



Alma Mater Studiorum – Università di Bologna

DOTTORATO DI RICERCA IN SCIENZE DELLA TERRA
XX° CICLO

Settore scientifico disciplinare GEO/02

Titolo di Tesi

EVIDENZE MICROPALAEONTOLOGICHE E SEDIMENTOLOGICHE
DI CICLI DEPOSIZIONALI E CLIMATICI CIRCA MILLENARI NEI DEPOSITI TARDOQUATERNARI
DELLA PIANA DELL' ARNO E DEL DELTA DEL PO

Presentata da: Dott. Veronica Rossi

Coordinatore dottorato:
Prof. William Cavazza

Relatore
Prof. Alessandro Amorosi

Esame finale anno 2008

INDICE

Introduzione

Paper 1: Late Quaternary climatic evolution of the Arno coastal plain (Western Tuscany, Italy) from subsurface data

Aguzzi, M., Amorosi, A., Colalongo, M.L., Ricci Lucchi, M., **Rossi, V.**, Sarti, G. and Vaiani, S.C.

Paper 2: Anatomy and sequence stratigraphy of the late Quaternary Arno valley fill (Tuscany, Italy)

Amorosi, A., Sarti, G., **Rossi, V.** and Fontana, V.

Paper 3: Climatic signature of millennial-scale parasequences from Lateglacial-Holocene transgressive deposits of Arno valley fill (Tuscany, Italy)

Amorosi, A., Ricci Lucchi, M., **Rossi, V.** and Sarti, G.

Paper 4: Late Quaternary palaeoenvironmental evolution of the Adriatic coastal plain and the onset of Po River Delta

Amorosi, A., Dinelli E., **Rossi, V.**, Vaiani, S.C. and Sacchetto, M.

Paper 5: Microfaunal response to sediment supply changes and fluvial drainage reorganization in Holocene deposits of the Po Delta, Italy

Rossi, V. and Vaiani, S.C.

Paper 6: The application of a subtidal foraminiferal-based transfer function to reconstruct Holocene palaeo-bathymetry of the Po delta, Northern Adriatic Sea

Rossi, V. and Horton, B.P.

Cicli deposizionali sub-milankoviani nelle aree costiere: record stratigrafico di eventi climatico-eustatici ad alta frequenza

Appendice: The Sedimentary Record of the 2005 Hurricane Season along the Gulf Coast

Horton, B.P., **Rossi, V.** and Hawkes, A.D.

INTRODUZIONE

Nel corso dell'ultimo decennio, l'Olocene (circa 11.500 anni calibrati ad oggi) è stato oggetto di numerosi studi interdisciplinari, finalizzati alla definizione e comprensione delle caratteristiche e delle cause di una comprovata variabilità climatica a scala millenaria (1.500-1.000 anni) e sub-millenaria (550 anni - Bond et al., 1997, 2001; Chapman e Shackleton, 2000).

Quale fattore, o più probabilmente quale meccanismo di fattori, abbia causato l'instaurarsi di eventi climatici freddi durante l'attuale interglaciale è ancora oggi una questione in buona parte aperta e a tal proposito sono state formulate varie ipotesi e relativi modelli, nessuno dei quali completamente risolutivo. Le cause più accreditate al momento riguardano variazioni nell'attività solare, evidenziate da fluttuazioni nella produzione di nuclidi cosmogenici (^{10}Be e ^{14}C), perturbazioni nel ciclo idrologico, e più precisamente nella circolazione oceanica profonda, indotte dall'improvviso rilascio di grandi quantità di acqua dolce, ed eruzioni vulcaniche (Mayewsky et al., 2004; Sbaffi et al., 2004).

La presenza a scala globale di almeno sei periodi di deterioramento climatico (*RCC-rapid climatic change*) di ridotta intensità e di durata circa millenaria è stata riconosciuta da Mayewsky et al. (2004), tramite l'integrazione di numerosi indicatori paleoclimatici ad alta risoluzione provenienti da aree geografiche ed ambienti differenti (ad esempio: valori di $\delta^{18}\text{O}$ registrati in carote di ghiaccio, depositi carbonatici lacustri o speleotemi, concentrazione di alkenoni in successioni marine, associazioni a foraminiferi planctonici in depositi di bacino oceanico, associazioni polliniche e a diatomee entro successioni lacustri). Le numerose datazioni disponibili in letteratura hanno permesso di evidenziare la contemporaneità di questi eventi climatici con le principali fasi di avanzamento globale dei ghiacciai continentali in Europa e in Nord America (Denton and Karlen, 1973), ed un buon grado di correlabilità con i cinque più recenti, fra gli otto di età olocenica, eventi freddi a ciclicità millenaria (*Bond's event*) riconosciuti nel Nord Atlantico da Bond et al. (1997, 2001) (vedi Tabella 1).

Fasi di avanzamento dei ghiacciai continentali in Europa e in Nord America (Denton and Karlen, 1973)	RCC- <i>rapid climatic change</i> (Mayewsky et al., 2004)	<i>Bond's event</i> - Nord Atlantico (Bond et al., 1997)	
		12.500 anni calibrati BP	YD
		11.100 anni calibrati BP	8
		10.300 anni calibrati BP	7
		9.500 anni calibrati BP	6
9.400-8.200 anni calibrati BP	9.000-8.000 anni calibrati BP	8.200 anni calibrati BP	5
5.800-5.200 anni calibrati BP	6.000-5.000 anni calibrati BP	5.900 anni calibrati BP	4
4.200-3.900 anni calibrati BP	4.200-3.800 anni calibrati BP	4.300 anni calibrati BP	3
3.000-2.400 anni calibrati BP	3.500-2.500 anni calibrati BP	2.800 anni calibrati BP	2
1.200-900 anni calibrati BP	1.200-1.000 anni calibrati BP	1.400 anni calibrati BP	1
500-150 anni calibrati BP	600-150 anni calibrati BP		

Tabella 1. Schema riassuntivo della ciclicità climatica circa millenaria riconosciuta nell’Emisfero settentrionale durante il periodo tardiglaciale-olocenico.

L’integrazione di *proxy* petrografici, litologici e micropaleontologici, registrati nelle successioni di bacino in carote provenienti da entrambi i lati del Nord Atlantico, ha rivelato brusche diminuzioni di temperatura subite dalle acque superficiali oceaniche durante il periodo tardiglaciale-olocenico. Tramite le analisi degli isotopi stabili e la comparazione con le associazioni attuali a foraminiferi planctonici del Mare del Nord, è stata ipotizzata una riduzione di circa 2°C e 5°C, rispettivamente per gli otto eventi di età olocenica e per lo *Younger Dryas* (Bond et al., 1997). Quest’ultimo appartiene al periodo pre-olocenico (ca. 13.000-11.500 anni calibrati) ed è l’unico evento ad essere chiaramente documentato nelle carote di ghiaccio della Groenlandia, assieme a quello datato circa 8.200 anni calibrati (Alley et al., 1997; Alley, 2000; Thomas et al., 2007), nonché in numerose serie polliniche mediterranee (Watts et al., 1996; Magri, 1999; Tinner e Lotter, 2001, 2006).

La presenza di una ciclicità climatica a scala millenaria (schematizzata in Tabella 1) ha verosimilmente influenzato l'evoluzione stratigrafico-deposizionale recente dei bacini oceanici, dei sistemi costieri e delle pianure alluvionali. In particolare, il susseguirsi quasi periodico di fasi di deterioramento e miglioramento climatico può avere indotto variazioni cicliche nella dinamica vegetazionale e nella produzione e distribuzione a mare dei sedimenti, fattori questi ultimi di fondamentale importanza nell'evoluzione deposizionale delle aree costiere suscettibili a pur minime variazioni fisico-ambientali.

Al momento risulta invece più incerta la presenza, a scala globale, di oscillazioni relative del livello marino correlabili a fasi climatiche di breve periodo (circa 1.000 anni). Superato l'ultimo massimo glaciale, datato a circa 20.000 anni calibrati fa, il livello marino ha iniziato a risalire da -120 metri rispetto al livello attuale, in seguito allo scioglimento delle calotte glaciali (Fairbanks, 1989).

Le tre curve glacio-eustatiche meglio datate attualmente disponibili, ricostruite utilizzando i *reef* corallini come paleoindicatori del livello marino, suggeriscono la presenza, durante la risalita post-glaciale, di brevi fasi di forte accelerazione, alternate a lunghi momenti di stasi o decelerazione (Fairbanks, 1989; Chappell and Polach, 1991; Bard et al., 1996). L'andamento di queste curve, che mantengono tuttavia un certo grado di incertezza dovuto all'influenza di fattori locali, suggerisce la presenza, a scala globale, di almeno due eventi di forte risalita del livello marino, in risposta a intense fasi di scioglimento delle calotte glaciali e la conseguente produzione di enormi volumi di acqua dolce rilasciati in mare (*MWP-Melt Water Pulse*). Il primo momento di forte risalita eustatica (MWP-1A) è datato a circa 14.300-14.000 anni calibrati, circa 1.000 anni prima dello *Younger Dryas*, mentre il secondo forte impulso (MWP-1B) coincide con l'inizio della trasgressione olocenica (circa 11.600-11.300 anni calibrati).

Rapidi episodi di accelerazione, seppur di minore intensità, hanno continuato a caratterizzare l'andamento del livello marino durante tutto il periodo olocenico. Liu et al. (2004) hanno distinto, tramite l'utilizzo di numerosi *proxy* continentali, costieri e marini provenienti dalla vasta area del Pacifico occidentale, altre due fasi di notevole risalita eustatica, denominate mwp-1c (circa 9.500-9.200 anni calibrati) e mwp-1d (8.000-7.500 anni calibrati) (Figura 1). Questi ultimi impulsi trasgressivi sono probabilmente relazionabili all'afflusso di grandi quantità di acqua dolce dovuti, più che allo

scioglimento delle calotte, oramai in buona parte scomparse, a episodi catastrofici come il collasso di grandi laghi glaciali (Clarke et al., 2003).

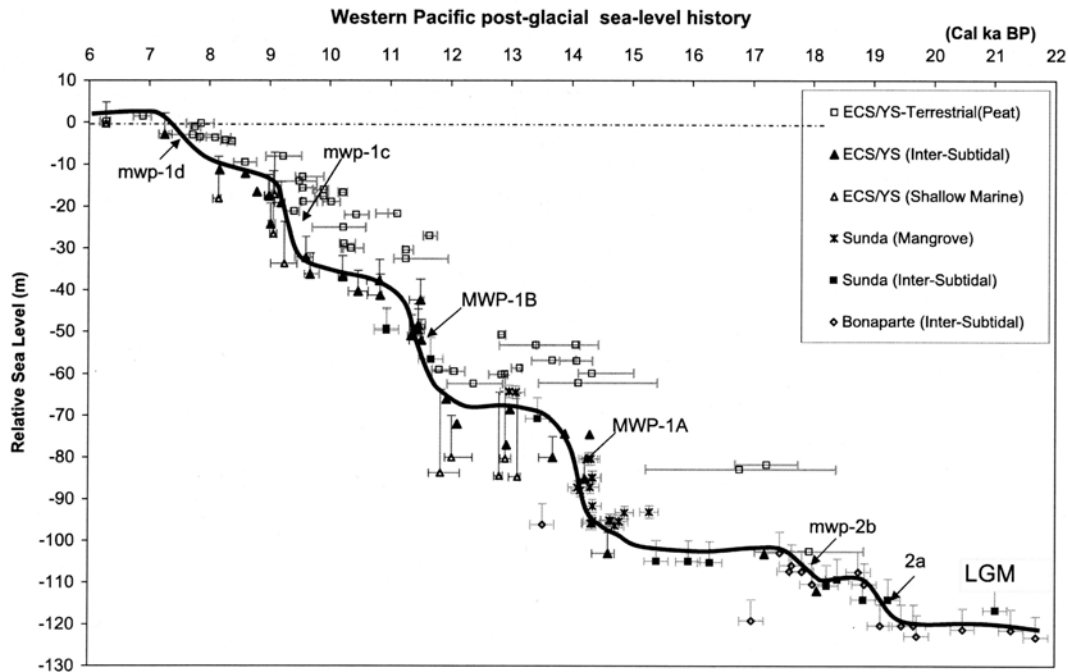


Figura 1. Risalita "a scatti" del livello marino durante il periodo post-glaciale nell'area del Pacifico occidentale. ECS: East China Sea; YS: Yellow Sea. LGM: Last Glacial Maximum (da Liu et al., 2004).

Rapide variazioni sia del tasso di risalita del livello marino che dell'apporto sedimentario a mare, entrambe relazionabili a cambiamenti climatici tramite complesse relazioni di causa-effetto, hanno chiaramente influenzato l'architettura deposizionale del sistema deltizio del Yellow River (Liu et al., 2004) e di altri fiumi sfocianti nel Pacifico occidentale, quali Song Hong (Tanabe et al., 2006; Li et al., 2006) e Yangtze (Hori et al., 2001; Yi et al., 2003).

Analogamente, è ipotizzabile che l'evoluzione recente delle aree costiere del Mediterraneo abbia risentito di una tale ciclicità climatico-eustatica. Eventuali variazioni di facies sedimentaria, faunistica e pollinica, riconosciute alla scala sub-milankoviana nelle successioni post-glaciali sepolte al di sotto delle attuali piane deltizie e costiere, possono quindi rappresentare il record deposizionale di eventi climatici circa millenari, la cui esistenza è oramai comprovata a scala mondiale.

Ciclicità deposizionali del quinto e sesto ordine di età tardiglaciale-olocenica, caratterizzate al loro interno da una chiara tendenza *shallowing-upward* e delimitate a base e a tetto da superfici trasgressive minori (parasequenze *sensu* Van Wagoner et al., 1990), sono state recentemente riconosciute nel sottosuolo del delta dell'Ebro in Spagna (Somoza et al., 1998), del delta del Rodano in Francia (Boyer et al., 2005), del delta del Tevere (Amorosi e Milli, 2001) e della piana costiera emiliano-romagnola (Amorosi et al., 2005).

Entro depositi trasgressivi datati circa 14.000-7.000 anni calibrati, queste parasequenze sono organizzate secondo un *trend* retrogradazionale e sembrano riflettere l'andamento di risalita "a scatti" del livello marino. Nessuna diretta correlazione fra questi cicli deposizionali e le fasi climatiche tardiglaciali-oloceniche è però al momento chiaramente documentata, in particolare per quanto concerne lo sviluppo della porzione "regressiva" di ogni parasequenza e il suo eventuale segnale climatico.

Obiettivi

o Obiettivo generale

L'obiettivo generale di questo lavoro è di fornire un contributo allo studio stratigrafico e paleoambientale di alcune successioni tardoquaternarie (tardiglaciali-oloceniche) dell'area mediterranea italiana. Questo studio ha lo scopo di evidenziare, entro l'attuale sequenza trasgressivo-regressiva (dalla fine dell'ultimo glaciale ad oggi), la presenza su base sedimentologica e micropaleontologica di ciclicità deposizionali di ordine minore, descrivendone le principali caratteristiche di facies e la geometria tridimensionale, e collocandole entro un preciso quadro cronologico che ne consenta la correlazione a scala extra-bacinale.

o Obiettivi specifici

1. Uno degli obiettivi specifici di questo lavoro è la comprensione delle relazioni di causa-effetto intercorrenti fra ciclicità eustatica e climatica circa millenaria, globalmente riconosciuta e documentata per il periodo tardiglaciale-olocenico, e ciclicità deposizionale alla scala sub-milankoviana in aree deltizie e di piana costiera. Questo studio vuole quindi contribuire allo sviluppo di un modello capace di prevedere le possibili conseguenze geologico-ambientali di future variazioni climatiche e relative oscillazioni del livello marino a breve periodo. Nell'immediato futuro, cambiamenti climatici ad alta frequenza e di chiara natura antropica sono stati infatti ipotizzati dal report internazionale sul clima (IPCC-*Intergovernmental Panel on Climate Change*) del 2007, così come il loro devastante impatto su ampi tratti di costa a scala mondiale.
2. Attraverso lo studio stratigrafico di dettaglio di cicli a scala circa millenaria, in contesti sia trasgressivi che di regressione deposizionale, ulteriore obiettivo di questo studio è la discussione dei meccanismi di interazione tra clima e produzione/apporto di sedimenti a mare, fattori di fondamentale importanza per l'evoluzione dei sistemi costieri presi in esame.

Scelta delle aree di studio

A questo scopo sono state selezionate due aree costiere italiane, diverse per contesto geologico-strutturale di appartenenza, quali la pianura deltizia dell'Arno, nell'area nord-tirrenica, e il Delta del Po nell'area nord-adriatica.

La scelta del Delta del Po è stata dettata dalla possibilità di contestualizzare, alla scala del bacino padano, dettagliate analisi di facies e relative ciclicità deposizionali di ordine inferiore al quarto, grazie alla presenza di un valido e ben conosciuto quadro stratigrafico generale di riferimento. I depositi di età tardoquaternario-olocenica della Pianura Padana (Amorosi et al., 1999, 2003, 2004) e della zona meridionale del Delta del Po (Stefani e Vincenzi, 2005; Bondesan et al., 2006) sono stati infatti oggetto di numerosi studi

sedimentologici e stratigrafici, che hanno permesso di ricostruire l'evoluzione e l'architettura deposizionale dell'area padana alla scala delle sequenze di quarto ordine (circa 100.000 anni).

Otto cicli di ordine gerarchico inferiore (parasequenze), di periodo circa millenario, sono stati recentemente riconosciuti entro la successione olocenica presente nel sottosuolo dell'area a sud del Po di Volano (Amorosi et al., 2005). Le caratteristiche di facies e la loro geometria tridimensionale, distinte tramite l'integrazione di analisi sedimentologiche e micropaleontologiche, rappresentano un valido quadro di comparazione per la vicina area del delta moderno.

Analogamente, un solido quadro di riferimento stratigrafico-sequenziale alla scala dei cicli di quarto ordine, sul quale impostare studi ad alta risoluzione, è disponibile per l'area della pianura costiera dell'Arno, grazie allo studio di sottosuolo recentemente intrapreso dallo stesso gruppo di ricerca al quale appartengo (Aguzzi et al., 2005; Aguzzi, 2006).

Metodi e Fasi della ricerca

Al fine di conseguire gli obiettivi sopra elencati, in entrambe le aree prese in esame è stata eseguita, in primo luogo, una ricostruzione stratigrafica tridimensionale di dettaglio dei depositi tardiglaciale-olocenici.

Sei sondaggi a carotaggio continuo, di profondità compresa fra 30-100 metri, due dei quali eseguiti nell'ambito della Tesi di Dottorato della dott.ssa Margherita Aguzzi, sono stati realizzati nella piana costiera dell'Arno, grazie alla collaborazione con il Dr. Giovanni Sarti del Dipartimento di Scienze della Terra dell'Università di Pisa. Tre sondaggi a 40 metri di profondità sono stati invece eseguiti espressamente per questo progetto nel Delta del Po, finanziati dal gruppo di ricerca del Prof. Amorosi.

La caratterizzazione di facies dei sondaggi è stata eseguita tramite l'integrazione di analisi sedimentologiche e micropaleontologiche di dettaglio (associazioni miste a foraminiferi ed ostracodi bentonici), entrambe condotte dalla scrivente.

Questi dati sono stati integrati con numerose analisi radiometriche (AMS ^{14}C), effettuate su campioni ricchi in carbonio (gusci di molluschi, resti vegetali e pezzi di legno, livelli arricchiti in materia organica o torba) e prelevati in corrispondenza di specifici livelli stratigrafici, al fine di fornire un inquadramento cronologico generale della successione tardoquaternario-olocenica e definire età e durata di cicli deposizionali minori.

Al fine di ottenere una ricostruzione completa e bi-tridimensionale della geometria dei corpi deposizionali identificati, le stratigrafie desunte dai sondaggi a carotaggio continuo sono state correlate, attraverso opportune griglie di sezioni stratigrafiche, con ulteriori dati di sottosuolo (sondaggi e CPTU) di minore qualità provenienti dalla banca dati di vari enti pubblici locali.

Lo studio stratigrafico dei cicli a scala circa millenaria è stato concentrato sulla porzione trasgressiva (*TST-transgressive system tract*) della successione sviluppatasi nelle aree in esame durante il Tardiglaciale e l'Olocene inferiore-medio (circa 14.000-7.000 anni calibrati), pur essendo documentata in letteratura la presenza di cicli deposizionali e climatici circa millenari anche in tempi più recenti, durante il periodo preistorico e storico (Bond et al., 1997; Somoza et al., 1998; Mayewsky et al., 2004; Leorri et al., 2006).

La scelta di focalizzare lo studio sui depositi trasgressivi è legata al fatto che in questo tratto di successione è possibile considerare trascurabile l'influenza sulla sedimentazione di numerosi fattori autociclici, quali variazioni locali nel tasso di subsidenza e fenomeni di avulsione fluviale, fra i più comuni (Amorosi e Milli, 2001). Quest'ultimi, comunemente preponderanti nel tratto "regressivo" delle sequenze (*HST-highstand system tract*) tendono infatti a complicare un quadro evolutivo di per sé molto articolato, indebolendo il segnale che consente il riconoscimento delle parasequenze.

La caratterizzazione climatica delle successioni in esame, alla scala sia delle sequenze di quarto ordine che dei cicli deposizionali di ordine minore (parasequenze) entro il TST, è stata possibile grazie alle analisi polliniche eseguite dalla dott.ssa Marianna Ricci Lucchi su due sondaggi chiave ubicati nella pianura costiera dell'Arno.

Riconosciuti e documentati gli effetti deposizionali ed ambientali della ciclicità circa millenaria climatico-eustatica nella piana dell'Arno e nell'area del delta padano, è stato

operato un confronto con simili evidenze climatiche e di facies in successioni coeve sepolte nel sottosuolo di altri sistemi costieri in varie parti del mondo. Questo procedimento ha consentito di mettere in relazione la ciclicità deposizionale ad alta frequenza delle aree in esame con eventi climatici di importanza globale.

Risultati

Il lavoro di ricerca condotto nell'ambito del Dottorato in Scienze della Terra ha portato alla realizzazione di 7 pubblicazioni scientifiche (da questo momento in poi indicate come Paper 1-6 + un appendice), in corso di stampa/pubblicate, inviate o in procinto di essere inviate a riviste internazionali, e di un capitolo di confronto e correlazione dati a completamento del progetto di ricerca.

Paper 1: pubblicato su *Sedimentary Geology* (2007) vol. 202, pp. 211-229.

Paper 2: in stampa su *GeoActa Special Publication on "Sequence Stratigraphy"* (A. Amorosi, B.U. Haq e L. Sabato Editors).

Paper 3: inviato a *The Holocene*.

Paper 4: inviato a *Palaeogeography, Palaeoclimatology, Palaeoecology*.

Paper 5: inviato a *Marine Micropaleontology*.

Paper 6: da inviare a *Journal of Foraminiferal Research*.

Capitolo "Cicli deposizionali sub-milankoviani nelle aree costiere: record stratigrafico di eventi climatico-eustatici ad alta frequenza".

Appendice: accettato per pubblicazione su *Quaternary International special issue "Record of disasters and hurricanes"* (S.A.G. Leroy Editor).

Per ognuno dei paper che costituiscono questa Tesi di Dottorato, il rispetto dell'ordine alfabetico nell'elenco degli autori implica un contributo attivo di ognuno di essi, in parti uguali, sia all'interpretazione dei dati che alla stesura del manoscritto. Contributi minori sono evidenziati, come tradizione nella letteratura scientifica, dal rovesciamento

dell'ordine alfabetico degli autori.

Paper 1, 2 e 3 riguardano lo studio dei depositi post-glaciali della piana costiera dell'Arno. Alla luce di favorevoli caratteristiche paleomorfologiche, che hanno consentito l'accumulo di una successione post-glaciale di riempimento di valle incisa di circa 35-40 metri di spessore, quest'area si è dimostrata un esempio ottimale per lo sviluppo di modelli di analisi di facies ad alta risoluzione e per lo studio delle relazioni fra oscillazioni climatiche ad alta frequenza ed evoluzione ambientale.

Paper 4, 5 e 6 illustrano invece l'evoluzione deposizionale post-glaciale nel sottosuolo del delta padano che, a dispetto dell'enorme mole di studi recenti nell'area padana, non è mai stato investigato in dettaglio. La successione trasgressiva si sviluppa qui in un contesto opposto a quello dell'Arno (assenza di significativi riempimenti di valle incisa), mentre è presente una successione deltizia progradante particolarmente complessa ed estremamente sviluppata.

Infine, nel Capitolo di confronto e correlazione dati la ciclicità deposizionale e climatica distinta entro i depositi trasgressivi della pianura dell'Arno e del Delta del Po è inserita in un contesto di riferimento globale ottenuto tramite dati stratigrafici e climatici, presenti in letteratura e provenienti da numerose aree costiere mondiali.

In appendice è riportata la pubblicazione scientifica extra-progetto di Dottorato, realizzata in collaborazione con il Prof. Benjamin Peter Horton, durante il periodo di formazione trascorso all'estero presso Department of Earth and Environmental Science, University of Pennsylvania, e accettata per pubblicazione su Quaternary International.

Viene di seguito presentato un riassunto dei principali risultati ottenuti.

Paper 1 presenta i risultati di uno studio sedimentologico e micropaleontologico ad alta risoluzione (foraminiferi e ostracodi bentonici, pollini), condotto su un sondaggio a carotaggio continuo profondo (M1), ubicato in prossimità dell'attuale linea di costa nord-tirrenica. Il recupero praticamente continuo e indisturbato di 105 metri di successione di depositi tardoquaternari-olocenici ha permesso di documentare l'evoluzione stratigrafica

e paleoclimatico-ambientale della pianura costiera dell'Arno, dalla trasgressione tirreniana (circa 125.000 anni fa) ad oggi.

L'identificazione di due superfici trasgressive principali ha permesso di distinguere due sequenze trasgressivo-regressive, che grazie alle analisi polliniche sono state relazionate a precise fasi climatico-eustatiche di carattere globale. La porzione stratigraficamente inferiore di ogni sequenza è composta da depositi costieri e di mare basso, formati durante i due più recenti interglaciali (OIS/*oxygen isotopic stage* 1-Olocene e OIS 5e-Tirreniano), in un contesto climatico caldo e di risalita (e successivo stazionamento alto) del livello marino.

Le sequenze terminano in una successione alluvionale, sviluppatasi durante le fasi di caduta eustatica o di stazionamento basso del livello marino, avvenute in corrispondenza di fasi climatiche fredde/stadi glaciali (OIS 2-4 e 6).

In particolare, la sequenza deposizionale di età olocenica, con oltre 50 metri circa di spessore totale, documenta la presenza di una profonda valle incisa nel sottosuolo della piana costiera dell'Arno. Al di sopra di depositi fluviali riferibili all'ultimo glaciale, il riempimento della valle incisa dell'Arno è costituito quasi interamente da depositi estuarini, di età compresa tra circa 10.000 e 8.000 anni BP. Al di sopra di questi, depositi litorali, marini e infine di progradazione deltizia registrano il colmamento e il seguente seppellimento della paleovalle.

In questo lavoro mi sono occupata dell'analisi micropaleontologica del sondaggio e, in parte, dell'analisi di facies.

Paper 2, a partire dal dato puntiforme illustrato in Paper 1, illustra in dettaglio l'architettura deposizionale dei depositi tardiglaciale-olocenici (13.000-8.000 anni calibrati BP) che costituiscono il riempimento della paleovalle dell'Arno, ampia circa 5-7 km. Tramite la correlazione di sondaggi a carotaggio continuo e altri dati di sottosuolo di minore qualità, disposti lungo quattro sezioni trasversali ed una sezione allungata parallelamente all'asse della valle, è stato possibile ricostruire la geometria tridimensionale dei principali corpi deposizionali e definire tempi e modalità di sviluppo della valle incisa e del suo riempimento.

Durante il periodo tardiglaciale-olocenico, un'alternanza verticale di depositi trasgressivi di pianura costiera, *bay-head delta* ed estuario si sviluppa entro valle, per uno spessore totale di circa 35-40 metri. Analogamente, muovendosi lungo valle dalle aree più prossimali verso l'attuale linea di costa si registrano sottocorrente variazioni laterali di facies, da depositi palustri e debolmente salmastri a successioni prettamente estuarine.

Una dettagliata analisi di facies sui sondaggi a carotaggio continuo ha permesso di distinguere, entro la successione trasgressiva, tre cicli deposizionali minori (parasequenze) spessi circa 10 metri, delimitati da superfici trasgressive e caratterizzati internamente da un chiaro trend *shallowing-upward*. Queste parasequenze, di durata circa millenaria, mostrano un evidente sviluppo tridimensionale entro valle, suggerendo una risalita "a scatti" del livello marino durante le prime fasi della trasgressione.

In risposta alla continua risalita del livello marino, depositi di spiaggia e di piattaforma interna completano il riempimento della paleovalle e invadono le aree di interfluvio, fino a questo momento rimaste esposte con il conseguente sviluppo di un paleosuolo. Circa 17 metri di depositi tardo-trasgressivi e di progradazione deltizia costituiscono la successione olocenica formatasi in corrispondenza degli argini della paleovalle.

In questo lavoro mi sono occupata della descrizione sedimentologica dei sondaggi a carotaggio continuo e, in parte, delle correlazioni stratigrafiche.

Paper 3 si è occupato in dettaglio della caratterizzazione di facies, sia sedimentologico-faunistica che pollinica, dei depositi trasgressivi (circa 13.000-7.800 anni calibrati BP) di un sondaggio profondo circa 56 metri (S1), ubicato nella porzione prossimale della paleovalle dell'Arno.

L'elevato spessore della successione trasgressiva in esame (circa 36-37 metri), che corrisponde di fatto al riempimento della paleovalle dell'Arno in posizione opposta rispetto a quella investigata in Paper 1, e la presenza di depositi fini in facies lagunare-palustre, estremamente ricchi in microfauna bentonica, hanno favorito uno studio paleoambientale e climatico ad alta risoluzione.

Questo tipo di approccio multidisciplinare ha permesso di chiarire i rapporti esistenti fra cicli deposizionali a scala sub-milankoviana e ciclicità climatica millenaria,

affrontando il problema dell'interazione fra fattori autociclici e allociclici interdipendenti, quali clima, variazioni del livello marino, produzione e apporto di sedimenti.

In particolare, è chiaramente documentata per la prima volta la risposta deposizionale ed ambientale di un sistema costiero attuale a due specifiche fasi climatiche fredde, di impatto mondiale, come lo *Younger Dryas* e l'evento olocenico degli 8.200 anni calibrati.

Nell'area nord tirrenica l'instaurarsi di brevi fasi climatiche fredde, ma non aride come chiaramente evidenziato dalle analisi polliniche, ha causato uno spostamento verso mare quasi immediato degli ambienti e delle relative facies deposizionali. Una maggiore produzione di sedimenti, in concomitanza con una probabile fase di rallentamento o stasi della risalita del livello marino, ha infatti indotto il riempimento delle lagune sviluppatesi durante le fasi calde del Tardiglaciale-Olocene, tramite la deposizione di sedimenti di pianura costiera e sabbie di *bay-head delta*. Nel caso dell'evento degli 8.200 calibrati, la regressione deposizionale culmina con lo sviluppo di una pianura alluvionale e di un paleosuolo, presente ad una profondità comparabile con gli argini della paleovalle (circa 17 metri) e relazionabile ad una avulsione del fiume Arno. L'annegamento della paleovalle e lo sviluppo di una successione trasgressiva palustre-lagunare post-8.200 coincide con il ritorno a condizioni climatiche favorevoli, come indicato dalle analisi polliniche.

Il raggiungimento della massima trasgressione marina (*MFS-maximum flooding surface*), evidenziato dal passaggio da microfaune salmastre a marino-influenzate, avviene circa 7.800 anni fa, dopo il colmamento della paleovalle.

In questo lavoro mi sono occupata della descrizione sedimentologica dei sondaggi, dell'intera parte micropaleontologica, della ricerca paleoclimatica e, in parte, dell'interpretazione dei risultati e della stesura del testo.

Paper 4 tratta l'evoluzione paleogeografica e stratigrafica dell'area del Delta moderno del Po durante l'ultimo ciclo trasgressivo-regressivo, da circa 11.000 anni calibrati ad oggi. Tramite l'analisi di facies di tre sondaggi profondi circa 40 metri (indicati come Core 1, 2 e 3), e l'integrazione di quest'ultimi con altri dati di sottosuolo (sondaggi e CPTU), lungo una sezione trasversale orientata circa N-S, è stato possibile definire le principali fasi evolutive oloceniche e la formazione in età recente del sistema deltizio Po.

La porzione inferiore della successione tardoquaternaria in esame è composta da depositi di pianura alluvionale, organizzati in sequenza *fining-upward* e delimitati a tetto da un livello sovraconsolidato con evidenze di pedogenesi (paleosuolo), sviluppatosi probabilmente al passaggio dall'ultimo massimo glaciale alle prime fasi trasgressive.

Il brusco passaggio a torbe e depositi palustri ricchi in materia organica segna l'inizio della trasgressione olocenica attorno ai 10.000 anni calibrati. La progressiva risalita del livello marino induce un rapido spostamento verso terra delle facies, come chiaramente indicato dal susseguirsi di depositi trasgressivi di retrobarriera, spiaggia e piattaforma interna (TST-*transgressive system tract*, spesso circa 7 metri). Entro i depositi palustri di retrobarriera evidenze sedimentologico-stratigrafiche suggeriscono la presenza di almeno un ciclo deposizionale di ordine minore, relazionabile a un breve momento di rallentamento o di stasi nella curva di risalita del livello marino, avvenuto durante l'Olocene inferiore e databile fra i 9.900 e i 9.500 anni calibrati.

Raggiunto il momento di massima trasgressione marina (MFS-*maximum flooding surface*), distinto in sondaggio grazie a variazioni nella microfauna registrate entro i depositi di piattaforma interna, il sistema deposizionale inizia a progredire. Una spessa successione di depositi di prodelta (15-16 metri) passa verso l'alto a depositi di fronte deltizio e di piana deltizia, che chiudono la successione di *highstand*.

Nel sondaggio ubicato più a mare (Core 1), la combinazione di analisi micropaleontologiche e geochimiche di dettaglio (quest'ultime eseguite dal prof. Enrico Dinelli) ha permesso di distinguere, entro la successione di prodelta, l'inizio del sistema deltizio riferibile al Po di età moderna (post-Rotta di Ficarolo). Quest'ultimo infatti mostra sia alti contenuti in Cr e Ni, indicativi di una sedimentazione deltizia a chiaro segnale geochimico Po, che elevate percentuali di *Nonionella turgida*. Una microfauna comparabile è attualmente presente in Nord Adriatico lungo il margine occidentale della *mud-belt*, tipico prodelta dell'attuale sistema deltizio Po.

In questo lavoro mi sono occupata della descrizione sedimentologica dei sondaggi, delle correlazioni stratigrafiche e di gran parte della micropaleontologia, dell'interpretazione dei risultati e della stesura del testo.

Paper 5, che costituisce un approfondimento micropaleontologico di Paper 4, focalizza l'attenzione sull'evoluzione recente del sistema deltizio Po, tramite uno studio micropaleontologico di dettaglio di due sondaggi a carotaggio continuo, Core 1 (lo stesso di Paper 4) e Core S1, ubicati lungo un transetto Est-Ovest nella parte meridionale del Delta.

L'integrazione di analisi cluster e analisi qualitative eseguite, rispettivamente, sui foraminiferi e sugli ostracodi bentonici, ha permesso di distinguere 4 associazioni appartenenti a diversi ambienti e sub-ambienti di mare basso.

Variazioni in verticale e in laterale, nella distribuzione delle associazioni, riflettono i principali cambiamenti avvenuti, durante gli ultimi 5.500 anni calibrati circa (post massima trasgressione marina), nell'organizzazione del sistema fluviale e quindi nella produzione e distribuzione del sedimento.

Specifici cambiamenti nel contenuto microfossilifero sono stati relazionati a minori oscillazioni batimetriche accompagnate da variazioni nell'intensità e tipologia (apporto di acqua dolce e/o di sedimenti fini e soprattutto di nutrienti) dell'influenza fluviale nell'area in esame. In particolare, fin dalle prime fasi di progradazione deltizia risulta evidente la stretta relazione esistente fra microfauna e apporto di nutrienti.

I dati micropaleontologici di sondaggio, integrati con evidenze sedimentologiche, hanno permesso di distinguere quattro principali fasi evolutive nella storia del Delta (Fasi A-D), correlabili a specifici periodi storico-climatici, grazie alla disponibilità di datazioni al radiocarbonio e alla buona documentazione storico-idrografica presente in letteratura.

Durante il primo periodo-Fase A, compreso fra il momento di massima trasgressione marina e fine Alto Medioevo (circa 5.500-1.000 anni calibrati fa), si sviluppa un ambiente di prodelta in corrispondenza del Core S1. Contemporaneamente in posizione distale (Core 1) sono presenti depositi fini di piattaforma interna scarsamente fluvio-influenzata, in continuità con la successione marina trasgressiva sottostante.

Durante il Basso Medioevo (Fase B) l'approssimarsi del sistema deltizio Po induce la deposizione di sedimenti fini di prodelta, caratterizzati da una forte variabilità nel contenuto microfossilifero, anche in corrispondenza di Core 1. Una fitta alternanza di due associazioni marine fluvio-influenzate, una indicativa soprattutto di condizioni iposaline e profondità ridotte (alte percentuali di *Ammonia tepida* e *A. parkinsoniana*), l'altra di un

elevato contenuto in nutrienti e di profondità lievemente maggiori (alte percentuali di *Valvulineria perlucida* e *Criboelphidium granosum*), indica condizioni ambientali instabili, probabilmente causate dalle frequenti avulsioni fluviali avvenute durante questo periodo. Durante i primi secoli del Basso Medioevo, in corrispondenza di Core S1 i depositi argillosi di prodelta sono sostituiti da sabbie di fronte deltizio.

Il brusco passaggio, in Core 1, ad una associazione a *Nonionella turgida* segna l'inizio di una nuova fase evolutiva (Fase C-passaggio all'età Moderna), che vede l'instaurarsi di condizioni ambientali particolarmente stressanti (elevato contenuto in materia organica e limitata scarsità in ossigeno) nell'area in esame. Per la prima volta il record deposizionale di una *mud-belt* fossile, seppure la sua porzione marginale, è rinvenuto nel sottosuolo di un sistema deltizio moderno. Questo radicale cambiamento faunistico-ambientale è stato probabilmente indotto dall'avulsione di Ficarolo (Rotta di Ficarolo), avvenuta circa 800 anni calibrati fa.

La nuova configurazione della rete idrografica, unitamente alla circolazione superficiale adriatica diretta verso sud, ha infatti favorito l'accumulo di nutrienti e sedimenti fini di origine fluviale nell'area in esame. Al momento risulta invece difficile comprendere meglio il ruolo svolto dal clima in relazione all'attivazione dell'avulsione e alla produzione di sedimenti, sebbene un prolungato periodo di instabilità climatica abbia certamente interessato l'area mediterranea durante gli ultimi secoli del Medioevo e l'età Moderna (*Medieval Warm Period* e inizio *Little Ice Age*).

Infine, la Fase D segna la nascita del Delta Moderno, post-Taglio di Porto Viro (circa 350 anni calibrati fa), con conseguente deposizione di cordoni deltizi in corrispondenza di Core 1.

In questo lavoro mi sono occupata di gran parte dello studio micropaleontologico, dell'interpretazione dei risultati e della stesura del testo.

Paper 6 tratta la questione dell'applicabilità del metodo delle *transfer function* (WA-PLS *transfer function*) su successioni marine poco profonde. Tramite l'elaborazione statistica eseguita sulla distribuzione attuale dei foraminiferi bentonici in Nord Adriatico (*database* pubblicato da Jorissen nel 1988), è stato possibile sviluppare una WA-PLS

transfer function capace di riprodurre il dato batimetrico con uno scarto medio di circa 5,14 metri (RMSEP-*root mean square error of prediction*).

Precise e valide ricostruzioni paleobatimetriche sono dunque possibili come confermato anche dall'elevato valore del coefficiente di correlazione ($r^2=0,95$), indicativo di una forte relazione ambientale fra associazioni a foraminiferi bentonici e il parametro profondità nell'area in esame.

L'applicazione della *transfer function* (denominata NATF: *Northern Adriatic transfer function*) sulla successione marina olocenica di un sondaggio ubicato nella zona meridionale del Delta del Po (sondaggio Core 1-vedi Paper 4 e 5) ha fornito dati quantitativi di paleoprofondità, con un errore specifico di circa 5 metri, per 31 campioni contenenti abbondanti foraminiferi (microfauna autoctona contabile).

Questo grado di incertezza nella ricostruzione della curva paleobatimetrica dell'area del Delta non ha comunque impedito di evidenziare piccole oscillazioni di paleoprofondità entro il *trend* tendenzialmente regressivo/*shallowing-upward*, che ha caratterizzato gli ultimi 5.500 anni circa.

In accordo con la ben nota evoluzione paleoambientale dell'area in esame, i valori più alti di paleoprofondità, compresi fra $17,8 \pm 5,3$ metri e $28,9 \pm 5,6$ metri, caratterizzano i depositi tardo trasgressivi e primo regressivi di piattaforma interna contenenti alte percentuali di miliolidi e taxa ialini epifiti. Una brusca diminuzione di profondità (da 29 metri a 11,5 metri circa) coincide con il primo campione di prodelta, per poi attestarsi su valori inferiori a 18,7 metri entro l'intera successione deltizia, caratterizzata da alte percentuali di *Ammonia tepida* e *A. parkinsoniana*, *Valvulineria perlucida* e *Criboelphidium granosum*.

Seguendo un tipico andamento *shallowing-upward*, i valori più bassi di paleoprofondità (compresi fra 10,5-7,5 metri circa) sono registrati al top della successione deltizia progradante.

Nella successione di prodelta valori in media lievemente superiori di paleoprofondità caratterizzano i depositi di *mud-belt* contenenti alte percentuali di *Nonionella turgida*, in accordo con l'attuale gradiente batimetrico dell'Adriatico settentrionale.

La validità dei dati ottenuti è stata verificata statisticamente e in modo indipendente tramite l'applicazione della *Modern Analogue Technique* (MAT). Questo tipo di analisi

ha permesso infatti di distinguere i campioni aventi un analogo attuale nel *database* di riferimento (29 su un totale di 31), e per questo motivo adatti all'applicazione della *transfer function*.

In questo lavoro mi sono occupata dell'intero studio micropaleontologico e di gran parte della trattazione statistica, dell'interpretazione dei risultati e della stesura del testo.

Il capitolo "Cicli deposizionali sub-milankoviani nelle aree costiere: record stratigrafico di eventi climatico-eustatici ad alta frequenza" presenta, a completamento di questo progetto di ricerca, un quadro di confronto a scala mondiale fra parasequenze circa millenarie, documentate nel sottosuolo di pianure deltizie-costiere attuali, e ben note ciclicità climatico-eustatiche di età tardiglaciale-olocenica.

Partendo dai dati stratigrafici e climatici ottenuti dalle aree deltizie italiane prese direttamente in esame, pianura costiera dell'Arno (Paper 2-3) e Delta del Po (Paper 4), è stato attuato un tentativo di correlazione a scala globale con altri sistemi costieri mediterranei ed extra-mediterranei, utilizzando dati esistenti in letteratura. Questi ultimi sono stati in parte rivisti e interpretati in base allo scopo del lavoro e a esigenze metodologiche, come l'utilizzo di datazioni calibrate ottenute tramite un unico programma (CALIB versione 5.1., Stuiver e Reimer, 1993; Stuiver et al., 2005) e *dataset* di riferimento (IntCal04 da Reimer et al., 2004 e Marine04 da Hughen et al., 2004).

Età calibrate sono infatti indispensabili per garantire sia l'uniformità del dato temporale che la possibilità di confrontare record stratigrafici locali con specifiche fasi climatiche ed eustatiche di impatto globale.

Le maggiori fasi di risalita eustatica riconosciute in letteratura (MWP-*melt water pulse*), in particolare quelle di età olocenica, risultano chiaramente registrate nei depositi di sottosuolo di varie aree deltizie e costiere tramite superfici trasgressive. Caratteristiche paleomorfologiche locali, ereditate dal periodo glaciale, possono tuttavia causare un certo grado di ritardo nella registrazione delle trasgressioni.

Queste rapide fasi di accelerazione nella risalita del livello marino sono intervallate da altrettanti episodi di rallentamento o stasi della curva eustatica, ai quali corrispondono semi-coeve oscillazioni climatiche fredde circa millenarie, come lo Younger Dryas o l'evento degli 8.200 anni calibrati fra i più conosciuti.

Cicli stratigrafico-deposizionali comparabili per estensione temporale a ben noti eventi climatico-eustatici sono presenti in molte delle successioni sedimentarie in esame.

Considerando un certo grado di dispersione temporale, dovuto all'interpolazione di alcune datazioni e all'utilizzo di dati ottenuti tramite metodologie analitiche differenti, questi cicli trasgressivi-regressivi di breve periodo e di età tardiglaciale-olocenica mostrano una buona correlabilità fra loro e con le principali fasi trasgressive-MWP e "regressive"-eventi freddi mondiali. In particolare la trasgressione di età più recente (mwp-1d), immediatamente precedente il momento di massima trasgressione marina-MFS, e i due eventi climatici freddi principali (Younger Dryas e evento degli 8.200 calibrati) risultano essere chiaramente registrati dall'Oceano Atlantico settentrionale al Pacifico occidentale, passando per il bacino mediterraneo.

Tuttavia, per motivi paleomorfologico-ambientali di carattere locale, non tutti gli episodi trasgressivi e gli eventi climatici freddi post-glaciali riconosciuti in letteratura sono registrati nella totalità delle aree costiere prese in esame. In generale, una registrazione dettagliata ma soprattutto completa degli eventi climatico-eustatici avvenuti fra i 14.000 e i 7.000 anni calibrati è più facilmente riscontrabile entro le successioni trasgressive di riempimento di valli incise.

Appendice

Nell'articolo in appendice sono stati integrati e discussi dati geologici di superficie e di sottosuolo (tre *russian peat cores* di 50 cm), riguardanti il devastante impatto dell'uragano Katrina e Rita nell'area del Golfo del Messico nel 2005. Tre aree costiere (*salt-marsh*), due delle quali appartenenti allo stato del Mississippi ed una allo stato dell'Alabama, sono state prese in esame.

La massima altezza dell'onda di tempesta di Katrina è stata stimata più di 7,5 metri e di 3,43 metri, rispetto al *North American Vertical Datum 88* (NAVD88), rispettivamente per la zona costiera del Mississippi e per quella dell'Alabama. Inoltre è stata calcolata una massima estensione verso terra di circa 700 metri. Solo in una delle aree in esame sono state rinvenute evidenze del passaggio di Rita, con un'onda di tempesta di circa 3,43

metri (rispetto a NAVD 88) in altezza ed un'estensione entroterra massima di circa 370 metri.

I depositi di tempesta di Katrina e di Rita mostrano una superficie netta o erosiva al contatto con i sottostanti depositi di *marsh* ed un generale assottigliamento verso l'entroterra. Uno spessore variabile di circa 9-13 cm e di circa 7 cm caratterizza rispettivamente il record deposizionale di Katrina e di Rita.

I depositi di tempesta sono risultati grossolani e poveri in materia organica rispetto ai sedimenti sottostanti e virtualmente sterili in foraminiferi.

In questo lavoro mi sono occupata dell'analisi sedimentologica, micropaleontologica e dell'interpretazione di facies dei sondaggi.

Bibliografia

Aguzzi, M. 2006. Stratigrafia di sottosuolo di depositi tardoquaternari del Valdarno inferiore (Toscana). Tesi di dottorato, Università degli Studi di Bologna.

Aguzzi, M., Amorosi, A., Sarti, G. 2005. Stratigraphic architecture of Late Quaternary deposits in the lower Arno Plain (Tuscany, Italy). *Geologica Romana* 38, 1–10.

Alley, R. B. 2000. The Younger Dryas cold interval as viewed from central Greenland. *Quaternary Science Reviews* 19, 213–226.

Alley, R., Mayewski, P., Sowers, T., Stuiver, M., Taylor, K., Clark, P. 1997. Holocene climatic instability: a prominent widespread event 8200 yr ago. *Geology* 25, 483–486.

Amorosi, A., Colalongo, M. L., Pasini, G., Preti, D. 1999. Sedimentary response to Late Quaternary sea-level changes in the Romagna coastal plain (northern Italy). *Sedimentology* 46, 99–121.

Amorosi, A., Milli, S. 2001. Late Quaternary depositional architecture of Po and Tevere river deltas (Italy) and worldwide comparison with coeval deltaic successions. *Sedimentary Geology* 144, 357–375.

Amorosi, A., Centineo, M. C., Colalongo, M. L., Pasini, G., Sarti, G., Vaiani, S. C. 2003. Facies architecture and Latest Pleistocene-Holocene depositional history of the Po Delta (Comacchio area). Italy. *The Journal of Geology* 111, 39–56.

Amorosi, A., Colalongo, M. L., Fiorini, F., Fusco, F., Pasini, G., Vaiani, S. C., Sarti, G. 2004. Palaeogeographic and palaeoclimatic evolution of the Po Plain from 150-ky core records. *Global and Planetary Change* 40, 55–78.

Amorosi, A., Centineo, M. C., Colalongo, M. L., Fiorini, F., 2005. Millennial-scale depositional cycles from the Holocene of the Po Plain, Italy. *Marine Geology* 222-223, 7–18.

Bard, E., Hamelin, B., Arnold, M., Montaggioni, L., Cabioch, G., Faure, G., Rougerie, F. 1996. Deglacial sea-level record from Tahiti corals and the timing of global meltwater discharge. *Nature* 382, 241–244.

Bond, G., Showers, W., Cheseby, M., Lotti, R., Almasi, P., deMenocal, P., Priore, P., Cullen, H., Hajdas, I., Bonani, G. 1997. A pervasive millennial scale cycle in North Atlantic Holocene and glacial climate. *Science* 278, 1257–1266.

Bond, G., Kromer, B., Beer, J., Muscheler, R., Evans, M. N., Showers, W., Hoffmann, S., Lotti-Bond, R., Hajdas, I., Bonani, G. 2001. Persistent solar influence on North Atlantic climate during the Holocene. *Science* 294, 2130–2136.

Bondesan, M., Cibin, U., Colalongo, M. L., Pugliese, N., Stefani, M., Tsakiridis, E., Vaiani, S. C., Vincenzi, S. 2006. Benthic communities and sedimentary facies recording late Quaternary environmental fluctuations in a Po Delta subsurface succession (Northern Italy). In: Coccioni, R., Lirer, F., Marsili, A. (Eds.), *Proceedings of the Second and Third Italian Meeting of Environmental Micropaleontology*, The Grzybowski Foundation Special Publication 11, 21–31.

Boyer, J., Duvail, C., Le Strat, P., Gensous, B., Tesson, M. 2005. High resolution stratigraphy and evolution of the Rhône delta plain during Postglacial time, from subsurface drilling data bank. *Marine Geology* 222-223, 267–298.

Chapman, M. R., Shackleton, N. J. 2000. Evidence of 550-year and 1000-year cyclicities in North Atlantic circulation patterns during the Holocene. *The Holocene* 10, 287–291.

Chappell, J., Polach, H. 1991. Postglacial sea-level rise from a coral record at Huon Peninsula, Papua New Guinea. *Nature* 349, 147–149.

Clarke, G. K. C., Leverington, D. W., Teller, J. T., Dyke, A. S. 2003. Superlakes, megafloods, and abrupt climate change. *Science* 301, 922–923

Denton, G. H., Karlén, W. 1973. Holocene climatic variations: their pattern and possible cause. *Quaternary Research* 3, 155–205.

Fairbanks, R. G. 1989. A 17,000-year glacio-eustatic sea level record: influence of glacial melting rates on the Younger Dryas event and deep ocean circulation. *Nature* 342, 639–642.

Hori, K., Saito, Y., Zhao, Q., Cheng, X., Wang, P., Sato, Y., Li, C. 2001. Sedimentary facies of the tide-dominated paleo-Changjiang (Yangtze) estuary during the last transgression. *Marine Geology* 177, 331–351.

Hughen, K. A., Baillie, M. G. L., Bard, E., Beck, J. W., Bertrand, C. J. H., Blackwell, P.G., Buck, C. E., Burr, G. S., Cutler, K. B., Damon, P. E., Edwards, R. L., Fairbanks, R. G., Friedrich, M., Guilderson, T. P., Kromer, B., McCormac, G., Manning, S., Ramsey, C. B., Reimer, P. J., Reimer, R. W., Remmele, S., Southon, J. R., Stuiver, M., Talamo, S., Taylor, F. W., van der Plicht, J., Weyhenmeyer, C. E. 2004. Marine04 marine radiocarbon age calibration, 0–26 cal kyr BP. *Radiocarbon* 46, 1059–1086.

IPCC-Intergovernmental Panel on Climate Change 2007. Climate Change 2007: The Physical Science Basis.

Leorri, E., Martin, R., McLaughlin, P. 2006. Holocene environmental and parasequence development of the St. Jones Estuary, Delaware (USA): Foraminiferal proxies of natural climatic and anthropogenic change. *Palaeogeography, Palaeoclimatology, Palaeoecology* 241, 590–607.

Li, Z., Saito, Y., Matsumoto, E., Wang, Y., Tanabe, S., Vu, Q. L. 2006. Climate change and human impact on the Song Hong (Red River) Delta, Vietnam, during the Holocene. *Quaternary International* 144, 4–28.

Liu, J. P., Milliman, J. D., Gao, S., Cheng, P. 2004. Holocene development of the Yellow River's subaqueous delta, North Yellow Sea. *Marine Geology* 209, 45–67.

Magri, D. 1999. Late Quaternary vegetation history at Lagaccione near Lago di Bolsena (central Italy). *Review of Paleobotany and Palynology* 106, 171–208.

Mayewski, P. A., Rohling, E. E., Stager, J. C., Karlen, W., Maasch, K. A., Meeker, L. D., Meyerson, E. A., Gasse, F., van Kreveld, S., Holmgren, K., Lee-Thorp, J., Rosqvist, G., Rack, F., Staubwasser, M., Schneider, R. R., Steig, E. J. 2004. Holocene climate variability. *Quaternary Research* 62, 243–255.

Reimer, P. J., Baillie, M. G. L., Bard, E., Bayliss, A., Beck, J. W., Bertrand, C. J. H., Blackwell, P. G., Buck, C. E., Burr, G. S., Cutler, K. B., Damon, P. E., Edwards, R. L., Fairbanks, R. G., Friedrich, M., Guilderson, T. P., Hogg, A. G., Hughen, K. A., Kromer, B., McCormac, F. G., Manning, S. W., Ramsey, C. B., Reimer, R. W., Remmele, S., Southon, J. R., Stuiver, M., Talamo, S., Taylor, F. W., van der Plicht, J., Weyhenmeyer, C. E. 2004. IntCal04 Terrestrial radiocarbon age calibration. *Radiocarbon* 46, 1029–1058.

Sbaffi, L., Wezela F. C., Curzia, G., Zoppi, U. 2004. Millennial- to centennial-scale palaeoclimatic variations during Termination I and the Holocene in the central Mediterranean Sea. *Global and Planetary Change* 40, 201–217.

Somoza, L., Barnolas, A., Arasa, A., Maestro, A., Rees, J. G., Hernandez-Molina, F. J. 1998. Architectural stacking patterns of the Ebro delta controlled by Holocene high-frequency eustatic fluctuations, delta-lobe switching and subsidence processes.

Sedimentary Geology 117, 11–32.

Stefani, M., Vincenzi, S. 2005. The interplay of eustasy, climate and human activity in the late Quaternary depositional evolution and sedimentary architecture of the Po Delta system. *Marine Geology* 222-223, 19–48.

Stuiver, M., Reimer, P. J. 1993. Extended 14C data base and revised CALIB 3.0 14C Age calibration program. *Radiocarbon* 35, 215–230.

Stuiver, M., Reimer, P. J., Reimer, R. W. 2005. CALIB 5.0. <http://calib.qub.ac.uk/calib/>

Tanabe, S., Saito, Y., Vu, Q. L., Hanebuth, T. J. J., Ngo, Q. L., Kitamura, A. 2006. Holocene evolution of the Song Hong (Red River) delta system, northern Vietnam. *Sedimentary Geology*, 187 (1-2), 29–61.

Thomas, E. R., Wolff, E. W., Mulvaney, R., Steffensen, J. P., Johnsen, S. J., Arrowsmith, C., White, J. W. C., Vaughn, B., Popp, T. 2007. The 8.2 kyr event from Greenland ice cores. *Quaternary Science Reviews* 26 (1–2), 70–81.

Tinner, W., Lotter, A. F. 2001. Central European vegetation response to abrupt climate change at 8.2 ka. *Geology* 29, 551–554.

Tinner, W., Lotter, A. F. 2006. Holocene expansions of *Fagus silvatica* and *Abies alba* in Central Europe: where are we after eight decades of debate? *Quaternary Science Reviews* 25, 526–549.

Van Wagoner, J. C., Mitchum, R. M., Campion, K. M., Rahmanian, V. D. 1990. Siliclastic sequence stratigraphy in well logs, cores and outcrops: concepts for high resolution correlations of time and facies. *American Association of American Petroleum Geologists. Methods in Exploration* 7 Barbara H. Lidtz, Tulsa.

Watts, W. A., Allen, J. R. M., Huntley, B. 1996. Vegetation history and palaeoclimate of the Last Glacial period at Lago Grande di Monticchio, southern Italy. *Quaternary Science Review* 15, 133–153.

Yi, S., Saito, Y., Zhao, Q., Wang, P. 2003. Vegetation and climate changes in the Changjiang (Yangtze River) delta, China, during the past 13,000 years inferred from pollen records. *Quaternary Science Reviews* 22, 1501–1519.

Paper 1

Late Quaternary climatic evolution of the Arno coastal plain (Western Tuscany, Italy) from subsurface data

Aguzzi, M., Amorosi, A., Colalongo, M.L., Ricci Lucchi, M.,
Rossi, V., Sarti, G. and Vaiani, S.C.

Late Quaternary climatic evolution of the Arno coastal plain (Western Tuscany, Italy) from subsurface data

Margherita Aguzzi^a, Alessandro Amorosi^{a,*}, Maria Luisa Colalongo^a,
Marianna Ricci Lucchi^a, Veronica Rossi^a, Giovanni Sarti^b, Stefano Claudio Vaiani^a

^a *Dipartimento di Scienze della Terra e Geologico-Ambientali, Università di Bologna, Via Zamboni 67, 40126 Bologna, Italy*

^b *Dipartimento di Scienze della Terra, Università di Pisa, Via Santa Maria 53, 56126 Pisa, Italy*

Abstract

A multidisciplinary study of a 105-m-long core was carried out on the Tyrrhenian coast of Tuscany, Western Italy. Detailed description of sedimentary facies, foraminifer and ostracod assemblages, pollen, and ¹⁴C ages is presented in this paper.

Identification in core of two transgressive surfaces (TSs) as the most prominent stratigraphic markers allows subdivision of the Late Quaternary stratigraphic succession into two transgressive–regressive (T–R) sequences, attributed to the last 150 kyr BP. Sequence boundaries have no unequivocal physical expression in the core.

Detailed pollen analysis documents a direct relationship between vertical facies evolution and climate fluctuations. Coastal to shallow-marine sediments in the lower part of T–R sequences were deposited during the last two interglacial periods (OIS 1 and 5e), under rising sea-level conditions and during the following sea-level highstands. By contrast, alluvial sedimentation (upper part of T–R sequences) took place during periods of sea-level fall and subsequent sea-level lowstands, and was invariably linked to the onset of glacial periods (OIS 4–2 and 6, respectively).

This paper presents the first detailed facies documentation of a Late Quaternary incised-valley fill sequence from Italy. About 51 m of Holocene sediments are recorded beneath the present Arno River valley. Early transgression is documented in the lower part of the incised-valley fill by wave-dominated estuarine facies overlying lowstand fluvial deposits. Late transgression records the rapid landward migration of a beach-barrier system, followed by the establishment of an open-marine environment. Highstand sedimentation is represented by a shallowing-upward succession, which reflects progradation of the modern delta/strandplain.

© 2007 Elsevier B.V. All rights reserved.

Keywords: Late Quaternary stratigraphy; Sea-level change; Incised-valley system; Pollen; Micropalaeontology; Arno River

1. Introduction

Stratigraphic investigation of Late Quaternary deposits has become increasingly popular in the last decade, because of the unique opportunity to use tectonically undisturbed and easily datable sediments as a basis for the definition of realistic and accurate depositional models (Blum and Törnqvist, 2000; Cattaneo and Steel, 2003). These models may be successfully used for the prediction of possible scenarios of environmental

* Corresponding author. Tel.: +39 51 2094586; fax: +39 051 2094522.

E-mail addresses: MAguzzi@arpa.emr.it (M. Aguzzi),
alessandro.amorosi@unibo.it (A. Amorosi),
marianna.riccilucchi@unibo.it (M.R. Lucchi),
veronica.rossi4@unibo.it (V. Rossi), sarti@dst.unipi.it (G. Sarti),
stefano.vaiani@unibo.it (S.C. Vaiani).

change under rising sea-level conditions, and for the development of new conceptual models in the field of sequence stratigraphy (e.g. Saito, 1994; Blum and Törnqvist, 2000; Plint and Nummedal, 2000; Amorosi and Colalongo, 2005). Such models can also be applied to the interpretation of older successions and may serve to elucidate late Quaternary tectonic activity.

Facies analysis and sequence stratigraphy of Late Quaternary deposits traditionally deals with detailed reconstructions of Holocene successions buried in the uppermost few tens of metres beneath the modern alluvial and coastal plains (Lowrie and Hamiter, 1995; Somoza et al., 1998; Amorosi et al., 1999a; Hori et al., 2002; Amorosi et al., 2003; Overeem et al., 2003; Tanabe et al., 2003; Hori et al., 2004; Amorosi et al., 2005; Storms et al., 2005). Although a cyclic stacking pattern of facies in response to Milankovich-scale cycles has been observed within pre-Holocene deposits (Massari et al., 2004), there have been few attempts to depict the detailed facies architecture of the last two glacial–interglacial cycles (from OIS 6 onwards). This is mostly due to problems in the recovery of pre-Holocene data within

buried successions. Long-cored pollen series from continental successions in Europe have documented the climatic evolution of the last 150 ky (Wijmstra, 1969; Wijmstra and Smit, 1976; Woillard, 1978; Follieri et al., 1988; De Beaulieu and Reille, 1992; Tzedakis, 1993; Reille et al., 1998; Tzedakis, 1999), and have been shown to correlate with oxygen-isotope stratigraphy (see Tzedakis et al., 1997; Caspers and Freund, 2001; Guiter et al., 2003; Preusser, 2004). These studies, however, generally lack detailed facies analysis. Few studies have investigated in detail the response of coastal and deltaic depositional systems to the last two Quaternary glacio-eustatic cycles on the basis of multiple datasets (Amorosi et al., 1999b; Törnqvist et al., 2000, 2003; Lim and Park, 2003; Amorosi et al., 2004; Konradi et al., 2005; Hanebuth et al., 2006).

The aim of this paper is to present the first detailed example of an integrated sedimentological and micro-palaeontological study of late Quaternary deposits in the Tyrrhenian area, based on analysis of a 105 m-long core that was drilled in 2003 in western Tuscany (Italy), only 200 m from the present shoreline (Fig. 1). Specific

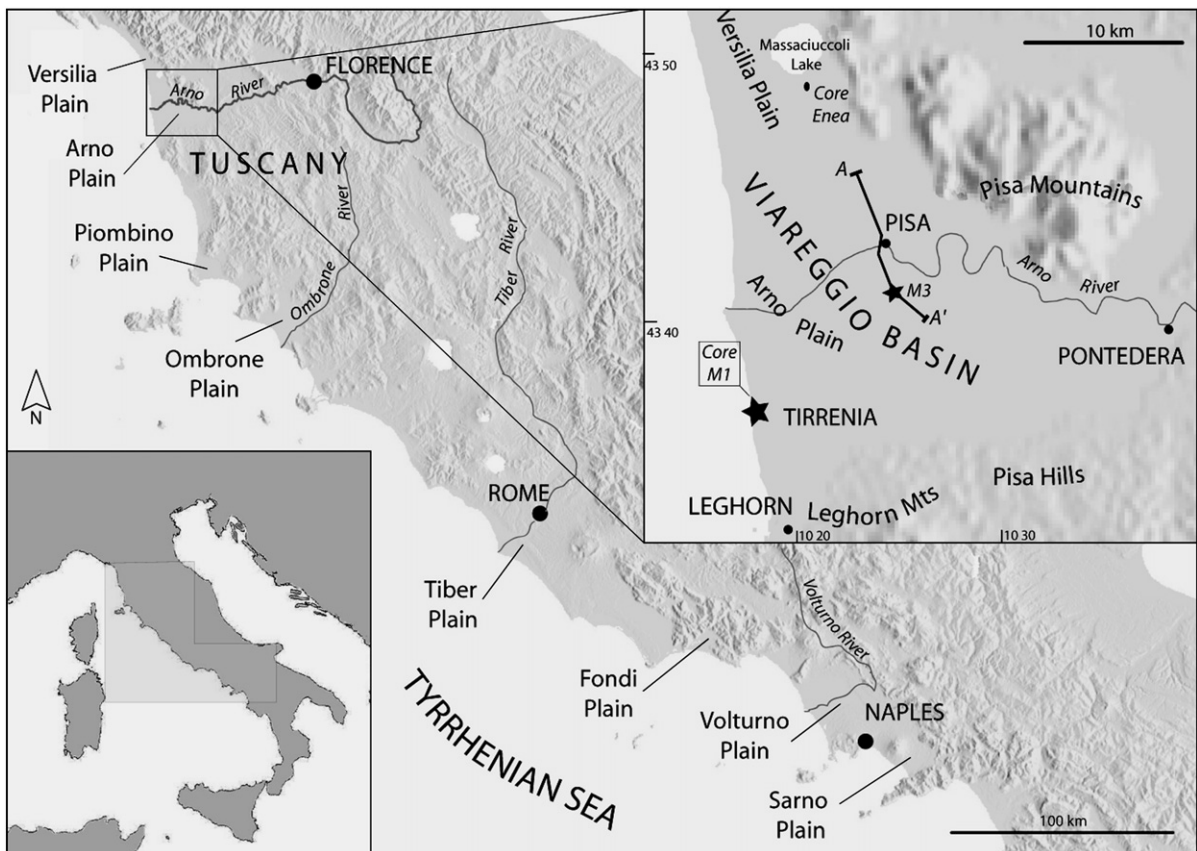


Fig. 1. Map of the study area with location of the major coastal plains along the Tyrrhenian coast of Italy. AA': section trace of Fig. 5.

objectives of this paper are: i) to reconstruct the depositional history of the Tuscan coastal plain in terms of its response to sea-level fluctuations during the past 150 ky, ii) to document the vertical stacking pattern of facies within the Holocene incised-valley fill beneath the Arno River, and iii) to establish a high-resolution chronology for the studied succession on the basis of pollen data.

2. OIS 5e deposits along the Tyrrhenian coast of Italy

The Quaternary evolution of the Tyrrhenian coast of Italy is difficult to unravel, due to complex superposition of tectonic uplift, subsidence and eustatic effects on sedimentation. A review of Late Quaternary tectonics along the Tyrrhenian coast and its influence on stratigraphic architecture was recently presented by Ferranti et al. (2006). Apart from a few detailed studies, however, stratigraphic information on the Late Quaternary succession is scarce in comparison with the well-documented Adriatic coast (Amorosi et al., 1999b; Cattaneo and Trincardi, 1999; Ridente and Trincardi, 2002; Amorosi et al., 2004). This applies especially to deposits of the last interglacial.

Early investigations of Late Quaternary deposits along the Tyrrhenian coast have been carried out in the Tiber Plain, around the city of Rome, where deposits attributed to the last interglacial (OIS 5e) have been encountered at depths ranging between 30 and 80 m below surface (Bellotti et al., 1994b, 1995; Milli, 1997). South of Rome, tidal notches referred to OIS 5e have been recognized at +7.3 m a.s.l. in outcrops bordering the Fondi Plain (Fig. 1), whereas lagoonal OIS 5e deposits have been encountered in subsurface at –6.5 m (Antonioli et al., 1988).

Close to Naples (Fig. 1), OIS 5e marine deposits have been identified at 50 m core depth in the Volturno plain (Romano et al., 1994), on the basis of $^{230}\text{Th}/^{234}\text{U}$ dating of coral *Cladocora coespitosa*. Further south, in the Sarno Plain (Fig. 1), marine deposits attributed to OIS 5 have been recognised at a depth of 25 m below surface (Barra et al., 1991).

In Tuscany, subsurface investigations carried out on the Ombrone coastal plain have been restricted to the post-OIS 5 succession (Carboni et al., 2002; Bellotti et al., 2004; Biserni et al., 2004). To the north, in the Piombino alluvial plain, lagoonal deposits assigned to OIS 5e on the basis of pollen data have been identified at 20 m core depth (Amorosi et al., 2004). Marine deposits attributed to OIS 5 on the basis of thermo-luminescence dates (Mauz, 1999) and amino-acid racemization (Hearty and Dai Pra,

1987) crop out patchily along the coast between Piombino and Leghorn, and are overlain by reddish weathered alluvial deposits (Cortemiglia et al., 1983; Hearty and Dai Pra, 1987; Mauz, 1999; Sarti et al., 2005).

The Arno coastal plain is located north of Livorno ('Leghorn'), in the southern part of the subsiding Viareggio Basin (Fig. 1). The Viareggio Basin includes the Versilia Plain and is bounded to the NE by the Pisa Mts. Its southern boundary, marked by the Livorno–Sillaro tectonic line (Bortolotti, 1966), is coincident with the foothills of the Leghorn Mountains. The depocentre of this basin, which is located close to the present coastline, was filled by up to 2500 m of upper Miocene–Present deposits (Pascucci, 2005). The Viareggio Basin is the northernmost of a series of extensional basins that developed on the south-western side of the Northern Apennines (Tuscany) during the early Messinian. This basin evolved as a half-graben, with NW–SE orientation, during a rifting phase in the Early Pliocene (Mariani and Prato, 1988; Argnani et al., 1997).

Aguzzi et al. (2005) established a stratigraphic framework for the Late Quaternary deposits beneath the lower Arno River valley. Approximately 20 km north of the study area, in the Versilia Plain (Fig. 1), $^{230}\text{Th}/^{234}\text{U}$ dating of a 90 m-long core has suggested the attribution of marine deposits to OIS 5e, at a depth of approximately 70 m (Antonioli et al., 1999). Unfortunately, no facies analysis has been performed on this core.

3. Materials and methods

The 105 m-long core (labelled M1) was drilled close to the village of Tirrenia, along the Tyrrhenian coast of Tuscany (Fig. 1). Drilling system consisted of a double corer, with 12 cm core diameter. Core recovery was 95%. The core was split lengthwise and carefully described in terms of colour, lithology, grain size, sedimentary structures and accessory materials (roots, wood fragments, organic material, peat, mollusc shells). Five AMS ^{14}C uncalibrated dates (performed at CEDAD, University of Lecce, Italy) were obtained from wood, organic-rich layers and mollusc shells, collected in the upper 50 m (Fig. 2).

A total of 179 samples of approximately 150 g were collected for micropalaeontological analyses. All samples were i) dried at 60 °C, ii) washed with H_2O through sieves of 63 μm (240-mesh), and iii) analyzed for ostracods and foraminifera. Qualitative analyses were performed for all samples on the >63 μm size fraction. Sixty-six samples with perfectly preserved foraminiferal specimens within the >125 μm size fraction were used for counting. These samples were split into small portions, which included at least 300 foraminifera. Identification of foraminifera and

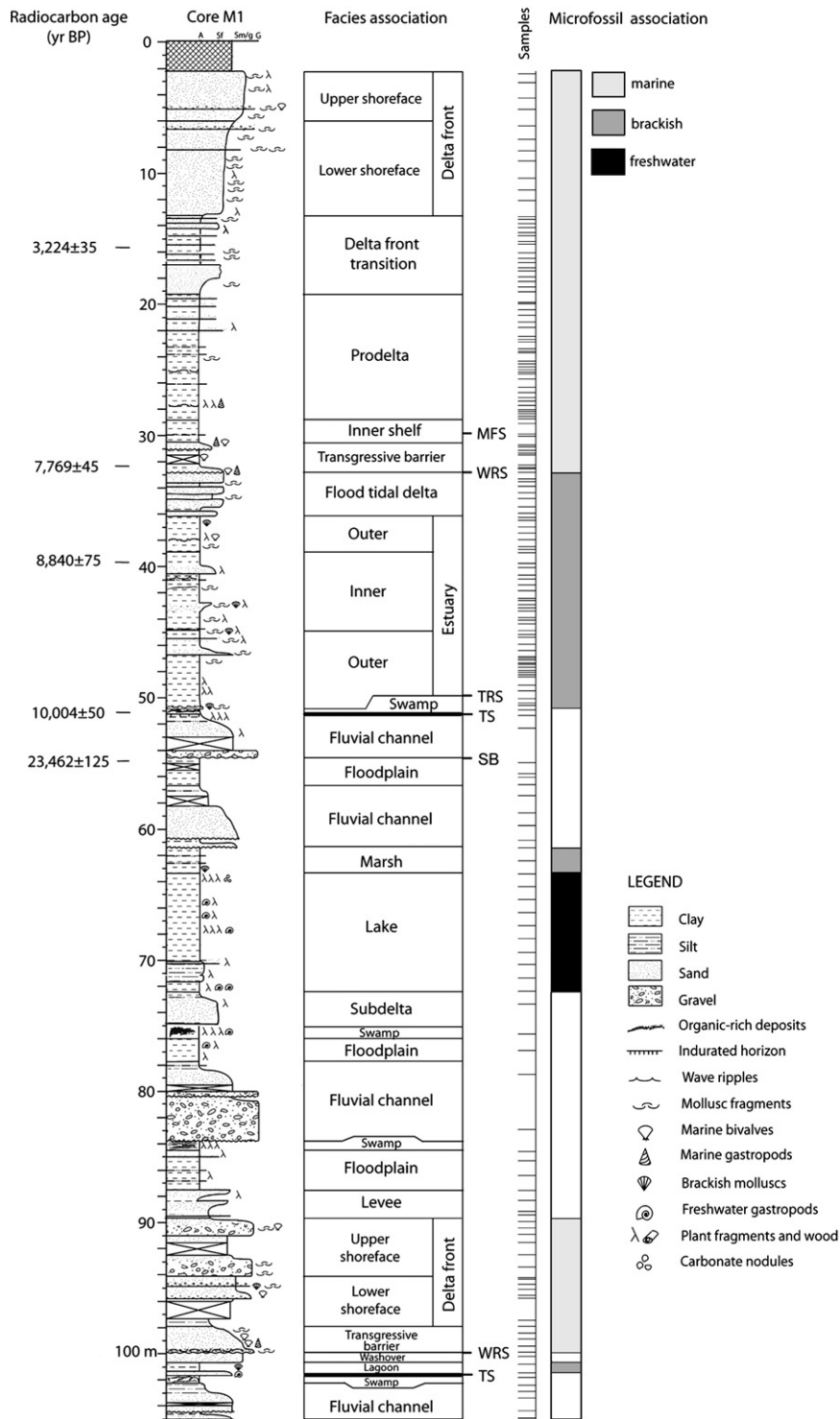


Fig. 2. Stratigraphic column of Core M1, inferred depositional environments, and general micropalaeontological divisions. TS: transgressive surface; TRS: tidal ravinement surface; WRS: wave ravinement surface; MFS: maximum flooding surface; SB: sequence boundary.

ostracods was based on the original microfossil descriptions, and a series of key papers (Bonaduce et al., 1975; Jorissen, 1988; Athersuch et al., 1989; Albani and Serandrei Barbero, 1990; Henderson, 1990; Cimerman and Langer, 1991; Sgarrella and Moncharmont Zei, 1993; Fiorini and Vaiani, 2001). Ecological information on species and palaeoenvironmental significance of assemblages are mainly provided by Blanc-Vernet (1969), Bonaduce et al. (1975), Jorissen (1987), Murray (1991), Pugliese and Stanley (1991), Yassini and Jones (1995), Debenay et al. (2000), Ruiz et al. (2000), Donnici and Serandrei Barbero (2002), Smith and Horne (2002), Amorosi et al. (2004) and Carboni et al. (2004).

Eighty-nine samples were analyzed for pollen. Sediment samples were dried and treated with HCl (20%), HF (40%) and NaOH (10%). Pollen concentration was calculated by addition of tablets with a known number of *Lycopodium* spores to a specific weight of sediment (Stockmarr, 1971). An average of 300 pollen grains per sample was counted. Only the synthetic pollen diagrams are shown, in which the pollen sum includes all pollens with the exception of aquatics. Arboreal pollen types (AP) are split into four classes: i) *Pinus*; ii) mixed deciduous oak-wood, including mesophilous and thermophilous trees living in warm and humid climates, such as *Quercus*, *Corylus*, *Carpinus betulus*, *Ostrya*, *Fraxinus*, *Hedera*, *Tilia*, *Ulmus*, *Acer*, *Betula*, and *Alnus*; iii) mountain taxa (*Abies*, *Picea* and *Fagus*), living at present at altitudes > 1500 m, and iv) Mediterranean taxa, living in Mediterranean climates characterized by high summer drought and including sclerophyllous and evergreen trees/shrubs, such as *Quercus ilex*, *Erica arborea*, *Phillyrea* type, *Pistacia* and *Olea*. Similarly, non-arboreal types (NAP) are subdivided in three classes: 1) steppic shrubs and herbs (*Artemisia*, Chenopodiaceae, *Ephedra*, *Hippophae*) withstanding cold and dry conditions; 2) Poaceae and 3) ubiquitous, represented by all other herbs without any particular ecological demand. The aquatics are represented by hygro-hydrophyte plants growing in humid environments, such as *Sparganium* type, *Typha*, *Myriophyllum* and Cyperaceae.

4. Sedimentology and micropalaeontology of core M1

Core M1 (Fig. 2) was drilled in the car park of a bathing establishment close to the present shoreline. The uppermost 2 m are of anthropogenic origin. The succession can be divided into a series of twenty-six depositional units, the sedimentological and micropalaeontological (foraminifers, ostracods, pollen) characteristics of which are described in descending order.

4.1. 2.10–13.15 m: delta front facies association

The upper part of this facies association, between 2.10 and 6.00 m core depth, consists of well sorted, medium to coarse sand, with scattered pebbles. This shows a gradation into the underlying fine to medium sand, with local silty sand intercalations. Wood fragments and plant debris are abundant, and shell material is widespread throughout this unit. Poorly preserved foraminifers (*Ammonia*, *Elphidium* and Miliolidae) and ostracods (*Pontocythere turbida* and *Loxoconcha turbida*) are locally observed within this facies association. No pollen were found in this interval.

On the basis of its stratigraphic position and morphological features of the present coastal plain, this facies association is attributed to the delta front of a prograding wave-dominated delta system. The coarser part is interpreted to reflect upper shoreface deposits, whereas the underlying finer-grained deposits are attributed to the lower shoreface. The presence of few microfossils within this facies association, characteristic of littoral environments, is consistent with this interpretation, and suggests transport under high-energy conditions.

4.2. 13.15–19.15: prodelta–delta front transition facies association

This facies association includes a rhythmic alternation of silty clay and very fine, sharp-based sand layers. A 2 m thick sand body is recorded between 17 and 19 m core depth. Shell material and wood fragments are abundant. The silty clays include a foraminiferal assemblage dominated by *Ammonia tepida* and *A. parkinsoniana* (46–73%), with common *Criboelphidium* spp. (mainly *C. granosum* and *C. poeyanum*). *L. turbida* with subordinate *P. turbida*, *Carinocythereis whitei* and *Leptocythere* spp. characterize the ostracod fauna (Fig. 3). Microfauna is scarce within the sandy deposits, with rare and poorly preserved foraminifers, similar to the fauna recorded in the overlying unit. A ^{14}C age of 3224 ± 35 yr BP was obtained at 15.75 m core depth (Fig. 2).

High percentages of arboreal pollen (AP about 65%), with mixed deciduous oak-wood, *Pinus* and Mediterranean taxa, characterize this interval (Fig. 4). Also significant is the relative abundance of cultivated trees (such as *Olea* and *Castanea*).

This facies association is interpreted to reflect the gradual transition from a prodelta to a delta front, occurring during a period of intense human activity. The microfauna is diagnostic of a shallow-marine environment with strong influence by fluvial discharge. The sharp-based sand layers are interpreted as the result of flood events.

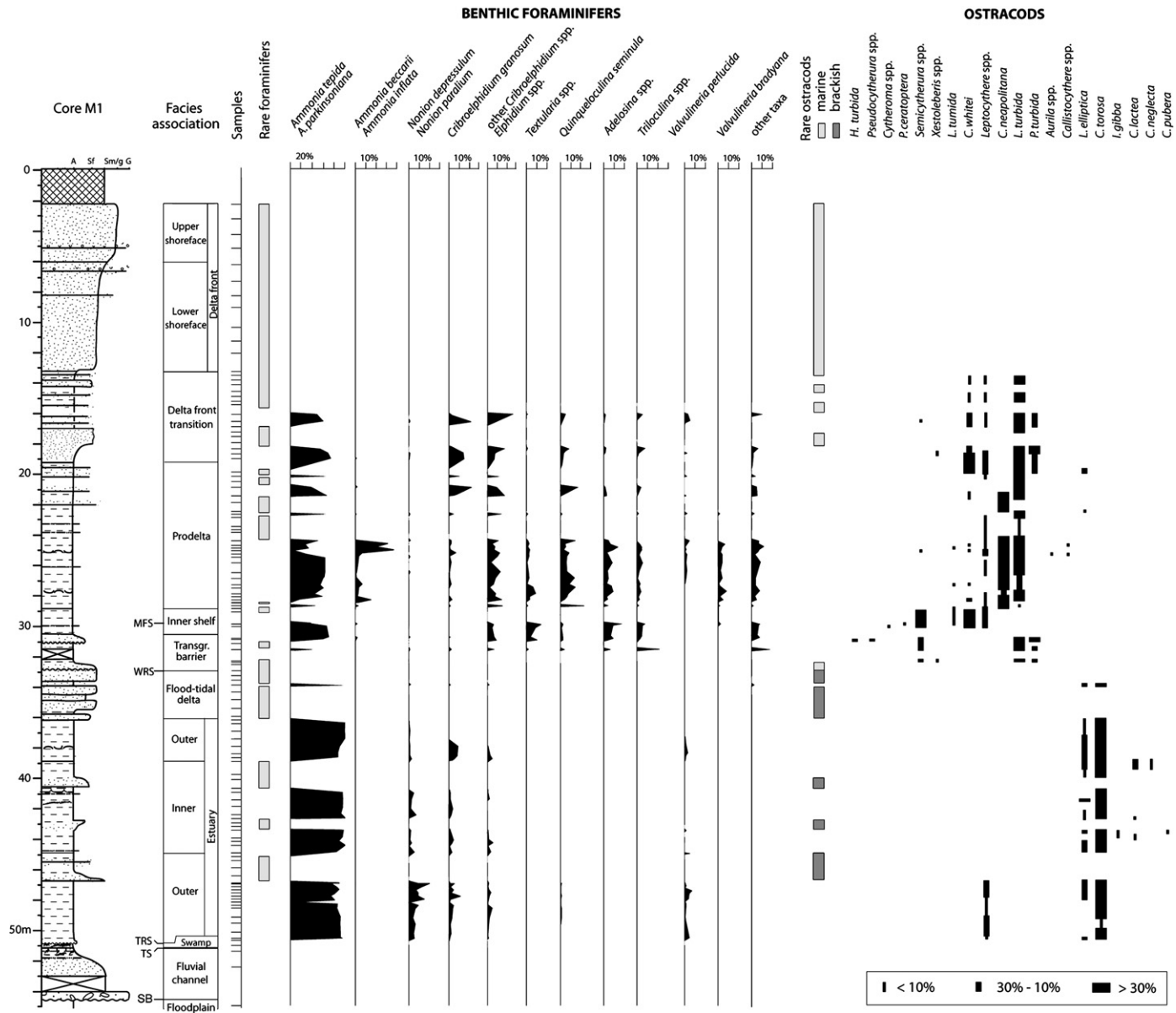


Fig. 3. Distribution of benthic foraminifers and ostracods in the upper 50 m of core M1. TS: transgressive surface; TRS: tidal ravinement surface; WRS: wave ravinement surface; MFS: maximum flooding surface; SB: sequence boundary.

4.3. 19.15–28.90 m: prodelta facies association

This facies association differs from the overlying deposits by the generally lower sand/mud ratio, which increases from bottom to top of the interval, and the lower amount of shells and wood fragments. The foraminiferal assemblage is characterized by the dominance of *A. tepida* and *A. parkinsoniana* (30–70%), with subordinate *Criboelphidium* and *Quinqueloculina seminulum* (Fig. 3). Relatively high frequencies of *Adelosina* spp., *Ammonia beccarii*, *Ammonia inflata*, *Textularia* spp. and *Valvulineria bradyana* are observed in the lower part of this interval, below 24 m core depth. Quantitative palaeontological data are not available for several sand-rich samples from the upper part of this facies association, for which less than 300 foraminiferal tests were observed. The ostracod assemblage includes mainly *Cytheridea neapolitana* and *L. turbida*, with local high concentrations of *P. turbida* and *C. whitei*.

Pollen data record a progressive downward increase in AP percentages, reaching about 85% (Fig. 4). In the uppermost part, forests were characterized by a mixed sclerophyllous (Mediterranean taxa) and deciduous broadleaved vegetation typical of a subMediterranean climate, with irregular and short summer drought (Jalut et al., 2000). Starting at 25–26 m depth, particularly significant is the relative abundance (about 20% on average) of mountain taxa, whose components (mainly *Abies* and *Fagus*) grow only under high humidity conditions.

This facies association represents a prodelta environment developed during an interglacial period. The microfauna consists of shallow-marine foraminifers and ostracods commonly observed in recent Mediterranean deltas (e.g. Colalongo, 1969; Jorissen, 1988; Bellotti et al., 1994a); the abundance of the euryhaline foraminifers *A. tepida* and *A. parkinsoniana* reflects a significant fluvial influence. Upward increase in sand/mud ratio and decreasing amounts of *Adelosina*, *Valvulineria* and *Textularia* suggest increasing freshwater influx with the progressive approach to the fluvial mouth.

4.4. 28.90–30.50 m: inner-shelf facies association

This facies association is characterized by a homogeneous succession of bioturbated silty clay. Apart from a general abundance of *Ammonia*, this interval records the highest specific diversity of both foraminifers and ostracods, and is characterized by the highest percentages of *Adelosina*, *Triloculina* and *Textularia* (Fig. 3).

These are coupled with low frequencies of *Q. seminulum* and *Criboelphidium* spp. The ostracod assemblage is dominated by *Semicytherura* spp. and *Carinocytherei whitei*, with subordinate *Leptocythere* spp., *L. tumida*, *Cytheroma* spp., and *Pterygocythereis ceratoptera*.

This interval records the highest percentages of AP (about 90%) and a significant increase in total pollen concentration (Fig. 4).

The microfauna observed in this facies association is typical of a relatively open-marine environment, with scarce fluvial influence, and is here interpreted as an inner-shelf, slightly below the wave base level. Pollen data point to a phase of maximum forest cover under interglacial climate conditions.

4.5. 30.50–32.95 m: transgressive barrier facies association

This facies association displays a typical fining-upward tendency, from fine sand to silty sand, with local intercalations of silty clays. This unit displays an erosional lower boundary, marked by a veneer of mollusc shells. The microfauna consists in the lower part of poorly preserved ostracods (*Aurila* and *Loxoconcha*) and foraminifers (*Elphidium* and *Ammonia*), passing upwards to a foraminiferal association similar to that described for the inner-shelf facies association, except for the lower abundance of *Textularia* (Fig. 3). The ostracods include *L. turbida*, *P. turbida* and *Semicytherura* spp. In the uppermost part of the unit *Hiltermannocythere turbida* and *Pseudocytherura* spp. have been observed.

Pollen samples from this facies association, collected within two fine-grained intercalations, show a similar proportion of AP groups relative to the overlying unit (Fig. 4). A remarkable peak of Poaceae is recorded in the lowermost sample, paralleled by high values of aquatics and total pollen concentration. A silt intercalation at 32.30 m core depth yielded a ^{14}C age of 7769 ± 45 yr BP (Fig. 2).

This facies association formed in a high-energy, coastal environment. The basal erosion surface is interpreted as a wave ravinement surface (WRS in Fig. 2) (Swift, 1968; Nummedal and Swift, 1987). This unit, as a whole, has been interpreted as a transgressive sand sheet, reflecting the landward migration of a barrier during the Holocene transgression. The fining-upward trend and the microfauna suggest rapid transition to relatively deeper water environments. Pollen characteristics of the lowest sample suggest an environmental control on the pollen association, possibly related to proximity to marsh environments.

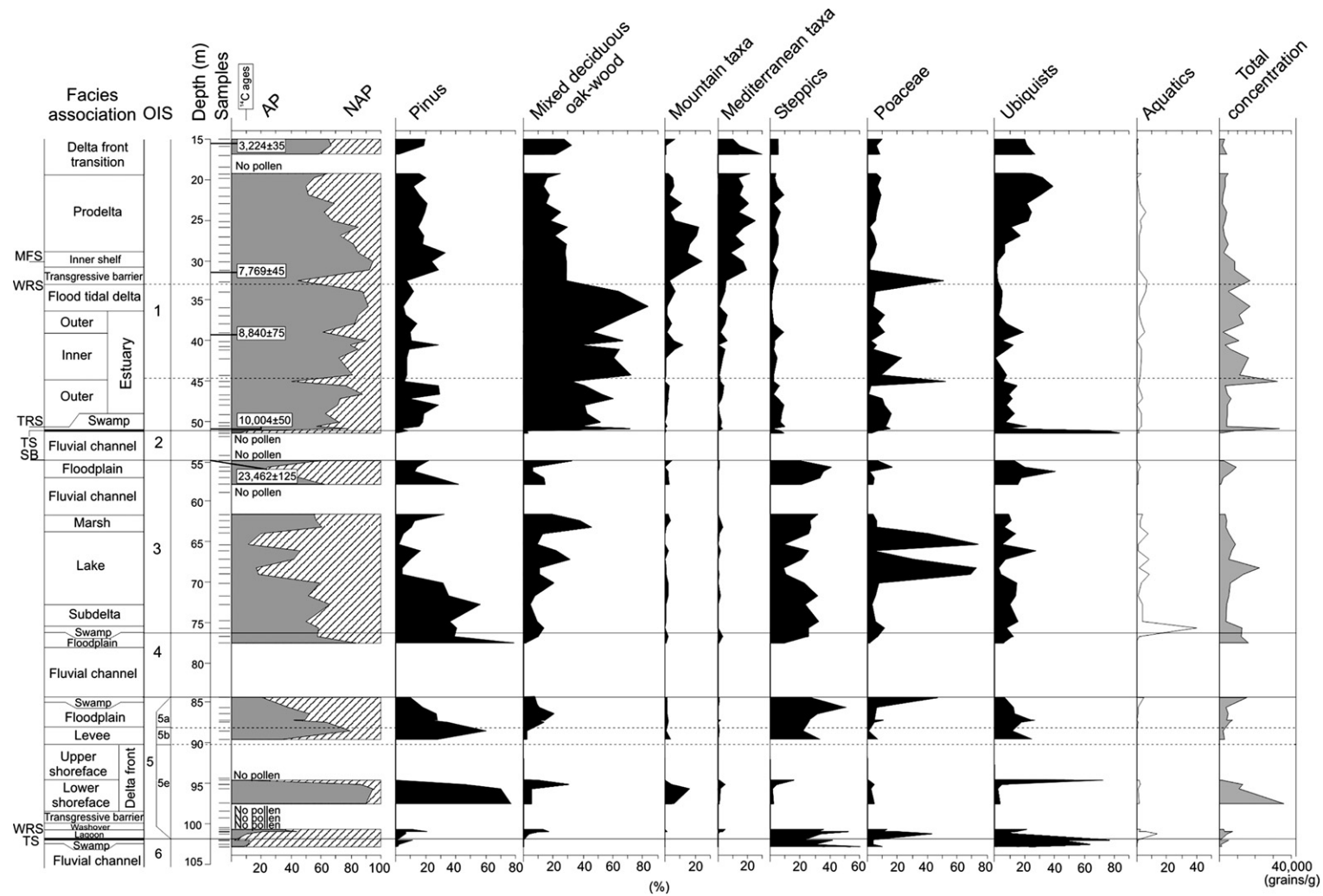


Fig. 4. Synthetic pollen and total concentration diagrams of core M1. Facies associations, oxygen-isotope stages and ^{14}C ages are indicated. Dotted lines mark minor divisions based on pollen spectra. AP, arboreal pollen; NAP, non-arboreal pollen. For main composition of pollen groups, see text.

4.6. 32.95–36.10 m: flood tidal delta facies association

This facies association consists of alternating silty sand and fine-grained to medium sand layers, a few dm thick. Small fragments of mollusc shells are present. A rare, poorly preserved microfauna, consisting of *A. tepida*, *A. parkinsoniana*, *Brizalina* spp., *Bulimina* spp. and *Cyprideis torosa*, characterizes the sand layers (Fig. 3); a well preserved microfauna composed almost entirely of *A. tepida* and *A. parkinsoniana* (95% of the foraminiferal assemblage), in association with brackish ostracods *C. torosa* and *Loxoconcha elliptica*, was observed in a silt intercalation at 33.85 m core depth. Very high pollen concentration values and maximum percentages (85%) of mixed deciduous oak-wood are recorded within this interval (Fig. 4).

The diagnostic microfauna of this facies association, showing the co-existence of brackish/euryhaline (*A. tepida*, *A. parkinsoniana*, *C. torosa*, *L. elliptica*) and open-marine (*Brizalina* spp., *Bulimina* spp.) taxa, suggest that deposition of this unit took place in a brackish-water environment, with local input of sediment material of marine origin. In view of the textural features and the stratigraphic relationships with the overlying and underlying units, this facies association is interpreted as a flood tidal delta, i.e. a sedimentary body located in the back-barrier area behind a tidal inlet. Maximum development of the mesophilous forest suggests a stable warm-temperate climate.

4.7. 36.10–50.90 m: estuary facies association

This facies association includes a thick, homogeneous succession of dark grey silty clay. Sand layers, displaying both fining-upward and coarsening-upward tendencies and wave ripples at their tops, are commonly encountered between about 39 and 47 m core depth. Wood and shell fragments are also scattered throughout this interval. A 5 cm-thick layer, entirely made up of mollusc shells, with abundant *Cerastoderma glaucum*, is present at the base of this facies association.

The foraminiferal assemblage consists almost entirely of *A. tepida* and *A. parkinsoniana* (about 80–100%), with local occurrences (up to 20%) of *Haynesina depressula* (Fig. 3). Among the ostracods *C. torosa* is the dominant species, with subordinate *L. elliptica*. Changes in the proportion of foraminiferal and ostracod specimens allow subdivision of this facies association into three intervals (Fig. 2): ostracods are more abundant than foraminifers between 39 and 45 m core depth, where mesohaline to freshwater ostracod species (*Candona lactea*, *C. neglecta*, *Cypris pubera* and *Ilyo-*

cypris gibba) are recorded. A reverse proportion of these taxa is recorded above and below this interval.

With regard to pollen data, this interval can be subdivided into two parts (Fig. 4): similar to the overlying facies association, the upper interval is characterized down to the depth of about 45 m by a dominance of mixed deciduous oak-wood and low values of the other arboreal groups. In the lower interval, the relative proportion of *Pinus* increases significantly, while total pollen concentration decreases. A sample at 39.40 m core depth yielded a ^{14}C age of 8840 ± 75 yr BP (Fig. 2).

The sedimentological features, combined with the very low microfaunal diversity and the presence of dominant brackish assemblages suggest that deposition of this facies association took place within a wave-dominated estuary (“central basin deposits” of Dalrymple et al., 1992), in which two distinct subenvironments can be identified. The lower and upper intervals, showing maximum foraminiferal abundance, are interpreted to reflect an outer estuary environment. By contrast, the ostracod-rich stratigraphic interval including mesohaline to freshwater species, which displays a significantly stronger fluvial influence, is interpreted as an inner estuary deposit. The basal shell layer, with a characteristic brackish fauna, is interpreted as a transgressive lag, representing the initial stage of the estuarine transgression, and corresponds to the tidal ravinement surface (TRS in Fig. 2) of Allen and Posamentier (1993) and Zaitlin et al. (1994), or the bay ravinement surface of Nummedal and Swift (1987) and Foyle and Oertel (1997).

Pollen data from the lower part of this facies association indicate a scattered warm-temperate forest vegetation, with significant occurrence of drought-tolerant trees (*Pinus*), growing under early interglacial climate conditions. Subsequently, a mixed deciduous mesophilous forest was established.

4.8. 50.90–51.20 m: swamp facies association

This facies association is composed of a few dm-thick grey clay beds with abundant organic material. No microfauna was observed within this interval.

A ^{14}C age of $10,004 \pm 50$ yr BP was obtained close to the base of this facies association, at 51.15 m core depth (Fig. 2).

The pollen spectrum available for this interval displays a remarkable peak in total pollen concentration and high values of AP (80%), mainly represented by mixed deciduous oak-wood taxa (Fig. 4).

This facies association is interpreted as a freshwater swamp deposit that formed at the onset of the Holocene transgression, and could represent the initial expression

of a transgressive phase (TS in Fig. 2). Pollen characteristics support this interpretation, indicating well-developed forest vegetation typical of interglacial climate conditions.

4.9. 51.20–54.60 m: fluvial-channel facies association

This facies association consists of gravelly sand, sand and dark brown sandy silt, with a distinctive fining-upward trend and a sharp erosional lower boundary. An overconsolidated, dark horizon, approximately 50 cm thick, caps the succession. No microfossils are present in this interval.

Pollen are very scarce or absent throughout this unit. Pollen analysis of two samples collected within the stiff deposits at top of this facies association, between 51.40 and 51.20 m core depth, showed dominance of a single herbaceous taxon (Asteraceae, belonging to ubiquists), with parallel very low AP values (Fig. 4).

This facies association is interpreted as fluvial-channel sediments, discharged by the ancient Arno River, and formed during a cold climatic period. The fining-upward trend is interpreted to mark the progressive channel abandonment, with subsequent soil development on top. The unusual pollen spectrum recorded close to the top of the facies association, including grains that are very resistant to oxidation and corrosion (Bottema, 1975), is consistent with its interpretation as a palaeosol. In this case, the high dominance of Asteraceae should be interpreted as due to differential pollen preservation and has no value as open vegetation indicator (Havinga, 1984).

4.10. 54.60–56.70 m: floodplain facies association

This facies association consists of a monotonous succession of silty clay. No microfossils are present, with the exception of scattered, poorly preserved ostracods.

Despite the general low pollen content, a vegetation association dominated by NAP, with scattered trees of mixed deciduous oak-wood and *Pinus*, is observed (Fig. 4). Of note, are the very high values of steppics.

A ^{14}C age of $23,462 \pm 125$ yr BP was obtained from a sample at 54.95 m core depth (Fig. 2).

This facies association has been attributed to a floodplain environment. The characteristic pollen spectrum indicates the development of open vegetation typical of cold and arid climate conditions.

4.11. 56.70–61.40 m: fluvial-channel facies association

This facies association shows a distinctive fining-upward trend from coarse to fine sand, with an erosional

lower boundary. No microfauna was observed within this interval.

Samples from this interval are very poor in pollen and display an association similar to that recorded in the overlying deposits (Fig. 4).

Similarly to the stratigraphic interval between 50.90 m and 54.60 m core depth, this facies association is interpreted to represent a fluvial-channel deposit.

4.12. 61.40–63.30 m: marsh facies association

This facies association is composed of grey clay, with a few silt intercalations in the uppermost 60 cm. The microfauna records the occurrence throughout this interval of an ostracod assemblage dominated by *C. torosa*, with rare *Leptocythere lagunae* (Fig. 2).

The pollen spectra show relatively high values of mixed deciduous oak-wood (about 40% in average), and a consequent reduction of NAP (Fig. 4).

These deposits, characterized by a typical brackish microfauna, are inferred to have formed in a brackish-water environment, such as a marsh, in close proximity to a marine environment (bay or estuary). Pollen data suggest a moderate expansion of mesophilous forests within an open vegetation landscape, indicating a slightly warmer and more humid climate.

4.13. 63.30–72.40 m: lake facies association

This facies association includes a thick, homogeneous succession of clays. Horizontal lamination with laminae of different colours (from yellowish grey to light grey, dark grey and black) is common. The darker colours are due to the abundance of organic material. A considerable concentration of freshwater molluscs was observed. The microfauna of this interval consists uniquely of rare oligohaline to freshwater ostracods, such as *C. lactea*, *C. neglecta* and *Cyclocypris* spp. (Fig. 2).

Pollen data display very high values of Poaceae and moderate percentages of mixed deciduous oak-wood, decreasing downward (Fig. 4). A significant occurrence of aquatics is recorded throughout this interval.

The laminated clays are believed to reflect a lake deposit. Lack of connection with the open sea is supported by the diagnostic fossil content. The anomalously high values of Poaceae and aquatics are an additional, obvious indication of humid environment.

4.14. 72.40–74.80 m: subdelta facies association

This facies associations consists of silty clay and fine to medium sand. No microfossils are present in this

interval and no samples were found suitable for pollen analysis.

In view of the stratigraphic relationships with the overlying and underlying units (see next section), this facies association is presumed to reflect a sub-delta deposit, formed at the boundary between a wet coastal plain and an alluvial plain. This sand body could be linked to overflow events of either a river or a distributary channel into an enclosed freshwater terrestrial area.

4.15. 74.80–76.20 m: *swamp facies association*

This facies association is composed of grey and dark grey clay, with rare silt layers. *Planorbis* molluscs and carbonized wood fragments are abundant. Dark laminae, due to concentration of organic material, are common.

The pollen association is characterized by high values of NAP, mainly steppics and Poaceae, and low values of AP (Fig. 4). *Pinus* is the most significant tree and the aquatics show a remarkable peak (about 40%).

The sedimentological characteristics suggest that this facies association formed in a quiet, freshwater paludal environment. This interpretation is strongly supported by the anomalously high values of aquatics.

4.16. 76.20–77.70 m: *floodplain facies association*

This facies association is made up of grey silty clay, with plant debris and rare terrestrial gastropods (*Helix*). No microfossils were found within this interval.

Pollen analysis shows considerably high percentages of *Pinus* and lack of aquatics (Fig. 4).

This facies association is interpreted to represent the finest portion of deposits which settle in the alluvial plain and are afterwards exposed to subaerial processes. Lack of aquatic plants indicates the occurrence of dry paleoenvironmental conditions.

4.17. 77.70–83.90 m: *fluvial-channel facies association*

This facies association consists of sandy gravel, grey sand and silty sand, with a distinctive fining-upward trend and a sharp erosional lower boundary. No microfossils are present in this interval. This facies association yielded no samples suitable for pollen analysis.

These deposits are interpreted as fluvial-channel sediments, discharged by the palaeo-Arno river possibly during a cold period.

4.18. 83.90–84.50 m: *swamp facies association*

These sediments consist of brown peaty clay with abundant wood fragments and plant debris. Small freshwater gastropods (*Bithynia*, *Planorbis*) are present. No microfauna was found in this interval.

This unit displays a high content of pollen with dominant Poaceae and significant percentages of aquatics (Fig. 4).

This association appears to have been deposited in a humid, terrestrial environment, such as a swamp.

4.19. 84.50–87.70 m: *floodplain facies association*

This facies association includes grey silty clay, with plant debris and rare terrestrial gastropods. No microfauna was found in this interval.

Pollen of NAP dominate this interval, while AP are represented by remarkable values of mixed deciduous oak-wood (reaching a maximum of 22%) and *Pinus* (Fig. 4).

This facies association reflects a floodplain environment developed during a moderately warm and humid period.

4.20. 87.70–89.40 m: *levee facies association*

This facies association shows a sharp lower boundary with the underlying facies association, and consists of a rhythmic alternation of silty clay and fine to medium sand layers. Plant debris is present. The clay intercalations contain calcareous nodules. No microfauna was found in this interval.

Pollen samples are characterized by high percentages of *Pinus*, an abundance of NAP, and very scarce occurrence of mixed deciduous oak-wood and low total pollen concentration (Fig. 4).

This facies association formed in a terrestrial environment, probably as an overbank deposit on a levee. The pollen spectrum suggests the development of open vegetation with scattered trees and shrubs, typical of cold climate conditions.

4.21. 89.40–97.90 m: *delta front facies association*

This facies association is dominated by coarse to medium sand, with abundant shell material, grading upward into gravelly sand. Wood fragments are present throughout this interval. Rare and poorly preserved foraminifers (*Ammonia*, *Elphidium*, Miliolidae) and ostracods (*Aurila*, *Loxoconcha* and *P. turbida*) have been observed (Fig. 2).

The available pollen spectra show very high mean values of *Pinus* (60%), a considerable amount of mixed deciduous oak-wood (30% in the uppermost sample), mountain and Mediterranean taxa, and very low NAP values (Fig. 4).

This facies association is interpreted to reflect a shallowing-upward succession within a high-energy, delta-front environment, with sandy lower shoreface deposits grading upward into gravel rich, upper shoreface deposits.

The pollen association and the high total pollen concentration are indicative of a dense, mixed evergreen and deciduous forest vegetation, indicating a cool-temperate climate. A superposed environmental control on pollen association is suggested by the extremely high percentages of *Pinus*, as the result of selective preservation of pollen grains within these beach deposits.

4.22. 97.90–100.00 m: transgressive barrier facies association

This facies association includes fine to medium sand with an erosional lower boundary and a remarkable abundance of shell materials. The microfauna is very similar to that from the above interval. No pollen have been found in this interval.

This unit is interpreted to reflect a transgressive sand sheet due to the landward migration of a transgressive barrier. The erosional lower boundary corresponds to the wave ravinement surface (WRS in Fig. 2).

4.23. 100.00–100.85 m: washover facies association

This facies association consists of fine to medium sands, with rare small fragments of mollusc shells. No microfauna was found in this interval.

Total pollen concentration is low (Fig. 4). Although NAP are predominant, moderate amounts of mixed deciduous oak-wood and Mediterranean taxa also characterize this interval.

Given the stratigraphic relationships with the adjacent units, this facies association is interpreted to have formed in a back-barrier environment. Particularly, this deposit could have accumulated on the landward side of a beach-barrier, due to barrier overstepping by storm processes (washover sand). The low total pollen concentration is consistent with such a peculiar depositional environment.

4.24. 100.85–101.70 m: lagoon facies association

This facies association includes a sandy layer with a characteristic brackish-water mollusc fauna (*C. glau-*

cum); this is overlain by peaty silty clay with shell material and carbonized wood fragments. A typical brackish microfauna is recorded in the fine-grained deposits of this interval (Fig. 2). The foraminiferal assemblage is dominated by *A. tepida* and *A. parkinsoniana*, while the ostracod association is mainly composed of *C. torosa*.

The pollen association is dominated by NAP (mostly Poaceae and steppics) and shows increasing-upward values of mixed deciduous oak-wood (Fig. 4). The abundance of aquatics is significantly high.

The lower boundary of this facies association represents the initial phase of a marine incursion and corresponds to the transgressive surface (TS in Fig. 2). The sedimentological and micropalaeontological features of this facies association are typical of a brackish lagoon environment. Pollen spectra suggest that sedimentation took place during a transitional phase of reforestation under warming climate conditions. The abundance of aquatics indicates the local presence of stagnant waters.

4.25. 101.70–102.20 m: swamp facies association

This facies association consists of dark sandy clay, with abundant wood fragments and plant debris. No microfossils are present in this interval.

Pollen data record very high amounts of NAP (90%), while AP display low values, with very low quantities of *Pinus* and abundant aquatics (Fig. 4).

This facies association is typical of an enclosed wet terrestrial environment, such as a swamp. The characteristic pollen association is indicative of a steppe environment developed under very cold and arid climate conditions.

4.26. 102.20–105.00 m: fluvial-channel facies association

This facies association consists of fine to medium sands, with a distinctive fining-upward trend. No microfauna was recorded in this interval.

The pollen spectrum available records the highest values of NAP (98%) of the whole succession and a very low pollen concentration (Fig. 4).

This facies association is interpreted as fluvial-channel sediments discharged by the palaeo-Arno river during a cold and arid phase. This is documented by pollen data, suggesting the presence of scattered vegetation, characterized mainly by steppic herbs.

5. Palaeoenvironmental and climatic evolution

The vertical stacking pattern of facies observed in core M1 shows that the Late Quaternary succession of the Arno coastal plain consists of a repeated alternation

of coastal and alluvial deposits (Fig. 2). The two major transgressive surfaces (TSs) detected at about 51 and 102 m core depth, respectively, appear as the two most valuable stratigraphic markers in the core. These may enable a pragmatic subdivision of the stratigraphic succession into two vertically stacked transgressive–regressive (T–R) sequences (sensu Embry, 1993, 1995), of Holocene and Late Pleistocene age, respectively. A minor transgression surface could be represented by the lower boundary of swamp deposits resting on floodplain deposits at 76 m core depth.

Sediments deposited in brackish-water environments directly overlie the TSs, which are generally developed on top of alluvial sediments. These early transgressive deposits are overlain by nearshore and shallow-marine sediments (late transgressive+highstand). The upper parts of T–R sequences show an upward transition to continental deposits, formed during periods of sea-level fall and subsequent sea-level lowstand.

Similar to recent observations by Amorosi and Colalongo (2005) from the Late Quaternary deposits of the Po Plain, in Northern Italy, transgressive sediments above the TSs carry a distinctive pollen signature, corresponding to: i) maximum expansion of forest vegetation (AP), ii) abrupt decrease in non-arboreal pollen (NAP), and iii) major peaks in total pollen concentration (Fig. 4). These characteristics point to an obvious relationship between transgressive episodes and the onset of warm (interglacial) phases. By contrast, alluvial plain deposits beneath the TSs show pollen assemblages dominated by open vegetation communities (NAP) and significantly lower concentration values, which are typical of glacial periods.

Given the uncertain age attribution of the lower T–R sequence, for which no absolute age data are available, we will discuss our core data from top to bottom.

5.1. The upper T–R sequence (OIS 1)

The upper TS identified at about 51 m core depth records the onset of the Holocene transgression (Fig. 2), as inferred from five radiocarbon dates. Of particular interest is the remarkable thickness (about 20 m) of early transgressive, brackish-water facies between the tidal ravinement surface (TRS) and the wave ravinement surface (WRS), suggesting that sedimentation between 10 and 7.8 kyr BP took place within a wave-dominated estuary (Dalrymple et al., 1992; Nichol et al., 1994). This interpretation is consistent with recent work from a more landward location in the Arno coastal plain, showing the presence of an incised-valley fill, about 25 m thick, roughly perpendicular to the present shore-

line and corresponding to the modern Arno River course (Fig. 5). Away from the valley axis, the Holocene succession is less than 20 m thick and overlies an indurated and weathered palaeosurface. This surface, corresponding to an interfluvial sequence boundary (Van Wagoner et al., 1990; Aitken and Flint, 1996; McCarthy and Flint, 1998), was formed during the last glacial period and was transgressed by brackish waters around 7.8 kyr BP (see core M3 in Fig. 5).

The thick estuarine complex observed in core M1 thus appears to constitute the SW prolongation of the incised-valley (see Fig. 1). A similar estuary infilling by clayey sediments during the last transgression has been reported from several incised-valley systems (Hori et al., 2001; Ta et al., 2001; Boski et al., 2002; Li et al., 2002).

The transgressive barrier sands dated to about 7800 yr BP document the rapid landward migration of a beach-barrier system during the late stage of transgression. These sands, in turn, are overlain by thin inner-shelf clays, indicating rapidly increasing water depth. The maximum flooding surface, identified at 29.85 m core depth within lithologically homogeneous inner-shelf deposits (Fig. 2), was recognized on the basis of subtle micropalaeontological evidence (Fig. 3), such as the highest percentages of *Textularia* (17%) and *Adelosina* (18%), associated with relatively low contents of *A. tepida* and *A. parkinsoniana* (see also Fiorini and Vaiani, 2001; Amorosi and Colalongo, 2005).

Late transgressive marine sediments are significantly thinner (3 m) than the overlying highstand succession of prograding deltaic deposits, which attains a total thickness of 30 m. This asymmetry is characteristic of the Holocene transgressive–regressive sedimentary wedges described from the major coastal plains all around the world (see review in Amorosi and Milli, 2001).

Detailed pollen analysis enables the reconstruction of a three-fold palaeoclimatic evolution for the Holocene of core M1, documenting a direct relationship between vertical facies patterns and vegetation history (Fig. 4). The first phase, marking the transition from glacial to interglacial conditions, was characterized by the abrupt spread of a mixed deciduous oak-wood, which took place in response to a pronounced phase of climate warming at the beginning of the Holocene. This remarkable change in climatic conditions was paralleled by the onset of transgressive sedimentation within the incised-valley, showing transition from fluvial to paludal, and then outer-estuarine deposits (see also Zaitlin et al., 1994; Hori et al., 2002). Similar to other pollen sequences of the Mediterranean area (Pérez-Obiol and Julià, 1994; Nicol-Pichard and

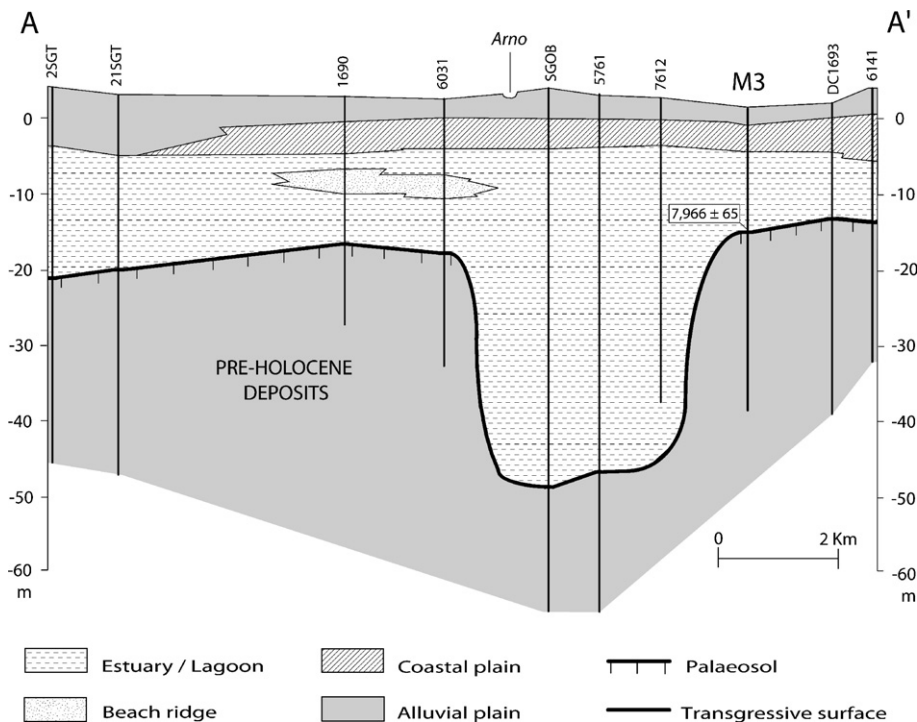


Fig. 5. Cross-section showing the geometry of the Holocene Arno incised-valley fill, 10 km NE of core M1. For detailed facies description of core M3, see Aguzzi (2006). For section trace, see Fig. 1.

Dubar, 1998; Carrión and Van Geel, 1999), early Holocene vegetation is associated with the presence of drought-tolerant *Pinus* woodland (Fig. 4). Although masked by a peak in Poaceae, which probably reflects proximity to a paludal environment, the first vegetation phase terminates at 45 m core depth with a small, but significant decline of temperate trees. This is accompanied by a slight “regressive” tendency within the incised-valley, recorded in the core by rapid transition from an outer-to inner-estuarine environment.

During the second phase, extending up to about 7800 yrs BP, *Pinus* woodland was largely replaced by the oak-wood, which shows a considerable expansion and culmination. This vegetation phase, suggesting a progressive increase in temperature and humidity, matches the progressive landward shift of the shoreline, shown by upward transition from inner estuary to outer estuary, and then flood tidal-delta deposits.

Maximum AP values, corresponding to the maximum development of trees and thus suggesting the most favourable temperature and humidity conditions, are recorded at the onset of marine sedimentation, within transgressive-barrier and inner-shelf deposits. After peak transgression, forest composition underwent an important change: the mixed deciduous oak-wood

declined and the Mediterranean and *Pinus* woodland spread. The development of the Mediterranean forest, mainly characterized by *Q. ilex*, represents a significant palaeovegetation event recorded in many Italian sites, such as Valle di Castiglione (Follieri et al., 1988), Lago di Vico (Magri and Sadori, 1999), Lagaccione (Magri, 1999), Ripasottile (Ricci Lucchi et al., 2000), and the Tyrrhenian Sea (Russo Ermolli and di Pasquale, 2002). This event suggests a change toward a more Mediterranean climate that persisted and probably increased its characteristic summer drought during the second half of the Holocene, when the Mediterranean vegetation became dominant and a progressive reduction in other forest components was recorded (mixed deciduous oak-wood and mountain taxa), parallel to an expansion of open vegetation.

5.2. The lower T–R sequence (OIS 5e-2)

No direct age attribution is available for the nearshore sands overlying the lower TS, at about 102 m core depth. Although additional chronological control must be obtained to constrain the exact timing of deposition of this unit, we are inclined to assign these sands to the last interglacial period, corresponding to the Tyrrhenian or

Eemian (Oxygen-Isotope Substage 5e — 128–116 kyr BP), in view of the absence of marine deposits between this interval and the Holocene sediments (Fig. 2). This attribution is consistent with data from the Enea core in the adjacent Versilia Plain (Fig. 1), which have provided an age of 129.2 and 132.8 kyr BP at about 69 m and 72 m core depth, respectively (Antonioli et al., 1999; Ferranti et al., 2006).

Pollen from the swamp and the fluvial deposits below the TS (102–105 m core depth) provide strong indication of glacial climate conditions (dominance of NAP and particularly steppics) corresponding to OIS 6 (Fig. 4). Pollen data within the lagoonal sediments just above the TS record a progressive increase of arboreal taxa, mainly deciduous oak-wood and Mediterranean, which can be related to the onset of the last interglacial (OIS 5e). This is followed by a no-pollen zone, coincident with the deposition of washovers and transgressive barrier sands, which likely records the maximum warming phase of the Eemian. Scattered pollen samples within the overlying, “regressive” lower-shoreface sediments indicate the presence of a dominant coniferous forest (characterized by *Pinus* and mountain taxa), with scarcity of mesophilous trees belonging to the oak-wood. This pollen association could be the result of the progressive cooling typical of the latest phase of the Eemian (Guiot et al., 1989; De Beaulieu and Reille, 1992; Zagwijn, 1996; Tzedakis et al., 2003; Preusser, 2004).

An abrupt facies change separates the Eemian marine deposits from the overlying alluvial sediments, suggesting the presence of a significant stratigraphic hiatus. Pollen data available for the levee deposits capping the delta front succession indicate open vegetation, characterized mainly by steppics and *Pinus*, which can be related to an early Weichselian stadial phase (possibly corresponding to OIS 5b). The pollen association recorded within the overlying floodplain and swamp deposits represents a significant expansion of mesophilous forest (mixed deciduous oak-wood) that can be associated with an interstadial phase (OIS 5a).

The alluvial (fluvial-channel and floodplain) deposits between about 76 and 84 m core depth have been assigned to OIS 4, in view of their stratigraphic position, sedimentological characteristics and pollen assemblage dominated by *Pinus*, which indicate the onset of glacial climate conditions. Accordingly, we assume that the overlying swamp, subdelta, lake and marsh deposits (61–76 m) were primarily formed during OIS 3, which implies that the minor transgressive surface at 76 m core depth marks the OIS 4/3 transition. This is, again, suggested by pollen data, which indicate the persistence

of a considerable mesophilous forest typical of interstadial climate conditions within an open vegetation landscape.

The two erosional surfaces marking the base of fluvial-channel deposits at 61.40 and 54.60 m core depth, respectively, are both potential candidates for the sequence boundary (SB), corresponding to the OIS 3/2 transition. On the basis of the radiocarbon date of 23.4 ka at about 55 m core depth, which would translate after calibration (Stuiver et al., 1998) into about 27.5 ka (late OIS 3), we are inclined to place the SB at the upper unconformable surface.

6. Conclusions

Through integrated sedimentological and micropalaeontological (foraminifer, ostracod and pollen) analyses of a 105-m-long core from western Tuscany, new insights were obtained into the response of this coastal system to combined sea-level and climate fluctuations during the last 150 kyr.

Two prominent intervals with marine sedimentation permit us to define two distinct transgressive–regressive (T–R) sequences, of Holocene and Late Pleistocene age, respectively. Stratigraphic correlation with the marine oxygen-isotope record on the basis of pollen data documents strict relationships between T–R sequences and interglacial/glacial cycles, which shows that transgressive surfaces correlate invariably with the onset of forested conditions during interglacials, whereas the return to alluvial sedimentation correlates with an abrupt change to open vegetation conditions during glacials. An attempt to delineate the palaeoenvironmental evolution of the study area in response to sea-level fluctuations and climate forcing resulted in the establishment of a well-resolved chronology for the studied succession, from OIS 6 to Present. The transgressive surfaces are much more readily identifiable surfaces than sequence boundaries.

This paper presents the first detailed facies documentation of an incised-valley sequence from the Late Quaternary of Italy. The Holocene succession is 51 m thick and includes about 20 m of early transgressive estuarine deposits above a tidal ravinement surface. These are capped by a wave ravinement surface, overlain by a thin succession of late transgressive barrier-beach and inner-shelf deposits. Highstand deposits above the maximum flooding surface are represented by a shallowing-upward succession of prodelta to delta-front sediments.

The detailed reconstruction of palaeoenvironmental evolution and vegetation changes in the Tuscan area

during the last 150 kyr may help significantly in refining our knowledge of sea-level fluctuations and climate changes in the Mediterranean area during the Late Quaternary.

Acknowledgements

This study was funded by the Bologna University as part of *Progetto Strategico d'Ateneo* (co-ordinator: A. Amorosi). We are grateful to M. Gibling and M.G. Carboni for their accurate reviews, and to C. Fielding and G.J. Weltje for the editorial advice.

References

- Aguzzi, M., 2006. Stratigrafia di sottosuolo di depositi tarsoquaternari del Valdarno inferiore (Toscana). PhD Thesis. University of Bologna.
- Aguzzi, M., Amorosi, A., Sarti, G., 2005. Stratigraphic architecture of Late Quaternary deposits in the lower Arno Plain (Tuscany, Italy). *Geol. Rom.* 38, 1–10.
- Aitken, J.F., Flint, S.S., 1996. Variable expressions of interfluvial sequence boundaries in the Breathitt Group (Pennsylvanian), eastern Kentucky, USA. In: Howell, J.A., Aitken, J.F. (Eds.), *High Resolution Sequence Stratigraphy: Innovations and Applications*. *Geol. Soc. London Spec. Publ.*, vol. 104, pp. 193–206.
- Albani, A., Serandrei Barbero, R., 1990. I Foraminiferi della Laguna e del Golfo di Venezia. *Mem. Sci. Geol.* 42, 271–341.
- Allen, G.P., Posamentier, H.W., 1993. Sequence stratigraphy and facies model of an incised valley fill: the Gironde Estuary, France. *J. Sediment. Petrol.* 63, 378–392.
- Amorosi, A., Colalongo, M.L., 2005. The linkage between alluvial and coeval nearshore marine successions: evidence from the Late Quaternary record of the Po River Plain, Italy. In: Blum, M.D., Marriott, S.B., Leclair, S.F. (Eds.), *Fluvial Sedimentology VII*. International Association of Sedimentologists Special Publ., vol. 35, pp. 257–275.
- Amorosi, A., Milli, S., 2001. Late Quaternary depositional architecture of Po and Tevere river deltas (Italy) and worldwide comparison with coeval deltaic successions. *Sediment. Geol.* 144, 357–375.
- Amorosi, A., Colalongo, M.L., Pasini, G., Preti, D., 1999a. Sedimentary response to Late Quaternary sea-level changes in the Romagna coastal plain (northern Italy). *Sedimentology* 46, 99–121.
- Amorosi, A., Colalongo, M.L., Fusco, F., Pasini, G., Fiorini, F., 1999b. Glacio-eustatic control of continental-shallow marine cyclicity from Late Quaternary deposits of the south-eastern Po Plain (Northern Italy). *Quat. Res.* 52, 1–13.
- Amorosi, A., Centineo, M.C., Colalongo, M.L., Pasini, G., Sarti, G., Vaiani, S.C., 2003. Facies architecture and Latest Pleistocene–Holocene depositional history of the Po Delta (Comacchio area). *Italy. J. Geol.* 111, 39–56.
- Amorosi, A., Colalongo, M.L., Fiorini, F., Fusco, F., Pasini, G., Vaiani, S.C., Sarti, G., 2004. Palaeogeographic and palaeoclimatic evolution of the Po Plain from 150-ky core records. *Glob. Planet. Change* 40, 55–78.
- Amorosi, A., Centineo, M.C., Colalongo, M.L., Fiorini, F., 2005. Millennial-scale depositional cycles from the Holocene of the Po Plain, Italy. *Mar. Geol.* 222–223, 7–18.
- Antonioli, F., Dai Pra, G., Hearty, P.J., 1988. I sedimenti quaternari nella fascia costiera della Piana di Fondi (Lazio meridionale). *Boll. Soc. Geol. Ital.* 107, 491–501.
- Antonioli, F., Girotti, O., Impronta, S., Nisi, M.F., Puglisi, C., Verrubbi, V., 1999. Nuovi dati sulla trasgressione marina olocenica e sulla subsidenza della Pianura Versiliese attraverso in sondaggio di 90 metri. *Atti del Convegno “Le Pianure. Conoscenza e salvaguardia”*, Regione Emilia Romagna, Bologna, Italy, pp. 214–218.
- Argnani, A., Bernini, M., Di Dio, G.M., Papani, G., Rogledi, S., 1997. Stratigraphic record of crustalscale tectonics in the Quaternary of the Northern Apennines (Italy). *Quaternario* 10, 595–602.
- Athersuch, J., Home, D.J., Whittaker, J.E., 1989. Marine and brackish water ostracods. In: Kermack, D.M., Barnes, R.S.K. (Eds.), *Synopses of the British Fauna (New Series)*, vol. 43, Brill E.J., Leiden.
- Barra, D., Cinque, A., Gedwelt, M., Hurtgen, C., 1991. L'ospite caldo *Sylvestra seminis* (Bunaduce, Masoli and Pugliese, 1976) (Crustacea, Ostracoda): un possibile marker dell'ultimo interglaciale dell'area mediterranea. *Quaternario* 4, 327–332.
- Bellotti, P., Carboni, M.G., Di Bella, L., Palagi, I., Valeri, P., 1994a. Benthic foraminiferal assemblages in the depositional sequence of the Tiber Delta. *Boll. Soc. Paleontol. Ital., Spec. Vol.* 2, 29–40.
- Bellotti, P., Chiocci, F.L., Milli, S., Tortora, P., Valeri, P., 1994b. Sequence stratigraphy and depositional setting of the Tiber delta: integration of high-resolution seismics, well logs, and archeological data. *J. Sediment. Res., Sect. B Stratigr. Glob. Stud.* 64, 416–432.
- Bellotti, P., Milli, S., Tortora, P., Valeri, P., 1995. Physical stratigraphy and sedimentology of the Late Pleistocene–Holocene Tiber Delta depositional sequence. *Sedimentology* 42, 617–634.
- Bellotti, P., Caputo, C., Davoli, L., Evangelista, S., Garzanti, E., Pugliese, F., Valeri, P., 2004. Morpho-sedimentary characteristics and Holocene evolution of the emergent part of the Ombrone River delta (southern Tuscany). *Geomorphology* 61, 71–90.
- Biserni, G., Berendsen, H.J.A., Sandrelli, F., 2004. Shape reconstruction of the Pleistocene/Holocene unconformity in the Grosseto Plain (Tuscany, Italy). *Quaternario* 17, 443–451.
- Blanc-Vernet, L., 1969. Contribution à l'étude des foraminifères de Méditerranée. *Travaux de la Station Marine d'Endoume, Marseille*.
- Blum, M.D., Törnqvist, T.E., 2000. Fluvial response to climate and sea-level change: a review and look forward. *Sedimentology* 47 (Suppl. 1), 2–48.
- Bonaduce, G., Ciampo, G., Masoli, M., 1975. Distribution of Ostracoda in the Adriatic Sea. *Pubbl. Stn. Zool. Napoli* 40, 1–304.
- Bortolotti, V., 1966. La tettonica trasversale dell'Appennino I. La linea Livorno–Sillarò. *Boll. Soc. Geol. Ital.* 85, 529–540.
- Boski, T., Moura, D., Veiga-Pires, C., Camacho, S., Duarte, D., Scott, D.B., Fernandes, S.G., 2002. Postglacial sea-level rise and sedimentary response in the Guadiana Estuary, Portugal/Spain border. *Sediment. Geol.* 150, 103–122.
- Bottema, S., 1975. The interpretation of pollen spectra from prehistoric settlements (with special attention to Liguliflorae). *Palaeohistoria* 17, 17–35.
- Carboni, M.G., Bergamin, L., Di Bella, L., Iamundo, F., Pugliese, N., 2002. Late Quaternary sea-level changes along the Tyrrhenian Sea. Paleocological evidences for foraminiferal and ostracod assemblages. *Geobios* 35, 40–50.
- Carboni, M.G., Frezza, V., Bergamin, L., 2004. Distribution of Recent foraminifers in the Ombrone River Basin (Tuscany Continental Shelf, Tyrrhenian Sea, Italy): relations with fluvial run-off. In: Coccioni, R., Galeotti, S., Lirer, F. (Eds.), *Proc. First Ital. Meeting Environ. Micropal., Grzybowski Found. Spec. Publ.*, vol. 9, Krakow, Poland, pp. 7–16.
- Carrión, J.S., Van Geel, B., 1999. Fine-resolution Upper Weichselian and Holocene palynological record from Navarrés (Valencia,

- Spain) and a discussion about factors of Mediterranean forest succession. *Rev. Palaeobot. Palynol.* 106, 209–236.
- Caspers, G., Freund, H., 2001. Vegetation and climate in the Early-Pleni-Weichselian in northern central Europe. *J. Quat. Sci.* 16, 31–48.
- Cattaneo, A., Steel, R.J., 2003. Transgressive deposits: a review of their variability. *Earth-Sci. Rev.* 62, 187–228.
- Cattaneo, A., Trincardi, F., 1999. The Late Quaternary transgressive record in the Adriatic epicontinental sea: basin widening and facies partitioning. In: Bergman, K.M., Snedden, J.W. (Eds.), *Isolated Shallow Marine Sand Bodies: Sequence Stratigraphic Analysis and Sedimentologic Interpretation*. Soc. Econ. Paleontol. Mineral. Spec. Publ., vol. 64, pp. 127–146.
- Cimerman, F., Langer, M.R., 1991. Mediterranean Foraminifera. *Academia Scientiarum et Artium Slovenica, Ljubljana*, p. 30. Classis IV.
- Colalongo, M.L., 1969. Ricerche sugli Ostracodi nei fondali antistanti il delta del Po. *G. Geol.* 36, 335–362.
- Cortemiglia, G.C., Mazzanti, R., Parea, G.C., 1983. Geomorfologia della Baia Baratti (Livorno–Toscana) e della sua spiaggia. *Geogr. Fis. Din. Quat.* 6, 148–173.
- Dalrymple, R.W., Zaitlin, B.A., Boyd, R., 1992. Estuarine facies models: conceptual basis and stratigraphic implications. *J. Sediment. Petrol.* 62 (6), 1130–1146.
- De Beaulieu, J.-L., Reille, M., 1992. The last climatic cycle at La Grande Pile (Vosges, France). A new pollen profile. *Quat. Sci. Rev.* 11, 431–438.
- Debenay, J.-P., Guillou, J.-J., Redois, F., Geslin, E., 2000. Distribution trends of foraminiferal assemblages in paralic environments. A base for using foraminifera as bioindicators. In: Martin, E.R. (Ed.), *Environmental Micropaleontology. Topics in Geobiology*, vol. 15, Kluwer Academic/Plenum Publishers, New York, pp. 39–67.
- Donnici, S., Serandrei Barbero, R., 2002. The benthic foraminiferal communities of the northern Adriatic continental shelf. *Mar. Micropaleontol.* 44, 93–123.
- Embry, A.F., 1993. Transgressive–regressive (T–R) sequence analysis of the Jurassic succession of the Sverdrup Basin, Canadian Arctic Archipelago. *Can. J. Earth Sci.* 30, 301–320.
- Embry, A.F., 1995. Sequence boundaries and sequence hierarchies: problems and proposals. In: Steel, R.J., Felt, V.L., Johanneses, E.P., Mathieu, C. (Eds.), *Sequence stratigraphy on the Northwest European Margin*. Norwegian Petr. Soc. Spec. Publ., vol. 5, pp. 1–11.
- Ferranti, L., Antonioli, F., Mauz, B., Amorosi, A., Dai Pra, G., Mastronuzzi, G., Monaco, C., Orrù, P., Pappalardo, M., Radtke, U., Renda, P., Romano, P., Sansò, P., Verrubbi, V., 2006. Markers of the last interglacial sea-level high stand along the coast of Italy: tectonic implications. *Quat. Int.* 145–146, 30–54.
- Fiorini, F., Vaiani, S.C., 2001. Benthic foraminifera and transgressive–regressive cycles in the Late Quaternary subsurface sediments of the Po Plain near Ravenna (Northern Italy). *Boll. Soc. Paleontol. Ital.* 40, 357–403.
- Follieri, M., Magri, D., Sadori, L., 1988. 250,000-year pollen record from Valle di Castiglione (Roma). *Pollen Spores* 30, 329–356.
- Foyle, A.M., Oertel, G.F., 1997. Transgressive systems tract development and incised-valley fills within a Quaternary estuary-shelf system: Virginia inner shelf, USA. *Mar. Geol.* 137, 227–249.
- Guitier, F., Andrieu, V., de Beaulieu, J.-L., Cheddadi, R., Calvez, M., Ponel, P., Reille, M., Keller, T., Goeury, C., 2003. The last climatic cycles in Western Europe: a comparison between long continuous lacustrine sequences from France and other terrestrial records. *Quat. Int.* 111, 59–74.
- Guiot, J., Pons, A., de Beaulieu, J.L., Reille, M., 1989. A 140,000 years continental climate reconstruction from two European pollen records. *Nature* 338, 309–313.
- Hanebuth, T.J.J., Saito, Y., Tanabe, S., Vu, Q.L., Ngo, Q.T., 2006. Sea levels during late marine isotope stage 3 (or older?) reported from the Red River delta (northern Vietnam) and adjacent regions. *Quat. Int.* 145–146, 119–134.
- Havinga, A.J., 1984. A 20-year experimental investigation into the differential corrosion susceptibility of pollen and spores in various soil types. *Pollen Spores* 26, 541–558.
- Hearty, P.J., Dai Pra, G., 1987. Ricostruzione paleogeografica degli ambienti litoranei quaternari della Toscana e del Lazio settentrionale con l'impiego dell'aminostatigrafia. *Boll. Serv. Geol. Ital.* 106, 189–224.
- Henderson, P.A., 1990. Freshwater ostracods. In: Kermack, D.M., Barnes, R.S.K. (Eds.), *Synopses of the British Fauna (New Series)*, vol. 42, Brill E.J., Leiden.
- Hori, K., Saito, Y., Zhao, Q., Cheng, X., Wang, P., Sato, Y., Li, C., 2001. Sedimentary facies of the tide-dominated paleo-Changjiang (Yangtze) estuary during the last transgression. *Mar. Geol.* 177, 331–351.
- Hori, K., Saito, Y., Zhao, Q., Wang, P., 2002. Evolution of the coastal depositional systems of the Changjiang (Yangtze) River in response to Late Pleistocene–Holocene sea-level changes. *J. Sediment. Res.* 72, 884–897.
- Hori, K., Tanabe, S., Saito, Y., Haruyama, S., Nguyen, V., Kitamura, A., 2004. Delta initiation and Holocene sea-level change: example from the Song Hong (Red River) delta, Vietnam. *Sediment. Geol.* 164, 237–249.
- Jalut, G., Amat, A.E., Bonnet, L., Gauquelin, T., Fontugne, M., 2000. Holocene climatic changes in the Western Mediterranean, from south-east France to south-east Spain. *Palaeogeogr. Palaeoclimatol. Palaeoecol.* 160, 255–290.
- Jorissen, F.J., 1987. The distribution of Benthic Foraminifera in the Adriatic Sea. *Mar. Micropaleontol.* 12, 21–48.
- Jorissen, F.J., 1988. Benthic Foraminifera from the Adriatic Sea; principles of phenotypic variation. *Utrecht Micropaleontol. Bull.* 37, 1–176.
- Konradi, P.B., Larsen, B., Sørensen, A.B., 2005. Marine Eemian in the Danish eastern North Sea. *Quat. Int.* 133–134, 21–31.
- Li, C., Wang, P., Sun, H., Zhang, J., Fan, D., Den, G.B., 2002. Late Quaternary incised-valley fill of the Yangtze delta (China): its stratigraphic framework and evolution. *Sediment. Geol.* 152, 133–158.
- Lim, D.I., Park, Y.A., 2003. Late Quaternary stratigraphy and evolution of a Korean tidal flat, Haenam Bay, Southeastern Yellow Sea, Korea. *Mar. Geol.* 193, 177–194.
- Lowrie, A., Hamiter, R., 1995. Fifth and sixth order eustatic events during Holocene, fourth order highstand influencing Mississippi delta-lobe switching. In: Finkl Jr., C.W. (Ed.), *Holocene Cycles: Climate, Sea Levels and Sedimentation*. *J. Coastal Res.*, vol. 17, pp. 225–229.
- Magri, D., 1999. Late Quaternary vegetation history at Lagaccione near Lago di Bolsena (central Italy). *Rev. Palaeobot. Palynol.* 106, 171–208.
- Magri, D., Sadori, S., 1999. Late Pleistocene and Holocene pollen stratigraphy at lago di Vico, central Italy. *Veget. Hist. Archaeobot.* 8, 247–260.
- Mariani, M., Prato, R., 1988. I bacini neogenici costieri del margine tirrenico: approccio sismico stratigrafico. *Mem. Soc. Geol. Ital.* 41, 519–531.
- Mauz, B., 1999. Late Pleistocene records of littoral processes at the Tyrrhenian Coast (Central Italy): depositional environments and luminescence chronology. *Quat. Sci. Rev.* 18, 1173–1184.

- Massari, F., Rio, D., Serandrei Barbero, R., Asioli, A., Capraro, L., Fornaciari, E., Vergerio, P.P., 2004. The environment of Venice area in the past two million years. *Palaeogeogr. Palaeoclimatol. Palaeoecol.* 202, 273–308.
- McCarthy, P.J., Plint, A.G., 1998. Recognition of interfluvial sequence boundaries: integrating paleopedology and sequence stratigraphy. *Geology* 26, 387–390.
- Milli, S., 1997. Depositional setting and high-frequency sequence stratigraphy of the Middle-Upper Pleistocene to Holocene deposits of the Roman Basin. *Geol. Rom.* 33, 99–136.
- Murray, J.W., 1991. *Ecology and Palaeoecology of Benthic Foraminifera*. Longman Scientific & Technical, London.
- Nichol, S.L., Boyd, R., Penland, S., 1994. Stratigraphic response of wave-dominated estuaries to different relative sea-level changes and sediment supply histories: Quaternary case studies from Nova Scotia, Louisiana and Eastern Australia. In: Dalrymple, R.W., Boyd, R., Zaitlin, B.A. (Eds.), *Incised-Valley Systems: Origin and Sedimentary Sequences*. Soc. Econ. Paleontol. Mineral. Spec. Publ., vol. 51, pp. 266–283.
- Nicol-Pichard, S., Dubar, M., 1998. Reconstruction of Late-glacial and Holocene environments in south-east France based on the study of a 66-m long core from Biot, Alpes Maritimes. *Veget. Hist. Archaeobot.* 7, 11–15.
- Nummedal, D., Swift, D.J.P., 1987. Transgressive stratigraphy at sequence-bounding unconformities: some principles derived from Holocene and Cretaceous examples. In: Nummedal, D., Pilkey, O.H., Howard, J.D. (Eds.), *Sea-Level Fluctuation and Coastal Evolution*. Soc. Econ. Paleontol. Mineral. Spec. Publ., vol. 41, pp. 241–260.
- Overeem, I., Kroonenberg, S.B., Veldkamp, A., Groenesteijn, K., Rusakov, G.V., Svitoch, A.A., 2003. Small-scale stratigraphy in a large ramp delta: recent and Holocene sedimentation in the Volga delta, Caspian Sea. *Sediment. Geol.* 159, 133–157.
- Pascucci, V., 2005. Neogene evolution of the Viareggio Basin Northern Tuscany (Italy). *Geoacta* 4.
- Pérez-Obiol, R., Julià, R., 1994. Climatic change on the Iberian Peninsula recorded in a 30,000-yr pollen record from Lake Banyoles. *Quat. Res.* 41, 91–98.
- Plint, A.G., Nummedal, D., 2000. The falling stage systems tract: recognition and importance in sequence stratigraphic analysis. In: Hunt, D., Gawthorpe, R.L. (Eds.), *Sedimentary Response to Forced Regressions*. Geol. Soc. London, Spec. Publ., vol. 172, pp. 1–17.
- Preusser, F., 2004. Towards a chronology of the Late Pleistocene in the northern Alpine Foreland. *Boreas* 33, 195–210.
- Pugliese, N., Stanley, D.J., 1991. Ostracoda, depositional environments and Late Quaternary evolution of the eastern Nile delta, Egypt. *Quaternario* 4, 275–302.
- Reille, M., Andrieu, V., de Beaulieu, J.-L., Guenet, P., Goeury, C., 1998. A long pollen record from Lac du Bouchet, Massif Central, France, for the period ca. 325 to 100 ka (OIS 9c to OIS 5e). *Quat. Sci. Rev.* 17, 1107–1123.
- Ricci Lucchi, M., Calderoni, G., Carrara, C., Cipriani, N., Esu, D., Ferrelli, L., Girotti, O., Gliozzi, E., Lombardo, M., Longinelli, A., Magri, D., Nebbiai, M., Ricci Lucchi, F., Vigliotti, L., 2000. Late Quaternary record of the Rieti Basin, central Italy: paleoenvironmental and paleoclimatic evolution. *G. Geol.* 62, 105–135.
- Ridente, D., Trincardi, F., 2002. Eustatic and tectonic control on deposition and lateral variability of Quaternary regressive sequences in the Adriatic basin (Italy). *Mar. Geol.* 184, 273–293.
- Romano, P., Santo, A., Voltaggio, M., 1994. L'evoluzione morfologica della pianura del fiume Volturno (Campania) durante il tardo Quaternario. *Quaternario* 7, 41–56.
- Ruiz, F., Gonzalez-Regalado, M.L., Baceta, J.I., Menegazzo-Vitturi, L., Pistolato, M., Rampazzo, G., Molinaroli, E., 2000. Los ostrácodos actuales de la laguna de Venecia (NE de Italia). *Geobios* 33, 447–454.
- Russo Ermolli, E., di Pasquale, G., 2002. Vegetation dynamics of south-western Italy in the last 28 kyr inferred from pollen analysis of a Tyrrhenian Sea core. *Veget. Hist. Archaeobot.* 11, 211–219.
- Saito, Y., 1994. Shelf sequence and characteristic bounding surfaces in a wave-dominated setting: Latest Pleistocene–Holocene examples from Northeast Japan. *Mar. Geol.* 120, 105–127.
- Sarti, G., Zanchetta, G., Ciulli, L., Colonese, A., 2005. Late Quaternary oligotypical non-marine mollusc fauna from southern Tuscany: climatic and stratigraphical implications. *Geoacta* 4.
- Sgarrella, F., Moncharmont Zei, M., 1993. Benthic Foraminifera of the Gulf of Naples (Italy): systematics and autoecology. *Boll. Soc. Paleontol. Ital.* 32, 145–264.
- Smith, A.J., Horne, D.J., 2002. Ecology of marine, marginal marine and nonmarine ostracodes. In: Holmes, J.A., Chivas, A.R. (Eds.), *The Ostracoda Applications in Quaternary Research*. Geophysical Monograph, vol. 131, AGU, Washington DC, pp. 37–64.
- Somoza, L., Barnolas, A., Arasa, A., Maestro, A., Rees, J.G., Hernandez-Molina, F.J., 1998. Architectural stacking patterns of the Ebro delta controlled by Holocene high-frequency eustatic fluctuations, delta-lobe switching and subsidence processes. *Sediment. Geol.* 117, 11–32.
- Stockmarr, J., 1971. Tablets with spores in absolute pollen analysis. *Pollen Spores* 13, 615–621.
- Stoms, J.E.A., Hoogendoorn, R.M., Dam, R.A.C., Hoitink, A.J.F., Kroonenberg, S.B., 2005. Late-Holocene evolution of the Mahakam delta, East Kalimantan, Indonesia. *Sediment. Geol.* 180, 149–166.
- Stuiver, M., Reimer, P.J., Braziunas, T.F., 1998. High-precision radiocarbon age calibration for terrestrial and marine samples. *Radiocarbon* 40 (3), 1127–1151.
- Swift, D.J.P., 1968. Coastal erosion and transgressive stratigraphy. *J. Geol.* 76, 444–456.
- Ta, T.K.O., Nguyen, V.L., Tateishi, M., Kobayashi, I., Saito, Y., 2001. Sedimentary facies, diatom and foraminifer assemblages in a late Pleistocene–Holocene incised-valley sequence from the Mekong River Delta, Bentre Province, Southern Vietnam: the BT2 core. *J. Asian Earth Sci.* 20, 83–94.
- Tanabe, S., Saito, Y., Sato, Y., Suzuki, Y., Sinsakul, S., Tiyapairach, S., Chaimanee, N., 2003. Stratigraphy and Holocene evolution of the mud-dominated Chao Phraya delta, Thailand. *Quat. Sci. Rev.* 22, 789–807.
- Törnqvist, T.E., Wallinga, J., Murray, A.S., De Wolf, H., Cleveringa, P., De Gans, W., 2000. Response of the Rhine–Meuse system (west-central Netherlands) to the last Quaternary glacio-eustatic cycles: a first assessment. *Glob. Planet. Change* 27, 89–111.
- Törnqvist, T.E., Wallinga, J., Busschers, F.S., 2003. Timing of the last sequence boundary in a fluvial setting near the highstand shoreline — insights from optical dating. *Geology* 31, 279–282.
- Tzedakis, P.C., 1993. Long term tree populations in northwest Greece through multiple Quaternary climatic cycles. *Nature* 364, 437–440.
- Tzedakis, P.C., 1999. The last climatic cycle at Kopais, central Greece. *J. Geol. Soc.* 156, 425–434.
- Tzedakis, P.C., Andrieu, V., de Beaulieu, J.-L., Crowhurst, S., Follieri, M., Hooghiemstra, H., Magri, D., Reille, M., Sadori, L., Shackleton, N.J., Wijmstra, T.A., 1997. Comparison of terrestrial and marine records of changing climate of the last 500,000 years. *Earth Planet. Sci. Lett.* 150, 171–176.
- Tzedakis, P.C., Frogley, M.R., Heaton, T.H.E., 2003. Last Interglacial conditions in southern Europe: evidence from Ioannina, northwest Greece. *Glob. Planet. Change* 36, 157–170.

- Van Wagoner, J.C., Mitchum, R.M., Campion, K.M., Rahmanian, V.D. (Eds.), 1990. Siliciclastic Sequence Stratigraphy in Well Logs, Cores, and Outcrops: Concepts for High-Resolution Correlation of Time and Facies. *Am. Assoc. Petrol. Geol. Methods in Exploration Series*, vol. 7, AAPG, Tulsa (55 pp.).
- Wijmstra, T.A., 1969. Palynology of the first 30 m of a 120 m deep section in Northern Greece. *Acta Bot. Neerl.* 18, 511–527.
- Wijmstra, T.A., Smit, A., 1976. Palynology of the middle part (30–78 meters) of the 120 m deep section in Northern Greece. *Acta Bot. Neerl.* 25, 297–312.
- Woillard, G.M., 1978. Grand Pile peat bog: a continuous pollen record for the last 140,000 years. *Quat. Res.* 9, 1–21.
- Yassini, I., Jones, B.G., 1995. Foraminiferida and Ostracoda from Estuarine and Shelf Environments on the Southeastern Coast of Australia. University of Wollongong Press, Wollongong.
- Zaitlin, B.A., Dalrymple, R.W., Boyd, R., 1994. The stratigraphic organization of incised-valley systems associated with relative sea-level change. In: Dalrymple, R.W., Boyd, R., Zaitlin, B.A. (Eds.), *Incised-Valley Systems: Origin and Sedimentary Sequences*. Soc. Econ. Paleontol. Mineral. Spec. Spec. Publ., vol. 51, pp. 45–60.
- Zagwijn, W.H., 1996. An analysis of Eemian climate in western and central Europe. *Quat. Sci. Rev.* 15, 451–469.

Paper 2

Anatomy and sequence stratigraphy of the late Quaternary

Arno valley fill (Tuscany, Italy)

Amorosi, A., Sarti, G., **Rossi, V.** and Fontana, V.

Anatomy and sequence stratigraphy of the late Quaternary Arno valley fill (Tuscany, Italy)

Alessandro Amorosi¹, Giovanni Sarti², Veronica Rossi¹ and Vincenzo Fontana²

¹Dipartimento di Scienze della Terra e Geologico-Ambientali, Università di Bologna, Via Zamboni 67, 40126 Bologna, Italy. E-mail: alessandro.amorosi@unibo.it,
veronica.rossi4@unibo.it

²Dipartimento di Scienze della Terra, Università di Pisa, Via Santa Maria 53, 56126 Pisa, Italy. E-mail: sarti@dst.unipi.it

Abstract

The late Quaternary Arno valley fill, in western Tuscany, was formed during the last glacio-eustatic cycle. It exhibits a total thickness of 35-40 m, and is 5-7 km wide. It consists almost entirely of a single transgressive succession emplaced during the post-Last Glacial Maximum transgression, between latest Pleistocene (13 cal. ka BP) and early Holocene (8 cal. ka BP). An indurated horizon, intensively reworked by pedogenic features, occurs lateral to the deep incision.

Above a fluvial deposit flooring the valley, the incised valley fill includes an early transgressive succession of coastal plain, bay head-delta, and estuarine deposits. As sea-level rise continued, the valley was filled and the interfluves flooded. Above the interfluve sequence boundary, the late transgressive Holocene succession is about 17 m thick, and includes a transgressive-regressive succession of coastal, shallow-marine and modern deltaic deposits.

Facies analysis of continuous cores and stratigraphic correlation of borehole data from the lower Arno coastal plain allow detailed reconstruction of three-dimensional facies architecture of the valley body. Alternating freshwater and brackish deposits form the valley fill at proximal-most locations. West of Pisa, the valley fill includes amalgamated estuary-mouth sand bodies, whereas at distal locations (beneath the present shoreline) it consists almost entirely of estuarine mud.

Subtle vertical facies changes within the Arno valley fill allow identification and lateral tracing of three vertically stacked, shallowing-upward successions, about 10 m thick and bounded by flooding surfaces, which are interpreted as parasequences. Parasequence architecture suggests that sea-level rise close to the Pleistocene-Holocene boundary was punctuated by at least two distinct stillstand phases.

Keywords: Incised Valley Fill, Sequence stratigraphy, Parasequence, Arno River, Quaternary.

Introduction

The fluvial to marine transition is one of the most complex depositional environments, because of the large number of terrestrial and marine processes that interact there (Dalrymple and Choi, 2007). Valley fills that developed in response to Quaternary glacio-eustatic cycles, are typical features of this realm.

In early sequence-stratigraphic models (Posamentier et al., 1988; Posamentier and Vail, 1988; Van Wagoner et al., 1990), incised valley fills (IVF) and their estuarine components were defined as characteristic lowstand features of depositional sequences. Attribution of the estuarine portion of IVF to the transgressive phase dates to a subsequent paper by Dalrymple et al. (1992). A high-resolution sequence-stratigraphic interpretation for IVF has been offered by Dalrymple and Zaitlin (1994), and recently refined by Dalrymple (2006). A recent paper by Gibling (2006) summarizes the criteria for valley-classification, based upon their three-dimensional geometry, rather than internal structure.

Following the theoretical models of Dalrymple et al. (1992; 1994), Nichol et al. (1994), Schumm and Ethridge (1994), and Zaitlin et al. (1994), several papers have provided detailed facies documentation of Quaternary valley, from different geological settings (Allen and Posamentier, 1993; Blum et al., 1994; Thomas and Anderson, 1994; Foyle and Oertel, 1997; Heap and Nichol, 1997; Hori et al., 2002; Li et al., 2002, 2006; Wellner and Bartek, 2003; Weber et al., 2004; Fenies and Lericolais, 2005; Blum and Aslan, 2006). In Italy, after the early work from the Tiber coastal plain (Bellotti et al., 1994, 1995; Milli, 1997; Milli et al., this volume), another Late Quaternary valley-fill succession from the Tyrrhenian coastal area has been recently identified, on the basis of a deep core (M1) and scattered subsurface data (Aguzzi et al., 2005; 2007): the Arno valley fill, in western Tuscany.

The aim of this paper is to offer detailed 3-D facies documentation of the late Quaternary Arno valley-fill on the basis of an entirely new dataset (Fig. 1). The purpose of stratigraphic correlation is

to document facies changes within the valley fill, from distal-to-proximal location, and to show how high-resolution sequence-stratigraphic analysis of this valley fill may enable identification of lower-rank, high-frequency depositional cycles that can be traced throughout the valley body.

Geological Setting

The Arno coastal plain (Fig. 1), about 450 km² wide, is bounded by Pisani Mountains to the NW and by the well known “Livorno-Sillaro” tectonic line (Ghelardoni et al., 1968; Martini and Sagri, 1993; Carmignani et al., 1994; Boccaletti et al., 1997; Cantini et al., 2001; Cerrina et al., 2001), which runs along the foothills of Leghorn and Pisa hills, to the south. The boundary to the north with the Versilia plain is not clearly defined (Federici and Mazzanti 1989), and approximately corresponds with Massacciuccoli lake.

From a structural point of view, the Arno coastal plain represents the south inshore portion of the subsiding half-graben Viareggio basin (Argnani et al., 1997; Martini et al., 2001; Pascucci, 2005). This basin was formed since the Late Tortonian due to the opening of the Tyrrhenian Sea and the counter-clockwise migration of the Apenninic foredeep-foreland system (Malinverno and Ryan, 1986; Sartori, 1989; Patacca et al., 1990; Martini and Sagri, 1993; Pascucci et al., 2001).

Seismic investigations (Mariani and Prato, 1988; Pascucci, 2005) reveal that the depocentre of Viareggio basin is located beneath the present shoreline, and is filled by up to 2500 meters of upper Miocene to Holocene deposits. These have been grouped into five unconformity-bounded units (Pascucci, 2005). The late Quaternary deposits (sequence II of Mariano and Prato, 1988; sequence 6b of Pascucci, 2005) consist predominantly of undisturbed continental to shallow-marine deposits (Romagnoli, 1957; Sartori, 1978; Fancelli et al., 1986; Della Rocca et al., 1987; Baldacci et al., 1994; Mazzanti, 2000).

Recently, Aguzzi et al. (2005, 2007) supplied a new stratigraphic framework for the uppermost Viareggio Basin strata in the Arno coastal area, identifying on the basis of radiometric and pollen

data two transgressive-regressive sequences related to the last two interglacial-glacial cycles (base of OIS 1 and 5e, respectively). On the basis of remarkable differences in Holocene section thickness these authors suggested the presence of a late Quaternary incised valley, filled primarily with estuarine deposits.

The Holocene succession is > 50 m thick in Core M1 (Fig. 2) and includes, above a tidal ravinement surface, about 20 m of early transgressive estuarine deposits. These are overlain, through a wave ravinement surface, by a thin succession of late transgressive barrier-beach and inner-shelf deposits. Above the maximum flooding surface, highstand deposits are represented by a shallowing-upward succession of prodelta to delta-front sediments. The valley fill correlates laterally with an interfluvial sequence boundary, overlain by 17 m of Holocene sediments (Aguzzi et al., 2007).

Methods

A data set consisting of 20 continuous cores and 317 boreholes data around the city of Pisa (Fig. 1) provides an opportunity to examine the late Quaternary stratigraphic record of the study area, with special reference to the Arno valley fill. Three (M1, S2 and M3) out of 20 continuous cores have been detailed described in Aguzzi et al., (2005, 2007), while the 317 logs, provided by Geological Survey of Pisa Province, derive from boreholes drilled for water research purposes. These include poor-quality stratigraphic and sedimentological information. Vertical and lateral lithofacies relationships, sediment texture and grain size, colour, occurrence of accessory materials like plant and wood debris, and micropalaeontological content, provide the basis for facies characterization. Eleven AMS¹⁴C dates performed at Beta Analytic Inc. (Miami, Usa) and CEDAD (University of Lecce, Italy) from organic-rich layers and shell fragments constrain the chronostratigraphic framework. ¹⁴C ages younger than 20,000 yr BP are reported as cal. years BP.

Detailed micropalaeontological (ostracod and foraminifera) analyses carried out on six cores were used to refine facies interpretation.

The Late Quaternary Arno valley fill

Identification of the Arno valley fill is based primarily on remarkable thickness variations of the Holocene deposits and on peculiar facies attributes of the valley fill with respect to the adjacent interfluves. This allows us to reconstruct the planview geometry of the Arno palaeovalley (Fig. 1).

The Arno valley body (in the sense of Gibling, 2006) ranges between 5 and 7 km in width, and roughly coincides with the modern Arno River course. A significant change in palaeovalley direction is recorded near the Pisani Mountains, NE of Pisa, where a structural high affected the evolution of the river course. The Arno valley fill accords with the three major criteria established by Fielding and Gibling (2005) as diagnostic for valley fills (Figs. 3 and 4): i) a wide basal erosion surface that can be traced laterally in extra-channel deposits, ii) a dimension an order of magnitude larger than individual channels; iii) a scale of erosion that is several times the depth of scour evident from component channel fills.

Downstream facies changes along the Arno valley fill can be depicted through examination of a set of shore-parallel cross-sections, transverse to the valley axis (Figs. 3 and 4). Transgressive deposits are readily identifiable from core data, and for this reason are shown in colours. In contrast, there is no clear evidence of the basal valley scour in all sections.

The cross-sections show that the transgressive valley fill has a remarkably homogeneous thickness of about 35 m, which tends to increase seaward, to more than 40 m. With a width/thickness range of 125-200, the Arno valley fill fits the general range of width and thickness reported by Gibling (2006) for “valley fills within alluvial and marine strata”.

Detailed facies description of the Arno valley fill at distal-most locations is provided by Core M1 stratigraphy (see Aguzzi et al., 2007 - Fig. 2), and will not be repeated here in detail. In this area,

early transgressive stratigraphy consists of a monotonous succession of predominantly outer estuarine facies, overlain by a 30 m thick, late transgressive-regressive succession of littoral, shallow-marine and modern deltaic deposits (Fig. 3a). Limited core coverage and patchy terrace distribution commonly hamper recognition of fluvial terrace deposits in the geological record of buried valley fills (Gibling, 2006). However, the presence of gravel bodies, with erosional bases and fining-upward trends, suggests that alluvial terrace deposits could be present along the valley flanks, although difficult to map.

In a more landward position, halfway between Pisa and the Tyrrhenian coast (Fig. 3b), the valley fill consists predominantly of central estuarine clays, with subordinate organic-rich sands and clays, which are interpreted to represent coastal-plain and bay-head delta deposits. At this location, the valley fill is overlain by a thinner (20 m) succession of predominantly littoral sandy deposits, representing the landward equivalent of uppermost Core M1.

A few kilometres landwards (Fig. 4a), the valley fill consists primarily of thick, amalgamated bay-head delta systems, which are separated by thin intercalations of organic-rich paludal horizons, with very subordinate lagoonal clays. The upper part of the valley fill is characterized by alluvial plain deposits that are capped by an indurated horizon, containing calcareous glaebulae and rhizoconcretions, which is interpreted as a palaeosol. This overconsolidated horizon is observed approximately at the same stratigraphic level as the valley interfluves, forming a continuous horizon of stiff clays. Above the valley fill, Holocene stratigraphy includes a transgressive-regressive succession of coastal plain, lagoonal, coastal plain, and alluvial deposits, which are interpreted to represent the landward equivalents of the coastal succession recorded at seaward locations. A radiocarbon date from Core P1 allows attribution of the post-valley fill succession to about the last 8,000 cal. years BP.

In the landward-most transect, east of Pisa (Fig. 4b), where a thin fluvial deposit is preserved on the valley floor, the IVF is made up of a characteristic alternation of coastal plain and lagoonal deposits. These form vertically stacked, shallowing upward successions, approximately 10 m thick,

bounded by flooding surfaces, and interpreted as parasequences (A-C in Fig. 4b). These parasequences are restricted to the valley fill, and are overlain by a transgressive-regressive cycle that can also be recognized above the interfluvial unconformity. Radiocarbon dating constrains the base of the IVF to the late Pleistocene (about 13 cal. ka BP). Similarly to what is observed in Core P1, the valley was filled around 8 cal. ka BP, as documented by a ^{14}C date from Core S1.

Proximal to distal facies variations within Arno IVF are shown in a shore-perpendicular section (Fig. 5), where the parasequence boundaries identified in Figure 4b are tentatively traced parallel to the palaeovalley.

Sequence stratigraphy

The sequence bounding unconformity (SB) of the late Quaternary depositional sequence in the study area is a composite erosional surface (see Foyle and Oertel, 1997) that shows remarkably different characteristics from site to site. SB can be easily recognized lateral to the valley body, where it corresponds with a characteristic indurated and pedogenized horizon (“interfluvial sequence boundary” of Van Wagoner et al., 1990; Gibling and Bird, 1994; Aitken and Flint, 1996; McCarthy and Flint, 1998). In coincidence with this weathered palaeosurface, no lowstand deposition took place, and SB and the transgressive surface merge.

In contrast, SB identification on the valley flanks and on the valley floor based upon core data alone is not an unambiguous operation, especially in case of alluvium-on-alluvium contacts (see discussion in Gibling, 2006). In the Arno coastal plain, the limited number of continuous cores and the generally poor stratigraphic descriptions available from boreholes do not allow prompt differentiation between local scours, fluvial terraces and valley-base scours, making identification of SB difficult (Aguzzi et al., 2007). Lowstand fluvial deposits above a fluvial erosion surface, interpreted as SB, are only locally preserved, suggesting that erosion by tidal processes may have occurred during the following sea-level rise (Nichol et al., 1994).

The transgressive surface (TS), which coincides with the bay ravinement surface of Nummedal and Swift (1987) and Foyle and Oertel (1997), is marked throughout the valley fill by an abrupt facies shift from alluvial to overlying estuarine deposits (Fig. 5). The estuarine valley fill, *i.e.* coastal plain, estuary-mouth, central estuary and outer estuary deposits, forms the lower part of the transgressive systems tract (TST). The lower boundary of estuary-mouth sands with underlying estuarine deposits corresponds to the tidal ravinement surface of Demarest and Kraft (1987), Posamentier and Allen (1993) and Foyle and Oertel (1997).

The lower part of the TST is separated from overlying (upper part of the TST) shoreface and shelf deposits by a wave ravinement surface (Swift, 1968; Nummedal and Swift, 1987). The maximum flooding surface (MFS), which separates TST from the overlying highstand systems tract (HST), occurs within a relatively homogeneous clay succession (Bellotti et al., 1994; 1995; Li et al., 2002) and has no obvious physical expression. However, it can be defined from core data on the basis of subtle micropalaeontological variations, at the turnaround from deepening (transgressive) to shallowing (highstand) conditions (Aguzzi et al., 2007).

Several facies referable to a prograding Arno delta and adjacent strandplain are developed within the HST, but are not discussed in detail in this paper.

Origin and evolution of the incised-valley system

One of the most debated issues about late Quaternary valley fills is timing of valley incision. Incised valleys of Quaternary age have been interpreted to have formed in response to either sea-level fall (Fisk, 1944; Bernard and LeBlanc, 1965; Posamentier and Vail, 1988; Dabrio et al., 2000; Boski et al., 2002) or enhanced meltwater discharge during subsequent sea-level rise (Khadkikar and Rajshekhar, 2005; Blum and Aslan, 2006), or a combination of the two (Li et al., 2002). This results in uncertain attribution of the basal fluvial deposits within the valley-fill to LST or TST.

In the Arno coastal plain, two radiocarbon dates from alluvial deposits a few meters beneath the interfluvial sequence boundary, at 18-21 m core depth (Core P2 in Fig. 3a), indicate that valley incision started at an unspecified time, after about 38 uncalibrated ka BP (Fig. 6). Fluvial incision was punctuated by multiple episodes of alluvial aggradation (Muto and Steel, 2004), as documented by the remnants of two distinct levels of fluvial terraces (Figs. 3a and 4a) along the valley flank, forming small-scale allostratigraphic units (see Blum and Price, 1998). The lowermost (youngest) terrace deposit is dated to about 23.5 uncalibrated ka BP in Core M1. This interpretation constrains the end of fluvial incision to after this time (Fig. 6).

It is likely that valley incision originated in response to rapid sea-level fall at OIS 3/2 transition (around 30-25 uncalibrated ka BP), and probably continued during the entire OIS 2 period, when base level reached its lowest position (Aguzzi et al., 2007). Valley widening, which is a typical feature of decelerating rates of relative sea-level fall and relative sea-level rise (Strong and Paola, 2006), was associated with significant erosion of the valley walls. Extensive rooting and pedogenesis occurred in time-equivalent interfluvial segments adjacent to the deep incision (Plink-Björklund, 2005). When sea-level fall ceased, tectonic subsidence was able to generate new accommodation space, thus favouring the valley filling. The late lowstand phases (and possibly the early stages of post-glacial transgression) were characterized by fluvial sedimentation onto the valley floor. During the late stage, rapid sea-level rise induced drowning and landward shifting of the river mouth, with subsequent estuary formation.

The basal erosion surface thus appears as a composite regional incision that can be correlated with stiff, overconsolidated horizons in the interfluvial areas, and an overlapping geometry onto the valley walls can be reconstructed for the estuarine infilling (Zaitlin et al., 1994). Radiocarbon dates from the transgressive valley fill show post-13 cal. ka BP ages, documenting that the valley fill was simple (see Rahmani, 1988; Wood and Hopkins, 1989; Zaitlin et al., 1994), *i.e.* the valley was filled completely during the post-LGM phase.

Early transgressive sedimentation (parasequences A-C in Figs. 3-5) was confined in a narrow,

funnel-shaped geometry (see Dalrymple et al., 1992; Zaitlin et al., 1994) for about 5 ka, between 13 and 8 cal. ka. The bipartite record of stacked brackish and freshwater deposits within individual parasequences suggests a change from an estuary-dominated mode to a mode of coastal-plain/estuary-mouth evolution that was less affected by marine processes. The back-and-forth migration of depositional environments was probably due to stepwise sea-level rise, which allowed a brief re-establishment of terrestrial environments after each transgressive pulse. A similar pattern of parasequences formed during the same time interval has been reported by Lowrie and Hamiter (1995), Somoza et al. (1998), Amorosi et al. (2005), and Boyer et al. (2005). Lack of clearly recognizable parasequences west of Pisa (see Fig. 5) could be the result of sediment removal in high-energy mouth-bar sub-environments.

Valley filling neared completion around 8 cal. ka BP. The presence of a palaeosol at the same stratigraphic level as the interfluvial palaeosols (see Fig. 4) suggests a phase of non-deposition that could have been triggered by an episode of fluvial avulsion when Arno river was able to flow across the entire coastal plain, spreading onto the former valley interfluvies.

Conclusions

Detailed stratigraphic correlations and facies analysis from cores of the Arno coastal plain reveal an incised-valley system of late Quaternary age, interpreted as a transgressive estuary (*sensu* Dalrymple et al., 1992), roughly coinciding with the modern Arno River course.

The major results of this study may be summarized, as follows:

- 1) The Arno valley fill is a late Quaternary sedimentary body that can be traced in the subsurface of Arno coastal plain, beneath the town of Pisa, about 15 km inland from the Tyrrhenian coast. The valley fill is 5-7 km wide and total depth of incision can be estimated as 35-40 m.

- 2) The valley fill is transgressive in character, with thin fluvial deposits overlain by a thick succession of early transgressive deposits. At comparatively distal locations, estuarine facies associations constitute the principal component of the early transgressive valley fill. Landwards, these show lateral transition to estuary-mouth and then coastal plain deposits. A late transgressive succession of coastal to shallow-marine deposits caps the Arno valley fill and the adjacent interfluves. Prograding deltaic and strandplain deposits form the highstand succession.

- 3) The sequence-bounding unconformity is a composite surface that can be easily identified on the interfluves. In contrast, it is difficult to recognize on the valley flanks and on the valley floor, due to alluvium-on-alluvium contacts with underlying, pre-LGM deposits. The transgressive (bay ravinement) surface, the tidal ravinement surface and the wave ravinement surface are readily identified by abrupt landward shifts of facies. The maximum flooding surface has no physical expression, but can be recognized on the basis of subtle micropalaeontological variations.

- 4) Detailed facies analysis of the fluvial-marine transition enables identification, within the transgressive valley fill, of three distinct parasequences. Each parasequence is approximately 10 m thick and comprises a distinctive assemblage of lithofacies, with a lower brackish unit (estuary) showing upward transition to freshwater deposits (coastal plain). Parasequence development suggests that relative sea-level change during latest Pleistocene-Holocene was episodic and punctuated by rapid phases of sea-level rise, followed by periods of stillstand.

- 5) On the basis of radiocarbon dating, the onset of valley incision appears to be related to the

remarkable sea-level fall that accompanied OIS 3/2 transition. It can not been ruled out, however, that incision also continued during early stages of transgression.

Acknowledgements

This project received funding from Bologna University, as part of *Progetto Strategico d'Ateneo*, grant to A. Amorosi. We would like to thank Margherita Aguzzi for early work on the Arno valley fill. We are strongly indebted to Martin Gibling and Salvatore Milli for their very accurate reviews.

Figure captions

Fig. 1. Planview geometry of the late Quaternary Arno valley fill, with indication of the dataset used for stratigraphic correlations.

Fig. 2. Stratigraphy of core M1 (see Fig. 1, for its location), showing detailed facies characteristics of the Arno valley fill at distal-most locations (after Aguzzi et al., 2007, slightly modified). SB: Sequence Boundary, TS: Transgressive Surface. ^{14}C dates younger than 20,000 yr BP are expressed as calibrated ages BP.

Fig. 3. Cross-sections transversal to the Arno valley fill (see Fig. 1, for their location), showing internal facies architecture at relatively distal locations. ^{14}C dates younger than 20,000 yr BP are expressed as calibrated ages BP. Continuously-cored boreholes for which detailed facies analysis is available are shown in red.

Fig. 4. Cross-sections transversal to the Arno valley fill (see Fig. 1, for their location), showing internal facies architecture at relatively proximal locations. ^{14}C dates are expressed as calibrated ages BP. Continuously-cored boreholes for which detailed facies analysis is available are shown in red.

Fig. 5. Three-dimensional architecture of the late Quaternary Arno valley fill, showing distinctive along-dip variability in facies architecture (see transversal cross-sections of Figs. 3 and 4). SB: Sequence Boundary, TS: Transgressive Surface, BRS: Bay Ravinement Surface, TRS: Tidal Ravinement Surface, WRS: Wave Ravinement Surface, MFS: Maximum Flooding Surface.

Fig. 6. Schematic representation of the Arno valley fill with geologic interpretation. ^{14}C dates

younger than 20,000 yr BP are expressed as calibrated ages BP. Hatched lines show interpretation of fluvial deposits on the valley flanks as fluvial terraces (not shown in Figs. 4 and 5). Cores are projected from different transversal cross-sections.

References

- AGUZZI M., AMOROSI A. and SARTI G., 2005. Stratigraphic architecture of Late Quaternary deposits in the lower Arno Plain (Tuscany, Italy). *Geologica Romana* 38, 1-10.
- AGUZZI M., AMOROSI A., COLALONGO M.L., RICCI LUCCHI M., ROSSI V., SARTI G. and VAIANI S.C., 2007. Late Quaternary climatic evolution of the Arno coastal plain (Western Tuscany, Italy) from subsurface data. *Sedimentary Geology*, 202, 211-229.
- AITKEN J.F. and FLINT S., 1996. Variable expressions of interfluvial sequence boundaries in the Breathitt Group (Pennsylvanian), eastern Kentucky, USA. In: Howell J.A. and Aitken J.F. (eds.) *High resolution sequence stratigraphy: Innovations and applications. Geological Society London Special Publication* 104, 193-206.
- ALLEN G.P. and POSAMENTIER H.W., 1993. Sequence stratigraphy and facies model of an incised valley fill: the Gironde estuary, France. *Journal of Sedimentary Petrology* 63, 378-391.
- AMOROSI A., CENTINEO M.C., COLALONGO M.L. and FIORINI F., 2005. Millennial-scale depositional cycles from the Holocene of the Po Plain, Italy. *Marine Geology* 222-223, 7-18.
- ARGNANI A., BERNINI M., DI DIO G.M., PAPANI G. and ROGLEDI S., 1997. Stratigraphic record of crustal scale tectonics in the Quaternary of the Northern Apennines (Italy). *Il Quaternario* 10, 595-602.
- BALDACCI F., BELLINI L. and RAGGI G., 1994. Le risorse idriche sotterranee della Pianura di Pisa. *Atti*

della Società Toscana di Scienze Naturali Memorie Serie A 101, 241-322.

BELLOTTI P., CHIOCCI F.L., MILLI S., TORTORA P. and VALERI P., 1994. Sequence stratigraphy and depositional setting of the Tiber delta: integration of high-resolution seismics, well logs, and archeological data. *Journal of Sedimentary Research* B64, 416-432.

BELLOTTI P., MILLI S., TORTORA P. and VALERI P., 1995. Physical stratigraphy and sedimentology of the Late Pleistocene-Holocene Tiber Delta depositional sequence. *Sedimentology* 42, 617-634.

BERNARD H.A. and LEBLANC R.J., 1965. Resume of the Quaternary geology of the northwestern Gulf of Mexico Province. In: Wright H.E. and Frey D.G. (eds.) *The Quaternary of the United States*. Princeton University Press, 137-185.

BLUM M.D. and ASLAN A., 2006. Signatures of climate vs. sea-level change within incised valley-fill successions: Quaternary examples from the Texas Gulf Coast. *Sedimentary Geology* 190, 177-211.

BLUM M.D. and PRICE D.M., 1998. Quaternary alluvial plain construction in response to interacting glacio-eustatic and climatic controls, Texas Gulf Coastal Plain. In: Shanley K.W. and McCabe P.W. (eds.) *Relative Role of Eustasy, Climate, and Tectonism in Continental Rocks. SEPM Special Publication* 59, 31-48.

BLUM M.D., TOOMEY R.S. III and VALASTRO S., 1994. Fluvial response to Late Quaternary climatic and environmental change, Edwards Plateau, Texas. *Palaeogeography Palaeoclimatology Palaeoecology* 108, 1-21.

BOSKI T., MOURA D., VEIGA-PIRES C., CAMACHO S., DUARTE D., SCOTT D.B. and FERNANDES S.G., 2002. Postglacial sea-level rise and sedimentary response in the Guadiana Estuary, Portugal/Spain border. *Sedimentary Geology* 150, 103-122.

BOYER J., DUVAIL C., LE STRAT P., GENSOUS B. and TESSON M., 2005. High resolution stratigraphy and resolution of the Rhône delta plain during Postglacial time, from subsurface drilling data bank. *Marine Geology* 222-223, 267-298.

CANTINI P., TESTA G., ZANCHETTA G. and CAVALLINI R., 2001. The Plio-Pleistocene evolution of extensional tectonics in northern Tuscany, as constrained by new gravimetric data from the Montecarlo Basin (lower Arno Valley, Italy). *Tectonophysics* 330, 25-43.

CARMIGNANI L., DECANDIA F.A., FANTOZZI P.L., LAZZAROTTO A., LOTTA D. and MECCHERI M., 1994. Tertiary extensional tectonics in Tuscany (northern Apennines, Italy). *Tectonophysics* 238, 295-315.

CERRINA FERONI A., LEONI L., MARTELLI L., MARTINELLI P., OTTRIA G. and SARTI G., 2001. The Romagna Apennines, Italy; an eroded duplex. *Geological Journal* 36/1, 39-54.

DABRIO C.J., ZAZO C., GOY J.L., SIERRA F.J., BORJA F., LARIO J., GONZÁLEZ J.A. and FLORES J.A., 2000. Depositional history of estuarine infill during the last postglacial transgression (Gulf of Cádiz, southern Spain). *Marine Geology* 162, 381-404.

DALRYMPLE R.W., 2006. Incised valleys in time and space: introduction to the volume and an examination of the controls on valley formation and filling. In: Dalrymple R.W., Leckie D.A. and Tillman R. (eds.) *Incised Valleys in Time and Space. SEPM Special Publication* 85, 5-12.

DALRYMPLE R.W., and CHOI K., 2007. Morphologic and facies trends through the fluvial–marine transition in tide-dominated depositional systems: A schematic framework for environmental and sequence-stratigraphic interpretation. *Earth-Science Reviews* 81, 135-174.

DALRYMPLE R.W. and ZAITLIN B.A., 1994. High-resolution sequence stratigraphy of a complex, incised valley succession, the Cobequid Bay- Salmon River estuary, Bay of Fundy, Canada. *Sedimentology* 41, 1069-1091.

DALRYMPLE R.W., ZAITLIN B.A. and BOYD R., 1992. Estuarine facies models: conceptual basis and stratigraphic implications. *Journal of Sedimentary Petrology* 62, 1130-1146.

DALRYMPLE R.W., BOYD, R., and ZAITLIN, B.A., 1994. History of research, types and internal organization of incised-valley systems: Introduction to the volume. In: Dalrymple R.W., Boyd R. and Zaitlin B.A. (eds.) *Incised-Valley Systems: Origin and Sedimentary Sequences. SEPM Special Publication* 51, 3–10.

DELLA ROCCA R., MAZZANTI R. and PRANZINI E., 1987. Studio geomorfologico della Pianura di Pisa (Toscana). *Geografia Fisica e Dinamica Quaternaria* 10, 56-84.

DEMAREST II J.M. and KRAFT J.C., 1987. Stratigraphic record of Quaternary sea levels: implications for more ancient strata. In: Nummedal D., Pilkey O.H. and Howard J.D. (eds.) *Sea-Level Fluctuation and Coastal Evolution. Society of Economic Paleontologists and Mineralogists Special Publication* 41, 223-239.

FANCELLI R., GRIFONI R., MAZZANTI R., MENCHELLI S., NENCINI C., PASQUINUCCI M. and TOZZI C., 1986. Evoluzione della Pianura di Pisa. In: Mazzanti R., Grifoni Cremonesi R., Pasquinucci M. and

Pult Quaglia A.M. (eds.) *Terre e Paduli. Reperti, documenti, immagini per la storia di Coltano*.
Bandedecchi e Vivaldi, Pontedera, 23-29.

FEDERICI P.R. and MAZZANTI R., 1989. The Pisa plain (Italy) and its hydrological hazards.
Supplementi Geografia Fisica e Dinamica Quaternaria 2, 41-49.

FENIES H. and LERICOLAIS G., 2005. Internal architecture of an incised valley-fill on a wave- and
tide-dominated coast (the Leyre incised valley, Bay of Biscay, France). *Comptes Rendus
Geosciences* 337, 1257-1266.

FIELDING C.R., and GIBLING M.R., 2005. Distinguishing between channel and valley fills:
definitions, diagnostic criteria and dimensional data. *8th International Conference on Fluvial
Sedimentology: Delft, Netherlands, Abstracts*, 101.

FISK H.N., 1944. *Geological investigation of the alluvial valley of the lower Mississippi River*.
Vicksburg, U.S. Army Corps of Engineers, Mississippi River Commission.

FOYLE A.M. and OERTEL G.F., 1997. Transgressive systems tract development and incised-valley
fills within a Quaternary estuary-shelf system: Virginia inner shelf, USA. *Marine Geology* 137,
227-249.

GIBLING M.R., 2006. Width and thickness of fluvial channel bodies and valley fills in the geological
record: a literature compilation and classification. *Journal of Sedimentary Research* 76, 731-770.

GIBLING M.R. and BIRD D.J., 1994. Late Carboniferous cyclothems and alluvial paleovalleys in the
Sydney basin, Nova Scotia. *Geological Society America Bulletin* 106, 105-117.

GHELARDONI R., GIANNINI E. and NARDI R., 1968. Ricostruzione paleogeografia dei bacini neogenici e quaternari nella bassa valle dell'Arno sulla base dei sondaggi e dei rilievi sismici. *Memorie della Società Geologica Italiana* 7, 91-106.

HEAP A.D. and NICHOL S.L., 1997. The influence of limited accommodation space on the stratigraphy of an incised-valley succession: Weiti River Estuary, New Zealand. *Marine Geology* 144, 229-252.

HORI K., SAITO Y., ZHAO Q. and WANG P., 2002. Evolution of the coastal depositional systems of the Changjiang (Yangtze) River in response to late Pleistocene–Holocene sea-level changes. *Journal of Sedimentary Research* 72, 884-897.

KHADKIKAR A.S. and RAJSHEKHAR C., 2005. Holocene valley incision during sea level transgression under a monsoonal climate. *Sedimentary Geology* 179/3-4, 295-303.

LI C.X., WANG P., SUN H.P., ZHANG J.Q, FAN D.D. and DENG B., 2002. Late Quaternary incised-valley fill of the Yangtze delta (China): its stratigraphic framework and evolution. *Sedimentary Geology* 152, 133-158.

LI Z., SAITO Y., MATSUMOTO E., WANG Y., TANABE S. and VU Q.L., 2006. Climate change and human impact on the Song Hong (Red River) delta, Vietnam, during the Holocene. *Quaternary International* 144, 4-28.

LOWRIE, A. and HAMITER, R., 1995. Fifth and sixth order eustatic events during Holocene, fourth order highstand influencing Mississippi delta-lobe switching. In: Finkl C.W., Jr. (ed.) *Holocene cycles: climate, sea Levels and sedimentation*. *Journal of Coastal Research* 17, 225-229.

MALINVERNO A. and RYAN W.B.F., 1986. Extension in the Tyrrhenian sea and shortening in the Apennines as a result of arc migration driven by sinking of the lithosphere. *Tectonics* 5, 227-245.

MARIANI M. and PRATO R., 1988. I bacini Neogenici costieri del margine tirrenico: approccio sismico-stratigrafico. *Memorie della Società Geologica Italiana* 41, 519-531.

MARTINI I.P. and SAGRI M., 1993. Tectono-sedimentary characteristic of late Miocene-Quaternary extensional basin of Northern Apennines. *Earth Science Reviews* 34, 197-233.

MARTINI I.P., SAGRI M. and COLELLA A., 2001. Neogene-Quaternary basins of the inner Apennines and Calabrian Arc. In: Vai G.B. and Martini I.P. (eds.) *Anatomy of an Orogen: the Apennines and Adjacent Mediterranean basin*. Kluwer Academic Publ., Dordrecht, 375-400.

MAZZANTI R., 2000. Geomorfologia del bacino Versiliese-Pisano con particolare riferimento alla "Gronda dei Lupi", scarpata fossile che separa le Colline Livornesi, con i loro terrazzi eustatici, dalla pianura alluvionale pisana. *Atti della Società Toscana di Scienze Naturali Memorie Serie A* 107, 165-189.

MCCARTHY P.J. and PLINT A.G., 1998. Recognition of interfluvial sequence boundaries: Integrating paleopedology and sequence stratigraphy. *Geology* 26, 387-390.

MILLI S., 1997. Depositional setting and high-frequency sequence stratigraphy of the Middle-Upper Pleistocene to Holocene deposits of the Roman Basin. *Geologica Romana* 33, 99-136.

MILLI S., MOSCATELLI M., PALOMBO M.R., PARLAGRECO L. and PACIUCCI M., this volume. Incised valleys, their filling and mammal fossil record: a case study from the Middle-Upper Pleistocene

deposits of the Roman Basin (Latium, Italy). In: Amorosi A., Haq B., Sabato L. and Tropeano M. (eds.). *GeoActa Special Publication*.

MUTO T. and STEEL R., 2004. Autogenic response of fluvial deltas to steady sea-level fall; implications from flume-tank experiments. *Geology* 32, 401-404.

NICHOL S.L., BOYD R. and PENLAND S., 1994. Stratigraphic response of wave-dominated estuaries to different relative sea-level and sediment supply histories: Quaternary case studies from Nova Scotia, Louisiana and Eastern Australia. In: Dalrymple R.W., Boyd R. and Zaitlin B.A. (eds.) *Incised-Valley Systems: Origin and Sedimentary Sequences. SEPM Special Publication* 51, 265-283.

NUMMEDAL D. and SWIFT D.J.P., 1987. Transgressive stratigraphy at sequence-bounding unconformities: some principles derived from Holocene and Cretaceous examples. In: Nummedal D., Pilkey O.H. and Howard J.D. (eds.) *Sea-Level Fluctuation and Coastal Evolution. SEPM Special Publication* 41, 241-260.

PASCUCCI V., 2005. Neogene evolution of the Viareggio Basin, Northern Tuscany (Italy). *GeoActa* 4, 123-138.

PASCUCCI V., FONTANESI G., MERLINI S. and MARTINI I.P., 2001. Neogene tuscan shelf-western Tuscany extension evidences of the early post-compressional deposits (Tyrrhenian Sea - Northern Apennines, Italy). *Ofioliti* 26/2a, 187-196.

PATACCA E., SARTORI R. and SCANDONE P., 1990. Tyrrhenian basin and Apenninic arcs: kinematic relations since late Tortonian times. *Memorie della Società Geologica Italiana* 45, 425-451.

PLINK-BJORKLUND P., 2005. Stacked fluvial and tide-dominated estuarine deposits in high frequency (fourth-order) sequences of the Eocene central Basin, Spitsbergen. *Sedimentology* 52, 391-428.

PLINT A.G., MCCARTHY P.J. and FACCINI U.F., 2001. Nonmarine sequence stratigraphy: Updip expression of sequence boundaries and systems tracts in a high-resolution framework, Cenomanian Dunvegan Formation, Alberta foreland basin, Canada. *American Association Petroleum Geologists Bulletin* 85, 1967-2001.

POSAMENTIER H.W. and ALLEN G.P., 1993. Siliciclastic sequence stratigraphic patterns in foreland ramp-type basins. *Geology* 21, 455-458.

POSAMENTIER H.W. and VAIL P.R., 1988. Eustatic controls on clastic deposition II – Sequence and systems tract models. In: Wilgus C.K., Hastings B.S., Kendall C.G.St.C., Posamentier H.W., Ross C.A. and Van Wagoner J.C. (eds.) *Sea-Level Changes: an Integrated Approach. Society of Economic Paleontologists and Mineralogists Special Publication* 42, 125-154.

POSAMENTIER H.W., JERVEY M.T. and VAIL P.R., 1988. Eustatic controls on clastic deposition I: Conceptual framework. In: Wilgus C.K., Hastings B.S., Kendall C.G.St.C., Posamentier H.W., Ross C.A. and Van Wagoner J.C. (eds.) *Sea Level Changes: An Integrated Approach. SEPM Special Publication* 42, 109-124.

RAHMANI R.A., 1988. Estuarine tidal channel and nearshore sedimentation of a Late Cretaceous epicontinental sea, Drumheller, Alberta, Canada. In: de Boer P.L., van Gelder A. and Nio S.D. (eds.) *Tide-influenced Sedimentary Environments and Facies*. Reidel Publishing Co., Dordrecht, 433-471.

ROMAGNOLI L., 1957. Sondaggi a 200 m di profondità nel Quaternario recente presso Pisa. Studio delle facies attraversate e considerazioni sulla sedimentazione costiera a carattere ciclico. *Bollettino della Società Geologica Italiana* 76, 21-35.

SARTORI F., 1978. Studi sedimentologici e mineralogici delle alluvioni recenti della pianura pisana. I sedimenti del sondaggio della Bigattiera, presso S. Piero a Grado (Pisa). *Atti della Società Toscana di Scienze Naturali Memorie Serie A* 85, 61-93.

SARTORI R., 1989. Evoluzione neogenico-recente del bacino tirrenico e suoi rapporti con la geologia delle aree circostanti. *Giornale di Geologia* 51, 1-30.

SCHUMM, S.A. and ETHRIDGE F.G., 1994. Origin, evolution and morphology of fluvial Valleys. In: Dalrymple R.W., Boyd R. and Zaitlin B.A. (eds.) *Incised-Valley Systems: Origin and Sedimentary Sequences. SEPM Special Publication* 51, 11-27.

SOMOZA L., BARNOLAS A., ARASA A., MAESTRO A., REES J.G. and HERNANDEZ-MOLINA F.J., 1998. Architectural stacking patterns of the Ebro delta controlled by Holocene high-frequency eustatic fluctuations, delta-lobe switching and subsidence processes. *Sedimentary Geology* 117, 11-32.

STRONG N. and PAOLA C., 2006. Fluvial landscapes and stratigraphy in a flume. *The Sedimentary Record* 4, 4-8.

SWIFT D.J.P., 1968. Coastal erosion and transgressive stratigraphy. *Journal of Geology* 76, 444-456.

THOMAS M.A. and ANDERSON J.B., 1994. Sea-level controls on the facies architecture of the Trinity/Sabine incised-valley system, Texas continental shelf In: Dalrymple R.W., Boyd R. and

Zaitlin B.A. (eds.) *Incised-Valley Systems: Origin and Sedimentary Sequences. SEPM Special Publication 51*, 63-82.

VAN WAGONER J.C., MITCHUM R.M., CAMPION K.M. and RAHMANIAN V.D. (eds.), 1990. *Siliclastic sequence stratigraphy in well logs, cores and outcrops: concepts for high resolution correlations of time and facies*. American Association of American Petroleum Geologists. Methods in Exploration 7 Barbara H. Lidtz, Tulsa.

WEBER N., CHAUMILLON E., TESSON M. and GARLAN T., 2004. Architecture and morphology of the outer segment of a mixed tide and wave-dominated-incised valley, revealed by HR seismic reflection profiling: the paleo-Charente River, France. *Marine Geology* 207, 17-38.

WELLNER R.W. and BARTEK L.R., 2003. The effect of sea level, climate, and shelf physiography on the development of incised-valley complexes: a modern example from the East China Sea. *Journal of Sedimentary Research* 73, 926-940.

WOOD J.W. and HOPKINS J.C., 1989. Reservoir sandstone bodies in estuarine valley fill: Lower Cretaceous Glauconitic Member, Little Bow Field, Alberta, Canada. *American Association of Petroleum Geologists Bulletin* 73, 1361-1382.

ZAITLIN B.A., DALRYMPLE R.W. and BOYD R., 1994. The stratigraphic organization of incised-valley systems associated with relative sea-level change. In: Dalrymple R.W., Boyd R. and Zaitlin B.A. (eds.) *Incised-Valley Systems: Origin and Sedimentary Sequences. SEPM Special Publication 51*, 45-60.

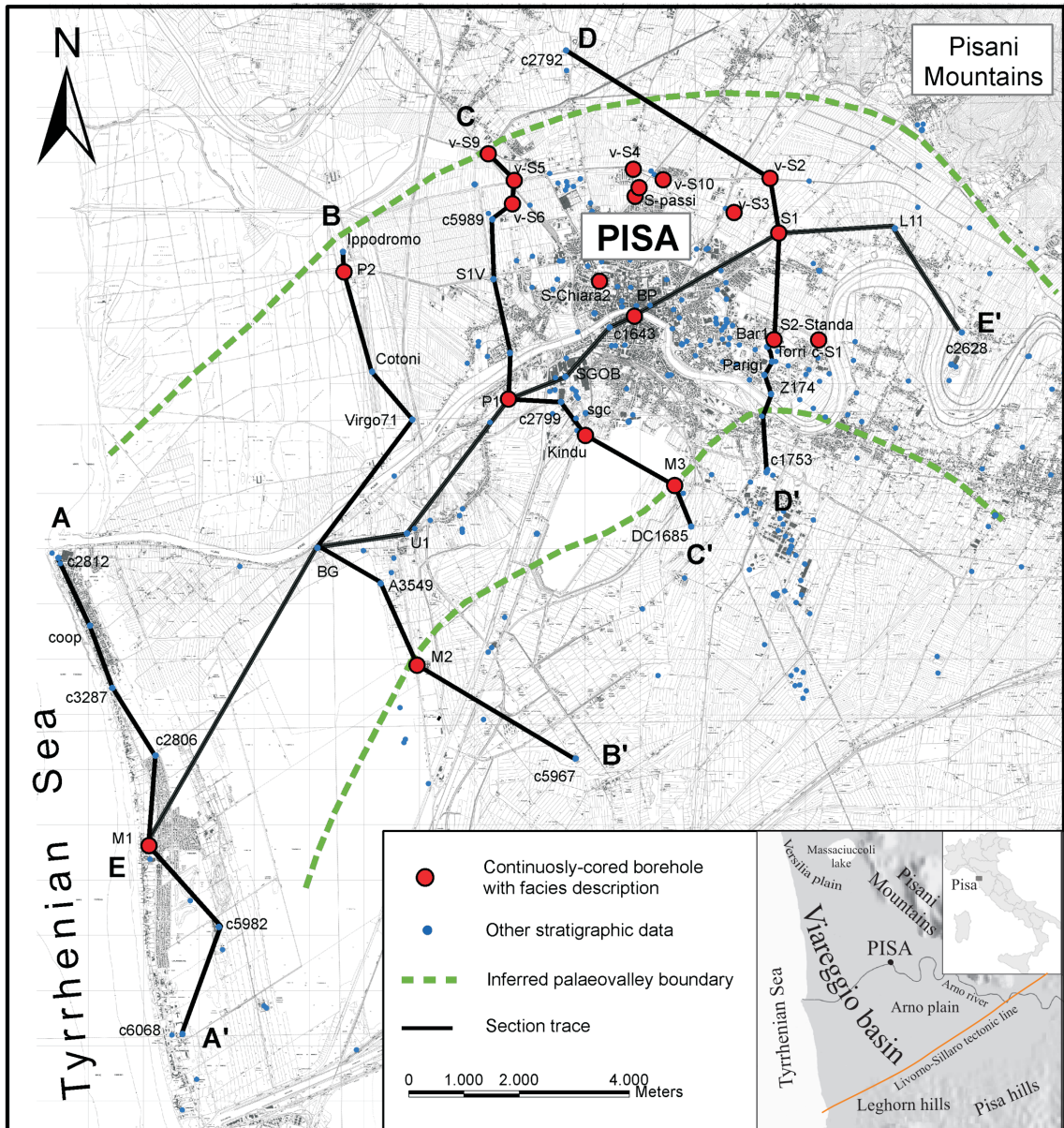


Figure 1

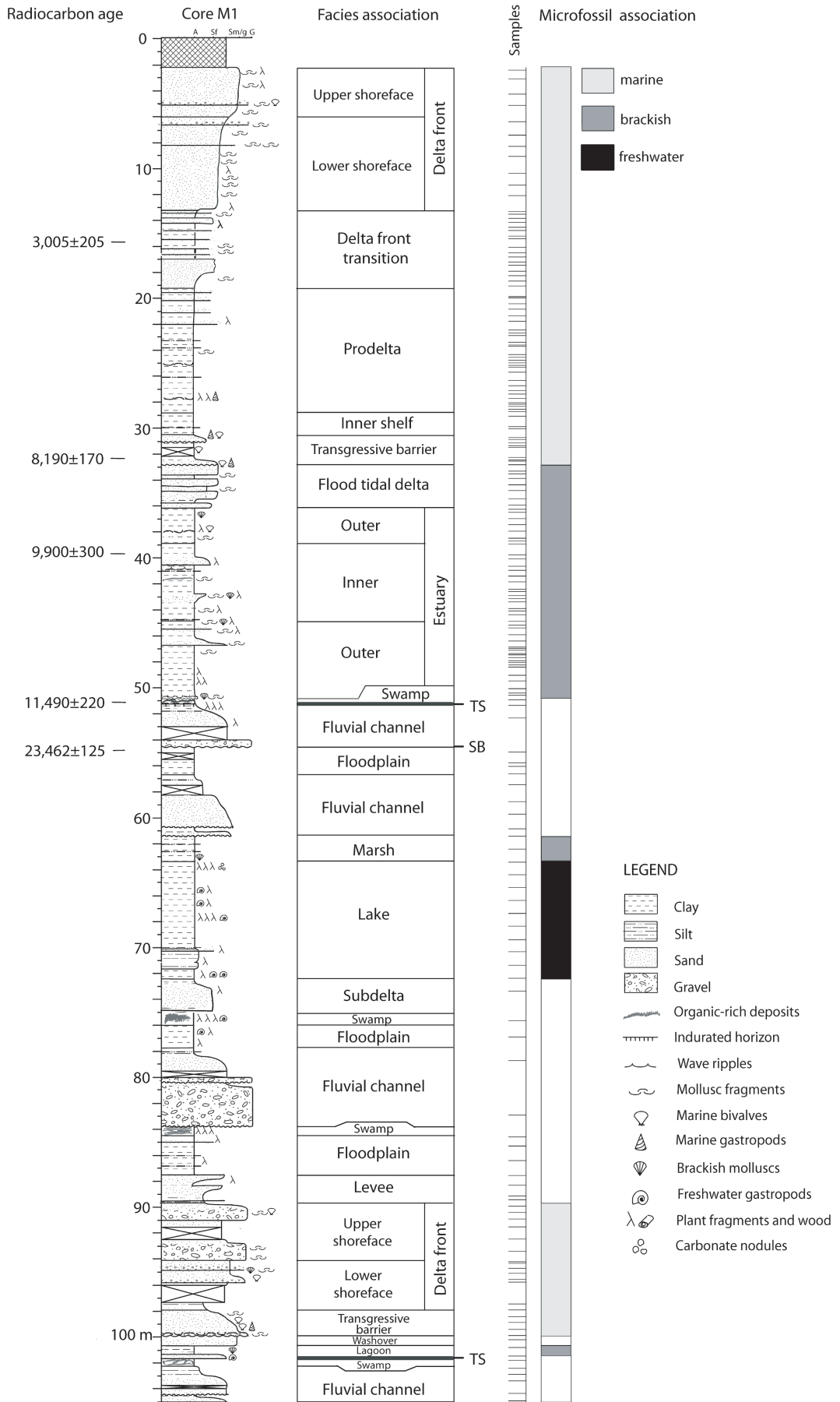


Figure 2

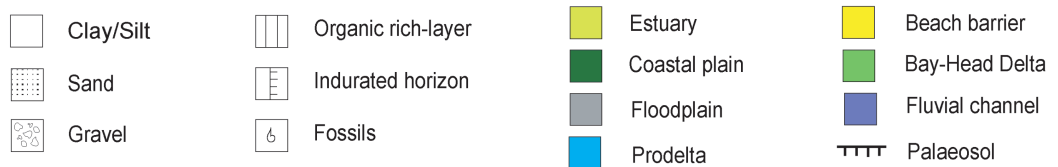
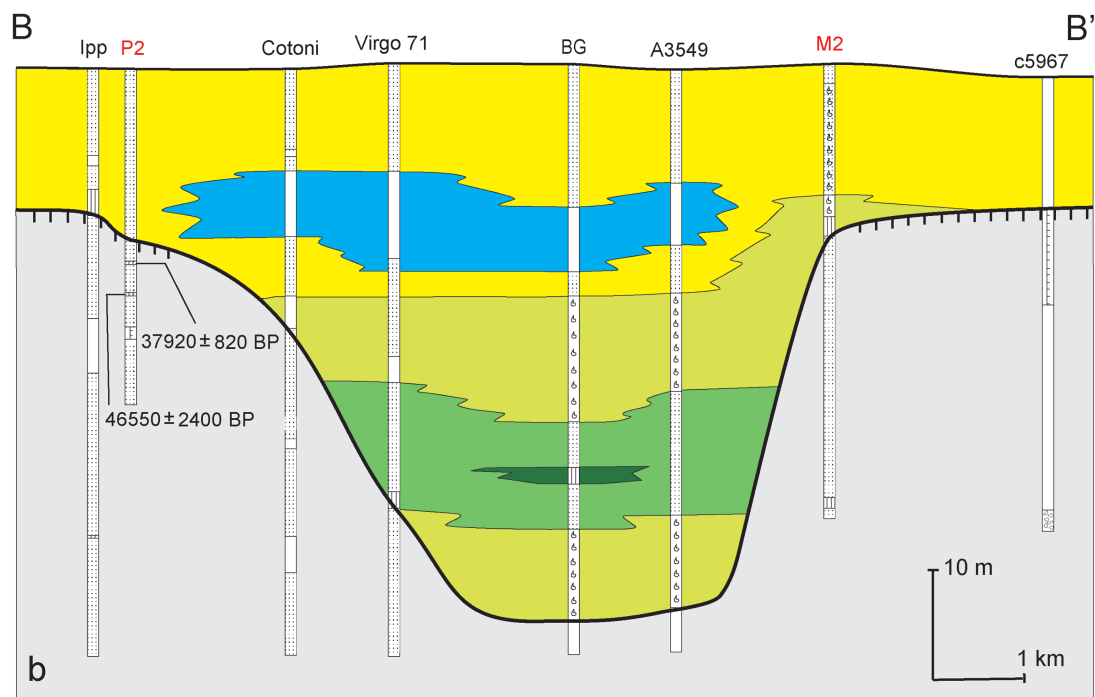
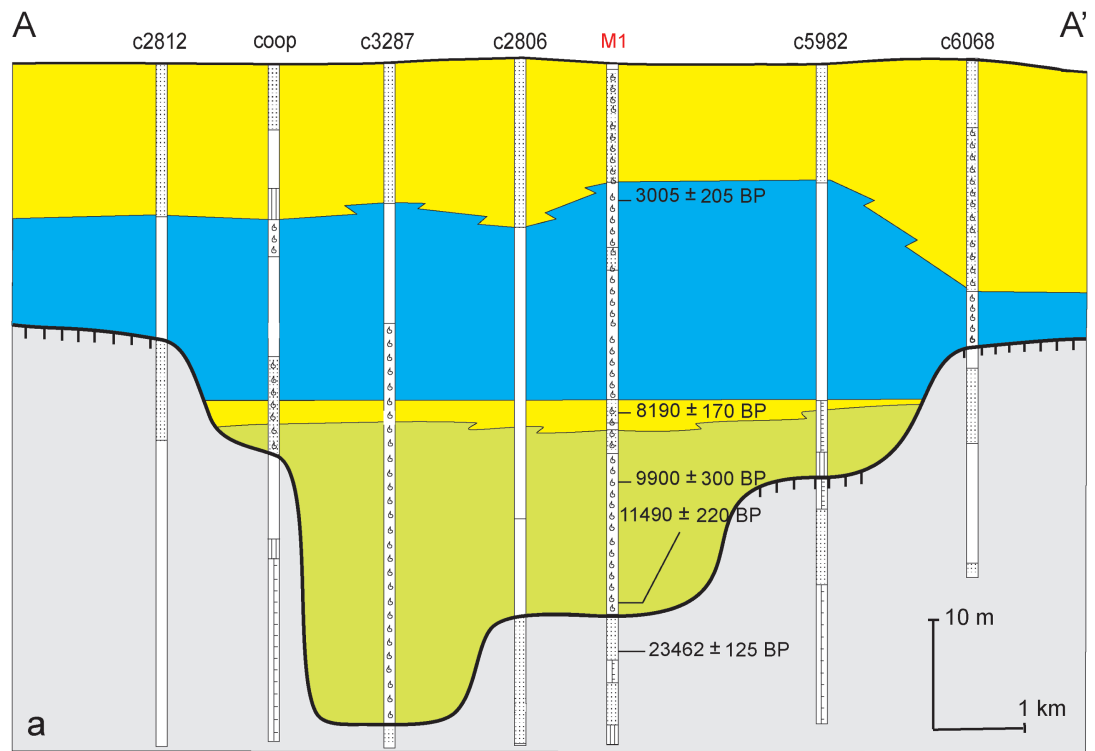


Figure 3

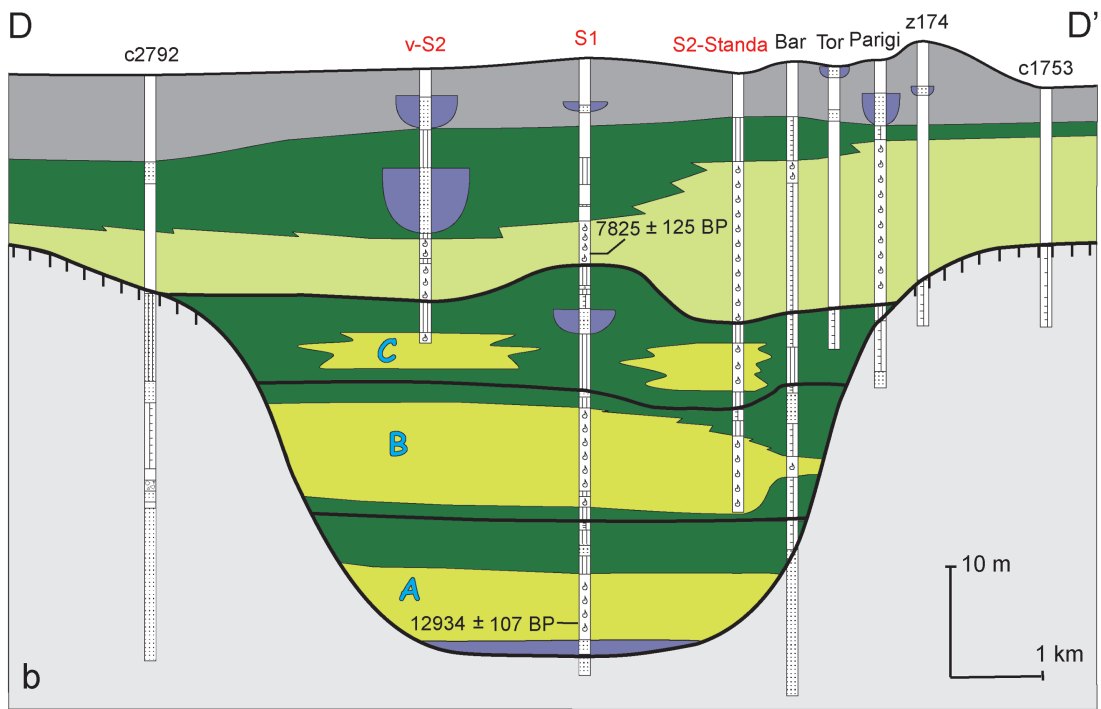
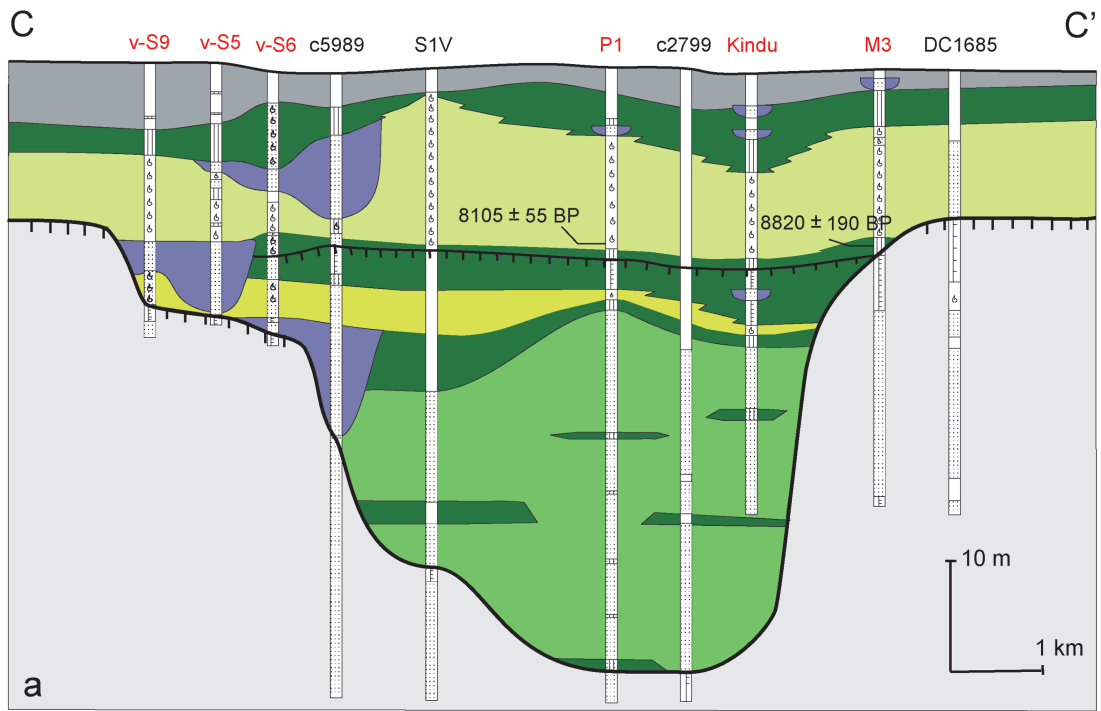


Figure 4

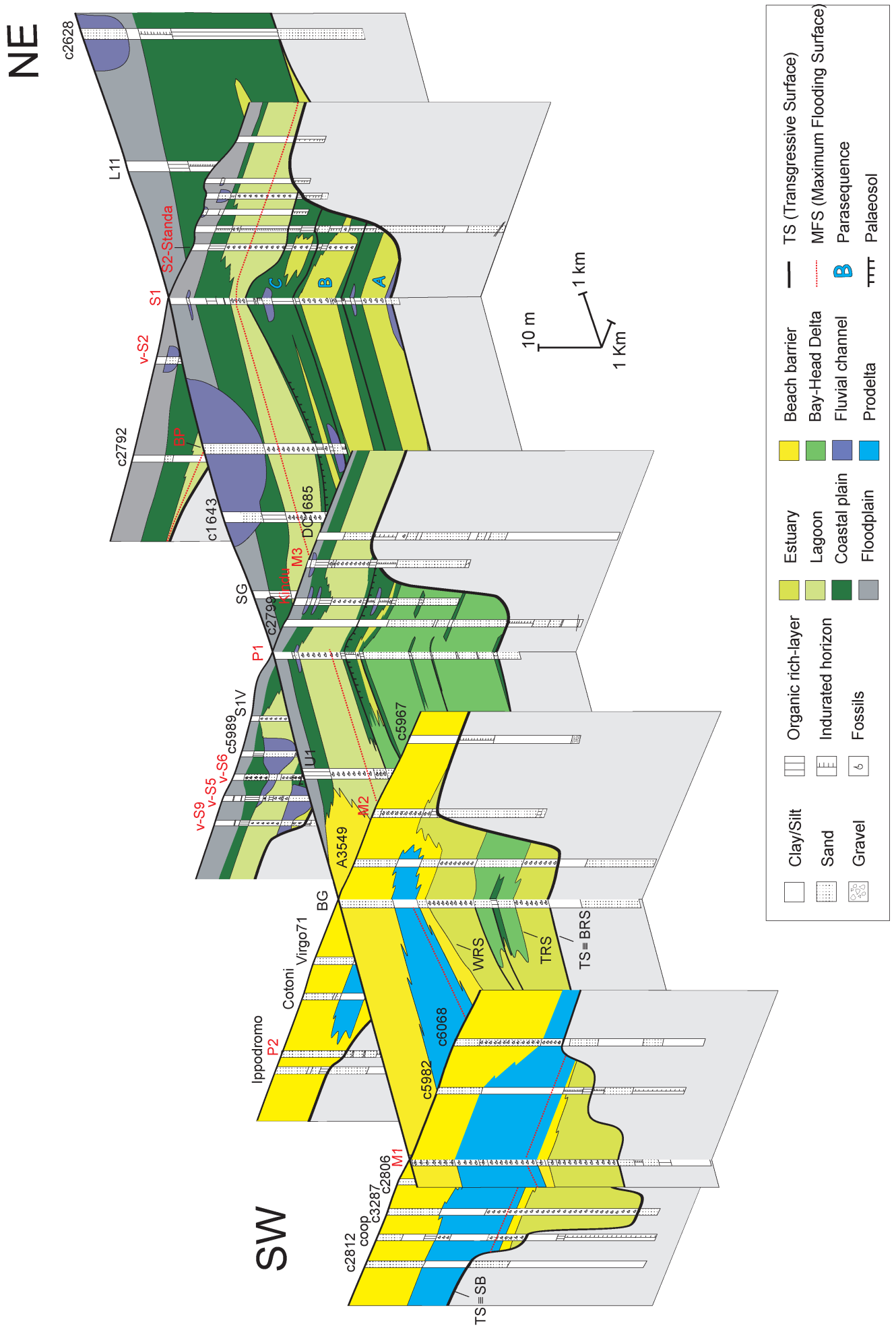


Figure 5

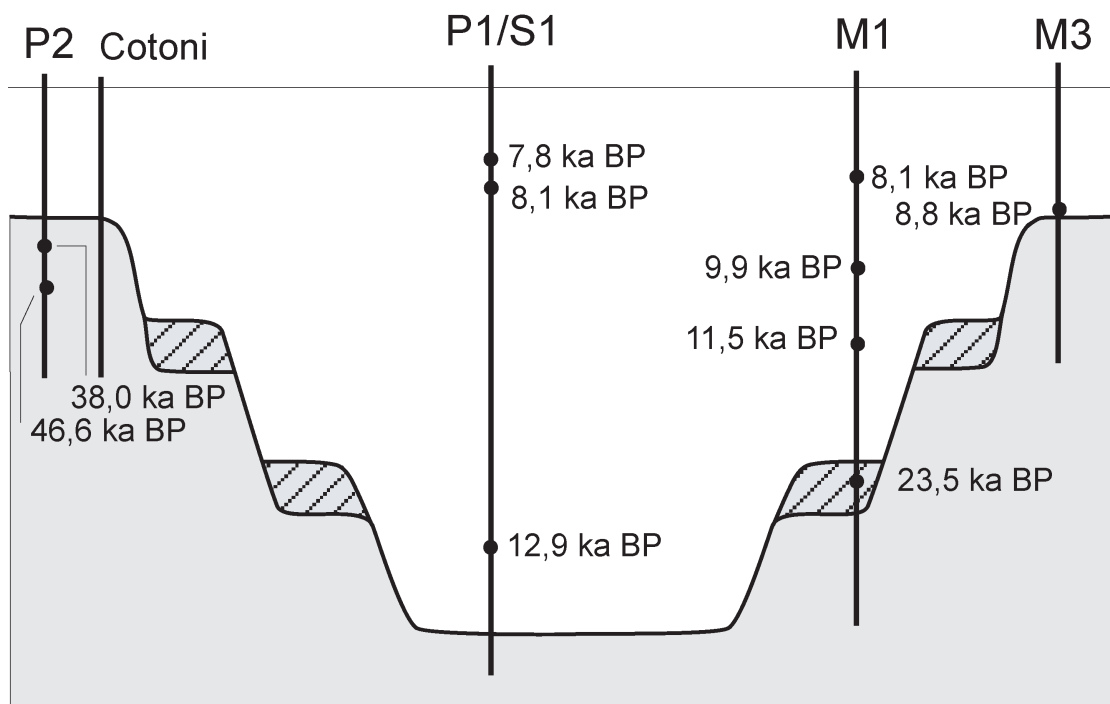


Figure 6

Paper 3

Climatic signature of millennial-scale parasequences from Lateglacial-Holocene transgressive deposits of Arno valley fill (Tuscany, Italy)

Amorosi, A., Ricci Lucchi, M., **Rossi, V.** and Sarti, G.

Climatic signature of millennial-scale parasequences from Lateglacial-Holocene transgressive deposits of Arno valley fill (Tuscany, Italy)

Alessandro Amorosi^{1*}, Marianna Ricci Lucchi¹, Veronica Rossi¹ and Giovanni Sarti²

¹Dipartimento di Scienze della Terra e Geologico-Ambientali, Università di Bologna, Via Zamboni 67, 40126 Bologna, Italy

²Dipartimento di Scienze della Terra, Università di Pisa, Via Santa Maria 53, 56126 Pisa, Italy

*Corresponding author: Tel: +39 051 2094586; Fax: +39 051 2094522; E-mail: alessandro.amorosi@unibo.it

Abstract

Despite recent report of millennial-scale cyclicality from Lateglacial-Holocene deposits of several coastal plains worldwide, no precise documentation of the key factors controlling cyclic facies architecture has been made available by previous work.

Detailed sedimentological analysis of a continuously-cored borehole, around the town of Pisa, in western Tuscany, provides evidence for the occurrence of three millennial-scale, transgressive-regressive cycles within the post-Last Glacial Maximum (LGM) transgressive succession (13-8 cal. kyr BP) of the Arno incised-valley fill. These cycles, which are bounded by lateral equivalents of marine flooding surfaces, are 8-12 m thick and correspond to small-scale parasequences. Micropalaeontological (foraminifers and ostracods) investigations based upon differentiation of eight microfaunal associations, allow to refine the stratigraphic framework, emphasizing subtle changes in palaeosalinity across parasequence boundaries.

Diagnostic changes in vegetation patterns, driven by opposite climate conditions, enable precise documentation of parasequence development as a function of climate change. Pollen spectra invariably show expansions of broad-leaved forests at parasequence boundaries, suggesting that rapid shifts to warmer climate conditions accompanied episodes of rapid sea-level rise. In contrast, stillstand phases saw the development of cold-temperate communities (upper parts of parasequences), suggesting transition to temporary colder climate conditions.

Reconstruction of parasequence architecture on the basis of adjacent stratigraphic data, combined with palaeoclimate characterization and radiometric dating enable identification, within the transgressive Arno valley body, of three major “regressive” pulsations, two of which may be correlated with the most important cooling events of the post-LGM period: the Younger Dryas and the 8,200 cal. yr BP event, respectively. The sedimentary response to these short-term phases of climatic cooling is clearly documented by episodes of widespread coastal-plain and bay-head delta

progradation, leading to partial estuary infilling and temporary establishment of continental environments in the proximal and central sectors of the valley.

Keywords

Climate change, Millennial-scale cycles, Parasequence, Palinology, Holocene, Tuscany.

Introduction

The need to predict characteristics of future climate change and their potential environmental and social consequences has stimulated, during the last decade, an increasing interest of the scientific community toward Lateglacial and Holocene climate variability (e.g., IPCC, 2001, 2007; National Research Council-NRC, 2002; Alley *et al.*, 2003).

There is widespread evidence today of rapid, millennial-scale climate oscillations for the post-glacial period (ca. 15,000 cal. yr BP to present), and the occurrence of Holocene, millennial- to centennial-scale climate events is globally well documented, although the driving factors of this cyclicity are not completely understood (Bond *et al.*, 1997; Mayewski *et al.*, 2004).

In the Northern Hemisphere, six periods of significant Holocene climatic deterioration (rapid climate changes-RCC in Mayewski *et al.*, 2004), coeval with the main phases of glacier fluctuations in Europe and North America (Denton and Karlén, 1973), have been identified from high- to low-latitudes, within a varied depositional record (e.g. ice cores, marine and lacustrine successions, speleothems).

Potential correlative cold events have been identified by Bond *et al.* (1997) within the sedimentary record of two North Atlantic deep-sea cores, by means of integrated petrographic and micropalaeontological analyses. High-resolution AMS radiocarbon dating has enabled identification in this succession of a millennial-scale cyclicity, with periodicity of about $1,470 \pm 500$ years, encompassing about the last 13,000 cal. yr BP.

The vertical stacking of millennial-scale depositional cycles, bounded by marine flooding surfaces or their lateral equivalents, and characterized by shallowing-upward tendencies (parasequences *sensu* Van Wagoner *et al.*, 1990 and Kamola and Van Wagoner, 1995), has been reported from late Quaternary, post-Last Glacial Maximum (LGM) successions worldwide: namely, Mississippi Delta (Lowrie and Hamiter, 1995), Ebro Delta (Somoza *et al.*, 1998), Gulf of Cadiz

(Gonzales *et al.*, 2004), Po Coastal Plain (Amorosi *et al.*, 2005), Rhône Delta (Boyer *et al.*, 2005), and St. Jones estuary (Leorri *et al.*, 2006). A combination of small-scale sea-level fluctuations with rapid climate change has been invoked in these works as the major controlling factor of stratigraphic architecture. However, no unambiguous evidence of a direct link between post-LGM parasequence development and specific climatic events has been documented, so far.

The objective of this work is to provide, for the first time, detailed documentation of the sedimentary response to Lateglacial and Holocene climate variability, through pollen characterization of vertically-stacked, millennial-scale parasequences. The overwhelming control of glacioeustasy during post-LGM transgression makes the transgressive systems tract (TST) of the late Quaternary depositional sequence as an ideal site to test the direct influence of small-scale climatic and eustatic fluctuations on the stacking pattern of high-frequency depositional cycles (Amorosi and Milli, 2001).

Recent identification in the Arno coastal plain, Western Tuscany (Fig. 1), of a 35-40 m thick succession of Holocene, transgressive incised-valley fill deposits (see Core M1 in Aguzzi *et al.*, 2007) makes this area suitable for high-resolution palaeoenvironmental and palaeoclimatic studies. The valley fill in Core M1 consists of a relatively monotonous succession of estuarine deposits. In order to detect more subtle facies variations at the estuarine-continental transition, a continuously-cored borehole, 56 m deep, was drilled about 15 km landwards along the palaeovalley axis, close to the town of Pisa (Core S1 in Fig. 1). Core S1 was submitted to detailed sedimentological, micropalaeontological and palynological investigations.

Post-LGM stratigraphy of Arno coastal plain

Few studies only have focused on post-LGM subsurface stratigraphy of Arno coastal plain. Unfortunately, most of them are based upon interpretation of poor-quality data, *i.e.* boreholes drilled for water research that lack detailed stratigraphic information and reliable chronologic control (Romagnoli, 1957; Sartori, 1978; Della Rocca *et al.*, 1987; Baldacci *et al.*, 1994; Federici and Mazzanti, 1995; Mazzanti, 2000).

On the basis of pollen data from 19 continuously-cored boreholes drilled south of Arno River, near Leghorn (Fig. 1), Galletti Fancelli (1978) assigned the uppermost 30 m to the Sub-Atlantic and Boreal phases, in agreement with an uncalibrated radiocarbon age of 6659 ± 153 y BP reported from the same area, at 22 m depth (Ferrara *et al.*, 1961).

An example of high-frequency (centennial-scale resolution) climatic control on the Arno River dynamics during the late Holocene has been supplied by Benvenuti *et al.* (2006), who furnished a detailed sedimentological and stratigraphic description of an archaeological site from Pisa urban area, reconstructing the history of a riverine harbour erected in the Etruscan age. This study documents the strict relationships between recurrent episodes of harbour destruction and high-magnitude flood events caused by high-frequency climatic and eustatic changes.

A recent multidisciplinary study of a 105m-long core, drilled about 4.5 km south of Arno River mouth (Core M1 in Fig. 1), combined with stratigraphic correlations with adjacent wells, has shown the presence of a late Quaternary incised valley, broadly coinciding with the present Arno river course. Thickness of the Holocene succession in coincidence of the valley body exceeds 50 m, whereas the entire Holocene succession above the palaeovalley interfluvies is just 17 m thick (Aguzzi *et al.*, 2007). The valley-fill consists almost entirely of thick, early transgressive estuarine facies, which are overlain by a thin late transgressive succession of beach-barrier and then shallow-

marine deposits. The overlying highstand succession records progradation of modern Arno delta and adjacent coastal systems.

Methods

Core S1 was drilled about 1 km NE of Pisa, in the inner portion of the palaeovalley fill (Fig. 1). The core was performed through a continuous perforating system that guaranteed high recovery percentages (86%). The core was split lengthwise and carefully described in terms of mean grain size, colour, sedimentary structures and accessory materials, including peat, organic matter, wood fragments and plant debris, calcareous nodules, mollusc fragments, marine and brackish bivalves, marine and pulmonate gastropods. Sedimentological features of Core S1 were integrated with detailed micropalaeontological analyses to obtain an accurate facies characterization.

A total of 82 samples were collected along the cored succession for micropalaeontological analyses. Approximately 150 g of each sample were initially dried for 8 hours at 60 °C, washed with water plus hydrogen peroxide (35% vol.), wet sieved through 63 µm (240-mesh) sieves and then dried again. The benthic microfauna (ostracods and foraminifers) contained in the > 63 µm size fraction was qualitatively analyzed. Thirty-one samples, showing well-preserved foraminifers, were dried sieved and the fraction > 125 µm quantitatively analyzed. When possible, more than 300 specimens were counted and related percentages elaborated for each species.

Forty-eight samples, collected from clay and silt deposits of Core S1, were sub-sampled for pollen analysis. Sediment samples were first dried and then treated with HCl (20%), HF (40%) and NaOH (10%). An average of 300 pollen grains per sample were counted. In the synthetic pollen diagrams, the pollen sum includes all pollen types, with the exception of aquatics, which are plotted separately. Arboreal pollen types (AP) were split into five classes: i) *Quercus* group is dominated

by deciduous oak and includes other mesophilous and thermophilous trees, such as *Corylus*, *Carpinus betulus*, *Ostrya*, *Fraxinus*, *Hedera*, *Tilia*, *Ulmus*, *Acer*, *Betula*; *Pinus*, living in warm and humid climates; ii) Mediterraneans include sclerophyllous and evergreen trees/shrubs, such as *Quercus ilex*, *Erica arborea*, *Phillyrea* type, *Pistacia* and *Olea*, living in Mediterranean climates characterized by high summer drought; iii) riparians are represented by trees/shrubs, such as *Alnus* and *Salix*, which live in flooded areas close to river channels; iv) mountains (*Abies*, *Picea* and *Fagus*), living at present at altitudes > 1500 m; and v) *Pinus*, which includes species living in very different environments, from mountains to Mediterranean, but consistently having high tolerance for drought. Similarly, non-arboreal types (NAP) were subdivided into three classes: i) ubiquists, represented by herbs with no particular ecological demand; ii) Poaceae; and iii) steppic herbs withstanding cold and dry conditions (*Artemisia* and Chenopodiaceae). The aquatics are represented by hygro-hydrophyte plants growing in humid environments, such as *Sparganium*-type, *Typha*, *Myriophyllum* and Cyperaceae.

The chronological framework benefited from two AMS ¹⁴C dates, performed at Beta Analytic Inc. (Miami, USA) on estuarine samples from Core S1, and two AMS ¹⁴C dates from correlative Core M1. Five additional radiocarbon dates carried out on continental deposits few cm away from parasequence boundaries furnished unreliable (> 30 ky) results, due to reworking of older material. Ages are reported as calibrated year BP.

Microfossil associations and sedimentology of Core S1

Detailed microfossil analyses were carried out on Core S1, in order to obtain an accurate facies characterization and depict subtle palaeoenvironmental changes, especially in terms of small salinity oscillations. Eight mixed, benthic foraminifers and ostracods microfossil associations were

recognized and grouped into three main ecological categories, labelled M, B, F and R (Table I) following terminology by Amorosi *et al.* (2004). Specific sub-environments and their related microfauna were distinguished by lower case letters. Associations M are indicative of shallow-marine environments, whereas associations B and F correspond to brackish and freshwater environments, respectively. Finally, associations R include a transported and reworked microfauna.

Palaeoenvironmental interpretation in Table I is based upon several key papers dealing with modern microfauna (Bonaduce *et al.*, 1975; Athersuch *et al.*, 1989; Albani and Serandrei Barbero, 1990; Henderson, 1990; Cimerman and Langer, 1991; Murray, 1991; Sgarrella and Moncharmont Zei, 1993; Ruiz *et al.*, 2000; Debenay *et al.*, 2006). Similar microfossil assemblages from late Quaternary successions of the Mediterranean area (Carboni *et al.*, 2004; Fiorini, 2004) were also taken into account for comparison.

Sedimentary facies of Core S1 are similar to those described at length by Aguzzi *et al.* (2007) from Core M1 (Fig. 1), and for this reason will not be repeated here. The reader is referred to that paper, for detailed facies description.

Similarly to Core M1, where the total thickness of post-LGM succession is about 51 m (Aguzzi *et al.*, 2007), the lower boundary of transgressive sedimentation in Core S1 was encountered at about 54 m depth (Fig. 2). Above a fluvial-channel deposit, which is interpreted to represent a lowstand unit flooring the Arno palaeovalley (see Aguzzi *et al.*, 2007), the early transgressive Arno valley fill, beneath late transgressive Holocene coastal sands, consists predominantly of estuarine and coastal plain deposits, with a subordinate proportion of alluvial plain facies (Fig. 2).

Unlike Core M1 (Aguzzi *et al.*, 2007), where the valley fill includes relatively homogeneous outer estuarine facies *sensu* Dalrymple *et al.* (1992), the landward equivalent succession of Core S1 shows a distinctive cyclic pattern of estuarine and coastal plain facies, documented by cyclic changes in sedimentary facies and palaeosalinity indicators, which suggest continuous, small-scale landward and seaward shifts in shoreline position. The Arno valley fill can thus be subdivided into three small-scale transgressive-regressive cycles (Fig. 2), 8-12 m thick, bounded by flooding

surfaces (or their lateral equivalents – see Cant, 1998), which are defined here as parasequences (PS1, PS2 and PS3) in the sense of Van Wagoner *et al.* (1990).

Rapid transgression at the base of PS1 is documented by the presence, above a thin swamp interval, of a transgressive lag, rich in mollusc shells, which is overlain by a 5m-thick succession of estuarine deposits (microfossil associations Bd and Ma – see Figs. 2 and 3a). A radiocarbon date from this facies association provided an age of $12,934 \pm 107$ cal. yr BP. The upper, sandy portion of PS1, about 4 m thick, records the progressive infilling of the estuary by prograding bay-head delta (or estuary-mouth) sand bodies. This “regressive” succession is capped by a few metres of coastal plain deposits, typically pedogenized at their top (Fig. 3b).

Above a few metres of marsh and central estuarine deposits (Figs. 2 and 3b), the lower, transgressive, portion of PS2 is characterized by the re-establishment of enduring central estuarine conditions (microfossil association Bc – see Fig. 2). Upward transition to microfossil association Bb (inner estuary) precedes estuary infilling by coastal plain deposits (Fig. 2).

Renewed “transgression” is suggested, at the base of PS3 (around 30 m core depth), by deposition of thick, freshwater swamp deposits, which are overlain by marsh clays (microfossil association Bb). Unlike PS1 and PS2, PS3 does not record a significant landward shift of facies, as documented by lack of estuarine deposits. Coastal plain and alluvial plain facies form the thick, regressive portion of PS3, which is topped by a stiff, pedogenized horizon (Figs. 2 and 3c).

A fourth flooding surface, overlain by a transgressive succession of swamp, lagoonal and open-bay deposits dated to $7,825 \pm 125$ cal. yr BP, is recorded above PS3 (Fig. 3d). The maximum flooding surface is placed in coincidence of microfossil assemblage Mb (Fig. 2), showing the highest marine affinity (Table I). This succession is overlain by thick, prograding Arno delta deposits, which form the highstand systems tract (Fig. 2).

Pollen stratigraphy of Core S1

Despite an overall dominance of arboreal pollen (AP), which is a distinctive feature of Holocene deposits, the transgressive record of Core S1 shows high-frequency vegetation changes that parallel facies architecture (Fig. 2). The pollen diagram is described and interpreted from bottom to top, taking into account the stratigraphic subdivision into parasequences discussed in the previous section.

The lower part of PS1, corresponding to early transgressive estuarine deposits, is characterized by an abundance (45% on average) of deciduous broad-leaved trees of *Quercus* group, and relatively high percentages (20-30%) of mountain trees, mostly represented by *Abies* and *Fagus*. Significant, among *Quercus* group, is the percentage (around 5%) of *Tilia*, which almost disappears higher up in the stratigraphic column.

The upper, regressive portion of PS1 is sand-dominated, and for this reason very few samples only are suitable for pollen analysis. Lower percentages (< 30%) of *Quercus* group are recorded in the lower part of the bay-head delta succession; these are accompanied by a slight expansion of *Pinus* and herbs (NAP). Pollen within a fine-grained interval at 45 m core depth is characterized by high contents of mountain trees and abundant *Carpinus betulus* (*Quercus* group), while more thermophilous taxa like *Quercus*, *Corylus*, *Tilia* and *Ulmus* show extremely low values.

The lower, transgressive part of PS2, showing central estuary development following alternating marsh and estuarine conditions, is characterized by the dominance (> 50%) of *Quercus* group and relatively high percentages (15-20%) of Mediterranean trees and shrubs, among which *Quercus ilex* and *Erica arborea* are most abundant. In contrast, *Pinus* and mountain trees show very low values.

A remarkable change in pollen association is recorded in the overlying, regressive part of PS2, where inner estuary and marsh deposits show a sharp increase in *Pinus* and mountain trees, together

representing 50% of the whole flora, while *Quercus* group and Mediterranean trees undergo an abrupt decline.

An increasing trend of deciduous broad-leaved trees (mainly *Quercus* group and riparians) characterizes swamp deposits in the lower, transgressive part of PS3. This trend is paralleled by stabilization of mountain trees to moderate, but significant, values and by the decrease of *Pinus*.

Pollen content in the overlying, regressive portion of PS3 is scarce and strongly influenced by local environmental conditions. In particular, the exceptionally high percentages of riparian trees within two channel abandonment facies are due to the specific depositional environment. Swamp deposits provide a more realistic picture of vegetation, characterized by relatively low values (25%) of deciduous broad-leaved trees (*Quercus* group) and abundant *Pinus* (25%) and mountain trees (35%).

The transgressive deposits overlying PS3 display, again, a remarkable increase in *Quercus* group, Mediterranean and riparian trees, representing altogether > 50% of the whole flora. Moderate, but significant values of *Abies* (about 8%) as unique component of mountain trees, are recorded close to the MFS. In more detail, outer lagoon and bay deposits at peak transgression show a major increase in Mediterranean elements, particularly *Quercus* evergreen, which achieves here its maximum values.

Palaeoclimatic signature and age attribution of parasequences

The overall pollen characteristics of the transgressive record of Core S1 indicate a major phase of forest development that took place under interglacial and/or interstadial climate conditions. This interpretation is consistent with the two radiocarbon dates available, which constrain parasequence development between about 13 and 8 cal. kyr BP (Fig. 2).

Pollen association from lower PS1 indicates a mixed, broad-leaved and coniferous forest vegetation, which is typical of fresh-temperate, interstadial climate conditions. As a whole, pollen spectra are very similar to those reported from Late Glacial pollen series of central Italy (Follieri *et al.*, 1988; Lowe *et al.*, 1996; Magri, 1999; Magri and Sadori, 1999) and southern Italy (Watts *et al.*, 1996). Diagnostic of the Late Glacial interstadial is maximum expansion of *Tilia*, a mesophilous taxon which does not withstand competition with other termophilous trees, like *Quercus* and *Corylus*, and that typically declines during the Holocene, when these trees become widespread (Watts *et al.*, 1996; Magri, 1999). The upward decrease, in upper PS1, of all termophilous taxa, leaving mountain trees (typical of higher altitudes) free to expand, is interpreted as the result of a significant fall in palaeotemperature, probably related to the incoming Younger Dryas (YD) cold event. Pollen signature of YD in central Italy is commonly characterized by abrupt return to open vegetation, dominated by steppic herbs (Follieri *et al.*, 1988; Lowe *et al.*, 1996; Watts *et al.*, 1996; Magri, 1999; Magri and Sadori, 1999; Drescher-Schneider *et al.*, 2007).

The dominance of termophilous forests observed in lower PS2 is indicative of warm climate conditions typical of the onset of the Holocene interglacial. In particular, the mixed character of the forests, with minor sclerophyllous evergreen taxa and dominant deciduous broad-leaved trees, points to a sub-Mediterranean climate, with short and irregular summer drought (Jalut *et al.*, 2000). The decline of these forests and the spread of cold-temperate trees (mainly *Abies*) reconstructed from upper PS2 imply an abrupt decrease in palaeotemperature, which can thus be related to an early-Holocene cold event. A correlative, early Holocene expansion of *Abies* in the study area has been recently dated to 10,385±165 cal. yr BP from estuarine deposits of Core M1 (Ricci Lucchi, submitted) and to 9,590±60 uncal. yr BP at Massaciuccoli Lake (Mariotti Lippi *et al.*, 2007 – see Fig. 1, for location).

Pollen association from lower PS3 suggests the re-expansion of warm-temperate forests, probably favoured by warmer and more humid climate conditions. The following decline of these forests (upper PS3), associated to maximum occurrence of *Abies*, is interpreted, similarly to what

reported by Tinner and Lotter (2006) from central Europe, as the result of climate change towards cooler and more humid summer conditions, which these authors attribute to the 8.2 cal. kyr BP cold event. Moisture availability, in particular, is considered to be responsible for the expansion of drought-sensitive trees, such as *Abies*. Magny *et al.* (2003) have reported an increase in humidity of about 50%, in central Europe, during the 8.2-cold event. In Tuscany (Core M1), *Abies* becomes the dominant element, together with *Pinus*, at 8,190±170 cal. yr BP (Ricci Lucchi, submitted). At Lago dell'Accesa, about 120 km south of Pisa, a short rise in lake level accompanied by the expansion of *Abies* has been also recently correlated to the 8.2 cold event (Drescher-Schneider *et al.*, 2007). This interpretation is consistent with radiometric age of about 7,825 cal. yr BP obtained from transgressive lagoonal deposits overlying PS3 (see Fig. 2).

Pollen association above PS3 suggests rapid transition to optimal warm and humid climate conditions. In addition, the gradual upward expansion of sclerophyllous evergreen forests points to an increase in the Mediterranean character of climate, including major periods of summer drought (Jalut *et al.*, 2000).

Post-LGM parasequence architecture of Arno coastal plain

Detailed facies analysis of two continuous cores (BP and S2), < 3 km away from Core S1, concurrently with stratigraphic data available from Core BG (8 km SW of Core S1), enable the construction of a cross-section along the Arno valley axis (Fig. 4), transversal to the palaeoshoreline. This section forms the basis for the characterization of parasequence architecture within the valley body, from proximal to distal locations.

A peculiar cyclic alternation of coastal plain and estuarine deposits, reflecting a continuous back and forth migration of coastal depositional environments, is the diagnostic feature of post-LGM

stratigraphy in the study area (Fig. 4). In particular, lateral tracing of three stratigraphically distinct intervals of estuarine clays, approximately 3-5 m thick, which overlie thin coastal plain deposits, allows their prompt correlation with the lower, transgressive parts of parasequences PS1 to PS3 identified in Core S1.

The regressive, upper portions of parasequences PS1 to PS3 invariably display return to subaerial conditions. Specifically, the estuarine clays are overlain by either coastal plain deposits or thick bay-head delta sands. In this latter case (see Core BG), non-deposition in coincidence of topographic highs and erosion processes related to the high-energy, estuary-mouth setting may result in poor identification of parasequence boundaries.

PS3, which is dominated by coastal plain deposits in Core S1, can be much more easily recognized in a seaward direction (Fig. 4), where this facies is replaced by a gradually thickening estuarine deposit. The local presence, at top of PS3, of alluvial plain deposits capped by a pedogenized horizon (see Core S1), marks the maximum seaward shift of facies in the study area during the Holocene transgression, further supporting the hypothesis of a major “regressive” event around 8,000 cal. yr BP.

Renewed transgression above PS3 is documented by the development of a 15 m thick succession of estuarine-lagoonal deposits, showing lateral transition seaward to beach-barrier sand and shallow-marine clay (Core BG). Vertically stacked coastal plain and thick alluvial plain deposits form the overlying highstand succession, recording progradation and the building up of the modern Arno coastal plain.

Discussion

Identification and facies/pollen characterization of three small-scale depositional cycles (parasequences) from the post-LGM transgressive succession of Arno valley fill provides a solid stratigraphic framework against which assess our data, to better understand the effects of specific climatic changes on facies evolution and sediment dispersal patterns in the study area. Lateral tracing, throughout the valley body, of the three parasequences (PS1 to PS3) identified in Core S1 suggests that these transgressive-regressive cycles of Lateglacial-early Holocene age do reflect an allocyclic control, and that they are not due to local, mostly autocyclic, factors, such as subsidence or distributary channel-delta lobe switching.

Pollen characterization of parasequences PS1 to PS3 shows that these millennial-scale cycles have a distinctive climatic connotation. The post-LGM early transgression in the study area was punctuated by three distinct episodes of marine flooding, recorded by the lower parts of parasequences, which led to widespread development of estuarine conditions throughout the Arno palaeovalley. Landward shifts in shoreline position were accompanied by major expansions of mixed, broad-leaved vegetation, suggesting the establishment of relatively warmer climate conditions.

Episodes of rapid sea-level rise were followed by subsequent phases of relative sea-level stillstand, which favoured extensive progradation of bay-head delta and coastal plain systems, with rapid seaward shift of the estuarine facies. Progradation, which was accompanied by a significant increase in sediment supply, took place in coincidence of the transition to relatively cooler phases, as documented by forests decline and spreading of cold-temperate trees in the upper parts of parasequences.

The diagnostic pollen spectra and radiocarbon dates available provide a relatively well constrained chronological framework for the study parasequences. Particularly, PS1 developed entirely during the Lateglacial, whereas PS2 and PS3 record early Holocene deposition.

The two regressive episodes corresponding to upper PS1 and PS3 are here assigned to the two most prominent and widespread cold phases recorded in the North Atlantic region during the last deglaciation: Younger Dryas (YD) and 8,200-event or Bond's event 5 (Stuiver *et al.*, 1995; Alley *et al.*, 1997; Klitgaard-Kristensen *et al.*, 1998; Alley, 2000; Rasmussen *et al.*, 2007; Thomas *et al.*, 2007), respectively. These cooling events were probably triggered by the sudden weakening of North Atlantic thermohaline circulation, induced by the release of massive freshwater fluxes from Laurentide proglacial lakes, such as Lake Agassiz (Barber *et al.*, 1999). Enormous volumes of fresh-waters, stored in the ice-dammed lakes, were periodically released into the oceans through Hudson Bay (Teller *et al.*, 2002; Clarke *et al.*, 2003). The timing of two of the largest outbursts of water just preceded the Younger Dryas and 8,200-cold events, respectively at ca. 12,900 and 8,500 cal. yr BP (Barber *et al.*, 1999; Teller *et al.*, 2002). This interpretation is also supported by several climate models and numerical simulations, which confirm the slowdown of North Atlantic thermohaline circulation and the subsequent global alteration of ocean-climate patterns, in response to massive freshwater fluxes (Clarke *et al.*, 2003; Rohling and Pälike, 2005; Renssen *et al.*, 2007). A secondary forcing role for these cooling events was possibly played by the millennial-scale variability in solar activity, as proposed by Bond *et al.* (2001).

The YD-event, which occurred between ca. 12,900 and 11,600 cal. yr BP, has been interpreted to reflect return to near-glacial conditions shortly before the onset of the Holocene warming (Mayewski *et al.*, 1993; Denton and Hendy, 1994). Pollen data recovered from several areas of Europe show, around 12,000 cal. yr BP, a prompt change in coastal and inland vegetation patterns, which is indicative of cool and arid conditions (Pons and Reille, 1988; de Beaulieu *et al.*, 1994; Watts *et al.*, 1996). Several palaeoclimatic records, from both lacustrine and marine successions, have documented the impact of the YD-event across different latitudes (Trincardi *et al.*, 1996;

Magny and Bégeot, 2004; Sbaffi *et al.*, 2004; Carboni *et al.*, 2005; Diefendorf *et al.*, 2006). In the study area, the YD-event was characterized by a sudden increase in total sand volume (see Fig. 4), which led to temporary estuary infilling through progradation of thick mouth-bar complexes.

A shorter-lived and smaller climatic anomaly relative to YD-event (Alley *et al.*, 1997; Bond *et al.*, 1997), and dated around 8,200 cal. yr BP, has been identified within different geological records, such as lacustrine and marine successions, speleothems and tree-rings (Klitgaard-Kristensen *et al.*, 1998; Nesje and Dahl, 2001; Baldini *et al.*, 2002; Sbaffi *et al.*, 2004; Diefendorf *et al.*, 2006). Lack of an unambiguous palynological response to the 8,200 climatic deterioration in northern Europe (Tinner and Lotter, 2001; Spurk *et al.*, 2002; Seppä and Poska, 2004) is probably due to the moderate decrease in temperature (about 2 °C) and irregular distribution of wetness/aridity conditions. However, in the Mediterranean area, pollen record of the 8,200-event has been reported by Magri (1999). In the study area, the 8,200-event records the last episode of widespread coastal/alluvial plain progradation, preceding the ultimate flooding of the study area after 8,000 cal. yr BP.

In summary, this study shows that very high accommodation settings, such as the late Quaternary Arno incised valley, may allow preservation of exceptionally thick packages of early transgressive (Lateglacial to early Holocene) deposits. In this instance, the overwhelming predominance of sea-level rise during the post-LGM transgression may strengthen the effects of small-scale, sea-level and climate change on the sedimentary record relative to other factors (tectonics, subsidence, changes in sediment supply). As a general rule, this may imply that valley fills can be regarded as ideal sites to investigate the sedimentary response of coastal areas to high-frequency, millennial-scale eustatic and climatic fluctuations. On the other hand, autocyclic processes, such as channel avulsion, delta lobe abandonment, and local subsidence due to sediment compaction are likely to become increasingly important during deposition of the highstand systems tract, leading to poor parasequence development in this tract of the sequence.

Conclusions

Detailed sedimentological, micropalaeontological (benthic foraminifers and ostracods) and palynological analyses were performed on a continuous core, 56 m long, drilled in the axial zone of the late Quaternary Arno River valley fill, in Western Tuscany, close to the town of Pisa.

Three distinctive small-scale transgressive-regressive cycles, bounded by lateral equivalents of marine flooding surfaces (parasequences PS1 to PS3), form the early transgressive (Lateglacial to early Holocene) succession. PS1 developed entirely during the Lateglacial, whereas PS2 and PS3 record early Holocene valley-fill sedimentation. Each parasequence is characterized by a lower, transgressive portion, showing rapid upward transition to estuarine clays, which is overlain by a shallowing-upward succession of bay-head delta, coastal plain, and locally alluvial plain deposits. Palaeosol development may locally occur on top of individual parasequences.

Parasequences PS1 to PS3, which are 8-12 m thick and exhibit the same periodicity as Bond's cycles, display a peculiar climatic connotation that reflects obvious fluctuations in vegetation cover. The lower, transgressive (estuarine) portion of parasequences invariably records the generalized expansion of warm-temperate forests. In contrast, the re-establishment of coastal plain environments in the valley was marked by forest decline and expansion of cold-temperate vegetation.

Stratigraphic correlation with adjacent wells allows lateral tracing of parasequence boundaries along the palaeovalley axis, leading to detailed reconstruction of overall parasequence architecture.

The two regressive episodes recorded by upper PS1 and PS3 are attributed to Younger Dryas (YD) and 8,200-event, respectively, *i.e.* the two most prominent and widespread cold phases recorded in the North Atlantic region during the last deglaciation. This paper thus provides for the

first time detailed documentation of the sedimentary response to Lateglacial and Holocene climate variability, through pollen characterization of vertically-stacked, millennial-scale parasequences.

Figure and table captions

Fig. 1. Location of the Arno coastal plain, with plan view indication (dotted lines) of the post-LGM valley body and section trace of Fig. 4.

Fig. 2. Sedimentology, micropalaeontology and pollen characteristics of Core S1 (see Fig. 1, for location). PS1 to PS3: parasequences (regressive portions are shown in grey), TS: Transgressive surface, FS: Flooding surface, MFS: Maximum flooding surface. Interpolated ages are based upon pollen correlation with Core M1 (see text).

Fig. 3. Representative photographs of Core S1, depicting facies changes at parasequence boundaries (see Fig. 2, for stratigraphic location). a: late Pleistocene fluvial-channel sands (FC), interpreted as lowstand deposits, overlain by a transgressive succession of swamp (S), transgressive lag (T), inner estuary (IE) and outer estuary (OE) deposits, forming lower PS1. The red line indicates the transgressive surface; white lines correspond to facies boundaries. b: pedogenized bay-head delta (BD) and floodplain (FP) deposits, separated by thin marsh (M) deposits at top PS1, overlain by transgressive central estuarine (CE) deposits of lowermost PS2. c: Fluvial-channel (FC) and indurated floodplain (FP) deposits of upper TS3, overlain by swamp (S) deposits. The red line represents the uppermost flooding surface beneath the maximum flooding surface. d: Close-up of uppermost PS3 from Core P1 (continuously-cored borehole drilled in the Arno valley, about 6 km SW of S1), with indurated floodplain (FP) deposits overlain by a transgressive succession of swamp (S) and lagoonal (L) deposits.

Fig. 4. Stratigraphic section of the Arno valley fill (see Fig. 1, for section trace), showing parasequence architecture from proximal (NE) to distal (SW) locations. Red line: parasequence

boundary. Ages are reported as calibrated year BP. Samples for micropaleontological analyses are shown right of Core S1 and Core S2.

Table I. Characteristic benthic foraminifers and ostracods taxa of the eight microfossil associations recorded within Core S1, and correlative depositional environments. Very abundant: > 70%; Abundant: 30-70%; Common: 10-30%; Rare: < 10%. For each microfossil association the dominant taxa are in bold.

References

- Aguzzi, M., Amorosi, A., Colalongo, M.L., Ricci Lucchi, M., Rossi, V., Sarti, G. and Vaiani, S.C.** 2007: Late Quaternary climatic evolution of the Arno coastal plain (Western Tuscany, Italy) from subsurface data. *Sedimentary Geology* 211, 211–29.
- Albani, A. and Serandrei Barbero, R.** 1990: I Foraminiferi della Laguna e del Golfo di Venezia. *Memorie Scienze Geologiche Padova* 42, 271–341.
- Alley, R.B.** 2000: The Younger Dryas cold interval as viewed from central Greenland. *Quaternary Science Reviews* 19, 213–26.
- Alley, R.B., Mayewski, P., Sowers, T., Stuiver, M., Taylor, K. and Clark, P.** 1997: Holocene climatic instability: a prominent widespread event 8200 yr ago. *Geology* 25, 483–86.
- Alley, R.B., Marotzke J., Nordhaus W.D., Overpeck J.T., Peteet, D.M., Pielke Jr. R.A., Pierrehumbert, R.T., Rhines, P.B., Stocker, T.F., Talley, L.D. and Wallace, J.M.** 2003: Abrupt Climate Change. Review. *Science* 299.
- Amorosi, A. and Milli, S.** 2001: Late Quaternary depositional architecture of Po and Tevere river deltas (Italy) and worldwide comparison with coeval deltaic successions. *Sedimentary Geology* 144, 357–75.

Amorosi, A., Colalongo, M. L., Fiorini, F., Fusco, F., Pasini, G., Vaiani, S. C. and Sarti, G. 2004: Palaeogeographic and palaeoclimatic evolution of the Po Plain from 150-ky core records. *Global and Planetary Change* 40, 55–78.

Amorosi, A., Centineo, M.C., Colalongo, M.L. and Fiorini, F. 2005: Millennial-scale depositional cycles from the Holocene of the Po Plain, Italy. *Marine Geology* 222–223, 7–18.

Athersuch, J., Horne, D.J. and Whittaker, J.E. 1989: Marine and brackish water ostracods. In Kermack, D.M., Barnes, R.S.K., editors, *Synopses of the British Fauna* (New Series) 43, Brill E.J., Leiden.

Baldacci, F., Bellini, L. and Raggi, G. 1994: Le risorse idriche sotterranee della Pianura di Pisa. *Atti della Società Toscana di Scienze Naturali Memorie Serie* 101 (A), 241–322.

Baldini, J. U. L., McDermott, F. and Fairchild, I. J. 2002: Structure of the 8200-year cold event revealed by a speleothem trace element record. *Science* 296, 2203–06.

Barber, D.C., Dyke, A., Hillaire-Marcel, C., Jennings, A.E., Andrews, J.T., Kerwin, M.W., Bilodeau, G., McNeely, R., Southon, J., Morehead, M.D. and Gagnon, J.M. 1999: Forcing of the cold event of 8,200 years ago by catastrophic drainage of Laurentide lakes. *Nature* 400, 344–48.

Benvenuti, M., Mariotti –Lippi, M., Pallecchi, P. and Sagri, M. 2006: Late-Holocene catastrophic floods in the terminal Arno River (Pisa, Central Italy) from the story of a Roman riverine harbour. *The Holocene* 16, 863–76.

Bonaduce, G., Ciampo, G. and Masoli, M. 1975: Distribution of Ostracoda in the Adriatic Sea. *Pubblicazione Stazione Zoologica di Napoli* 40.

Bond, G., Showers, W., Cheseby, M., Lotti, R., Almasi, P., deMenocal, P., Priore, P., Cullen, H., Hajdas, I. and Bonani, G. 1997: A pervasive millennial scale cycle in North Atlantic Holocene and glacial climate. *Science* 278, 1257–66.

Bond, G., Kromer, B., Beer, J., Muscheler, R., Evans, M. N., Showers, W., Hoffmann, S., Lotti-Bond, R., Hajdas, I. and Bonani, G. 2001: Persistent solar influence on North Atlantic climate during the Holocene. *Science* 294, 2130–36.

Boyer, J., Duvail, C., Le Strat, P., Gensous, B. and Tesson, M. 2005: High resolution stratigraphy and evolution of the Rhône delta plain during Postglacial time, from subsurface drilling data bank. *Marine Geology* 222-223, 267–98.

Cant, D.J. 1998: Sequence stratigraphy, subsidence rates, and alluvial facies, Mannville Group, Alberta foreland basin. In Shanley, K.W., McCabe, P.J., editors, *Relative Role of Eustasy, Climate, and Tectonism in Continental Rocks*. Special Publication Society of Economic Paleontologists and Mineralogists 59, 49–63.

Carboni, M.G., Frezza, V. and Bergamin, L. 2004: Distribution of Recent foraminifers in the Ombrone River Basin (Tuscany Continental Shelf, Tyrrhenian Sea, Italy): relations with fluvial runoff. In Coccioni, R., Galeotti, S., Lirer, F., editors, *Proceedings of the First Italian Meeting of Environmental Micropaleontology*. The Grzybowski Foundation Special Publication 9, 7–16.

Carboni, M.G., Bergamin, L., Di Bella, L., Landini, B., Manfra, L. and Vesica, P. 2005: Late Quaternary paleoclimatic and paleoenvironmental changes in the Tyrrhenian Sea. *Quaternary Science Reviews* 24, 2069–82.

Cimerman, F. and Langer, M.R. 1991: *Mediterranean Foraminifera. Academia Scientiarum et Artium Slovenica Classis IV* 30, Ljubljana.

Clarke, G.K.C., Leverington, D.W., Teller and J.T., Dyke, A.S. 2003: Superlakes, megafloods, and abrupt climate change. *Science* 301, 922–23.

Dalrymple, R.W., Zaitlin, B.A., and Boyd, R. 1992: Estuarine facies models. Conceptual basis and stratigraphic implications. *Journal of Sedimentary Petrology* 62, 1130–46.

de Beaulieu, J.L., Andrieu, V., Ponel, P. and Reille, M. 1994 : The Weichselian Late-glacial in southwestern Europe (Iberian Peninsula, Pyrenees, Massif Central, northern Apennines). *Journal of Quaternary Science* 9 (2), 101-107.

Debenay, J.P., Bicchi, E., Goubert, E. and Armynot du Châtelet, E. 2006 : Spatio-temporal distribution of benthic foraminifera in relation to estuarine dynamics (Vie estuary, Vendée, W France). *Estuarine Coastal Shelf Science* 67, 181–97.

Della Rocca, R., Mazzanti R. and Pranzino, E. 1987: Studio geomorfologico della Pianura di Pisa (Toscana). *Geografia Fisica e Dinamica Quaternaria* 10, 56–84.

Denton, G.H. and Hendy, C.H. 1994: Younger Dryas age advance of Franz Josef Glacier in the Southern Alps of New Zealand. *Science* 264, 1434–37.

Denton, G.H. and Karlén, W. 1973: Holocene climatic variations: their pattern and possible cause. *Quaternary Research* 3, 155–205.

Diefendorf, A.F., Patterson, W.P., Mullins, H.T., Tibert, N. and Martini, A. 2006: Evidence for high-frequency late Glacial to mid-Holocene (16,800 to 5,500 cal yr B.P.) climate variability from oxygen isotope values of Lough Inchiquin, Ireland. *Quaternary Research* 65, 78–86.

Drescher-Schneider, R., de Beaulieu, J-L., Magny, M., Walter-Simonnet, A-V., Bossuet, G., Millet, L., Bruciapaglia, E. and Drescher, A. 2007: Vegetation history, climate and human impact over the last 15,000 years at Lago dell'Accesa (Tuscany, Central Italy). *Vegetation History and Archaeobotany* 16, 279–89.

Federici, P.R. and Mazzanti, R. 1995: Note sulle pianure costiere della Toscana. *Memorie Società Geografica Italiana* 53, 165–270.

Ferrara, G., Fornaca Rinaldi, G. and Tongiorgi, E. 1961: Carbon-14 dating in Pisa II. *Radiocarbon* 3, 99–104.

Fiorini, F. 2004: Benthic foraminiferal associations from Upper Quaternary deposits of southeastern Po Plain, Italy. *Micropaleontology* 50, 45–58.

Follieri, M., Magri, D. and Sadori, L. 1988: 250000-year pollen record from Valle di Castiglione (Roma). *Pollen et Spores* 30, 329–56.

Galletti Fancelli, M.L. 1978: Ricerche sulla subsidenza della pianura pisana. Analisi polliniche di sedimenti quaternari della pianura costiera tra Pisa e Livorno. *Bollettino Società Geologica Italiana* 97, 197–245.

Gonzalez, R., Dias, J.M.A., Lobo, F., and Mendes, I. 2004: Sedimentological and paleoenvironmental characterisation of transgressive sediments on the Guadiana Shelf (Northern Gulf of Cadiz, SW Iberia). *Quaternary International* 120, 133–44.

Henderson, P.A. 1990: Freshwater ostracods. In Kermack, D.M., Barnes, R.S.K., editors, *Synopses of the British Fauna* (New Series) 42, Brill E.J., Leiden.

IPCC 2001: *Climate Change 2001: Synthesis Report*. Summary for Policymakers. Intergovernmental Panel on Climate Change Third Assessment Report, Cambridge University Press, Cambridge.

IPCC 2007: *Climate Change 2007: Synthesis Report*. Summary for Policymakers. Intergovernmental Panel on Climate Change Fourth Assessment Report, Cambridge University Press, Cambridge.

Jalut, G., Amat, A.E., Bonnet, L., Gauquelin, T. and Fontugne, M. 2000: Holocene climatic changes in the Western Mediterranean, from south-east France to south-east Spain. *Palaogeography, Palaeoclimatology, Palaeoecology* 160, 255–90.

Kamola, D.L. and Van Wagoner, J.C. 1995: Stratigraphy and facies architecture of parasequences with examples from the Spring Canyon Member, Blackhawk Formation, Utah. In Van Wagoner,

J.C., Bertram, G.T., editors, *Sequence Stratigraphy of Foreland Basin Deposits*. American Association of Petroleum Geologists Memories 64, 27–54.

Klitgaard-Kristensen, D., Sejrup, H-P., Hafliðason, H., Johnsen, S. and Spurk, M. 1998: A regional 8200 cal yr BP cooling event in northwest Europe, induced by final stages of the Laurentide ice-sheet deglaciation? *Journal of Quaternary Science* 13, 165–69.

Leorri, E., Martin, R. and McLaughlin, P. 2006: Holocene environmental and parasequence development of the St. Jones Estuary, Delaware (USA): Foraminiferal proxies of natural climatic and anthropogenic change. *Palaeogeography, Palaeoclimatology, Palaeoecology* 241, 590–607.

Lowe, J.J., Accorsi, C.A., Bandini Mozzanti, M., Bishop, A., Van der Kaars, S., Forlani, L., Mercuri, A. M., Rivalenti, C., Torri, P. and Watson, C. 1996: Pollen stratigraphy of sediment sequences from lakes Albano and Nemi (near Rome) and from the central Adriatic, spanning the interval from oxygen isotope Stage 2 to the present day. *Memorie Istituto Italiano Idrobiologia* 55, 71–98.

Lowrie, A. and Hamiter, R. 1995: Fifth and sixth order eustatic events during Holocene, fourth order highstand influencing Mississippi delta-lobe switching. In Finkl Jr., C.W., editor, *Holocene Cycles: Climate, Sea Levels and Sedimentation*. *Journal of Coastal Research* 17, 225– 29.

Magny, M. and Bégeot, C. 2004: Hydrological changes in the European midlatitudes associated with freshwater outbursts from Lake Agassiz during the Younger Dryas event and the early Holocene. *Quaternary Research* 61, 181–92.

Magny, M., Begeot, C., Guiot, J. and Peyron, O. 2003: Contrasting patterns of hydrological changes in Europe in response to Holocene climate cooling phases. *Quaternary Science Reviews* 22, 1589–96.

Magri, D. 1999: Late Quaternary vegetation history at Lagaccione near Lago di Bolsena (central Italy). *Review of Paleobotany and Palynology* 106, 171–208.

Magri, D. and Sadori, L. 1999: Late Pleistocene and Holocene pollen stratigraphy at Lago di Vico (central Italy). *Vegetation History and Archaeobotany* 8, 247–60.

Mariotti Lippi, M., Guido, M., Menozzi, B.I., Bellini, C. and Montanari, C. 2007: The Massaciuccoli Holocene pollen sequence and the vegetation history of the coastal plains by the Mar Ligure (Tuscany and Liguria, Italy). *Vegetation History and Archaeobotany* 16, 267-277.

Mayewski, P.A., Meeker, L.D., Whitlow, S., Twickler, M. S., Morrison, M.C., Alley, R.B., Bloomfield, P. and Taylor, K. 2003: The Atmosphere During the Younger Dryas. *Science* 261, 195–97.

Mayewski, P.A., Rohling, E.E., Stager, J.C., Karlen, W., Maasch, K.A., Meeker, L.D., Meyerson, E.A., Gasse, F., van Kreveld, S., Holmgren, K., Lee-Thorp, J., Rosqvist, G., Rack, F., Staubwasser, M., Schneider, R.R. and Steig, E.J. 2004: Holocene climate variability. *Quaternary Research* 62, 243– 55.

Mazzanti, R. 2000: Geomorfologia del bacino Versiliese-Pisano con particolare riferimento alla "Gronda dei Lupi", scarpata fossile che separa le Colline Livornesi, con i loro terrazzi eustatici,

dalla pianura alluvionale pisana. *Atti della Società Toscana di Scienze Naturali Memorie Serie A* 107, 165-89.

Murray, J.W. 1991: *Ecology and Palaeoecology of Benthic Foraminifera*. Longman Scientific and Technical, London.

National Research Council (NRC) 2002: *Abrupt climate changes: Inevitable surprises*. National Academy Press, Washington, D.C.

Nesje, A. and Dahl, S.O. 2001: The Greenland 8200 cal yr BP event detected in loss-on ignition profiles in Norwegian lacustrine sediment sequences. *Journal of Quaternary Science* 16, 155–66.

Pons, A. and Reille, M. 1988: The Holocene and Upper Pleistocene pollen record from Padul (Granada, Spain). *Palaeogeography, Palaeoclimatology, Palaeoecology* 66, 243–63.

Rasmussen, S.O., Vinther, B.M., Clausen, H.B. and Andersen, K.K. 2007: Early Holocene climate oscillations recorded in three Greenland ice cores. *Quaternary Science Reviews* 26, 1907–14.

Renssen, H., Goosse, H. and Fichefet, T. 2007: Simulation of Holocene cooling events in a coupled climate model. *Quaternary Science Reviews* 26, 2019–29.

Ricci Lucchi, M. (submitted): Holocene vegetation history and human impact in the Arno coastal plain (Tuscany, Italy). *Vegetation History and Archaeobotany*.

Rohling, E.J. and Palike, H. 2005: Centennial-scale climate cooling with a sudden cold event around 8,200 years ago. *Nature* 434, 975–79.

Romagnoli L. 1957. Sondaggi a 200 m di profondità nel Quaternario recente presso Pisa. Studio delle facies attraversate e considerazioni sulla sedimentazione costiera a carattere ciclico. *Bollettino della Società Geologica Italiana* 76, 21–35.

Ruiz, F., Gonzalez-Regalado, M.L., Baceta, J.I., Menegazzo-Vitturi, L., Pistolato, M., Rampazzo, G. and Molinaroli, E. 2000: Los ostrácodos actuales de la laguna de Venecia (NE de Italia). *Geobios* 33, 447–54.

Sartori F. 1978: Studi sedimentologici e mineralogici delle alluvioni recenti della pianura pisana. I sedimenti del sondaggio della Bigattiera, presso S. Piero a Grado (Pisa). *Atti della Società Toscana di Scienze Naturali Memorie Serie A* 85, 61–93.

Sbaffi, L., Wezela F.C., Curzia, G. and Zoppi U. 2004: Millennial- to centennial-scale palaeoclimatic variations during Termination I and the Holocene in the central Mediterranean Sea. *Global and Planetary Change* 40, 201–17.

Seppä, H. and Poska, A. 2004: Holocene annual mean temperature changes in Estonia and their relationship to solar insolation and atmospheric circulation patterns. *Quaternary Research* 61, 22–31.

Sgarrella, F. and Moncharmont Zei, M. 1993: Benthic Foraminifera of the Gulf of Naples (Italy): systematics and autoecology. *Bollettino Società Paleontologica Italiana* 32, 145–264.

Somoza, L., Barnolas, A., Arasa, A., Maestro, A., Rees, J.G. and Hernandez-Molina, F.J. 1998: Architectural stacking patterns of the Ebro delta controlled by Holocene high-frequency eustatic fluctuations, delta-lobe switching and subsidence processes. *Sedimentary Geology* 117, 11– 32.

Spurk, M., Leuschner, H.H., Baillie, M.G.L., Briffa, K.R. and Friedrich, M. 2002: Depositional frequency of German subfossil oaks: climatically and non-climatically induced fluctuations in the Holocene. *The Holocene* 12, 707–15.

Stuiver, M., Grootes, P.M. and Braziunas, T.F. 1995: The GISP2 d18O climate record of the past 16,500 years and the role of the sun, ocean, and volcanoes. *Quaternary Research* 44, 341– 54.

Teller, J.T., Leverington, D.W. and Mann, J.D. 2002: Freshwater outbursts to the oceans from glacial Lake Agassiz and their role in climate change during the last deglaciation. *Quaternary Science Reviews* 21, 879–87.

Thomas, E.R., Wolff, E.W., Mulvaney, R., Steffensen, J.P., Johnsen, S.J., Arrowsmith, C., White, J.W.C., Vaughn, B. and Popp, T. 2007: The 8.2 kyr event from Greenland ice cores. *Quaternary Science Reviews* 26 (1–2), 70–81.

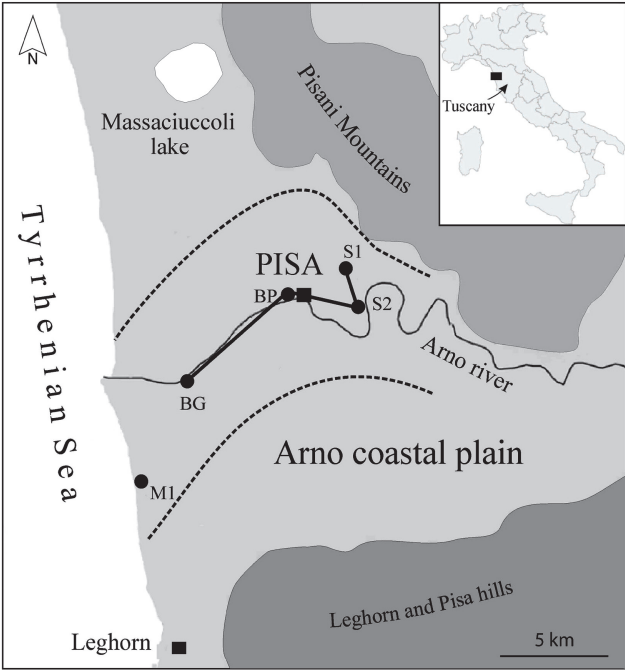
Tinner, W. and Lotter, A.F. 2001: Central European vegetation response to abrupt climate change at 8.2 ka. *Geology* 29, 551–54.

——— 2006: Holocene expansions of *Fagus sylvatica* and *Abies alba* in Central Europe: where are we after eight decades of debate? *Quaternary Science Reviews* 25, 526–49.

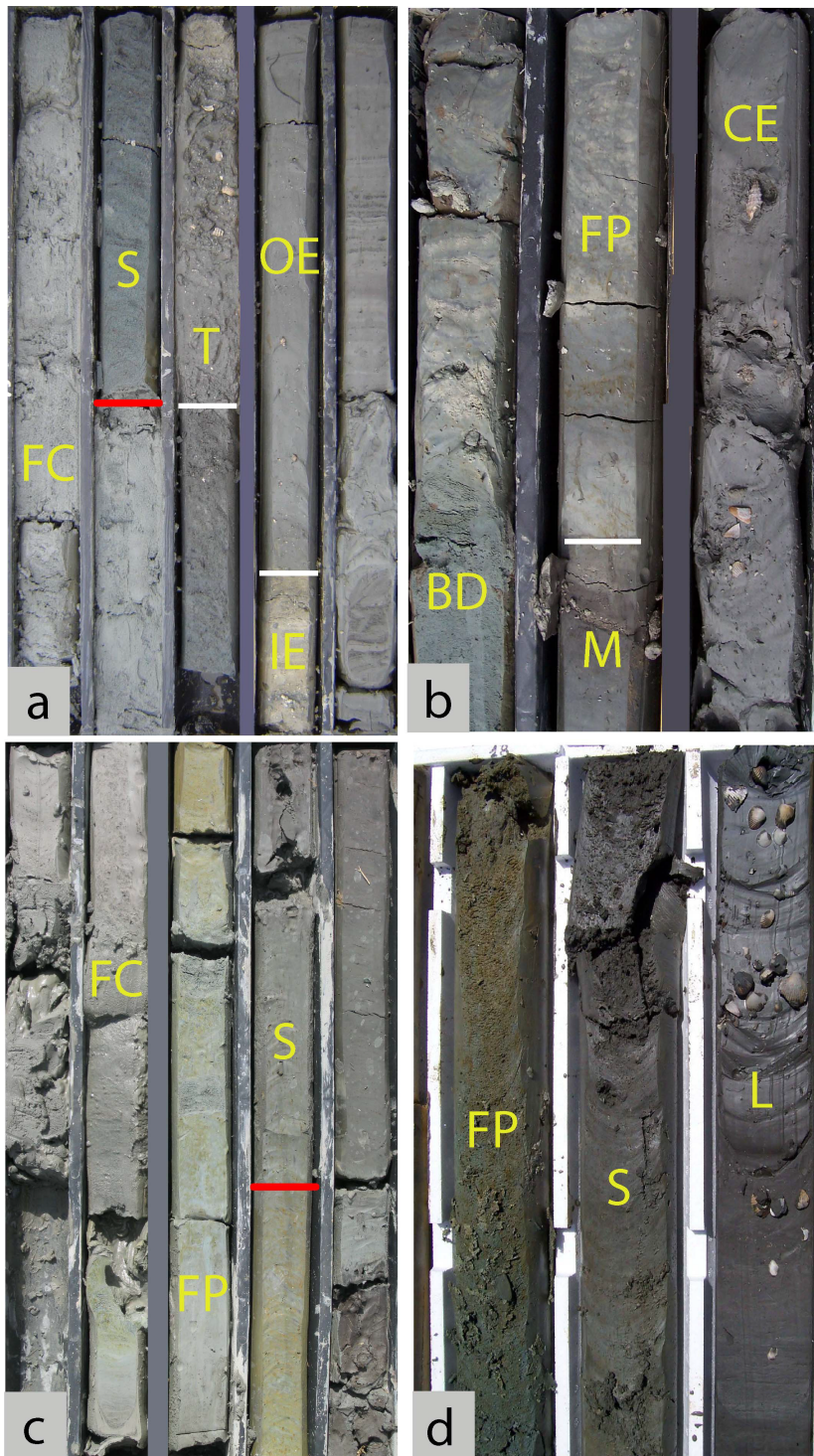
Trincardi, F., Asioli, A., Cattaneo, A., Correggiari, A., Vigliotti, L. and Accorsi C.A. 1996: Transgressive offshore deposits on the central Adriatic shelf: Architecture complexity and the record of the Younger Dryas short-term event. *Il Quaternario* 9, 753–62.

Van Wagoner J.C., Mitchum R.M., Campion K.M. and Rahmanian V.D. 1990: Siliclastic sequence stratigraphy in well logs, cores and outcrops: concepts for high resolution correlations of time and facies. *American Association of American Petroleum Geologists. Methods in Exploration* 7 Barbara H. Lidtz, Tulsa.

Watts, W.A., Allen, J.R.M. and Huntley, B. 1996: Vegetation history and palaeoclimate of the Last Glacial period at Lago Grande di Monticchio, southern Italy. *Quaternary Science Reviews* 15, 133–153.



Amorosi et al., Fig. 1



Amorosi et al., Fig. 3

Microfossil Association			Depositional environment
Name	Benthic Foraminifers	Ostracods	
Mb	Abundant <i>Ammonia tepida</i> (Cushman) and <i>Ammonia parkinsoniana</i> (d'Orbigny) (67%). Common <i>Valvulineria perlucida</i> (Heron-Allen and Earland) (11%) and Miliolids (15% - mostly <i>Miliolinella</i> spp. and <i>Quinqueloculina seminula</i> (Linnaeus)).	Abundant <i>Loxococoncha turbida</i> (G.W. Müller), <i>Leptocythere bacescoi</i> (Rome) and <i>L. ramosa</i> (Rome). Rare <i>Cytherois fischeri</i> (Sars), <i>Cytheridea neapolitana</i> (Kolmann) and <i>Carinocythereis whitei</i> (Baird).	Shallow, salinity-stressed marine environments (prodelta or bay).
Ma	Very abundant <i>Ammonia tepida</i> and <i>A. parkinsoniana</i> (87%). Common <i>Valvulineria perlucida</i> (11%) and rare <i>Haynesina germanica</i> (Herenberg) (1.5%).	Absent.	Mixed brackish-normal saline environments (proximal prodelta, outer lagoon/estuary, bay).
Bd	Very abundant <i>Ammonia tepida</i> and <i>A. parkinsoniana</i> (80-99%). Rare <i>Haynesina germanica</i> , <i>Criboelphidium</i> spp. and Miliolids (< 6%).	Very abundant <i>Cyprideis torosa</i> (Jones). Common <i>Loxococoncha elliptica</i> (Brady).	Brackish-water environments with high marine influence (outer lagoon/estuary).
Bc	Very abundant <i>Ammonia tepida</i> and <i>A. parkinsoniana</i> (> 73%). Common <i>Criboelphidium</i> spp. (mainly <i>C. granosum</i> (d'Orbigny)) up to 24% and <i>Miliolinella</i> spp. (mainly <i>M. elongata</i> (Kruit) and <i>M. subrotunda</i> (Montagu)) up to 12%.	Very abundant <i>Cyprideis torosa</i> . Rare <i>Loxococoncha elliptica</i> , <i>Xestoleberis dispar</i> (G.W. Müller) and <i>X. decipiens</i> (G.W. Müller).	Brackish-water environments with moderate marine influence (central lagoon/estuary).
Bb	Very abundant <i>Ammonia tepida</i> and <i>A. parkinsoniana</i> (88-99%). Rare <i>Criboelphidium</i> spp. (up to 10%) and <i>Miliolinella</i> spp. (up to 5%). Microfauna is usually not abundant and some samples result barren in foraminifers.	Very abundant <i>Cyprideis torosa</i> . Rare <i>Loxococoncha elliptica</i> and <i>L. stellifera</i> (G.W. Müller). Rare <i>Candona</i> spp. (mainly <i>C. lactea</i> (Baird)) within samples barren in foraminifers.	Brackish-water environments with low marine influence (inner lagoon/estuary or salt marsh).
F	Absent.	Very abundant <i>Candona</i> spp. (mainly <i>C. lactea</i>). Rare <i>Eucypris</i> spp.	Freshwater or oligohaline environments (swamp and pond).
Rb	Abraded and poorly preserved <i>Ammonia tepida</i> and <i>A. parkinsoniana</i> and <i>Cyprideis torosa</i> .		High-energy back-barrier environments (flood-tidal delta, washover and transgressive lag).
Rf	Poorly preserved marine foraminifers and few valves of brackish and freshwater ostracods.		High-energy environments with fossil reworking from older formations (fluvial and distributary channel, bay-head delta and subdelta).

Amorosi et al., Table I

Paper 4

Late Quaternary palaeoenvironmental evolution of the Adriatic coastal plain and the onset of Po River Delta

Amorosi, A., Dinelli, E., **Rossi, V.**, Vaiani, S.C. and Sacchetto, M.

Late Quaternary palaeoenvironmental evolution of the Adriatic coastal plain and the onset of Po River Delta

Alessandro Amorosi¹, Enrico Dinelli¹, Veronica Rossi^{1*}, Stefano Claudio Vaiani¹ and Massimo Sacchetto²

¹Dipartimento di Scienze della Terra e Geologico-Ambientali, Università di Bologna, Via Zamboni 67, 40126 Bologna, Italy

²S.P.G., Via dell'Artigianato 24, 45011, Adria, Italy

*Corresponding author: Tel: +39 051 2094565; Fax: +39 051 2094522;

E-mail: veronica.rossi4@unibo.it

Abstract

Despite an abundant geologic literature about the Po coastal plain, stratigraphic architecture beneath modern Po River Delta is virtually unknown. In this paper, combined sedimentological, micropalaeontological and geochemical investigations of three continuous cores (cores 1 to 3), about 40 m thick, enable for the first time the detailed reconstruction of subsurface stratigraphy in the Po River Delta area, along with its late Quaternary palaeoenvironmental evolution.

Lowstand deposits, formed during the Last Glacial Maximum, are expressed as a fining-upward succession of fluvial-channel and related overbank deposits, capped by a stiff, overconsolidated horizon. Above this unconformable surface, the lower post-glacial succession (transgressive systems tract or TST) is less than 7 m thick and includes a deepening-upward succession of back-barrier, shoreface and inner-shelf deposits. On the other hand, the overlying highstand systems tract is considerably thicker (up to 27 m) and comprises the bulk of recent delta progradation (*i.e.*, vertically stacked prodelta, delta front and delta plain deposits).

Stratigraphic correlations within early transgressive, back-barrier deposits show vertically stacked, thin shallowing-upward successions, reflecting an internal subdivision of TST into small-scale parasequences.

The homogeneous shallow-marine clay that accumulated at the turnaround from transgressive to highstand conditions can be palaeontologically differentiated into two packages (*Miliolidae*-dominated and *Ammonia/Cribrorhynchium*-dominated), reflecting open-marine and river-influenced conditions, respectively. Timing of maximum marine ingress (maximum flooding surface-MFS) is recorded within the open-marine clays at about 5,500 cal yr BP by minor changes in microfauna.

Geochemical characterization of Core 1 shows that distinct changes in sediment provenance accompanied the palaeoenvironmental evolution of the study area under changing relative sea-level conditions. At lowstand times, the study area was an alluvial plain under the influence of Adige River, as suggested by comparatively high Ba/Al values within pre-Holocene fluvial deposits.

Increasing upward values of Cr/Al₂O₃ and Ni/Mg within TST suggest an increasing sediment contribution from the Po River during early stages of transgression, via the longshore drift.

The onset of modern-age Po Delta in the study area is precisely identified in Core 1 at 25.10 m depth, and has a distinctive, double signature. In terms of microfaunal assemblages, Po River sediments are clearly marked by the development of a characteristic foraminiferal association dominated by the opportunistic species *Nonionella turgida*, a taxon typically abundant in the marginal zone of present northern Adriatic mud-belt. Po River deposits are also fingerprinted by a peculiar geochemical composition, corresponding to maximum Cr and Ni concentrations.

Keywords: Po Delta; Palaeogeography; Micropalaeontology; Sediment provenance; Adriatic mud-belt; Late Quaternary

Introduction

The Po Plain is one of Europe's major alluvial plain, which hosts a very dense population (about one third of the Italian population) and important agricultural and industrial activities. Owing to the considerable number of continuously-cored boreholes and cone penetration tests performed in the last decade, along with the construction of a solid database including thousands of pre-existing data, the Po Plain represents today an excellent archive for developing high-resolution stratigraphic studies. The possibility of tracing stratigraphic surfaces from the basin margin to the coastal plain makes the Po Plain a natural laboratory for the construction of detailed sequence-stratigraphic models (Amorosi and Colalongo, 2005).

Although several studies have documented in detail late Quaternary stratigraphic architecture in the Po coastal plain, mostly south of modern Po Delta (Rizzini, 1974; Bondesan et al., 1995; Amorosi and Marchi, 1999; Amorosi et al., 1999a, b, 2003, 2005; Stefani and Vincenzi, 2005; Curzi et al., 2006), no documentation exists about subsurface stratigraphy beneath the present delta plain.

Our research attempts to fill this gap, through combined sedimentological and micropalaeontological investigations of three continuously-cored boreholes (cores 1-3), 35-40 m deep, that were drilled in 2006 in the delta area, and the construction of a N-S oriented transect, roughly parallel to the coastline and perpendicular to Po River (Fig. 1). Specific objective of this paper is to examine the onset of deltaic sedimentation in the present Po Delta area, and frame it within a sequence-stratigraphic context. In this respect, detailed geochemical characterization of Core 1 is used as a tool for provenance discrimination and characterization of the key surfaces for sequence-stratigraphic interpretation.

Methods

The stratigraphic record was provided by three continuously-cored boreholes (cores 1, 2 and 3) performed by S.P.G. Adria through the wireline perforation system, which guaranteed very high (> 90%) recovery percentages. The cores were recovered in the modern delta plain, following a roughly north-south orientation, in order to obtain stratigraphic information about the entire delta system, from Po Levante to Po Tolle channel mouths (Fig. 1).

Each core was split lengthwise, macroscopically described in terms of mean grain size, sedimentary structures, colour and accessory material content, including peat, organic matter, plant and wood fragments, calcareous nodules, mollusk shells and bioclasts. A total of 191 samples were collected for micropalaeontological analysis. Due to its relatively distal (easternmost) position, which is confirmed by a continuous record of a thick succession of marine clays, Core 1 was selected as reference core for our study, and for this reason extensively sampled. Selected stratigraphic intervals were sampled for cores 2 and 3, in order to refine facies interpretation (Fig. 2). Approximately 150 g of sediment were dried in an oven for 8 hours at 60°C. They were washed with water plus hydrogen peroxide (35% vol.) through sieves of 63 µm (240 mesh), and then dried again for 24 hours.

The benthic microfauna (foraminifers and ostracods), encountered within the > 63 µm size fraction was qualitatively analyzed. Samples containing more than 300 foraminiferal specimens were dry sieved and quantitative analyzed in the size fraction > 125 µm. The relative abundance percentage of each foraminiferal species was finally calculated within 43 countable samples.

Identification of foraminiferal and ostracod species relies upon original descriptions and several key papers (Bonaduce et al., 1975; AGIP, 1982; Jorissen, 1988; Athersuch et al., 1989; Albani and Serandrei Barbero, 1990; Henderson, 1990; Cimerman and Langer, 1991; Sgarrella and Moncharmont Zei, 1993; Fiorini and Vaianni, 2001). Ecological interpretation of species and environmental significance of microfaunal associations are inferred from comparison with modern

benthic communities (Colalongo, 1969; D'Onofrio, 1969; Bonaduce et al., 1975; Breman, 1975; Jorissen, 1987; Murray, 1991; Van Der Zwaan and Jorissen, 1991; Barmawidjaja et al., 1992; Yassini and Jones, 1995; Debenay et al., 2000; Ruiz et al., 2000; Donnici and Serandrei Barbero, 2002; Smith and Horne, 2002) and similar microfaunal assemblages recorded within late Quaternary coastal successions of Italy. These include Po coastal plain (Amorosi et al., 2004, 2005; Fiorini, 2004; Bondesan et al., 2006) and Ombrone and Arno coastal plains (Carboni et al., 2004; Aguzzi et al., 2007).

Geochemical analyses were also performed on 59 samples from Core 1, in order to obtain specific information about sediment provenance. Samples were oven-dried at 40°C to complete dryness, and homogenized in an agate mortar. Chemical determinations were obtained by X-ray fluorescence spectrometry (Philips PW 1480) on pressed powder pellets, following the matrix correction methods of Franzini et al. (1972, 1975), Leoni and Saitta (1976), and Leoni et al. (1986). The estimated precision and accuracy for trace element determinations are better than 5%, except for those elements at 10 ppm and lower (10-15%). Loss on ignition (LOI) was evaluated after overnight heating at 950 °C.

Nine carbon-rich samples (organic clay, peat or well-preserved mollusk shells) were collected from cores 1 and 3 (Fig. 2) and analyzed by CEDAD laboratory (University of Lecce, Italy), providing a reliable chronological framework. The conventional radiocarbon dates were calibrated using software OxCal Ver. 3.10 and the dataset furnished by Reimer et al. (2004). For the calculation of ages from mollusk shells the marine calibration curve and the Northern Adriatic ΔR (-61 ± 50) were used. Ages are reported in text as calibrated yr BP.

Late Quaternary deposits beneath the modern Po Delta

Facies characterization of late Quaternary deposits in the Po Delta area relies upon detailed sedimentological and micropalaeontological study of cores 1-3 (Fig. 2). Seven facies associations were identified on the basis of core data (Fig. 3). The sequence in which each facies association is described and interpreted reflects their order of occurrence in the stratigraphic record, from bottom to top. Few metres (1-2 m) of anthropogenic deposits cap the cores succession.

Alluvial plain facies association (A)

Description

Facies association A exceeds 7 m in thickness, and occurs in the lowest part of the study cores (Fig. 2). Two major lithofacies (A1 and A2) were distinguished on the basis of sedimentological evidence.

Lithofacies A1 consists of medium to coarse sand, showing upward transition to fine sand, sandy silt and silt. The overall succession displays, in all cores, a characteristic fining-upward (FU) trend, with local erosional boundaries. No mollusc shells were found within this lithofacies. Plant debris is generally present and calcareous nodules may be observed within the silt layers.

This lithofacies includes in a few samples a rare and poorly preserved microfauna, composed of ostracods and foraminifers assigned to a variety of environments, from freshwater to open-marine. Valves of freshwater ostracods, mainly *Candona* (Baird), are usually encountered in association with specimens of marine foraminifers, such as *Cassidulina laevigata* (d' Orbigny), *Ammonia tepida* (Cushman) and *Bolivina* spp..

Lithofacies A1 is invariably overlain by lithofacies A2 (Fig. 3A), which consists of mottled grey clay and silt, with thin sand intercalations. Plant debris, wood fragments and calcareous nodules are

commonly present within this lithofacies. Few bioclasts of pulmonate gastropods are also locally found. This lithofacies is barren in microfossils.

Facies association A is capped by a stiff, pedogenized horizon, generally a few dm thick, which locally displays a characteristic dark colour (Fig. 3A). This horizon roughly corresponds to the Pleistocene-Holocene boundary.

Interpretation

Sedimentological and micropalaeontological features suggest that this facies association formed on an alluvial plain. Particularly, lithofacies A1 can be interpreted as a typical channel-fill succession, according to its peculiar facies characteristics and the presence of a transported and reworked microfauna. Lithofacies A2 is interpreted to represent channel abandonment and overbank sedimentation, including floodplain clays and minor crevasse/levee sand and silt deposits.

Similarly to what reported from adjacent areas (Amorosi et al., 1999a, 2003), deposition of Facies association A probably took place during the last glacial period, in the late Pleistocene, when lowstand conditions induced the development of a wide alluvial plain in the present coastal plain and in the northern Adriatic area. The indurated horizon at top of this facies association suggests a prolonged period of subaerial exposure, related to the early stages of transgression following the Last Glacial Maximum.

Back-barrier facies association (B)

Description

In all studied cores, the indurated horizon on top of Facies association A is abruptly overlain by characteristic dark, soft muds, attributed to Facies association B (Fig. 2). This facies association,

with a maximum thickness of 5 m (Core 1), can be subdivided primarily into three lithofacies. Basal lithofacies B1, 0.4-1.5 m thick, consists of peat layers, up to several tens of cm thick, and dark grey, organic-rich clay, with pulmonate gastropods and abundant wood fragments. Few valves of freshwater ostracods, such as *Candona albicans* (Brady), occur in this lithofacies.

Lithofacies B2, 0.5-1.5 m thick, is generally sandwiched within clayey layers of lithofacies B1 (see Fig. 3A - cores 1 and 3). It consists of fine to medium sand, with sharp lower boundaries. No fossils were encountered within this lithofacies.

The upper part of Facies association B includes lithofacies B3, 0.3-1.5 m thick. This lithofacies displays an obvious coarsening-upward trend, with transition from clay to fine sand (Fig. 3A). Clays are characterized by an oligotypic benthic assemblage, composed primarily of *Ammonia beccarii* (Linnaeus) and *Pontocythere turbida* (G.W. Müller). Shells of bivalves, mainly *Cardium* (Linnaeus), and marine gastropods are locally abundant in Core 2. On the other hand, scattered bioclasts of mollusc, small plant debris and a mixed marine-brackish microfauna (*Ammonia beccarii*; *Elphidium* spp., *Ammonia tepida*; *Cyprideis torosa* (Jones)) are usually recorded within the overlying sandy deposits.

Five radiocarbon dates are available from this facies association (Fig. 2). The basal peat horizon (lithofacies B1) is well constrained to lowermost Holocene (about 9,900 cal yr BP). A reliable age estimate for the top of Facies association B is around 7,500 cal yr BP, based upon radiocarbon age of 7685±175 from lithofacies B1 of Core 3 (Fig. 2).

Interpretation

Lithofacies B1 corresponds to backswamp deposits that accumulated in a coastal plain or on the landward side of a lagoon, in response to a rapid shift in sea-level rise close to the Pleistocene-Holocene boundary. Vertical transition to lithofacies B2 (cores 1 and 3) is suggestive of an increase in fluvial activity, which led to temporary swamp infilling by crevasse deposits. Superposition of

lithofacies B1 onto B2 documents the re-establishment of paludal environments in the study area around 9,500 calibrated yr BP, as shown by good correlation between ^{14}C dates in core 1 and 3 (Fig. 2).

The lower, muddy portion of lithofacies B3, with its characteristic faunal content, is interpreted to represent transition to a marine-influenced environment. On the basis of stratigraphic relationships with the overlying fossiliferous sand, this lithofacies is interpreted as a back-barrier environment, showing upper transition to a washover fan, containing a transported marine-brackish microfauna.

Transgressive barrier facies association (T)

Description

Facies association T, only few dm thick, consists of medium to fine sand, with very abundant bioclasts and shells of marine bivalves and gastropods (Fig. 3B), among which *Pecten* (Müller), *Murex* (Linnaeus), and *Turritella* (Lamarck) are the most common. An obvious erosional surface, marked by a veneer of mollusc shells, separates this facies association from underlying lithofacies B3.

Large-size specimens of marine benthic foraminifers and ostracods, such as *Ammonia beccarii* and *A. inflata* (Seguenza); *Elphidium crispum* (Linnaeus); *Adelosina* spp., *Semicytherura* spp. and *Loxoconcha exagona* (Bonaduce), showing traces of abrasion, are encountered throughout this facies association.

A radiocarbon date from this facies association (Core 1) provided an age of $5,805 \pm 175$ cal yr BP.

Interpretation

The sedimentological and faunal characteristics of this facies association, which displays strong similarities with sand deposits observed south of Po Delta in a correlative stratigraphic position (Curzi et al., 2006), suggest a high-energy coastal environment. The basal erosion surface is interpreted to be the result of wave ravinement that cut across back-barrier deposits, in response to rapid beach-barrier migration (Swift, 1968; Nummedal and Swift, 1987). The basal shell-rich layer corresponds to a transgressive lag, and the overlying sand is attributed to a shoreface environment.

Inner-shelf facies association (S)

Description

Facies association S (Fig. 3B) is made up predominantly of silty clay, with an overall fining-upward tendency. Concentration of fragments of marine bivalves is observed at distinct stratigraphic levels. Sand laminations are occasionally encountered.

The abundant foraminiferal microfauna includes high percentages of Miliolidae (18-41%) and hyaline epiphytic taxa (4.5-30.8%), mainly represented by *Asterigerinata mamilla* (Williamson), *Neocorbina terquemi* (Rzehak), with subordinate *Rosalina brady* (Cushman). Among Miliolidae, *Adelosina*, *Miliolinella* (Wiesner), *Pseudotriloculina* (Cherif), *Quinqueloculina* (d'Orbigny) and *Siphonaperta* (Vella) are common. Relatively low amounts of *Criboelphidium* (less than 18%) are observed in association with few specimens (less than 9%) of *Ammonia tepida* and *A. parkinsoniana* (d'Orbigny). *Valvulineria perlucida* (Heron-Allen and Earland) locally attains remarkably high values (26-50%).

The ostracod fauna is characterized by a high specific diversity, including several species of *Semicytherura* (Wagner) and *Loxoconcha* (Sars), such as *S. incongruens* (G.W. Müller), *S.*

acuticostata (Sars), *S. costata* (G.W. Müller), *S. striata* (Sars), *S. robusta* (Bonaduce), *L. tumida* (Brady), *L. turbida* (G.W. Müller), and *L. exagona*. Few valves of other taxa, as *Carinocythereis whitei* (Baird), *Hiltermannicythere turbida* (G.W. Müller), *Leptocythere* spp. and *Pterygocythereis ceratoptera* (Bosquet), are also present.

A radiocarbon date from this facies association (Core 1) provided an age of 4,700±155 cal yr BP.

Interpretation

Lithologic characteristics and faunal content of this facies association are consistent with deposition in an inner-shelf environment. Specifically, the foraminiferal assemblage is suggestive of open-marine conditions, with a flourished vegetation cover at sea bottom. The remarkable abundance of *Semicytherura* and *Loxococoncha* species, commonly found in infralittoral settings of the Adriatic Sea (Colalongo, 1969; Breman, 1975), supports this interpretation.

Facies association S records the relatively deepest marine conditions within the whole study succession. Radiocarbon dating from uppermost Facies association S deposits in Core 1 places this unit around time of maximum marine ingression.

Local high percentages of *Valvulineria perlucida*, a characteristic shallow-water taxon preferring environments with high food availability (Jorissen, 1988) and commonly found in living assemblages near the Po Delta (Donnici and Serandrei Barbero, 2002), suggest a local increase in fluvial influence.

Prodelta facies association (Pd)

Description

Facies association Pd has an average thickness of 15-16 meters and displays a transitional boundary to the underlying inner-shelf deposits (Facies association S). Three lithofacies (Pd1-Pd3) may be distinguished within this unit. Lithofacies Pd1 and Pd2 are vertically stacked, with an overall coarsening-upward trend (Fig. 3C). Lithofacies Pd3 was observed in Core 1 only, between 20.50 and 25.10 m depth.

Lithofacies Pd1 includes a monotonous, thick succession of silty clay, passing upward to dominant silt. Sand intercalations, a few mm to cm-thick, are increasingly abundant upwards. Scattered plant remains and rare bivalve bioclasts are recorded throughout this lithofacies.

Despite lithologic similarities with underlying Facies association S, lithofacies Pd1 shows a remarkably different micropalaeontological content. Specifically, the varied microfauna observed within the inner-shelf clays is here replaced by a relatively low number of foraminiferal species, including *Ammonia tepida* and *A. parkinsoniana* (generally 10-70%), with locally high amounts of *Valvulineria perlucida*, *Criboelphidium granosum* (d'Orbigny) and *Quinqueloculina seminulum* (Linnaeus). In the upper part of this facies association, the foraminiferal assemblage becomes more oligotypic, consisting almost entirely of *Ammonia tepida* and *A. parkinsoniana* (> 83%). The ostracod fauna is poorly diversified, with abundant *Loxoconcha turbida* and subordinate *Leptocythere ramosa* (Rome). Locally, numerous valves of *Semicytherura incongruens* and *Cytheridea neapolitana* (Kolmann) are encountered.

Lithofacies Pd2 consists of silt and sandy silt, with abundant intercalations of sand layers, up to 50 cm thick (Figs. 2 and 3C). Plant debris and organic-rich material are common. The microfauna is poor, and includes few specimens of *Ammonia tepida* and *A. parkinsoniana*, with rare valves of *Loxoconcha elliptica* (Brady). Sand intercalations are barren in microfossils.

Lithofacies Pd3 consists of silty clay with a peculiar microfauna dominated by *Nonionella turgida* (Williamson) (27-75%), with subordinate *Ammonia tepida* and *A. parkinsoniana*. The ostracod fauna is scarce, and mainly represented by few valves of *Loxoconcha turbida* and *Leptocythere ramosa*.

Deposition of this facies association is tightly constrained between 605 ± 65 and 380 ± 110 cal yr BP (Core 1).

Interpretation

The low interspecific microfaunal diversity of this facies association, combined with the dominance of taxa tolerant to stressed marine conditions, including low salinity, high nutrient fluxes and high turbidity, enable a prompt distinction of Facies association Pd from underlying inner-shelf deposits. These features allow to interpret this facies association as indicative of a prodelta environment. A comparable modern microfauna (*Ammonia* (Brünnich) and *Criboelphidium* (Cushman) assemblage) is commonly found in several deltaic systems, at relatively low water depths and within organic-rich deposits (10-22 meters in the North Adriatic area, Jorissen, 1988).

The upcore increase in *Ammonia tepida* and *A. parkinsoniana*, within lithofacies Pd1, and the generally poor microfauna of lithofacies Pd2, are suggestive of progressive approaching river mouths. A general shallowing-upward tendency within Facies association Pd also is documented by the upward increase in frequency and thickness of sand layers, which is paralleled by a decrease in the clay content. In this respect, lithofacies Pd2 could mark the transition from prodelta to delta-front sub-environments.

The *Nonionella turgida*-dominated foraminiferal assemblage recorded within lithofacies Pd3 displays strong similarities with the microfauna observed in the taphocoenoses that characterize the western flank of the Northern Adriatic mud-belt (Van der Zwaan and Jorissen, 1991). In the same area, *Nonionella turgida* (listed as *Nonionella opima* (Cushman)) is also dominant in living assemblages subjected to high organic matter inputs supplied by Po River (Donnici and Serandrei Barbero, 2002). In this respect, lithofacies Pd3 is considered to reflect the presence of a fossil mud-belt, in which Po River runoff products (fine-grained particles and nutrients) were concentrated by

longshore currents, inducing ample food availability and a limited oxygen deficiency at the sea bottom.

Delta front facies association (Df)

Description

Facies association Df, less than 5 m thick, consists of fine to medium sand, with a gradational lower boundary with the underlying fine-grained prodelta deposits (Facies association Pd) and an overall coarsening-upward trend (Fig. 3C). Two distinct sand bodies, separated by prodelta-delta front transition deposits (lithofacies Pd2), are recorded in cores 2 and 3.

Local accumulation of organic matter and bivalve bioclasts is common within this facies association, while wood fragments are scattered. A scarce microfauna, composed of poorly preserved specimens of benthic and planktonic foraminifers including *Bulimina* (d'Orbigny), *Cassidulina* (d'Orbigny) and *Orbulina* (d'Orbigny), is observed.

Interpretation

The sedimentological features of this facies association and the presence of foraminiferal assemblages possibly transported from nearby environments or reworked from older units, are indicative of a high-energy setting. Facies association Df, the top of which is just 2-7 m below the ground surface, corresponds to delta front deposits that accumulated in the study area during the 17th century (see radiocarbon age at upper boundary of Facies association Pd, in Core 1), following the Porto Viro diversion, which directed the main Po River trunk close to its present position (Ciabatti, 1967; Correggiari et al., 2005a, 2005b; Stefani and Vincenzi, 2005).

The presence of two superposed delta-front sand bodies (Fig. 2), separated by a variable thickness of prodelta clays, could be interpreted as alternate phases of delta lobe advance and retreat, possibly in response to a predominantly autocyclic control (distributary-channel avulsion and delta-lobe switching).

Delta plain facies association (Dp)

Description

Facies association Dp, less than 5 m thick, is encountered at top of the cored succession. It is mainly composed of fine-grained deposits and shows a sharp boundary with the underlying delta front sands.

Two lithofacies, with distinct micropalaeontological features, are observed. Lithofacies Dp1, which is recorded in proximity of the present coastline (cores 1 and 3), is composed primarily of homogeneous clay, including plants remains and scattered bioclasts. Several bioclasts and shells of *Cardium* were encountered within the clayey succession of Core 3, which was drilled along the outer margin of a present coastal lagoon. This lithofacies includes an oligotypic microfauna characterized by the overwhelming dominance of *Ammonia tepida* and *A. parkinsoniana*. In Core 3 these species are observed in association with numerous valves of *Cyprideis torosa*.

Lithofacies Dp2 occurs at top of cores 1 and 2 and is composed of clay and silt, with common sand intercalations. This lithofacies displays a higher content in organic matter. The mollusc fauna includes few shells of pulmonate gastropods, whereas bivalve bioclasts are lacking. No microfossils are present within this lithofacies.

Interpretation

Facies association Dp corresponds to the present Po Delta plain, which formed from ca. 350 cal yr BP to present (Correggiari et al., 2005a, 2005b). Particularly, lithofacies Dp1 corresponds to lower delta-plain deposits that accumulated in a complex environment strongly influenced by the sea (lagoon or bay), as suggested by the presence of a typical brackish-hypohaline microfauna. On the other hand, lithofacies Dp2 is interpreted to reflect an upper delta-plain setting, with no marine influence. The fine-grained succession corresponds to flood-basin deposits, while the thicker sand layers recorded in Core 2 can be interpreted as crevasse-splay sands.

Geochemistry of Core 1

Recent geochemical studies from Po coastal plain, carried out on late Quaternary cores (Amorosi et al., 2002, 2007; Curzi et al., 2006) and soil samples (Amorosi and Sammartino, 2005, 2007) have shown that selected elements, such as Cr and Ni, can be regarded as reliable geochemical indicators of sediment provenance from the Po River. Particularly, Cr/Al₂O₃ and Ni/Al ratios are not significantly influenced by changes in grain size (Dinelli et al., 2007), and may thus represent powerful tracers of this sediment source. The peculiar geochemical signal of Po River provenance has been interpreted to be the result of the abundance, in the Po drainage basin, of Cr- and Ni-bearing rocks (mainly ophiolites), deriving from both Alpine and Apenninic sources. On the other hand, geochemical studies from cores recovered in front of major Po distributary-channel mouths (Pila and Tolle), up to water depths of 36 m, have shown that Ba can be regarded as an indicator of sediment provenance from the Alpine Adige River (Picone et al., in press).

Four geochemical units (A to D in Fig. 4), with a marked stratigraphic significance, were identified on the basis of i) variations in bulk composition, which is dominated by the mixing of carbonates, coarse-grained silicates and fine-grained silicates, and ii) selected geochemical ratios

(Ba/Al, Cr/Al₂O₃ and Ni/Mg), used as indicators of sediment provenance in previous work (see above).

Geochemical unit A, corresponding to the alluvial-plain deposits in the lower part of the study succession, displays high Ba/Al values and the lowest Cr/Al₂O₃ and Ni/Mg values (Fig. 4). Bulk composition, not shown here in detail, is characterized by relatively low median concentrations of Al₂O₃, Fe₂O₃, V, Co, Cr, Ni, and Zn, concurrently with the highest median concentrations of CaO, Ba and Zr. The overlying Geochemical unit B, including samples from the back-barrier facies association, shows high Ba/Al values and increasing, although strongly fluctuating, Cr/Al₂O₃ and Ni/Mg values. An increase in Fe₂O₃, V, Cr, Ni and the highest median SiO₂ value are also recorded within this unit. Samples from organic-rich lithofacies B1 are strongly depleted in carbonates. Geochemical Unit C, corresponding to shelf and lowermost prodelta deposits, is characterized by a sharp decrease in Ba/Al and a slight increasing trend of Cr/Al₂O₃ and Ni/Mg. High concentrations of Fe₂O₃, V, Cr, Ni and Zn are also recorded in this interval, along with relatively low CaO values. Uppermost Geochemical unit D, including the vertical succession of prodelta, delta front and delta plain deposits, is characterized by the highest Cr/Al₂O₃ and Ni/Mg values. On the other hand, Ba/Al shows its lowest values and is constant throughout this interval. This unit has the lowest median CaO content, and the highest median concentrations of Fe₂O₃, V, Cr, Ni.

If plotted in the Ni/Mg *versus* Ba/Al diagram and compared with literature data (Fig. 5), fluvial samples from Geochemical unit A show a certain scattering and plot close to the compositional field of Adige River sediments. Despite a wide scattering, which appears to reflect the geochemical response to the variety of lithofacies within Facies association B (including organic-rich layers and peat), most back-barrier samples from Geochemical units B and C overlap with the field of fluvial sediments of Apenninic provenance, with a subordinate Po River influence. Finally, Geochemical unit D has a clearly distinct sediment provenance, plotting into the field of modern Po River sediments, with a limited dispersion.

Late Quaternary palaeoenvironmental evolution

Detailed correlation of cores 1-3, combined with stratigraphic data from core Scardovari (Roveri et al., 2001; Correggiari et al., 2005b) and adjacent wells (Fig. 6), allow to depict the late Quaternary (post-Last Glacial Maximum) palaeogeographic evolution of the study area. This follows the classic three-fold sequence-stratigraphic subdivision into lowstand, transgressive and highstand deposits.

The lowstand phase

Late Pleistocene sedimentation in the study area is recorded by the widespread development of fluvial-channel and overbank deposits (Facies association A). Although radiocarbon dates are not available for this stratigraphic interval, strong similarities with the stratigraphic framework reconstructed from adjacent areas (Amorosi et al., 1999a, 2003, 2005) suggest that these deposits accumulated during the Last Glacial Maximum, when sea level was approximately 120 m below its present position. In this respect, the stiff unit atop the alluvial succession can be readily correlated with the pedogenized horizon marking the Pleistocene-Holocene boundary throughout the Po Plain (Amorosi and Marchi, 1999) and the Venetian Plain (Tosi, 1994; McClennen et al., 1997; Mozzi et al., 2003).

During this period, the north Adriatic area was a huge alluvial plain drained by rivers of Alpine provenance. Sediment composition of fluvial deposits of Core 1 indicates a likely influence from Alpine Adige River (see Fig. 1), as suggested by the “anomalously” high Ba content of Geochemical unit A, which has no equivalents in sediments of Apenninic provenance. This implies that at lowstand conditions Po River flowed far from the study area, in a different position relative to its present course.

The Holocene transgression

Above the alluvial plain deposits, the post-glacial, transgressive succession consists of, from bottom to top, back-barrier, transgressive barrier and inner-shelf deposits (Figs. 2 and 6). Rapid sea-level rise close to the Pleistocene-Holocene boundary induced the flooding of the pre-Holocene alluvial plain, leading to the development of a variety of freshwater and brackish, back-barrier sub-environments.

Early stages of transgression (about 11,000 cal yr BP) are recorded by Facies association B in Core Scardovari only, where onlapped contacts onto the underlying substrate are observed (Fig. 6). The lower boundary of Facies association B, representing the transgressive surface, is sharp and depicts irregularities in substrate topography, suggesting that inherited Pleistocene morphology conditioned the geometry of backswamp and lagoonal deposits during the early Holocene. Generalized sedimentation in a back-barrier environment spread onto the entire study area around 9,850 cal yr BP (Fig. 6).

Superposition of lithofacies B2 onto B1 (Fig. 2) and the sheet-like geometry of sandy lithofacies (Fig. 6) suggest that a generalized phase of swamp infilling took place in the study area around 9,500 cal yr BP, possibly reflecting a stillstand episode within the generalized transgressive phase. In this respect, this shallowing-upward succession (parasequence in the sense of Van Wagoner et al., 1990; Kamola and Van Wagoner, 1995) could be correlative of one of the parasequences recently recognized within the Holocene transgressive deposits of Po coastal plain, 20 km south of the study area (Amorosi et al., 2005).

Renewed transgression is suggested by superposition of lithofacies B1 onto B2, and by upward transition to marine-influenced lithofacies B3, around 7,500 cal yr BP (see flooding surface in Fig. 6). As relative sea-level continued to rise, the back-barrier facies migrated further inland and a coastal environment took place in the study area, around 6,000 cal yr BP. The erosional contact

between Facies association B and overlying Facies association T is interpreted to reflect rapid backstepping of a barrier-lagoon system with continuing transgression.

A complex palaeogeography can be envisaged for the transgressive coastal system in the study area. Geochemical composition of back-barrier deposits (Geochemical unit B) suggests that, at early stages of transgression, Adige River was no longer able to supply sediments to the backstepping coastal system. During this phase, a dominant sediment contribution from the Apenninic rivers via the longshore drift is reconstructed, although a subordinate sediment supply from the Po River is recorded by a few samples.

Peak transgression and the maximum flooding surface

Maximum transgression was reached during deposition of Facies association S, when inner-shelf conditions established across the entire study area. As previously observed by Amorosi and Colalongo (2005), vertical distribution of benthic foraminiferal species may be useful to trace the maximum flooding surface within lithologically homogeneous deposits. This can be done in coincidence of the highest frequencies of relatively deep-marine species and the lowest frequencies of littoral and euryhaline taxa. These conditions are reached at 28.90 m within Core 1, where the highest concentrations of inner-shelf species, such as *Asterigerinata mamilla*, *Buccella granulate* (Di Napoli Alliata), *Siphonaperta aspera* (d'Orbigny) and *Textularia agglutinans* (d'Orbigny), are paralleled by the lowest concentrations of the euryhaline *Ammonia tepida* and *A. parkinsoniana*. Similarly, in cores 2 and 3 the maximum flooding surface lies few decimetres above the boundary with underlying Facies association T, suggesting that negligible deposition, with significant stratigraphic condensation, occurred in the study area during latest stages of transgression.

Composition of Geochemical unit C suggests that no significant changes in sediment dispersal patterns occurred in this period. A mixed sediment contribution to the inner shelf from the

Apenninic rivers and the Po River can be inferred from the Ni/Mg *versus* Ba/Al (Fig. 5), and from slightly increasing Cr/Al₂O₃ and Ni/Mg values (Fig. 4).

The highstand phase and the onset of Po River Delta

The upward increase in *Valvulineria perlucida* at top of Facies associations S is considered to reflect transition to prodelta deposits, and thus may serve as an indication of the onset of deltaic sedimentation in the study area. This is consistent with the ¹⁴C date of about 4,700 cal yr BP obtained within early regressive deposits (Figs. 2 and 6). The turnaround to regressive conditions, recording rapid delta progradation, took place when sediment supply overcame the rate of sea-level rise.

Coastal progradation in the Adriatic area is documented in the study cores by vertical superposition of prodelta (Facies association Pd), delta front (Df), and delta plain (Dp) deposits. This succession is approximately 25 m thick, resulting in strong asymmetry of the transgressive-regressive Holocene depositional cycle.

Inner shelf and lower prodelta deposits above the maximum flooding surface display strong stratigraphic condensation, and show geochemical features that are similar to those recorded within late transgressive shelf deposits (Geochemical unit C). This suggests that during the early highstand phase (between ca. 5,000 and 600 cal yr BP) the study area was sediment-starved, and received a markedly reduced sediment supply from the fringes of distinct prograding delta lobes (mixed Apenninic and Po River sediment contribution).

The onset of modern-age Po Delta in its present position is recorded within a lithologically homogeneous succession at about 600 cal yr BP, and is marked by identification of a mud-belt in the study area, at 25.10 m core depth (Core 1). The bulk of the shallowing-upward deltaic succession, starting with the mud-belt, also has an obvious Po River-supplied geochemical

signature, being marked by a sudden increase in Cr and Ni (abrupt shift to Geochemical unit D in Figs. 4 and 5).

Products of Po River runoff were brought to the sea and dispersed southward, parallel to the Adriatic coastline, by longshore currents. This induced the offshore accumulation of nutrients and fine-grained particles, probably at water depths comparable with the present record (20-40 m from Van der Zwaan and Jorissen, 1991), and led to the formation of a mud belt in the southern part of the study area (lithofacies Pd3 in Core 1 – See Fig. 2). Lack of a mud belt beneath the northern part of present delta plain is consistent with the southward-directed surface water circulation patterns (Core 3) and relatively proximal position (Core 2).

The growth of modern-age Po Delta in the study area took place after the abandonment of Primaro delta lobe and the northward shifting of the major Po distributary channel, both triggered by Ficarolo avulsion, in mid 12th Century AD (Correggiari et al., 2005b). This is confirmed by radiocarbon dates from basal prodelta deposits in Core Scardovari (750 cal yr BP – Roveri et al., 2001; Correggiari et al., 2005b) and Core 1 (ca. 600 cal yr BP - Fig. 2).

The remarkable thickness of the prodelta succession (Fig. 6) is indicative of very high sedimentation rates, induced by the combined effects of climate instability (Medieval Warm Period and Little Ice Age dated to 500-100 cal yr BP), and intense human interventions, such as deforestation and construction of artificial levees (Veggiani, 1990; Stefani and Vincenzi, 2005). During this period, at the transition to Modern Age, a marked phase of large delta outbuilding took place, leading to the formation of a multi-lobe supply-dominated system (“Renaissance lobes” of Correggiari et al., 2005a, b).

The Porto Viro cut, operated by the Venice Republic ca. 350 cal yr BP to prevent the infilling of Venice Lagoon, marked another intense progradational phase (outbuilding of modern Po Delta), which developed under a strong anthropogenic forcing (Correggiari et al., 2005b). Laterally continuous delta-front sand bodies, following an orientation parallel to the present shoreline, replaced prodelta sedimentation around 380 cal yr BP (see Core 1 in Fig. 2), suggesting the

development of a wave-dominated delta. Distinct stages of delta development are shown by alternating prodelta and delta front deposits (Fig. 6). The shallowing-upward succession is capped by recent delta-plain deposits.

Conclusions

Integrated sedimentological, micropalaeontological and geochemical analyses of three continuously-cored boreholes from subsurface of present Po Delta plain allow reconstruction of sequence-stratigraphic architecture, and may serve to identify palaeoenvironmental changes during the late Quaternary. Major results of this study can be summarized as follows:

- 1) The vertical stacking of seven major facies associations depicts the palaeoenvironmental evolution of the study area from the Last Glacial Maximum to Present. Identification of thirteen lithofacies on the basis of distinctive microfaunal (benthic foraminifer and ostracod) assemblages allows to refine palaeoenvironmental interpretation.
- 2) Above a fining-upward succession of lowstand alluvial deposits, stratigraphic architecture beneath Po Delta plain displays the traditional transgressive-regressive *suite* of backstepping barrier-lagoon (TST) and prograding deltaic systems (HST). Repeated phases of backswamp development and infilling by crevasse processes are likely to reflect a millennial-scale cyclicity of sea-level rise and stillstand, during early stages of transgression. Subtle micropalaeontological indicators enable precise identification of the maximum flooding surface (MFS) within otherwise undifferentiated shallow-marine clays.

- 3) The Holocene transgressive-regressive cycle of the Po Delta exhibits a marked asymmetry, with a thin (about 7 m) TST and a comparatively thicker (about 27 m) HST. Strong sediment condensation is recorded around MFS and in the early HST. The outbuilding of modern-age Po Delta is recorded within late HST by a microfauna showing strong similarities with the foraminiferal assemblage observed in the taphocoenoses of the Northern Adriatic mud-belt. Identification of this *Nonionella turgida*-dominated assemblage represents the first occurrence of a fossil mud-belt in the subsurface of the Po River Delta.

- 4) Vertical profiles of selected geochemical elements reveal distinctive changes in sediment provenance through time. Lowstand fluvial deposits display remarkably high Ba/Al values, which are interpreted to reflect sediment supply from Alpine (Adige River) sources. Transgressive sedimentation was characterized by a mixed (Apenninic and Po-derived) contribution to coastal environments. A remarkable shift toward the highest Cr and Ni concentrations is recorded at lower boundary of the mud-belt, reflecting the onset of modern-age Po River Delta in its present position.

Figure captions

Fig. 1. Location of the study area, with indication of the three cores (1-3) investigated in this study and section trace of Fig. 6. Dots indicate outcropping beach ridges in the Po Delta area (after Ciabatti, 1967). SC=Core Scardovari (described in Correggiari et al., 2005b). The mud-belt identified offshore the present Po Delta and the Adriatic surficial circulation pattern are also shown.

Fig. 2. Detailed stratigraphy of cores 1 to 3, with subdivision into lithofacies (see text) and indication of radiocarbon dates. Samples for micropalaeontological analysis are shown left of each stratigraphic column. TS: Transgressive surface, RS: Ravinement surface.

Fig. 3. Representative core photographs depicting the major facies associations and lithofacies identified in Core 1. A: late Pleistocene alluvial deposits (A1 and A2) overlain by a transgressive Holocene succession of back-barrier (B1-B3) and beach-barrier (T) sediments. The red line indicates the transgressive surface, while the yellow line shows the ravinement surface B: Close-up of A, showing the erosional boundary between washover sand (B3) and overlying transgressive barrier sand (T), with upward transition to shelf clay (S). C: Upward transition from prodelta (Pd1) and prodelta-delta front transition (Pd2) deposits to delta front (Df) sand, marked by the increasing proportion of sand within clay-sand alternations.

Fig. 4. Vertical profiles of selected geochemical indicators.

Fig. 5. Ba/Al vs Ni/Mg diagram of Core 1 samples. Compositional fields of sediments from the major rivers of the northern Adriatic area are shown for comparison: north Adriatic rivers (data from Dinelli and Lucchini, 1999), Adige River (data from Boldrin et al., 1989, 1992; Dinelli and Lucchini, 1999), Po River (data from Dinelli and Lucchini, 1999; Amorosi et al., 2002; Amorosi

and Sammartino, 2005, 2007), Apenninic rivers not tributaries of Po River (data from Dinelli and Lucchini, 1999; Amorosi et al., 2002). GU: Geochemical Unit.

Fig. 6. Stratigraphic cross-section beneath present Po Delta plain (see Fig. 1, for location of boreholes) showing facies architecture parallel to the shoreline, with sequence-stratigraphic interpretation (an approximate position of maximum flooding surface is shown). Unpublished data from cores ES1, E21 and LS1 were provided by S.P.G.

References

- AGIP, 1982. Foraminiferi Padani (Terziario e Quaternario): Plate I-LII. AGIP, Milano.
- Aguzzi, M., Amorosi, A., Colalongo, M.L., Ricci Lucchi, M., Rossi, V., Sarti, G., Vaiani, S.C., 2007. Late Quaternary climatic evolution of the Arno coastal plain (Western Tuscany, Italy) from subsurface data. *Sedimentary Geology* 202, 211-229.
- Albani, A., Serandrei Barbero, R., 1990. I Foraminiferi della Laguna e del Golfo di Venezia. *Memorie Scienze Geologiche Padova* 42, 271-341.
- Amorosi, A., Marchi, N., 1999. High-resolution sequence stratigraphy from piezocone tests: an example from the Late Quaternary deposits of the SE Po Plain. *Sedimentary Geology* 128, 69-83.
- Amorosi, A., Colalongo, M.L., 2005. The linkage between alluvial and coeval nearshore marine successions: evidence from the Late Quaternary record of the Po River Plain, Italy. In: Blum, M.D., Marriott, S.B., Leclair, S.F. (Eds.), *Fluvial Sedimentology VII*, International Association of Sedimentologists Special Publication, vol. 35, pp. 257-275.
- Amorosi, A., Sammartino, I., 2005. Geologically-oriented geochemical maps: a new frontier for geochemical mapping? *GeoActa* 4, 1-12.
- Amorosi, A., Sammartino, I., 2007. Influence of sediment provenance on background values of potentially toxic metals from near-surface sediments of Po coastal plain (Italy). *International Journal of Earth Sciences* 96, 389-396.

Amorosi, A., Colalongo, M.L., Pasini, G., Preti, D., 1999a. Sedimentary response to Late Quaternary sea-level changes in the Romagna coastal plain (northern Italy). *Sedimentology* 46, 99-121.

Amorosi, A., Colalongo, M.L., Fusco, F., Pasini, G., Fiorini, F., 1999b. Glacio-eustatic control of continental-shallow marine cyclicity from Late Quaternary deposits of the south-eastern Po Plain (Northern Italy). *Quaternary Research* 52, 1-13.

Amorosi, A., Centineo, M.C., Dinelli, E., Lucchini, F., Tateo, F., 2002. Geochemical and mineralogical variations as indicators of provenance changes in Late Quaternary deposits of SE Po Plain. *Sedimentary Geology* 151, 273-292.

Amorosi, A., Centineo, M.C., Colalongo, M.L., Pasini, G., Sarti, G., Vaiani, S.C., 2003. Facies architecture and Latest Pleistocene-Holocene depositional history of the Po Delta (Comacchio area). Italy. *The Journal of Geology* 111, 39-56.

Amorosi, A., Colalongo, M.L., Fiorini, F., Fusco, F., Pasini, G., Vaiani, S.C., Sarti, G., 2004. Palaeogeographic and palaeoclimatic evolution of the Po Plain from 150-ky core records. *Global and Planetary Change* 40, 55-78.

Amorosi, A., Centineo, M.C., Colalongo, M.L., Fiorini, F., 2005. Millennial-scale depositional cycles from the Holocene of the Po Plain, Italy. *Marine Geology* 222–223, 7-18.

Amorosi, A., Colalongo, M.L., Dinelli, E., Lucchini, F., Vaiani, S.C., 2007. Cyclic variations in sediment provenance from late Pleistocene deposits of the eastern Po Plain, Italy. In: Arribas, J.,

Critelli, S., Johnsson, M.J. (Eds.), *Sedimentary Provenance and Petrogenesis: Perspectives from Petrography and Geochemistry*, Geology Society of America Special Paper, vol. 420, pp. 13-24.

Athersuch, J., Horne, D.J., Whittaker, J.E., 1989. Marine and brackish water ostracods. In: Kermack, D.M., Barnes, R.S.K. (Eds.), *Synopses of the British Fauna (New Series)*, vol. 43. Brill E.J., Leiden.

Barmawidjaja, D.M., Jorissen, F.J., Puskaric, S., Van der Zwaan, G.J., 1992. Microhabitat selection by benthic foraminifera in the northern Adriatic Sea. *Journal Foraminiferal of Research* 22, 297-317.

Boldrin, A., Juracic, M., Menegazzo-Vitturi, L., Rabitti, S., Ramazzo, G., 1989. Geochemical considerations on trace element distributions in suspended matter and sediments at the river-sea interface, Adige River mouth, northern Adriatic Sea. *Applied Geochemistry* 4, 409-421.

Boldrin, A., Juracic, M., Menegazzo-Vitturi, L., Rabitti, S., Rampazzo, G., 1992. Sedimentation of riverborne material in a shallow shelf sea: Adige River, Adriatic Sea. *Marine Geology* 103, 473-485.

Bonaduce, G., Ciampo, G., Masoli, M., 1975. Distribution of Ostracoda in the Adriatic Sea. *Pubblicazione Stazione Zoologica di Napoli* 40.

Bondesan, M., Favero, V., Viniols, M.J., 1995. New evidence on the evolution of the Po-delta coastal plain during the Holocene. *Quaternary International* 29 (30), 105-110.

Bondesan, M., Cibin, U., Colalongo, M.L., Pugliese, N., Stefani, M., Tsakiridis, E., Vaiani, S.C., Vincenzi, S., 2006. Benthic communities and sedimentary facies recording late Quaternary environmental fluctuations in a Po Delta subsurface succession (Northern Italy). In: Coccioni, R., Lirer, F., Marsili, A. (Eds.), Proceedings of the Second and Third Italian Meeting of Environmental Micropaleontology, The Grzybowski Foundation Special Publication, vol. 11, pp. 21-31.

Breman, E., 1975. The distribution of Ostracodes in the bottom sediments of the Adriatic Sea. Thesis, Free University of Amsterdam, The Netherlands.

Carboni, M.G., Frezza, V., Bergamin, L., 2004. Distribution of Recent foraminifers in the Ombrone River Basin (Tuscany Continental Shelf, Tyrrhenian Sea, Italy): relations with fluvial run-off. In: Coccioni, R., Galeotti, S., Lirer, F. (Eds.), Proceedings of the First Italian Meeting of Environmental Micropaleontology, The Grzybowski Foundation Special Publication, vol. 9, pp. 7-16.

Ciabatti, M., 1967. Ricerche sull'evoluzione del Delta Padano. *Giornale di Geologia* 34, 381-406.

Cimerman, F., Langer, M.R., 1991. Mediterranean Foraminifera. *Academia Scientiarum et Artium Slovenica Classis IV* 30, Ljubljana.

Colalongo, M.L., 1969. Ricerche sugli Ostracodi nei fondali antistanti il delta del Po. *Giornale di Geologia* 36, 335-362.

Correggiari, A., Cattaneo, A., Trincardi, F., 2005a. The modern Po delta system: lobe switching and asymmetric prodelta growth. *Marine Geology* 222-223, 49-74.

Correggiari, A., Cattaneo, A., Trincardi, F., 2005b. Depositional patterns in the Holocene Po Delta system. In: Bhattacharya, J.P., Giosan, L. (Eds.), *River Deltas: Concepts, Models and Examples*. SEPM Special Publication, vol. 83, pp. 365-392.

Curzi, P.V., Dinelli, E., Ricci Lucchi M., Vaiani, S.C., 2006. Palaeoenvironmental control on sediment composition and provenance in the late Quaternary deltaic successions: a case study from the Po delta area (Northern Italy). *Geological Journal* 41, 591-612.

D'Onofrio, S., 1969. Ricerche sui Foraminiferi nei fondali antistanti il Delta del Po. *Giornale di Geologia* 36, 283-334.

Debenay, J.-P., Guillou, J.-J., Redois, F., Geslin, E., 2000. Distribution trends of foraminiferal assemblages in paralic environments. A base for using foraminifera as bioindicators. In: Martin, E.R. (Ed.), *Environmental Micropaleontology. Topics in Geobiology*, vol. 15. Kluwer Academic/Plenum Publishers, New York, pp. 39-67.

Dinelli, E., Lucchini, F., 1999. Sediment supply to the Adriatic Sea basin from the Italian rivers: geochemical features and environmental constraints. *Giornale di Geologia* 61, 121-132.

Dinelli, E., Tateo, F., Summa, V., 2007. Is there any influence of grain-size in the provenance signal of "fine-grained" sediments? Results from Pleistocene to recent sediments of the Po plain, northern Italy. In: Arribas, J., Critelli, S., Johnsson, M.J. (Eds), *Sedimentary Provenance and Petrogenesis: Perspectives from Petrography and Geochemistry*, Geological Society of America Special Paper, vol. 420, pp. 25-36.

Donnici, S., Serandrei Barbero, R., 2002. The benthic foraminiferal communities of the northern Adriatic continental shelf. *Marine Micropaleontology* 44, 93-123.

Fiorini, F., 2004. Benthic foraminiferal associations from Upper Quaternary deposits of southeastern Po Plain, Italy. *Micropaleontology* 50, 45-58.

Fiorini, F., Vaiani, S.C., 2001. Benthic foraminifers and transgressive-regressive cycles in the Late Quaternary subsurface sediments of the Po Plain near Ravenna (Northern Italy). *Bollettino della Società Paleontologica Italiana* 40, 357-403.

Franzini, M., Leoni, L., Saitta, M., 1972. A simple method to evacuate the matrix effects in X-ray fluorescence analysis. *X-ray Spectrom* 1, 151-154.

Franzini, M., Leoni, L., Saitta, M., 1975. Revisione di una metodologia analitica per fluorescenza-X basata sulla correzione completa degli effetti di matrice. *Rendiconti della Società Italiana di Mineralogia e Petrologia* 31, 365-378.

Henderson, P.A., 1990. Freshwater ostracods. In: Kermack, D.M., Barnes, R.S.K. (Eds.), *Synopses of the British Fauna (New Series)* 42. Brill E.J., Leiden.

Jorissen, F.J., 1987. The distribution of benthic foraminifera in the Adriatic Sea. *Marine Micropaleontology* 12, 21-48.

Jorissen, F.J., 1988. Benthic foraminifera from the Adriatic Sea; principles of phenotypic variation. *Utrecht Micropaleontology Bullettins* 37, 1-176.

Kamola, D.L., Van Wagoner, J.C., 1995. Stratigraphy and facies architecture of parasequences with examples from the Spring Canyon Member, Blackhawk Formation, Utah. In: Van Wagoner, J.C., Bertram, G.T. (Eds.), *Sequence Stratigraphy of Foreland Basin Deposits*, American Association of Petroleum Geologists, Memoir 64, pp. 27-54.

Leoni, L., Saitta, M., 1976. X-ray fluorescence analysis of 29 trace elements in rock and mineral standard. *Rendiconti della Società Italiana di Mineralogia e Petrologia* 32, 497-510.

Leoni, L., Menichini, M., Saitta, M., 1986. Determination of S, Cl, and F in silicate rocks by X-ray fluorescence analyses. *X-ray Spectrom* 11, 156-158.

McClennen, C.E., Ammerman, A.J., Schock, S.G., 1997. Framework stratigraphy for the Lagoon of Venice, Italy: revealed in new seismic-reflection profiles and cores. *Journal of Coastal Research* 13, 745-759.

Mozzi, P., Bini, C., Zilocchi, L., Becattini, R., Mariotti Lippi, M., 2003. Stratigraphy, paleopedology and palynology of Late Pleistocene and Holocene deposits in the landward sector of the lagoon of Venice (Italy), in relation to the caranto level. *Il Quaternario* 16 (1Bis), 193-210.

Murray, J.W., 1991. *Ecology and Palaeoecology of Benthic Foraminifera*. Longman Scientific and Technical, London.

Nummedal, D., Swift, D.J.P., 1987. Transgressive stratigraphy at sequence-bounding unconformities: some principles derived from Holocene and Cretaceous examples. In: Nummedal, D., Pilkey, O.H., Howard, J.D. (Eds.), *Sea-Level Fluctuation and Coastal Evolution*, Society of Economic Paleontologists and Mineralogists Special Publication, vol. 41, pp. 241-260.

Picone, S., Alvisi, F., Dinelli, E., Morigi, C., Negri, A., Ravaioli, M., Vaccaio, C., (in press). New insights on Late Quaternary paleogeographic setting in Northern Adriatic Sea (Italy). *Journal of Quaternary Sciences*.

Reimer, P.J., Baillie, M.G.L., Bard, E., Bayliss, A., Beck, J. W., Bertrand, C. J. H., Blackwell, P.G., Buck, C.E., Burr, G.S., Cutler, K.B., Damon, P.E., Edwards, R.L., Fairbanks, R.G., Friedrich, M., Guilderson, T.P., Hogg, A.G., Hughen, K.A., Kromer, B., McCormac, F.G., Manning, S.W., Ramsey, C.B., Reimer, R.W., Remmele, S., Southon, J.R., Stuiver, M., Talamo, S., Taylor, F.W., van der Plicht, J., Weyhenmeyer, C.E. 2004. IntCal04 terrestrial radiocarbon age calibration. *Radiocarbon* 46, 1029-1058.

Rizzini, A., 1974. Holocene sedimentary cycle and heavy mineral distribution, Romagna-Marche coastal plain, Italy. *Sedimentary Geology* 11, 17-37.

Roveri, M., Asioli, A., Correggiari, A., Trincardi, F., 2001. Ultra high-resolution marine record of paleoenvironmental changes in the last 5000 years. *Archaeo Oceanography Limnology* 22, 223-234.

Ruiz, F., Gonzalez-Regalado, M.L., Baceta, J.I., Menegazzo-Vitturi, L., Pistolato, M., Rampazzo, G., Molinaroli, E., 2000. Los ostrácodos actuales de la laguna de Venecia (NE de Italia). *Geobios* 33, 447-454.

Sgarrella, F., Moncharmont Zei, M., 1993. Benthic Foraminifera of the Gulf of Naples (Italy): systematics and autoecology. *Bollettino Società Paleontologica Italiana* 32, 145-264.

Smith, A.J., Horne, D.J., 2002. Ecology of marine, marginal marine and nonmarine ostracodes. In: Holmes, J.A., Chivas, A.R. (Eds.), *The Ostracoda Applications in Quaternary Research*. Geophysical Monograph, vol. 131, pp. 37-64.

Stefani, M., Vincenzi, S., 2005. The interplay of eustasy, climate and human activity in the late Quaternary depositional evolution and sedimentary architecture of the Po Delta system. *Marine Geology* 222–223, 19-48.

Swift, D.J.P., 1968. Coastal erosion and transgressive stratigraphy. *Journal of Geology* 76, 444-456.

Tosi, L., 1994. L'evoluzione paleoambientale tardo-aternaria del litorale veneziano nelle attuali conoscenze. *Il Quaternario* 7, 589-596.

Van der Zwaan, G.J., Jorissen, F.J., 1991. Biofacial patterns in river-induced shelf anoxia. In: Tyson, R.V., Pearson, T.H. (Eds.), *Modern and Ancient Continental Shelf Anoxia*, Geological Society Special Publication, vol. 58, pp. 65-82.

Van Wagoner, J.C., Mitchum, R.M., Campion, K.M., Rahmanian, V.D., 1990. Siliciclastic sequence stratigraphy in well logs, cores, and outcrops: concepts for high-resolution correlation of time and facies. *American Association of Petroleum Geologists Methods in Exploration, Series 7*.

Veggiani, A., 1990. Fluttuazioni climatiche e trasformazioni ambientali nel territorio imolese dall'alto medioevo all'età moderna. In: Mancini, F., Gioberti, M., Veggiani, A. (Eds.), *Imola nel Medioevo*. Imola, pp. 41-102.

Yassini, I., Jones, B.G., 1995. Foraminiferida and Ostracoda from Estuarine and Shelf Environments on the Southeastern Coast of Australia. University of Wollongong Press, Wollongong.

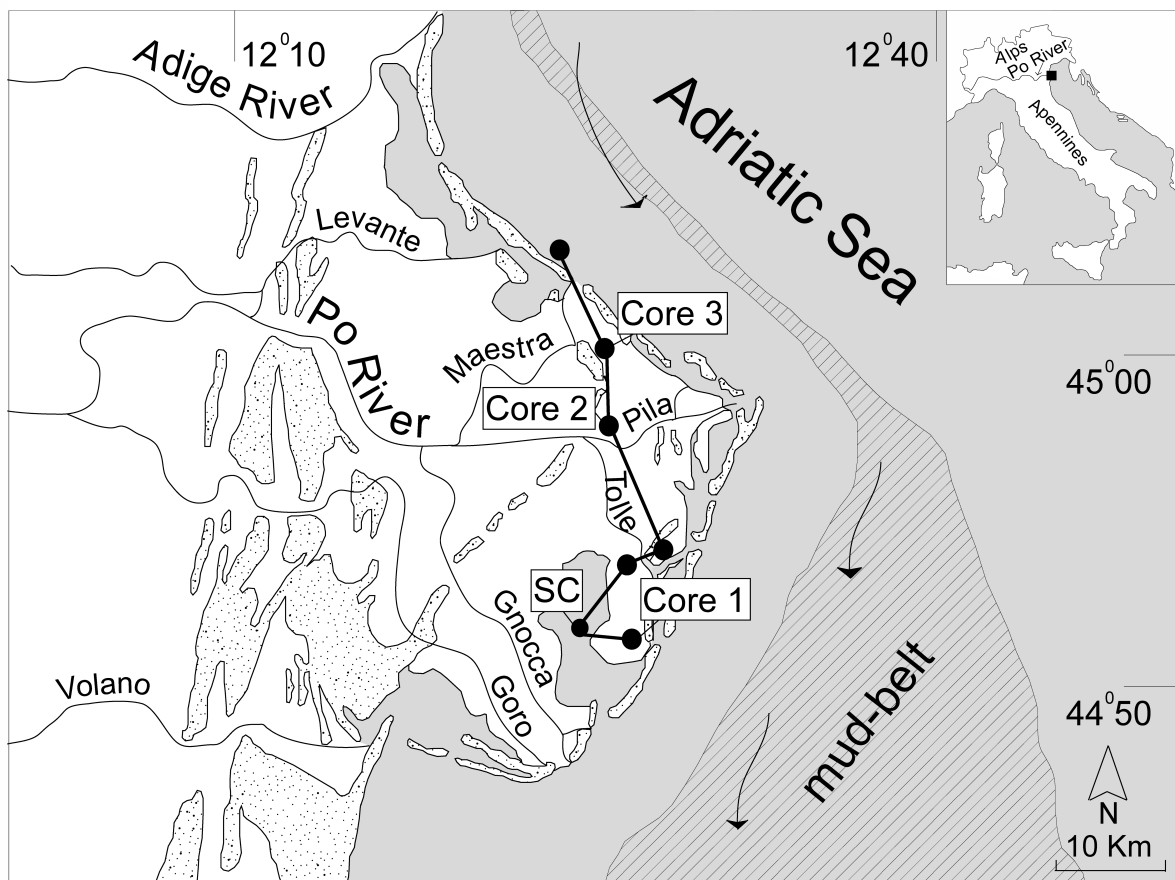


Figure 1

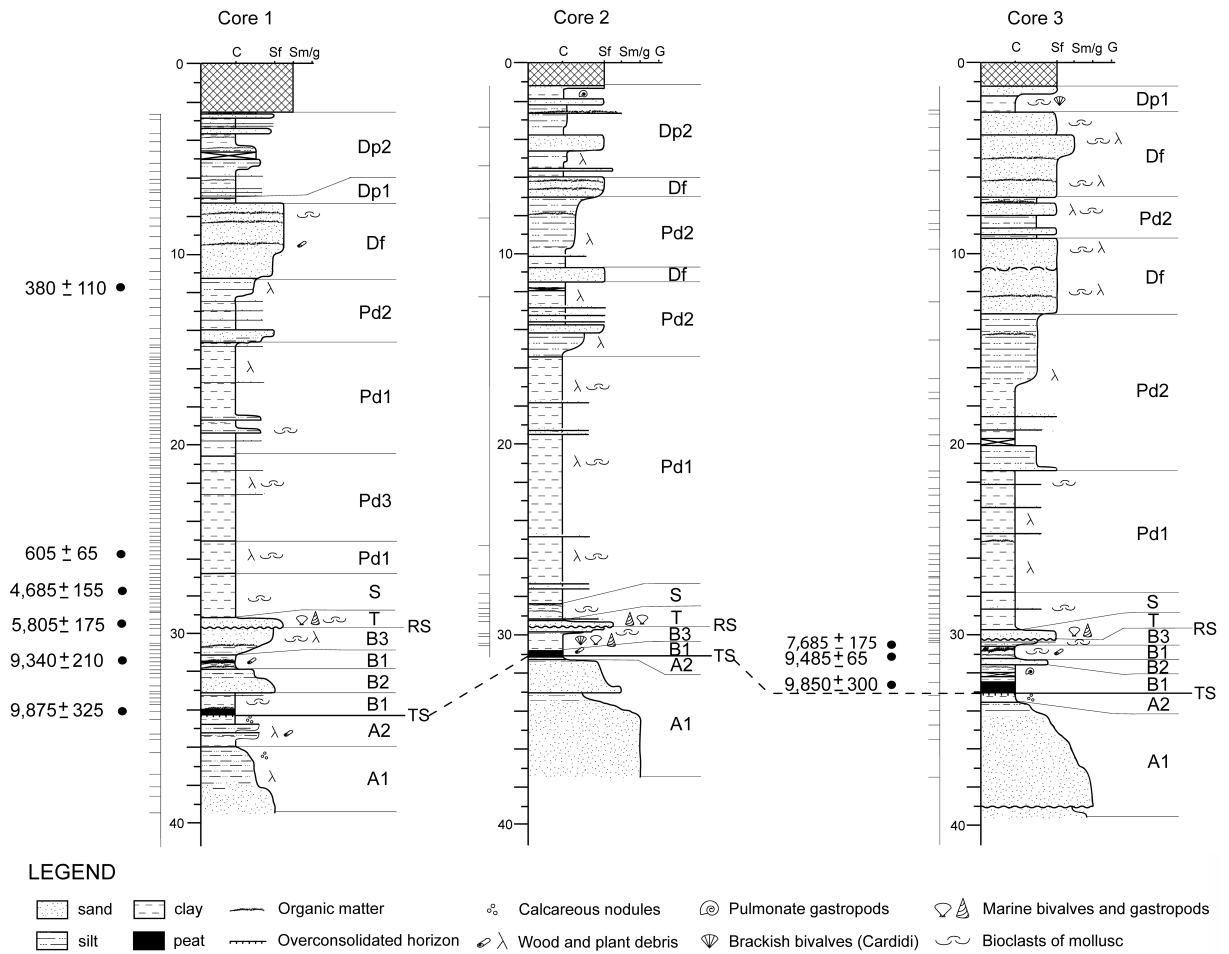


Figure 2

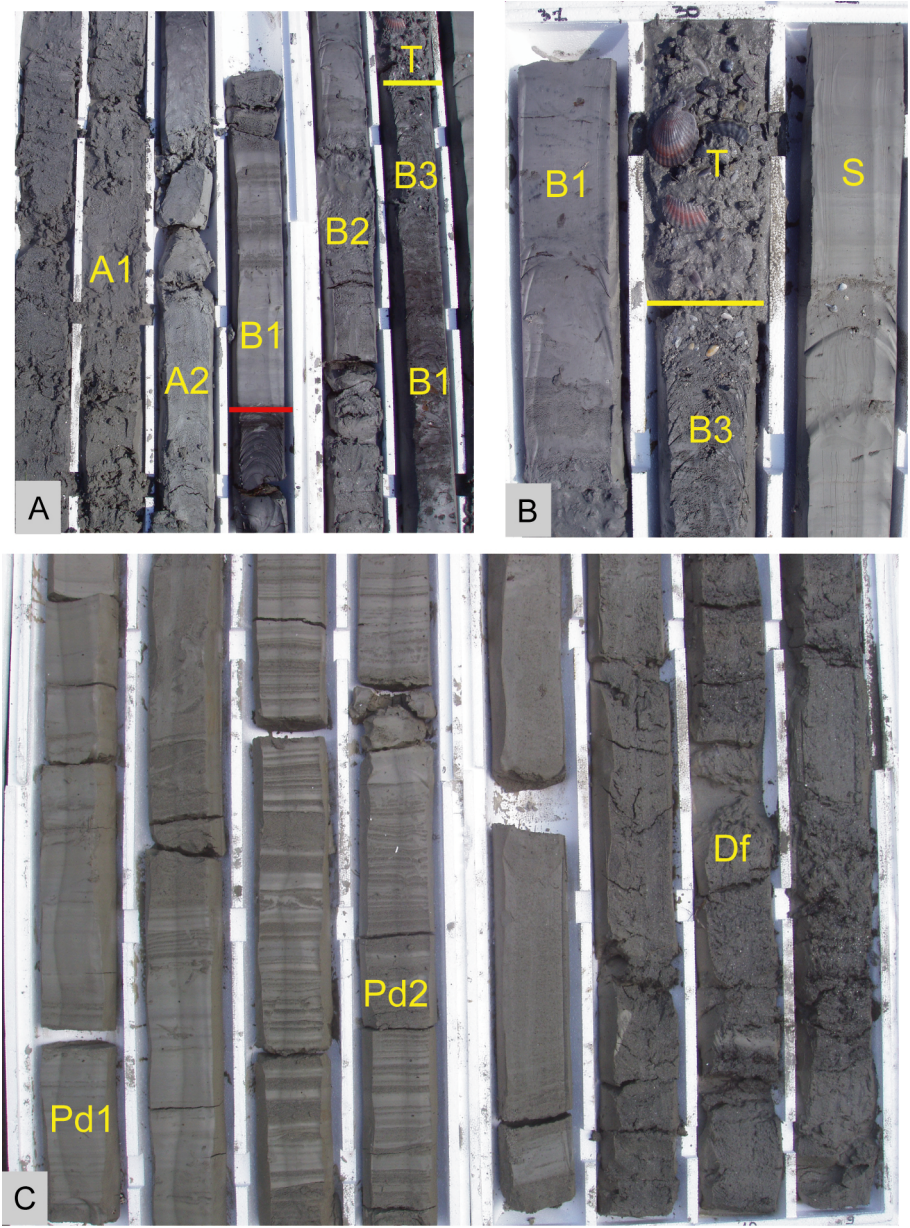


Figure 3

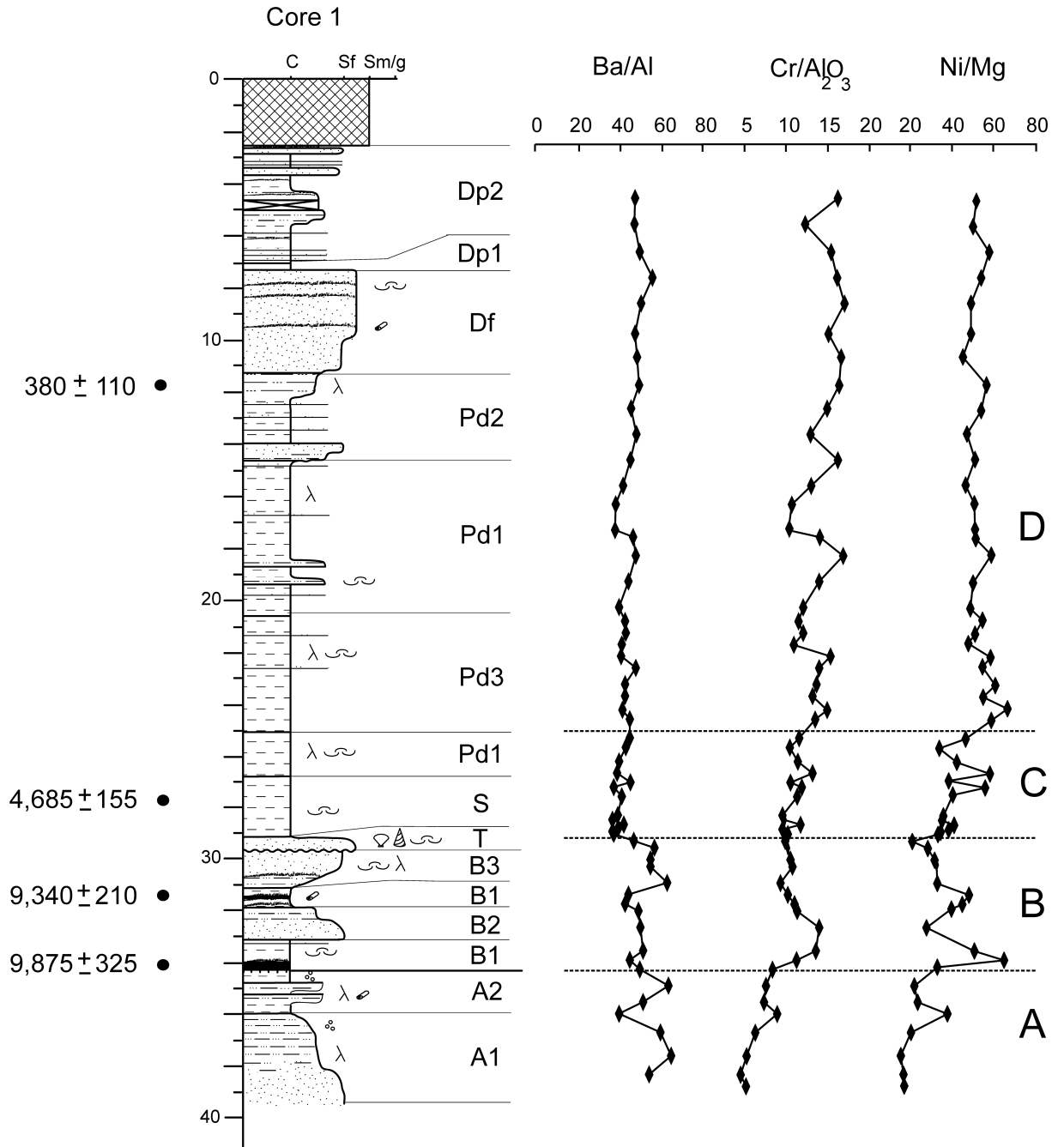


Figure 4

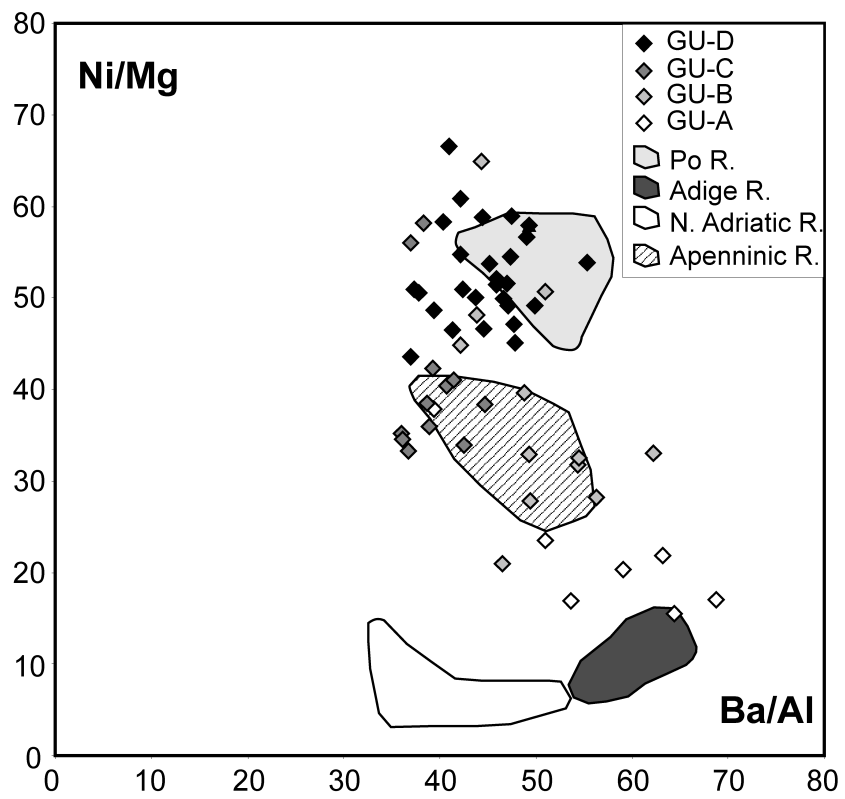


Figure 5

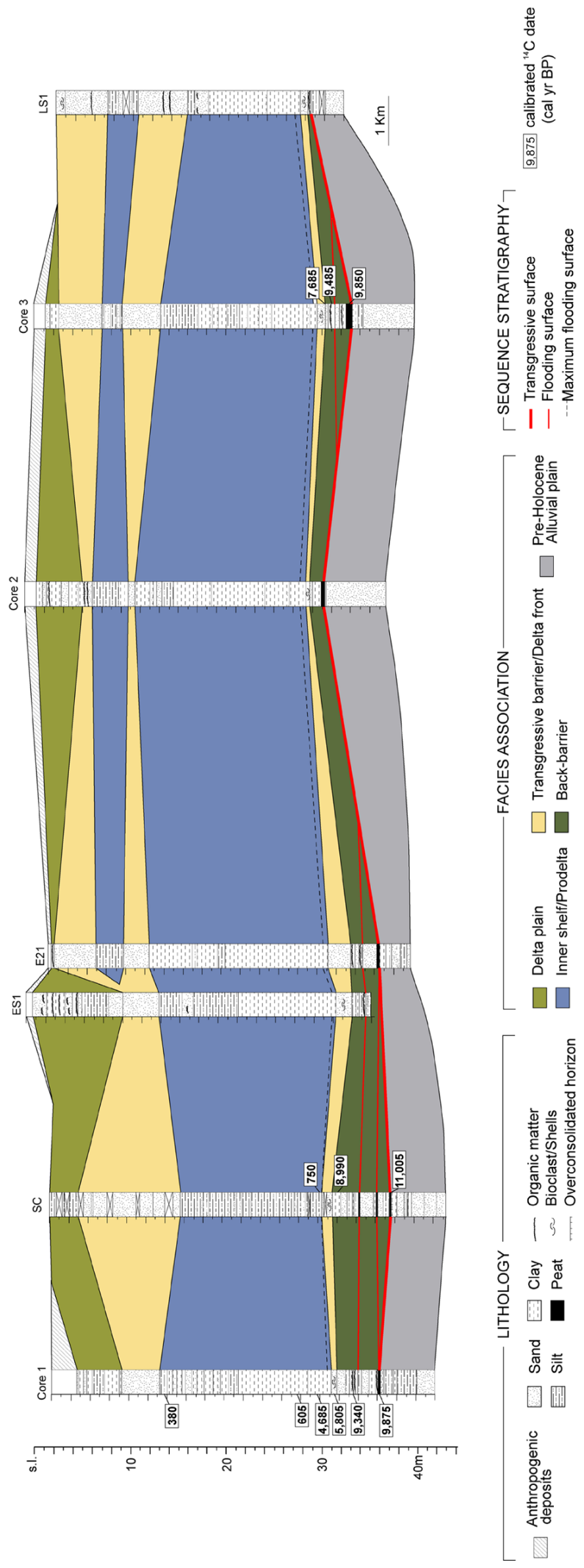


Figure 6

Paper 5

**Microfaunal response to sediment supply changes and fluvial drainage
reorganization in Holocene deposits of the Po Delta, Italy**

Rossi, V. and Vaiani, S.C.

**Microfaunal response to sediment supply changes and fluvial drainage
reorganization in Holocene deposits of the Po Delta, Italy**

Veronica Rossi ^{a,*} and Stefano Claudio Vaiani ^a

^a Dipartimento di Scienze della Terra e Geologico-Ambientali, Università di Bologna,

Via Zamboni 67, 40126 Bologna, Italy

* Corresponding author: Tel: +39 051 2094565; Fax: +39 051 2094522;

Dipartimento di Scienze della Terra e Geologico-Ambientali, Università di Bologna,

Via Zamboni 67, 40126 Bologna, Italy

E-mail: veronica.rossi4@unibo.it

Abstract

Detailed microfossil analyses performed on the Holocene subsurface deposits of modern Po Delta evidenced a complex palaeogeographic evolution. Foraminiferal cluster analyses integrated with qualitative description of ostracod fauna allowed to distinguish four microfossil assemblages, indicative of different marine environments and sub-environments. Temporal and spatial distribution patterns of benthic microfauna reflect changes in Po River discharge during delta evolution. The capability of microfossil assemblages to track nutrients and sediment supply oscillations permitted to recognize four main evolutionary phases (A-D), which took place after the maximum marine transgression (ca. 5 500 cal yr BP).

Prodelta and delta front deposits are accumulated in the western part of the study area between the first stages of progradation and the late Middle Age; these are paralleled, in a more distal position, by open marine sedimentation, replaced upward by prodelta sediments (phases A and B). Owing to the combined effect of a major avulsion (Rotta di Ficarolo) and the Adriatic circulation patterns, an organic-rich zone developed in the eastern part of the present Po Delta at the transition to the modern-age (phase C), around 600 cal yr BP. For the first time a fossil mud-belt, although its marginal fringe, along with its peculiar microfossil content (*Nonionella turgida* assemblage), is recorded beneath a modern delta plain. Prodelta deposits were replaced by delta front sands after the Porto Viro cut (ca. 350 cal yr BP), which marked the onset of Modern Delta (phase D).

Keywords: Po Delta; benthic microfauna; river discharge; mud-belt; Holocene

1. Introduction

Late Quaternary microfossil assemblages preserved in subsurface deltaic successions provide an useful tool to reconstruct the evolution of present coastal systems in response to recent sea-level oscillations, climatic changes and delta growth patterns.

Identification of major palaeoenvironmental factors controlling microfauna distribution in the recent past is commonly obtained by comparison with appropriate modern analogues.

For this reason, modern microbenthic assemblages from the Po Delta area (Northern Italy) have been extensively studied from the Sixties (e.g. Colalongo, 1969; D'Onofrio, 1969; Bonaduce et al., 1975; Fregni, 1980; Jorissen, 1988) and a characteristic zonation, explaining their distribution, depicted both for foraminifers (e.g. Jorissen, 1987; Donnici and Serandrei Barbero, 2002) and ostracods (Colalongo, 1969).

An obvious bathymetrical zonation parallel to the Adriatic coastline has been defined, particularly at great distance from the Po Delta system. Indeed, the high amount of freshwater and runoff products, discharged by Po River, induces local perturbations and significant environmental changes in the area adjacent the shoreline (Morigi et al., 2005).

A detailed picture of foraminifers distribution in proximity of Po River outlets reveals a close relationship between selected taxa and deposition of a mud-belt, composed by fine-grained and organic-rich sediments supplied by the Po River and distributed southward by long-shore currents. In this peculiar area of the Northern Adriatic Sea, between 20 and 40 m water depth, foraminiferal assemblages are dominated for increasing depths by *Nonionella turgida*, *Bulimina marginata* and *Valvulineria bradyana*, respectively, indicating high organic matter concentration and reduced oxygen conditions (Van der

Zwaan and Jorissen, 1991). Approaching the coastal area, the mud-belt is bounded on the western side by sandy deposits containing abundant *Ammonia* and *Elphidium* species, typical of littoral settings quite rich in nutrients (Jorissen, 1988; Donnici and Serandrei Barbero, 2002).

The initial stage of formation of the Northern Adriatic mud-belt is possibly connected with the onset of Po Delta system and the subsequent discharge of fine-grained deposits and nutrients. This event follows the Holocene transgressive period (ca. 10 000-6 000 yr BP), when the rate of relative sea-level rise slowed down and sediment discharge induced deltaic progradation in the study area (Amorosi et al., 2003; Amorosi and Colalongo, 2005).

Although the formation of the Holocene mud-belt has been recently investigated in the central Adriatic Sea, about 180 km SE of Po delta, by analyses of cores collected between 75.5 and 78.8 water depth (Morigi et al., 2005), no data are available from the subsurface of Po Delta system.

In this work we present the first record of a fossil mud-belt identified beneath the present Po delta plain, and discuss temporal and spatial distribution patterns of the benthic marine microfauna (foraminifers and ostracods) collected in two cores encompassing the last transgressive-regressive depositional cycle, of Holocene age. Specific aim of this paper is to document the response of microfossil assemblages to highly-variable, stressed environmental conditions that occurred in the study area during Po Delta progradation.

2. Geological setting and depositional evolution of the Po Delta

The Po River Delta is one of the largest and most studied delta systems of the Mediterranean Sea, representing a natural archive for sequence-stratigraphic and palaeoenvironmental studies (e.g. Ciabatti, 1966; Correggiari et al., 2005b). The combined effects of elevated subsidence rates and negligible tectonic deformations occurred during the Late Quaternary (Pieri and Groppi, 1981), guarantee favourable conditions for high-resolution stratigraphic analyses.

In the past decades, the origin and the sedimentary fill of Po basin, bounded by the Apennines to the south and the Alps to the north, have been extensively investigated. Structural and seismic analyses revealed a thick Plio-Quaternary succession buried beneath the Po Plain and alternately composed of marine and continental deposits, for a total thickness of ca. 700-800 meters (Pieri and Groppi, 1981; Castellarin et al., 1985; Castellarin and Vai, 1986; Vai, 1987).

Integrated sedimentological and palaeontological (benthic foraminifers, ostracods and pollen) studies have been recently carried out on the upper portion of this succession, evidencing, in the easternmost part of the plain, a cyclic stacking pattern of marginal marine and continental deposits formed in response to fluctuating sea-level (Amorosi et al., 1999, 2003, 2004). Particularly, subsurface data (Amorosi et al., 2005, submitted; Stefani and Vincenzi, 2005) revealed the development during the last glacial period of an alluvial plain that was abruptly inundated at the beginning of the Holocene transgression (ca. 10 000 yr BP). During the early stage of transgression a barrier-lagoon system developed, inducing the deposition of paludal and lagoonal sediments. In response to the

rapid landward migration of shoreline, brackish deposits were replaced by transgressive sand barriers and shallow marine clays. After maximum marine transgression (ca. 5 000-6 000 yr BP), an early wave-dominated Po Delta system took place (Amorosi and Milli, 2001; Amorosi and Colalongo, 2005), as documented by the geochemical record of an increasing supply by Po River sediments, paralleled by an increase in euryhaline foraminifers (Curzi et al., 2006).

During the earliest progradational stages, up to the Middle Ages-Renaissance transition, natural avulsion processes played a significant role in delta evolution, shifting the main distributary channels across the Po Plain (Correggiari et al., 2005b). The Po Delta system reached its present position and conformation (mixed wave- and river-dominated delta; Ciabatti, 1966) in the XVII century AD, after the Porto Viro cut operated by Venice Republic to preserve Venice Lagoon. The thick prodelta succession that rapidly accumulated offshore during the last ca. 350 years clearly records the high rates of sedimentation affecting the Po Delta area (Correggiari et al., 2005a, b).

Prodelta lobes, depicted by high-resolution seismic profiles at a water depth range of 5-30 m, show an evident asymmetric shape, induced by the southward flow of longshore currents that control and distribute the sediment flux from land to the Adriatic shelf (Correggiari et al., 2005a). At present, the interplay between this surficial circulation pattern and Po River discharge causes, in the Northern Adriatic basin, a prompt shore-parallel sediment distribution, which roughly consists of a littoral sandy zone and an organic-rich mud-belt area at 20-40 m water depth (Van Straaten, 1965; Van der Zwaan and Jorissen, 1991).

3. Material and methods

Two cores (Core S1 and Core 1) were performed in the southern portion of modern Po Delta in Northern Italy (Fig. 1) by wire line perforation, which guaranteed a continuous and undisturbed core stratigraphy, with very high recovery percentages (more than 90%). Core S1 was drilled near the Pomposa Abbey, about 8 km west of the present coastline and reached a depth of 188 m. Our attention is here focused on the upper 26 meters, recording the Holocene part of the succession. Following a roughly W-E orientation, Core 1 was located in an eastern position close to the present shoreline, in proximity of Po Tolle Harbour.

Detailed sedimentological analyses of the cores and a report of the main palaeontological features are provided by Bondesan et al. (2006), for Core S1, and Amorosi et al. (submitted), for Core 1. The distribution of several foraminiferal species from core S1 is shown in Amorosi et al. (2007); a more detailed picture of this distribution (including taxa with concentration > 4% in at least one sample) and data from four new samples are reported in this work.

164 samples of approximately 200-150 g (124 from Core 1, and 40 from Core S1) were collected for micropalaeontological analyses. All samples were (i) dried at 60°C for 8 hours, (ii) soaked in water or water plus hydrogen peroxide (35% vol.), (iii) wet sieved through sieves of 63 µm (240 mesh) and (iv) dried again. The grain size fraction > 63 µm was qualitatively analysed to describe the ostracods and foraminifers assemblages. The identification of foraminifers and ostracods species was supported by original

descriptions and several key papers as Bonaduce et al. (1975), AGIP (1982), Jorissen (1988), Albani and Serandrei Barbero (1990), Henderson (1990), Cimerman and Langer (1991), Sgarrella and Moncharmont Zei (1993), Fiorini and Vaiani (2001) and Rasmussen et al. (2005). Forty-nine samples (31 from Core 1 and 18 from Core S1), containing perfectly preserved and abundant benthic foraminifers, were split into small portions of almost 300 specimens and counted in the size fraction $> 125 \mu\text{m}$; relative percentages were finally elaborated for each species.

Matrix for cluster analyses was developed gathering selected species for each core in groups up to genera level, on the basis of their taxonomy and ecological characteristics, in order to make the data less dispersive and more comparable.

The 18 most abundant taxa (those $> 4\%$ in at least one sample and observed in both cores) were selected to compose the final matrix that was processed with a palaeontological statistical program (PAST-PAlaeontological SStatistic-ver. 1.55 by Hammer et al., 2007).

Hierarchical R-mode cluster analyses permitted to recognize the main microfossil assemblages occurring within the cored successions. The robustness of the foraminiferal groups was tested by running several unweighted pair group (UPGMA) cluster analyses with different similarity indexes, all of them consistent with the nature of our data.

Horn's (1966) modified version of Morisita's (1959) index was finally selected, because it guarantees the most realistic output data, downweighting the more abundant species.

Palaeoenvironmental interpretation of assemblages was inferred by a series of specific papers carried out on modern assemblages, particularly, the detailed comparison with the distribution patterns of modern Northern Adriatic microfauna allowed us to estimate

several environmental parameters, such as depth, salinity and organic matter (Colalongo, 1969; D'Onofrio, 1969; Breman, 1975; Jorissen, 1987, 1988; Murray, 1991; Van Der Zwaan and Jorissen, 1991; Barmawidjaja et al., 1992; Yassini and Jones, 1995; Bergamin et al., 1999; Debenay et al., 2000; Ruiz et al., 2000; Donnici and Serandrei Barbero, 2002; Frezza et al., 2005).

Further information were also provided by comparison with the microfossil associations recorded within the Late Quaternary successions buried beneath other coastal areas, such as SE Po Plain (Amorosi et al., 2004, 2005; Fiorini, 2004), inner Po Delta (Bondesan et al., 2006), Arno coastal plain (Aguzzi et al., 2007) and Ombrone coastal plain (Carboni et al., 2004).

The chronostratigraphic framework of cores was based upon six AMS ^{14}C dates for Core 1 (performed at CEDAD laboratory, University of Lecce, Italy), reported as calibrated yr BP, and one AMS ^{14}C date for Core S1 (Bondesan et al., 2006) here calibrated using CALIB version 5.1 (Stuiver and Reimer, 1993; Stuiver et al., 2005) and the calibration curve for terrestrial samples IntCal04 (Reimer et al., 2004).

4. Results

4.1. Microfossil assemblages

The sensitivity of benthic foraminifers and ostracods in deltaic environments to several physical parameters (e.g. Colalongo, 1969; Bizon and Bizon, 1984; Murray, 1991;

Barmawidjaja et al., 1992) can provide significant information about changes in salinity, food availability, oxygen concentration and other abiotic variables occurred in the past. Particularly, present data collected from river-influenced shelf areas evidence the capability of benthic foraminifers to track nutrients supply fluctuations (Van der Zwaan and Jorissen, 1991; Jorissen et al., 1992; Donnici and Serandrei Barbero, 2002). In this respect, microfossils could be a very useful tool to reconstruct river delta cycles (*sensu* Scruton, 1960; see also Amorosi et al., 2005) taking place during the highstand.

R-mode cluster analysis on foraminiferal assemblages of the cores provides information about the foraminiferal community structure, revealing three recurrent clusters and a separated species (Fig. 2). Foraminiferal distribution combined with ostracods data allow the identification of four microfossil assemblages (Figs. 3 and 4; foraminiferal counts are available as relative percentages in Supplementary data):

4.1.1. Assemblage 1

Assemblage 1 is characterized by species grouped in Cluster A and dominated by *Ammonia tepida* and *A. parkinsoniana* (> 35%), with subordinate *Ammonia beccarii*, *A. inflata* and *Quinqueloculina seminulum*. Low percentages of *Haynesina depressula* and *H. germanica*, *Criboelphidium granosum* and *Valvulineria perlucida*, are usually encountered in association with an oligotypic ostracod fauna, composed of numerous valves of *Loxoconcha turbida*.

At present, a comparable microfauna is recorded close to the Po River outlets along the Northern Adriatic coastline, at depth < 20 m and within quite organic-rich sediments

(Colalongo, 1969; D'Onofrio, 1969; Jorissen, 1988; Donnici and Serandrei Barbero, 2002).

Assemblage 1 indicates a shallow and proximal prodelta environment (< 20 m) subjected to low-salinity conditions and relatively high organic matter content.

4.1.2. Assemblage 2

Assemblage 2 consists of several taxa grouped to compose Cluster B (Fig. 2).

Foraminifers are very abundant and show a considerable variety of species, the highest recorded throughout the cored successions. Large amount of Miliolidae (18-63%) mainly *Adelosina*, *Quinqueloculina*, *Triloculina* and *Siphonaperta*, and hyaline epiphytic taxa (2-27%), such as *Asterigerinata* spp., *Rosalina* spp. and *Buccella granulata* are encountered (Figs. 3 and 4) in association with relatively low amounts of *Ammonia tepida* and *A. parkinsoniana*. Similarly, the ostracod fauna is quite diversified and contains numerous species of *Semicytherura* and *Loxoconcha*, as *S. incongruens*, *S. acuticostata*, *L. tumida* and *L. exagona*.

A similar foraminiferal assemblage is found in the modern Northern Adriatic shelf at about 20-40 m depth (Jorissen, 1988; Donnici and Serandrei Barbero, 2002); in this area a comparable diversified ostracod fauna is found at about 25-30 m depth (Colalongo, 1969). Variety and composition of assemblage 2 are consistent with a shallow-marine environment with low fluvial influence and vegetation cover at the bottom. Particularly, the abundance reached by epiphytic taxa suggests low turbidity conditions possibly far from river outlets (Massari et al., 2004).

4.1.3. Assemblage 3

Assemblage 3 is dominated by *Nonionella turgida* (27-75%) reported as a separated species in the cluster analysis (Fig. 2). Subordinate *Ammonia tepida* and *A. parkinsoniana* (4-29%) and *Quinqueloculina seminulum* (4-10%) are commonly found in this assemblage. Few to rare valves of *Loxoconcha turbida* and *Leptocythere ramosa* compose the ostracod fauna. A comparable foraminiferal microfauna characterizes the western flank of the present Northern Adriatic mud-belt at about 20 m depth. In correspondence of this peculiar area, high nutrient amounts are concentrated by the long-shore currents, inducing seasonal dysoxic conditions (Van der Zwaan and Jorissen, 1991). These conditions seem to be tolerated by *Loxoconcha turbida*, which can be considered a survivor-type species able to live in hypoxic environments (Bodergat et al., 1998).

The dominance of *Nonionella turgida*, an opportunistic species preferring high food availability and tolerant to reduced oxygen conditions (Van der Zwaan and Jorissen, 1991), indicates an environment strongly influenced by river discharge.

4.1.4. Assemblage 4

Assemblage 4 consists of two dominant species, *Criboelphidium granosum* (< 40%) and *Valvulineria perlucida* (up to 48.6%) grouped with the secondary taxa *Haynesina depressula* and *H. germanica* (less than 20%) to compose Cluster C (Figs. 2 and 3). This foraminiferal assemblage is found in association with a marine ostracod fauna, mainly composed of *Loxoconcha turbida*, *Cytheridea neapolitana* and *Semicytherura incongruens*. In the Adriatic Sea, taxa of clusters A and C are present in the near-shore

zone (Jorissen, 1987) and the dominant species show low tolerance for oxygen deficiency in areas with high organic matter content (Jorissen, 1988). In the south of the main active Po river mouth (Po Pila), the observed bathymetrical and organic matter gradients are paralleled by the relative increase of *Criboelphidium granosum* and *Valvulineria perlucida* (cluster C) and by the decrease of *Ammonia tepida* and *A. parkinsoniana* (cluster A). Beyond the 20 m-isobath, however, these taxa are replaced by foraminiferal assemblages typical of the modern mud-belt area (Jorissen, 1988).

Within the ostracods microfauna, *Semicytherura incongruens* and *Cytheridea neapolitana* are infralittoral species widely diffused in the Adriatic Sea (Bonaduce et al., 1975). Assemblage 4 are considered to reflect an organic rich-prodelta in which oxygen deficiency is probably not present, in spite of the influences of discharge products from the Po River. Compared with assemblage 1, the relative low amount of *Ammonia tepida* and *Ammonia parkinsoniana* and the presence of shallow marine ostracods not typical of salinity stressed conditions, are consistent with a slightly deeper environment.

4.2. Vertical microfaunal distribution

4.2.1. Core 1

The lower stratigraphic portion consists of an alluvial succession completely barren in microfossil and overlain, around 34 m core depth (Holocene transgressive surface-TS), by organic-rich deposits of back-barrier environment formed from 9 875 ±325 yr BP (Fig. 3). Few valves of freshwater ostracods, mainly *Candona albicans*, are encountered within the back-swamp clays. On the other hand, a rare and poorly preserved microfauna

(including *Ammonia tepida*; *Ammonia beccarii*; *Elphidium* spp.; *Adelosina* spp.; *Cyprideis torosa* and *Semicytherura* spp.), interpreted as transported from nearby environments, characterizes the upper part of back-barrier succession (washover sands) and the transgressive barrier sands deposited during the rapid onset of marine transgression around 6 000 cal yr BP, as documented by the radiocarbon date of a sample from the lower part of these sediments (Fig. 3). The erosional surface, marked by a veneer of mollusc shells, at the lower boundary of transgressive barrier sands, is interpreted as the ravinement surface-RS. Within the overlying inner-shelf clays microfossil assemblage 2 is continuously recorded up to 26.80 m, with the exception of two samples collected between 28 and 27 m containing a fluvio-influenced microfauna (assemblage 4). The highest abundance of species indicative of relatively open and deep marine environment, such as *Asterigerinata mamilla*, *Buccella granulata*, *Siphonaperta* spp. and *Textularia* spp., combined with the lowest percentage in euryhaline taxa (*Ammonia tepida* and *A. parkinsoniana*), are considered to reflect the maximum marine transgression (Amorosi et al., submitted), taking place in Core 1 area at 28.90 m (maximum flooding surface-MFS in Fig. 3).

Upcore, the change from inner-shelf to prodelta sedimentation is clearly documented by either the disappearance (see *Buccella granulata*, *Rosalina* and *Siphonaperta*) or the abrupt decrease of taxa belonging to assemblage 2, which are replaced by species tolerant to fluvial discharge, mainly *Ammonia tepida* and *A. parkinsoniana* (Fig. 3). The alternate record of three different fluvio-influenced marine assemblages (1, 3 and 4) is indicative of very unstable environmental conditions driven by the complex palaeogeographic evolution of Po Delta system.

The continuous presence of high percentages of the opportunistic species *Nonionella turgida* (25.10-20.50 m core depth) suggests the development of a mud-belt, although its marginal fringe. This record possibly indicates that from ca. 600 cal yr BP (as suggested by the radiocarbon age of a sample collected at 25.80 m core depth, Fig. 3), the suspended load (fine-grained particles and nutrients) delivered by Po River to the Adriatic shelf, was concentrated in proximity of Core 1, where the interplay of increasing food availability and low oxygen concentration determined the occurrence of this peculiar microfauna (assemblage 3).

The onset of these environmental conditions induced the substantial decrease of *Criboelphidium*, *Valvulineria perlucida*, *Ammonia tepida* and *A. parkinsoniana* (Fig. 3). *Quinqueloculina seminulum* seems to be the unique species able to pass through this critical ecological threshold without relevant effects. Whilst few information are available about the ecological behaviour of foraminiferal species with respect to specific environmental parameters, the common occurrence of *Q. seminulum* within marshes and lagoonal settings usually rich in organic matter and subject to oxygen deficiency (Scott et al., 1979; Albani and Serandrei Barbero, 1990), seems to be consistent with our data.

Upward, *Ammonia tepida* and *A. parkinsoniana* (assemblage 1) abruptly replace *Nonionella turgida*, marking the end of active mud-belt sedimentation. The overwhelming dominance of *Ammonia tepida* and *A. parkinsoniana*, recorded from 18 m up to the transition with delta front sands, suggests persisting hypohaline conditions induced by the progressive approaching of Po River outlets. The low number of specimens (commonly less than 50) collected within the upper part of prodelta sediments

(Fig. 3) hampers the quantitative analyses of foraminiferal microfauna; in these samples, however, the dominance of *Ammonia tepida* and *A. parkinsoniana* is observed.

One sample, collected at 16.55 m core depth, including a typical assemblage 4, maybe records a local increase of fluvial discharge products possibly linked to a flood event.

A transported microfauna composed of rare benthic and planktonic foraminifers (such as *Bulimina*; *Cassidulina*; and *Orbulina*) is found within the delta front sands. Delta plain deposits, recorded at the top of cored succession, result barren in microfossils.

4.2.2. Core S1

Above a thick alluvial succession assigned to the Last Glacial Maximum, Core S1 displays a transgressive-regressive depositional cycle of Holocene age, about 26 m thick; this is marked at the base by the TS (Fig. 4). The lowermost Holocene succession includes back-barrier deposits, containing an oligohaline ostracod fauna (mainly *Ilyocypris* and *Cyclocypris*). These are replaced, above the RS, by transgressive barrier sands marking the beginning of marine transgression and including rare and poorly preserved foraminifers (mainly *Ammonia beccarii*, Miliolidae and *Textularia*), probably transported from sublittoral environment during the landward migration of the barrier.

Upcore, two meters of offshore-transition clay-sand alternations are characterized by high amounts of Miliolidae in association with *Textularia* and *Elphidium* species (assemblage 2). Within these sediments, the MFS is traced at 19.75 m (Amorosi et al., 2007) by the highest concentration of relatively open and deep marine taxa (including *Textularia* spp. and *Buccella granulata*) and low amount in euryhaline species (*Ammonia tepida* and *A. parkinsoniana*), as previously defined for Core 1.

A monotonous succession of fine-grained prodelta deposits directly overlies offshore-transition deposits. The absence of any significant change in microfossil content (assemblage 1) and the rapid increase of *Ammonia tepida* and *A. parkinsoniana* (> 35%), suggest the development of a proximal prodelta environment, subjected to remarkable freshwater outflows since the first stages of deltaic progradation (Fig. 4).

The overlying delta front sands are characterised by a poorly preserved microfauna (mainly *Ammonia beccarii* and *Elphidium crispum*), coherent with a high-energy coastal environment related to the formation of beach barriers.

5. Po Delta evolution and mud-belt development: a high-resolution microfossil record

Micropalaeontological analyses performed on cores 1 and S1, integrating sedimentological data (Amorosi et al., 2007, submitted), allow an accurate facies characterization of the Holocene deposits beneath the southern portion of modern Po Delta.

The subsurface record of a thick and well-developed inner shelf/prodelta succession constitutes an ideal source of information for the reconstruction of the palaeoenvironmental evolution of Po Delta system. Several variations in microfossil content reflect the complex palaeogeographic evolution of the Po Delta area particularly after the maximum marine transgression (phases A-D, Fig. 5).

5.1. Phase A: From the maximum marine transgression to the early Middle Age

Following maximum marine transgression, possibly dated around 5 500 cal yr BP (according to the radiocarbon age of $5\,805 \pm 175$ cal yr BP from a sample collected 60 cm below the MFS in Core 1, Fig. 3), the combined effect of sea-level slowdown and increasing fluvial discharge forced the palaeoshoreline, located about 30 km west of its present position to prograde (Amorosi and Milli, 2001; Stefani and Vincenzi, 2005).

In the inland area of Core S1, the seaward migration of Po River mouths is possibly recorded by an abrupt increase in percentages of *Ammonia tepida* and *A. parkinsoniana* at the transition to prodelta deposits (Fig. 4, 5A).

In a more distal position (Core 1), the effects of deltaic progradation were subdued and an open-marine sedimentation went on (assemblage 2, Fig. 3) up to the late Middle Age (Fig. 5A). Within a distinct interval of shelf deposits (ca. 27-28 m core depth), Miliolids and hyaline ephyphitic taxa, composing assemblage 2, are replaced by assemblage 4. This change in microfossil content, dated at about $4\,685 \pm 155$ cal yr BP (Fig. 3), suggests a momentary increase in river discharge, maybe related to a minor avulsion (delta lobe switching).

Unstable palaeoenvironmental conditions probably affected the study area during the first phases of drainage reorganization. In this respect, Stefani and Vincenzi (2005) suggest the presence, after the maximum marine transgression, of an "indeterminate state" affecting the Po delta system with slow transgression and evidences of localised bays infilling. From the Bronze Age to the first centuries of late Middle Age (ca. 3 000-900/800 cal yr BP) several generations of cusped deltas developed across the Po Plain,

between Adria and Ravenna (Correggiari et al., 2005b; Stefani and Vincenzi, 2005), as recorded by outcropping coastal bodies. Through natural avulsion processes, frequent activations and abandonments of delta depositional lobes regulated the flux and distribution of fluvial runoff products in the Northern Adriatic Sea.

5.2. Phase B: Late Middle Age

Probably during the late Middle Age a prompt prodelta sedimentation reached Core 1 area (Fig. 5B), that however was affected by relative sediment-starvation up to the Modern Age as confirmed by the radiocarbon dating (605 ± 65 cal yr BP) from the lower part of prodelta deposits (Fig. 3).

Alternation of two different deltaic assemblages within lower prodelta deposits (assemblage 1 and 4, Fig. 3) possibly reflects fluvial discharge oscillations, induced by the combined effect of delta cycles and longshore drift. Brief episodes of intense sedimentary discharge are recorded by Core 1 microfauna (Fig. 3) through the abrupt decline of *Ammonia tepida* and *A. parkinsoniana* (assemblage 1) and the increasing abundance of species tolerant to ample food availability, such as *Valvulineria perlucida* and *Criboelphidium granosum* (assemblage 4).

At the beginning of the late Middle Age (ca. 1,000-900 cal yr BP) a large delta lobe (Po di Volano lobe) quickly developed in the area of Pomposa (Fabbri, 1985; Correggiari et al., 2005b), possibly leading to the deposition of delta front sands that capped Core S1 (Fig. 5B). This interpretation is supported by the ages available from the coastal sands outcropping close to this core (Stefani et al., 2003).

A key event that strongly influenced the recent evolution of Po Delta area occurred between AD 1152 and 1192, when a river avulsion took place near the village of Ficarolo (Fig. 5). This avulsion (“Rotta di Ficarolo”, Ciabatti, 1966; Fabbri, 1985) forced the entire Po River system to migrate northward, disabling Po Primario lobe and opening two new channels north of Ferrara (Po delle Fornaci and Po di Ariano-Goro, Fig. 5C). From this time, the main active Po branches remained in the northern sector of the Po Plain, marking the beginning of a new evolutive phase of the delta that characterizes the Po system in the Modern Age (Phase C).

5.3. Phase C: Transition to the Modern-age and the onset of Po River mud-belt

In response to the Ficarolo avulsion and the consequently overall fluvial drainage reorganization (Fig. 5C), a long period of alluvial-plain progradation and reduced deltaic sedimentation took place (Correggiari et al., 2005b).

Two hundreds years later, the integrated effects of Ficarolo avulsion and long-shore southward currents allowed the rapid accumulation of fine-grained sediments and nutrients in correspondence of Core 1 area, with consequent development of a mud-belt (Fig. 5C). During this period, the abrupt decline of typical shallow-marine taxa is paralleled by the remarkable increase of the opportunistic species *Nonionella turgida* (Fig. 3), a mud-dwelling epifaunal species tolerant to high nutrients concentration and periodic and limited dysoxic condition (Van der Zwaan and Jorissen, 1991; Barmawidjaja et al., 1992; Jorissen et al., 1992). The model proposed by Van der Zwaan and Jorissen (1991) explains modern benthic foraminiferal distribution along a generic Adriatic W-E

transect, under conditions of different seasonal oxygen concentration. In Figure 6 is reported the winter/spring seasonal condition, when the critical oxygen level is deep-lying and a complete fauna occurs. A similar foraminiferal pattern is observed throughout the fossil succession recovered by the study cores. The different microfossil content of the prodelta succession within cores 1 and S1 and the absence in the latter of assemblage 3 were mainly controlled by the surficial Adriatic currents, which accumulated fluvial products at a considerable distance from river mouths. Nearshore position of Core S1 prevented the development of a well-defined, nutrient-rich zone, as evidenced by the continuous record of assemblage 1 (comparable to the *Ammonia/Elphidium* assemblage of Van der Zwaan and Jorissen, 1991) throughout the prodelta succession (Figs. 4 and 6), whereas a foraminiferal association dominated by *Nonionella turgida* and the absence of *Valvulineria bradyana* are coherent with the deposition of a marginal mud-belt in correspondence of Core 1.

Although the total amount of fluvial discharge seems to play a secondary role for the development of a mud-belt zone in modern deltaic areas (Van der Zwaan and Jorissen, 1991), a persistent period of climatic variability (Veggiari, 1990), including the Little Ice Age-LIA (1450-1850 AD, ca. 500-100 cal yr BP) and the last centuries of late Middle Age (ca. 800-500 cal yr BP), chronologically overlap the onset and the development of Po mud-belt. It is reasonable that such climatic changes increased sediments and nutrients discharge, maybe supporting avulsion processes, such as the Rotta di Ficarolo, and the following formation of a prompt organic-rich area.

The progressive advance of Po Delta system shifted fluvial outputs further seaward, forcing mud-belt to move offshore close to its present position, about 4-5 km away from

the Po Pila mouth. In correspondence of Core 1, the end of mud-belt sedimentation is marked by the abrupt increase in *Ammonia tepida* and *A. parkinsoniana* microfauna in agreement with a shallowing-upward trend (Fig. 3).

5.4. Phase D: Modern Po Delta

At the beginning of the XVII century (1604 AD), Venice Republic forced the main trunk of Po River (Po delle Fornaci) to flow southward in correspondence of its present position, to preserve Venice Lagoon from sedimentary infilling (Bondesan, 1990). This event, known as Porto Viro cut, coincides with the new protruding morphological configuration of Po Delta (Modern Po Delta).

During this period, high sedimentation rates concurred to develop several delta lobes. The rapid delta outbuilding was enhanced by the combined effects of climatic changes (Veggiani, 1984) and more frequent human interventions that increased the sedimentary flux towards sea (Correggiari et al., 2005b; Stefani and Vincenzi, 2005).

The delta front and delta plain deposits recorded at the top of Core 1 were formed during the last centuries (as suggested by the radiocarbon dating of 380 ± 110 cal yr BP from a sample collected in the uppermost part of prodelta sediments, Fig. 3), confirming the rapid aggradation that has recently characterized the Po Delta area (Fig. 5D).

6. Conclusions

Temporal and spatial distribution patterns of benthic microfauna, from two continuous cores, reveal the main palaeoenvironmental changes occurred during the Holocene in the Po Delta area.

Transgressive sedimentation was mainly controlled by sea-level rise, as evidenced by the abrupt superposition of back-barrier and then marine deposits on an alluvial succession assigned to the Last Glacial Maximum.

Following time of maximum marine transgression ca. 5 500 cal yr BP, a combination of allocyclic and predominant autocyclic factors influenced depositional evolution of the delta system.

Four evolutionary phases (labeled A; B; C and D), corresponding to distinct palaeogeographic contexts, are distinguished and chronologically constrained on the basis of detailed micropalaeontological and radiocarbon analyses.

Complex palaeoenvironmental conditions, caused by the interplay of progressive shoreline progradation, surficial water circulation pattern and river avulsion processes, characterized the deltaic evolution and these are coupled by peculiar microfaunal content.

As shown for instance around 800 cal yr BP, when a major river avulsion, Rotta di Ficarolo, set the conditions for the development in the area adjacent Core 1 of a mud belt zone characterized by remarkable organic matter and reduced oxygen condition at the sea bottom, as indicated by the dominance of the opportunistic species *Nonionella turgida*.

Thanks to the capability of benthic foraminifers to track variations in nutrients flux, the deposition of a fossil mud-belt, although its marginal fringe, is clearly recognized and

chronologically constrained (around 600 cal yr BP) in the subsurface deposits of a present delta plain for the first time.

Past oscillations in river discharge (sediments plus nutrients), possibly induced by the combined effect of fluvial drainage reorganization and climatic changes, can be depicted by benthic microfauna in deltaic areas. On the other hand, as generally observed within highstand deposits, the presence of local parameters and the absence of a predominant factor prevent from discerning or quantifying consequences of the complex relationships between climate and deltaic evolution.

Acknowledgements

We are indebted to A. Amorosi and R. Barbieri for their constructive comments on an early version of the manuscript.

This research is supported by Bologna University as part of Progetto Strategico d'Ateneo (co-ordinator: A. Amorosi).

Appendix A: Taxonomic Reference List

This list includes Genus and Species of foraminifers and ostracods cited in the paper.

Foraminifers

Adelosina - *Adelosina* d'Orbigny, 1826; p. 303.

Ammonia – *Ammonia* Brünnich, 1772; p. 232.

Asterigerinata – *Asterigerinata* Bermúdez, 1949; p. 266.

Bulimina - *Bulimina* d'Orbigny, 1826; p. 269.

Cassidulina – *Cassidulina* d'Orbigny, 1826; p. 282.

Criboelphidium – *Criboelphidium* Cushman and Brönnimann, 1948; p. 18.

Elphidium – *Elphidium* de Montfort, 1808; p. 14.

Miliolinella – *Miliolinella* Wiesner, 1931; pp. 63, 65, 107.

Orbulina – *Orbulina* d'Orbigny, 1839; p. 2.

Quinqueloculina – *Quinqueloculina* d'Orbigny, 1826; p. 301.

Rosalina – *Rosalina* d'Orbigny, 1826; p. 271.

Siphonaperta – *Siphonaperta* Vella, 1957; p. 19 .

Textularia – *Textularia* DeFrance in de Blainsville, 1824; p. 177.

Triloculina - *Triloculina* d'Orbigny, 1826; p. 299.

Ammonia beccarii - *Nautilus beccarii* Linnaeus, 1758; p. 710, pl. 1 fig. 1, pl. 19 figs. h, i.

Ammonia inflata - *Rosalina inflata* Seguenza, 1862; p. 106, pl. 1 fig. 6.

Ammonia parkinsoniana - *Rosalina parkinsoniana* d'Orbigny, 1839; p. 99, pl. 4 figs. 25-27.

Ammonia tepida - *Rotalia beccarii* (Linné) var. *tepida* Cushman, 1926; p. 79, pl. 1.

Asterigerinata mamilla - *Rotalina mamilla* Williamson, 1858; p. 54, pl. 4 figs. 109-111

Buccella granulata - *Eponides frigidus granulatus* Di Napoli Alliata, 1952; p. 103,107, pl. 5 fig. 3.

Bulimina marginata - *Bulimina marginata* d'Orbigny, 1826; p. 269, pl. 12 figs. 10-12.

Criboelphidium granosum - *Nonionina granosa* d'Orbigny, 1846; p. 110, pl. 5 figs. 19-20.

Criboelphidium lidoense - *Elphidium lidoense* Cushman, 1936; p. 86, pl. 15 fig. 6.

Elphidium crispum - *Nautilus crispus* Linnaeus, 1758; p. 709, pl. 1 figs. 2 d-f.

Haynesina depressula - *Nautilus depressulus* Walker & Jacob, 1798; p. 641, pl. 14 fig. 33.

Haynesina germanica - *Nonionina germanica* Ehrenberg, 1840; p. 23.

Nonionella turgida - *Rotalina turgida* Williamson, 1858; p. 50, pl. 4 figs. 95-97.

Quinqueloculina seminulum - *Serpula seminulum* Linnaeus, 1758; p. 789, pl. 2 figs. 1a-c.

Valvulineria bradyana - *Discorbina bradyana* Fornasini, 1900; p. 393, fig. 43.

Valvulineria perlucida - *Rotalia perlucida* Heron-Allen and Earland, 1913; p. 139, figs. 7-9.

Ostracods

Cyclocypris – *Cyclocypris* Brady and Norman, 1889; p. 70.

Ilyocypris – *Ilyocypris* Brady and Norman, 1889; p. 106.

Loxoconcha - *Loxoconcha* Sars, 1866; p. 61.

Semicytherura - *Semicytherura* Wagner, 1957; pp. 80-81.

Candona albicans - *Candona albicans* Brady, 1864; p. 61, pl. 4 figs. 6-10.

Cyprideis torosa – *Candona torosa* Jones, 1850; p. 27, pl. 3 figs. 6a-e.

Cytheridea neapolitana - *Cytheridea neapolitana* Kolmann, 1958; p. 152, pl. 7 figs. 7-10.

Leptocythere ramosa - *Cythere ramosa* Rome, 1942; p. 22, pl. 4 fig. 52, pl. 5 figs. 53-54, pl. 6 fig. 51.

Loxoconcha exagona - *Loxoconcha exagona* Bonaduce, Ciampo and Masoli, 1975; p. 106, pl. 62 figs. 1-7, text-fig. 41.

Loxoconcha tumida - *Loxoconcha tumida* Brady, 1869; p. 48, pl. 8 figs. 11,12.

Loxoconcha turbida – *Loxoconcha levis* G.W. Müller, 1894; p. 344, pl. 27 figs. 8, 19, 22, pl. 28 figs. 4, 8. *Loxoconcha turbida* G.W. Müller, 1912; p. 308 (new name).

Semicytherura acuticostata – *Cytherura acuticostata* Sars, 1866; p. 76.

Semicytherura incongruens - *Cytherura incongruens* G.W. Müller, 1894; p. 296, pl. 17 figs. 2, 7, 8, pl. 19 fig. 7.

Appendix B: Supplementary data

Benthic foraminiferal data for the taxa reported in Figs. 2, 3 and 4. Data are given as relative percentages of the total benthic foraminiferal fauna from samples including more than 300 foraminiferal specimens.

Figure captions

Fig. 1. Location map of the study cores 1 and S1. Present-day Northern Adriatic mud-belt and simplified longshore current pattern (arrows) are reported.

Fig. 2. Dendrogram of the 18 most common foraminiferal taxa, based on R-mode cluster analysis (Horn's modified Morisita's index).

Fig. 3. Stratigraphy and vertical distribution of benthic foraminifers in Core 1. Mud-belt assemblage is highlighted in grey. TS: Transgressive surface, RS: Ravinement surface, MFS: Maximum Flooding Surface (stratigraphy after Amorosi et al., submitted). Ages are reported as calibrated year BP on the right of core.

Fig. 4. Stratigraphy and vertical distribution of benthic foraminifers in Core S1. TS: Transgressive surface, RS: Ravinement surface, MFS: Maximum Flooding Surface (stratigraphy after Amorosi et al., 2007). Age is reported as calibrated year BP on the right of core.

Fig. 5. Schematic reconstruction of four main evolutive phases (A-D) of the Po Delta system and relationship with palaeoenvironmental data recorded by analyses of the cores 1 and S1. For each phase, only the main active Po river branches are represented. Dotted line shows the present-day coastline (modified after Visentini, 1940; Ciabatti, 1966; Correggiari et al., 2005b; Stefani and Vincenzi, 2005).

Fig. 6. Spatial distribution pattern of modern benthic foraminifers along a generic W-E Adriatic transect, with the relative position of cores 1 and S1 (slightly modified after Van der Zwaan and Jorissen, 1991). Nearshore zone is dominated by *Ammonia* and *Elphidium* species. Following a bathymetric gradient, from shallow to deep water, the mud-belt area (showed in gray) is characterized by the dominance of *Nonionella turgida*, *Bulimina marginata* and *Valvulineria bradyana*.

References

AGIP, 1982. Foraminiferi Padani (Terziario e Quaternario): Plate I-LII. AGIP, Milano.

Aguzzi, M., Amorosi, A., Colalongo, M.L., Ricci Lucchi, M., Rossi, V., Sarti, G., Vaiani, S.C., 2007. Late Quaternary climatic evolution of the Arno coastal plain (Western Tuscany, Italy) from subsurface data. *Sedimentary Geology* 202, 211–229.

Albani, A., Serandrei Barbero, R., 1990. I Foraminiferi della Laguna e del Golfo di Venezia. *Memorie di Scienze Geologiche Padova* 42, 271–341.

Amorosi, A., Milli, S., 2001. Late Quaternary depositional architecture of Po and Tevere river deltas (Italy) and worldwide comparison with coeval deltaic successions. *Sedimentary Geology* 144, 357–375.

Amorosi, A., Colalongo, M.L., 2005. The linkage between alluvial and coeval nearshore marine successions: evidence from the Late Quaternary record of the Po River Plain, Italy. In: Blum, M.D., Marriott, S.B., Leclair, S.F. (Eds.), *Fluvial Sedimentology VII*, International Association of Sedimentologists, Special Publication 35. Blackwell Scientific Publications, Oxford, pp. 257–275.

Amorosi, A., Colalongo, M.L., Pasini, G., Preti, D., 1999. Sedimentary response to Late Quaternary sea-level changes in the Romagna coastal plain (northern Italy). *Sedimentology* 46, 99–121.

Amorosi, A., Centineo, M.C., Colalongo, M.L., Pasini, G., Sarti, G., Vaiani, S.C., 2003. Facies architecture and Latest Pleistocene-Holocene depositional history of the Po Delta (Comacchio area). Italy. *The Journal of Geology* 111, 39–56.

Amorosi, A., Colalongo, M.L., Fiorini, F., Fusco, F., Pasini, G., Vaiani, S.C., Sarti, G., 2004. Palaeogeographic and palaeoclimatic evolution of the Po Plain from 150-ky core records. *Global and Planetary Change* 40, 55–78.

Amorosi, A., Centineo, M.C., Colalongo, M.L., Fiorini, F., 2005. Millennial-scale depositional cycles from the Holocene of the Po Plain, Italy. *Marine Geology* 222–223, 7–18.

Amorosi, A., Colalongo, M.L., Dinelli, E., Lucchini, F., Vaiani, S.C., 2007. Cyclic variations in sediment provenance from late Pleistocene deposits of the eastern Po Plain, Italy. In: Arribas, J., Critelli, S., Johnsson, M.J. (Eds.), *Sedimentary Provenance and Petrogenesis: Perspectives from Petrography and Geochemistry*. Geology Society of America, Special Paper 420, pp. 13–24.

Amorosi, A., Dinelli, E., Rossi, V., Vaiani, S.C., Sacchetto, M., submitted. Late Quaternary palaeoenvironmental evolution of the Adriatic coastal plain and the onset of Po River Delta. *Palaeogeography, Palaeoclimatology, Palaeoecology*.

Barmawidjaja, D.M., Jorissen, F.J., Puskaric, S., Van der Zwaan, G.J., 1992. Microhabitat selection by benthic foraminifera in the northern Adriatic Sea. *Journal Foraminiferal of Research* 22, 297–317.

Bizon, G., Bizon, J.J., 1984. Ecologie des Foraminifères en Méditerranée nord-occidentale. P. Distribution des foraminifères sur le plateau continental au large du Rhône. In : Bizon, J.J., Burolet, P.F. (Eds.), *Ecologie des microorganismes en Méditerranée Occidentale*. ECOMED, AFTP, Paris, pp. 84–94.

Bodergat, A.M., Ikeya, N., Irzi, Z., 1998. Domestic and industrial pollution: use of ostracods (Crustacea) as sentinels in the marine coastal environment. *Journal Recherches Oceanographique* 23, 139–144.

Bonaduce, G., Ciampo, G., Masoli, M., 1975. Distribution of Ostracoda in the Adriatic Sea. *Pubblicazione Stazione Zoologica di Napoli* 40.

Bondesan, M., 1990. L'area deltizia padana: caratteri geografici e geomorfologici. In: Bondesan, M. (Ed.), *Il Parco dei delta del Po: studi ed immagini, Volume II*. Spazio Libri, pp. 10–48.

Bondesan, M., Cibir, U., Colalongo, M.L., Pugliese, N., Stefani, M., Tsakiridis, E., Vaiani, S.C., Vincenzi, S., 2006. Benthic communities and sedimentary facies recording late Quaternary environmental fluctuations in a Po Delta subsurface succession (Northern Italy). In: Coccioni, R., Lirer, F., Marsili, A. (Eds.), Proceedings of the Second and Third Italian Meeting of Environmental Micropaleontology, The Grzybowski Foundation Special Publication 11. Krakow, pp. 21–31.

Breman, E., 1975. The distribution of Ostracodes in the bottom sediments of the Adriatic Sea. Ph.D. Thesis, Free University of Amsterdam, Netherlands.

Carboni, M.G., Frezza, V., Bergamin, L., 2004. Distribution of Recent foraminifers in the Ombrone River Basin (Tuscany Continental Shelf, Tyrrhenian Sea, Italy): relations with fluvial run-off. In: Coccioni, R., Galeotti, S., Lirer, F. (Eds.), Proceedings of the First Italian Meeting of Environmental Micropaleontology, The Grzybowski Foundation Special Publication 9, pp. 7–16.

Castellarin, A., Vai, G.B., 1986. Southalpine versus po Plian Apenninic Arcs. In: Wezel, F.C. (Ed.), The origin of arcs. Elsevier, Amsterdam, pp. 253–280.

Castellarin, A., Eva, C., Giglia, G., Vai, G.B., Rabbi, E., Pini, G.A., Crestana, G., 1985. Analisi strutturale del Fronte Appenninico Padano. *Giornale di Geologia* 47, 47–75.

Ciabatti, M., 1966. Ricerche sull'evoluzione del Delta Padano. *Giornale di Geologia* 34 (2), 381–406.

Cimerman, F., Langer, M.R., 1991. Mediterranean Foraminifera. *Academia Scientiarum et Artium Slovenica Classis IV* 30: Ljubljana.

Colalongo, M.L., 1969. Ricerche sugli Ostracodi nei fondali antistanti il delta del Po. *Giornale di Geologia* 36, 335–362.

Correggiari, A., Cattaneo, A., Trincardi, F., 2005a. The modern Po delta system: lobe switching and asymmetric prodelta growth. *Marine Geology* 222-223, 49–74.

Correggiari, A., Cattaneo, A., Trincardi, F., 2005b. Depositional patterns in the Holocene Po Delta system. In: Bhattacharya, J.P., Giosan, L. (Eds.), *River Deltas: Concepts, Models and Examples*, SEPM Special Publication 83, pp. 365–392.

Curzi, P.V., Dinelli, E., Ricci Lucchi, M., Vaiani, S.C., 2006. Palaeoenvironmental control on sediment composition and provenance in the late Quaternary deltaic successions: a case study from the Po delta area (Northern Italy). *Geological Journal* 41, 591–612.

D'Onofrio, S., 1969. Ricerche sui Foraminiferi nei fondali antistanti il Delta del Po. *Giornale di Geologia* 36, 283–334.

Debenay, J.P., Guillou, J.J., Redois, F., Geslin, E., 2000. Distribution trends of foraminiferal assemblages in paralic environments. A base for using foraminifera as bioindicators. In: Martin, E.R. (Ed.), *Environmental Micropaleontology, Topics in Geobiology 15*. Kluwer Academic/Plenum Publishers, New York, pp. 39–67.

Donnici, S., Serandrei Barbero, R., 2002. The benthic foraminiferal communities of the northern Adriatic continental shelf. *Marine Micropaleontology* 44, 93–123.

Fabbri, C., 1985. Coastline variations in the Po delta since 2500 B.P. *Zeitschrift fuer Geomorphologie N.F.* 57, 155–167

Fiorini, F., 2004. Benthic foraminiferal associations from Upper Quaternary deposits of southeastern Po Plain, Italy. *Micropaleontology* 50, 45–58.

Fiorini, F., Vaianni, S.C., 2001. Benthic foraminifers and transgressive-regressive cycles in the Late Quaternary subsurface sediments of the Po Plain near Ravenna (Northern Italy). *Bollettino della Società Paleontologica Italiana* 40, 357–403.

Fregni, P., 1980. I Foraminiferi della piattaforma continentale Adriatica tra Ravenna e Chioggia. In: Colantoni, P., Galignani, P. (Eds.), *Ricerche sulla piattaforma continentale dell'alto Adriatico*, C.N.R. Quadern. 2. Bologna, pp. 43–53.

Frezza, V., Bergamin, L., Di Bella, L., 2005. Opportunistic benthic foraminifera as indicators of eutrophicated environments. Actualistic study and comparison with the Santeranian middle Tiber Valley (Central Italy). *Bollettino della Società Paleontologica Italiana* 44 (3), 193–201.

Hammer, Ø., Harper, D.A.T., Ryan, P.D., 2007. PAST—Palaeontological statistics, ver. 1.75 <http://folk.uio.no/ohammer/past>.

Henderson, P.A., 1990. Freshwater ostracods. In: Kermack, D.M., Barnes, R.S.K. (Eds.), *Synopses of the British Fauna (New Series)* 42. Brill E.J., Leiden.

Jorissen, F.J., 1987. The distribution of benthic foraminifera in the Adriatic Sea. *Marine Micropaleontology* 12, 21–48.

Jorissen, F.J., 1988. Benthic foraminifera from the Adriatic Sea; principles of phenotypic variation. *Utrecht Micropaleontology Bulletins* 37, 176.

Jorissen, F.J., Barmawidjaja, D.M., Puskaric, S., Van der Zwaan, G.J., 1992. Vertical distribution of benthic foraminifera in the northern Adriatic Sea: the relation with the organic flux. *Marine Micropaleontology* 19, 131–146.

Massari, F., Rio, D., Serandrei Barbero, R., Asioli, A., Capraio, L., Fornaciari, E., Vergerio, P.P., 2004. The environment of Venice area in the past two million years. *Palaeogeography, Palaeoclimatology, Palaeoecology* 202, 273–308.

Morigi, C., Jorissen, F.J., Fraticelli, S., Horton, B.P., Principi, M., Sabbatici, A., Capotondi, L., Curzi, P.V., Negri, A., 2005. Benthic foraminiferal evidence for the formation of the Holocene mud-belt and bathymetrical evolution in the central Adriatic Sea. *Marine Micropaleontology* 57, 25– 49

Murray, J.W., 1991. *Ecology and Palaeoecology of Benthic Foraminifera*. Longman Scientific and Technical, London.

Pieri, M., Groppi, G., 1981. Subsurface geological structure of the Po Plain, Italy. *Pubbl. 414 P.F. Geodinamica, C.N.R., Roma*.

Rasmussen, T.L., Hastrup, A., Thomsen, E., 2005. Lagoon to Deep-Water Foraminifera and Ostracods from the Plio-Pleistocene Kallithea Bay Section, Rhodes, Greece.

Cushman Foundation for Foraminiferal Research Special Publication 39, 290.

Reimer, P.J., Baillie, M.G.L., Bard, E., Bayliss, A., Beck, J.W., Bertrand, C.J.H., Blackwell, P.G., Buck, C.E., Burr, G.S., Cutler, K.B., Damon, P.E., Edwards, R.L., Fairbanks, R.G., Friedrich, M., Guilderson, T.P., Hogg, A.G., Hughen, K.A., Kromer, B., McCormac, F.G., Manning, S.W., Ramsey, C.B., Reimer, R.W., Remmele, S., Southon,

J.R., Stuiver, M., Talamo, S., Taylor, F.W., van der Plicht, J., Weyhenmeyer, C.E., 2004. IntCal04 terrestrial radiocarbon age calibration. *Radiocarbon* 46, 1029–1058.

Ruiz, F., Gonzalez-Regalado, M.L., Baceta, J.I., Menegazzo-Vitturi, L., Pisolato, M., Ramazzo, G., Molinaroli, E., 2000. Los ostrácodos actuales de la laguna de Venecia (NE de Italia). *Geobios* 33, 447–454.

Scott, D.B., Piper, D.J.W., Panagos, A.G., 1979. Recent salt marsh and intertidal mudflat foraminifera from the western coast of Greece. *Rivista Italiana di Paleontologia e Stratigrafia* 85, 243–266.

Scruton, P.C., 1960. Delta building and the deltaic sequence. In: Shepard, F.P., Phleger, F.B., van Andel, T.H. (Eds.), *Recent Sediments, Northwest Gulf of Mexico*, American Association of Petroleum Geologists Symposium. Tulsa, Oklahoma, pp. 82–102.

Sgarrella, F., Moncharmont Zei, M., 1993. Benthic Foraminifera of the Gulf of Naples (Italy): systematics and autoecology. *Bollettino Società Paleontologica Italiana* 32, 145–264.

Stefani, M., Vincenzi, S., 2005. The interplay of eustasy, climate and human activity in the late Quaternary depositional evolution and sedimentary architecture of the Po Delta system. *Marine Geology* 222–223, 19–48.

Stefani, M., Vincenzi, S., Cibin, S., 2003. Geological-stratigraphic map of the central portion of the Po Delta system at 1/50,000. Regione Emilia-Romagna. S.E.L.C.A.

Stuiver, M., Reimer, P.J., 1993. Extended 14C data base and revised CALIB 3.0 14C Age calibration program. Radiocarbon 35, 215–230.

Stuiver, M., Reimer, P.J., Reimer, R.W., 2005. CALIB ver. 5.0.
<http://calib.qub.ac.uk/calib/>.

Vai, G.B., 1987. Migrazione complessa del sistema fronte deformativo-avanfossa-cercine periferico: il caso dell'Appennino settentrionale. Memorie Società Geologica Italiana 38, 95–105.

Van der Zwaan, G.J., Jorissen, F.J., 1991. Biofacial patterns in river-induced shelf anoxia. In: Tyson, R.V., Pearson, T.H. (Eds.), Modern and Ancient Continental Shelf Anoxia, Geological Society Special Publication 58, pp. 65–82.

Van Straaten, L.M.J.U., 1965. Sedimentation in the North-Western of the Adriatic Sea. Colston Papers 17, 143–160.

Veggiani, A., 1984. Il deterioramento climatico dei Secoli XVI–XVIII ed i suoi effetti sulla bassa Romagna. Studi Romagnoli 35, 109–124.

Veggiani, A., 1990. Fluttuazioni climatiche e trasformazioni ambientali nel territorio imolese dall'alto medioevo all'età moderna. In: Mancini, F., Gioberti, M., Veggiani, A. (Eds.), *Imola nel Medioevo*. Imola, pp. 41–102.

Yassini, I., Jones, B.G., 1995. *Foraminiferida and Ostracoda from Estuarine and Shelf Environments on the Southeastern Coast of Australia*. University of Wollongong Press, Wollongong.

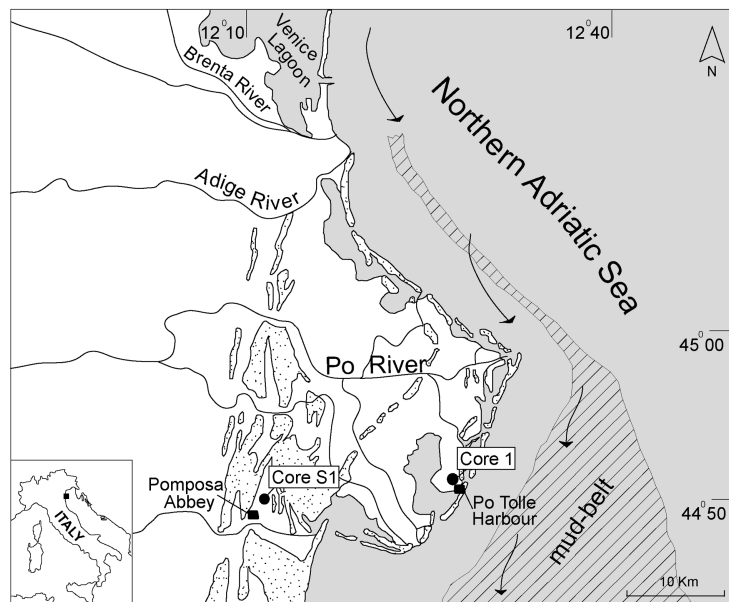


Figure 1

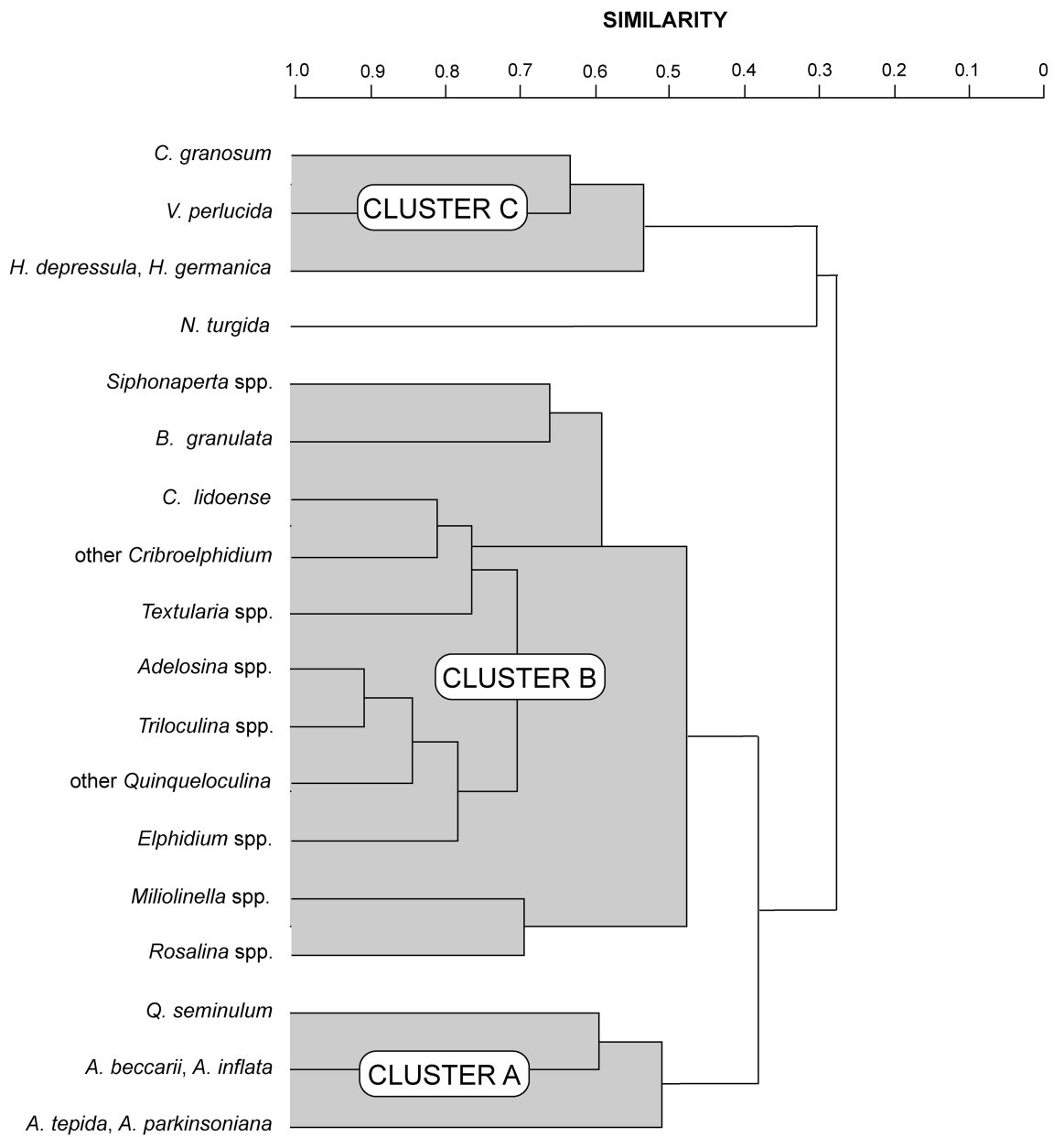


Figure 2

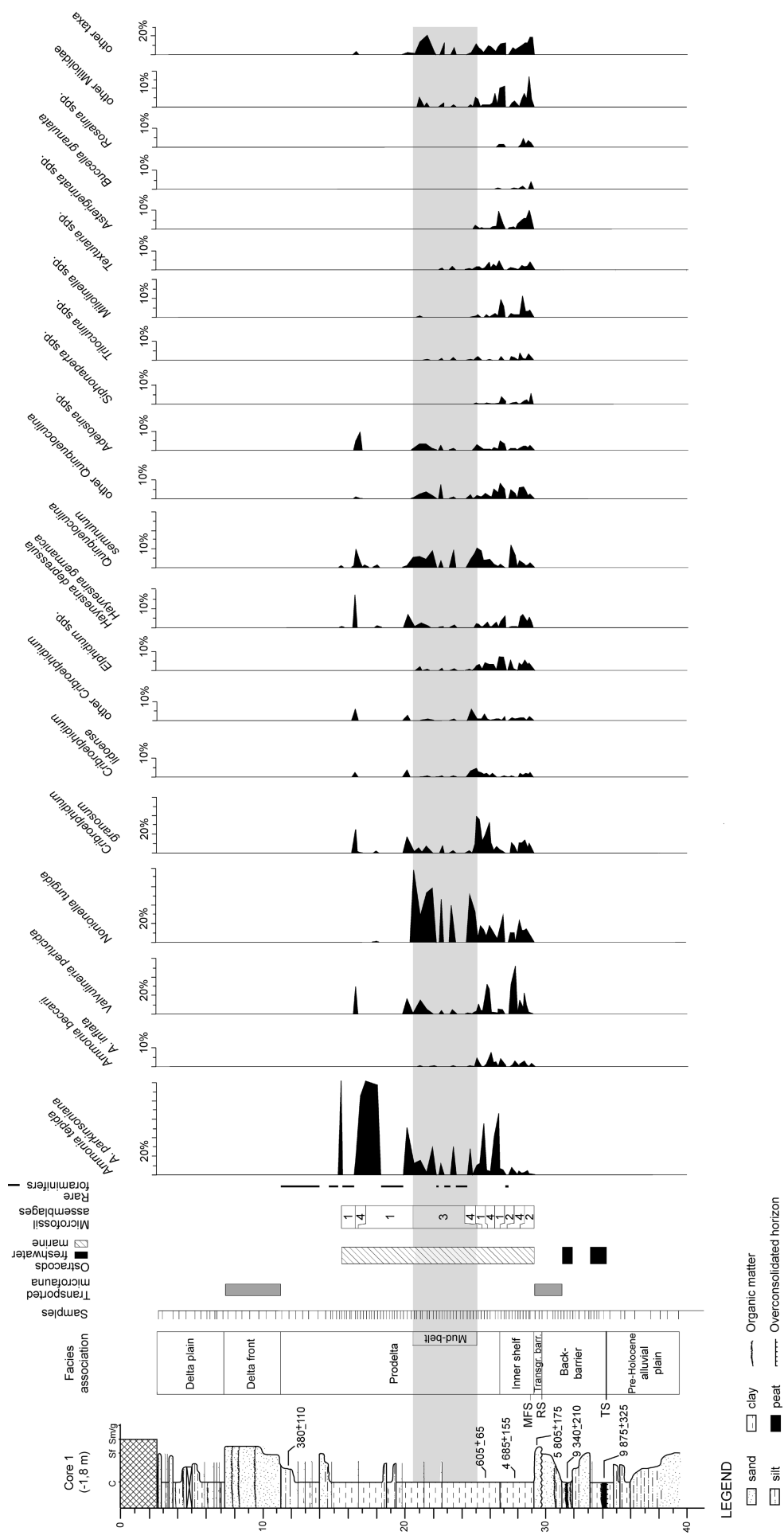


Figure 3

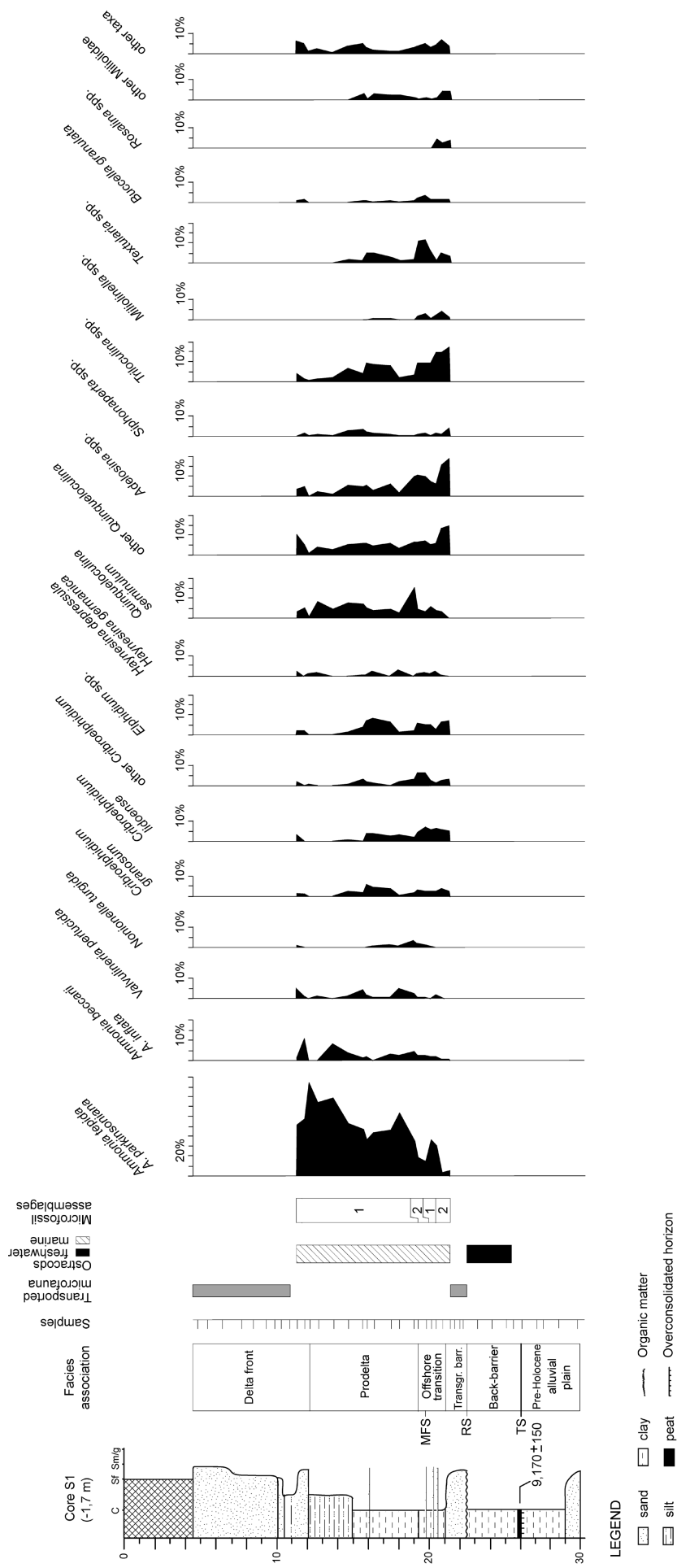


Figure 4

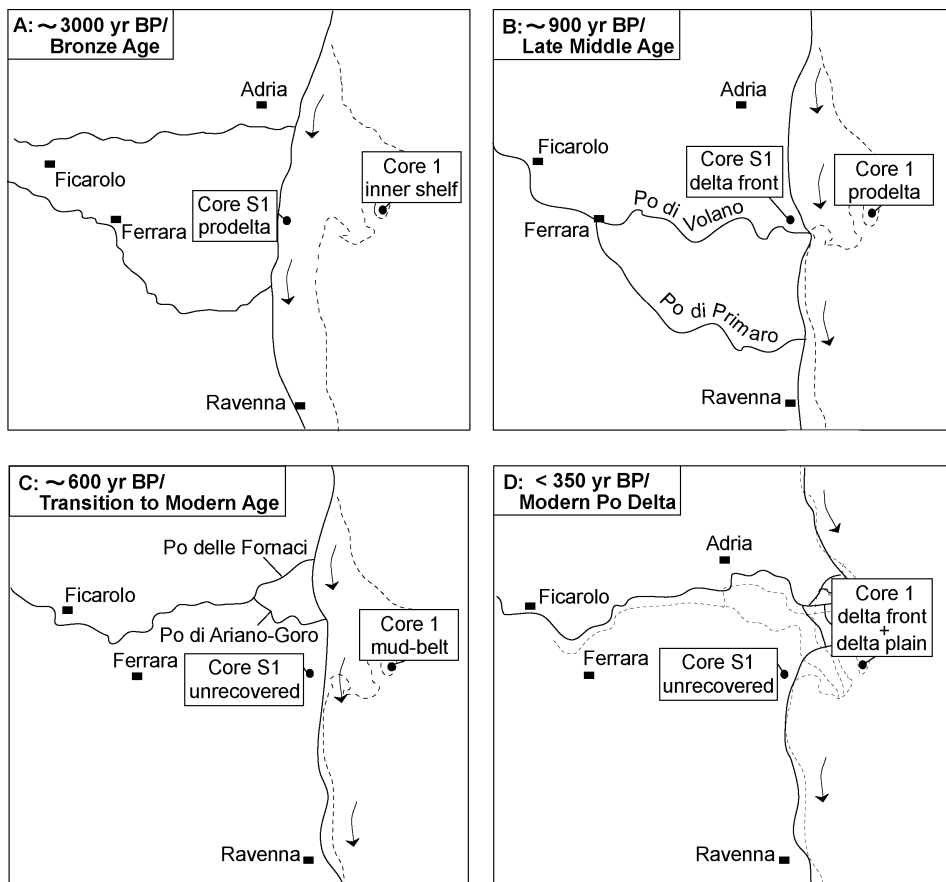


Figure 5

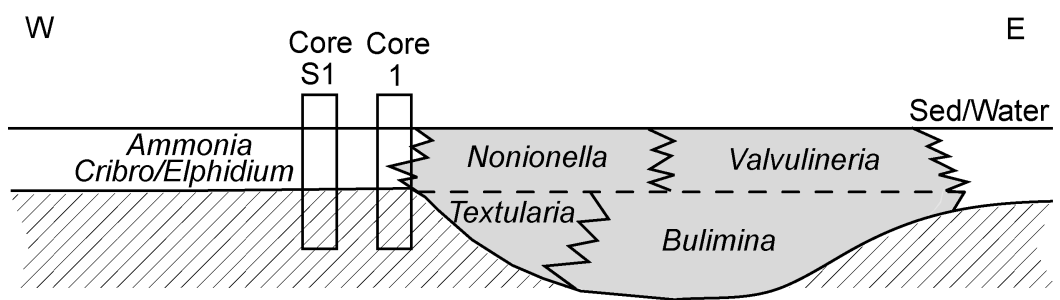


Figure 6

APPENDIX B: SUPPLEMENTARY DATA (ONLINE VERSION)

CORE 1 DATA

Sample Depth (m)	<i>Ammonia tepida</i> , <i>A. parkinsoniana</i>	<i>Ammonia beccarii</i> , <i>A. inflata</i>	<i>Valvulineria perlucida</i>	<i>Nonionella turgida</i>	<i>Criboelphidium granosum</i>
15.60	99.05	0.00	0.00	0.00	0.00
16.55	16.61	0.00	27.69	0.00	25.41
16.70	83.03	0.00	0.37	0.37	0.74
16.90	87.63	0.00	0.00	0.00	0.00
17.30	98.91	0.00	0.00	0.00	0.00
18.10	94.53	0.00	0.00	0.73	2.31
20.20	50.16	0.00	15.41	0.33	17.70
20.65	14.61	0.00	0.65	74.68	1.95
21.10	16.83	0.32	13.92	27.51	5.18
21.60	3.61	0.00	4.92	46.56	7.54
22.05	28.97	0.31	0.00	56.39	0.00
22.68	11.33	0.00	3.40	45.04	7.93
23.45	29.44	0.53	3.98	37.67	2.92
24.65	26.95	0.35	0.71	48.94	2.48
25.08	9.90	4.29	1.98	33.99	10.23
25.20	9.75	1.89	2.20	5.35	40.57
25.40	11.63	0.00	9.30	16.86	36.92
25.60	54.05	0.00	3.60	12.61	13.21
25.80	4.38	1.10	29.86	13.70	19.73
26.05	2.54	7.38	24.94	6.36	33.84
26.40	40.74	2.47	4.32	16.98	3.09
26.60	64.59	0.00	0.54	7.84	7.30
26.80	5.50	4.21	5.18	3.56	4.21
27.05	4.88	0.91	4.27	27.44	2.13
27.60	7.55	0.91	29.61	9.97	11.48
27.80	5.50	2.75	48.62	9.79	7.65
28.20	3.59	1.31	14.05	21.90	11.11
28.40	1.26	3.02	5.29	9.32	11.08
28.60	2.23	0.96	21.34	11.78	14.33
28.80	4.13	0.00	8.89	11.75	6.03
28.90	0.96	1.61	1.93	13.83	10.93

CORE 1 DATA

Sample Depth (m)	<i>Criboelphidium lidoense</i>	other <i>Criboelphidium</i>	<i>Elphidium</i> spp.	<i>Haynesina depressula</i> , <i>H. germanica</i>	<i>Quinqueloculina seminulum</i>
15.60	0.00	0.00	0.00	0.32	0.63
16.55	2.28	5.86	0.00	18.57	0.65
16.70	0.00	0.00	0.00	0.00	9.96
16.90	0.00	0.00	0.00	0.00	2.75
17.30	0.00	0.00	0.00	0.00	1.09
18.10	0.00	0.00	0.00	0.85	1.09
20.20	3.61	2.62	0.00	7.21	0.98
20.65	0.00	0.00	0.00	0.32	5.52
21.10	0.00	0.32	1.94	2.27	6.15
21.60	0.33	0.98	0.66	0.66	4.59
22.05	0.00	0.00	0.00	0.00	9.35
22.68	0.28	0.28	1.13	0.57	3.68
23.45	0.53	0.80	0.80	1.06	9.55
24.65	3.55	5.67	0.71	0.00	4.61
25.08	4.95	0.66	1.32	1.98	8.25
25.20	2.83	0.94	2.52	1.57	11.01
25.40	2.33	0.87	3.20	0.58	9.30
25.60	1.50	3.30	0.60	0.60	3.90
25.80	1.92	0.82	4.11	3.01	4.11
26.05	0.25	0.25	3.05	0.25	4.58
26.40	0.31	0.93	3.09	2.78	1.54
26.60	0.54	0.81	0.27	0.00	0.54
26.80	0.32	0.00	7.12	3.24	1.62
27.05	0.30	1.83	7.01	6.40	0.30
27.60	0.30	1.21	5.44	0.60	12.39
27.80	0.00	0.61	0.92	0.31	7.03
28.20	1.96	1.31	3.92	5.88	3.59
28.40	1.01	1.51	2.77	7.30	2.02
28.60	1.91	0.00	5.41	3.18	0.64
28.80	1.27	1.90	3.17	5.71	1.27
28.90	2.25	0.32	3.86	2.89	2.25

CORE 1 DATA

Sample Depth (m)	other <i>Quinqueloculina</i>	<i>Adelosina</i> spp.	<i>Siphonaperta</i> spp.	<i>Triloculina</i> spp.	<i>Miliolinella</i> spp.	<i>Textularia</i> spp.	<i>Asterigerinata</i> spp.
15.60	0.00	0.00	0.00	0.00	0.00	0.00	0.00
16.55	0.00	0.00	0.00	0.00	0.00	0.00	0.00
16.70	0.74	4.80	0.00	0.00	0.00	0.00	0.00
16.90	0.00	9.62	0.00	0.00	0.00	0.00	0.00
17.30	0.00	0.00	0.00	0.00	0.00	0.00	0.00
18.10	0.00	0.00	0.00	0.00	0.00	0.00	0.00
20.20	0.00	0.00	0.00	0.00	0.00	0.00	0.00
20.65	0.32	0.65	0.00	0.00	0.00	0.00	0.00
21.10	2.59	3.24	0.00	0.00	0.97	0.00	0.00
21.60	3.61	3.28	0.00	0.33	0.00	0.00	0.00
22.05	1.56	0.62	0.00	0.00	0.31	0.00	0.00
22.68	7.65	2.27	0.00	0.85	0.28	0.57	0.00
23.45	0.80	0.80	0.00	1.59	0.00	1.59	0.00
24.65	2.13	0.00	0.00	0.71	0.00	0.35	0.00
25.08	0.33	1.32	0.33	1.65	0.66	0.99	0.00
25.20	1.57	2.83	0.00	1.89	1.57	1.26	1.57
25.40	0.87	1.16	0.00	0.58	0.00	1.45	0.00
25.60	1.80	0.60	0.00	0.30	0.30	0.30	0.30
25.80	3.01	0.55	0.27	0.27	1.10	0.82	0.00
26.05	1.27	0.25	0.00	1.02	0.00	3.82	0.00
26.40	5.25	1.23	0.00	0.31	1.85	2.78	0.93
26.60	3.24	0.54	0.54	0.27	0.54	1.35	1.08
26.80	8.41	4.85	3.56	1.94	9.71	4.53	8.74
27.05	5.18	3.05	1.22	0.00	6.10	0.00	2.44
27.60	4.83	0.91	0.30	1.81	1.81	0.91	0.30
27.80	2.75	0.61	0.61	1.53	1.22	0.61	0.61
28.20	5.88	0.98	0.00	3.59	1.31	0.33	2.61
28.40	6.55	2.02	1.76	0.76	11.84	2.02	4.53
28.60	4.46	1.91	1.91	0.64	3.50	1.27	5.10
28.80	1.59	1.27	0.32	3.17	3.17	1.90	5.08
28.90	2.57	2.57	5.14	2.25	4.18	3.86	9.32

CORE 1 DATA

Sample Depth (m)	<i>Buccella granulata</i>	<i>Rosalina</i> spp.	other Miliolidae	other taxa
15.60	0.00	0.00	0.00	0.00
16.55	0.00	0.00	0.00	2.93
16.70	0.00	0.00	0.00	0.00
16.90	0.00	0.00	0.00	0.00
17.30	0.00	0.00	0.00	0.00
18.10	0.00	0.00	0.00	0.49
20.20	0.00	0.00	0.00	1.97
20.65	0.00	0.00	0.00	1.30
21.10	0.00	0.00	5.18	13.59
21.60	0.00	0.00	1.64	21.31
22.05	0.00	0.00	0.31	2.18
22.68	0.00	0.00	2.27	12.46
23.45	0.00	0.00	0.80	7.16
24.65	0.00	0.00	0.71	2.13
25.08	0.00	0.00	4.95	12.21
25.20	0.00	0.00	3.77	6.92
25.40	0.00	0.00	0.00	4.94
25.60	0.00	0.00	0.60	2.40
25.80	0.00	0.00	1.37	9.86
26.05	0.00	0.25	1.27	8.65
26.40	0.00	0.31	7.41	3.70
26.60	0.54	0.00	1.08	8.38
26.80	0.00	0.97	11.00	11.33
27.05	0.00	1.22	12.20	13.11
27.60	0.00	0.00	2.11	7.55
27.80	0.61	0.31	2.75	5.20
28.20	0.65	1.31	3.92	10.78
28.40	1.26	4.28	7.56	12.85
28.60	0.00	1.59	4.78	13.06
28.80	0.00	3.17	17.14	19.05
28.90	4.00	1.93	4.18	19.15

APPENDIX B: SUPPLEMENTARY DATA (ONLINE VERSION)

CORE S1 DATA

Sample Depth (m)	<i>Ammonia tepida</i> , <i>A. parkinsoniana</i>	<i>Ammonia beccarii</i> , <i>A. inflata</i>	<i>Valvulineria perlucida</i>	<i>Nonionella turgida</i>	<i>Criboelphidium granosum</i>	<i>Criboelphidium lidoense</i>
11.30	52.25	1.69	5.62	0.56	1.12	3.37
11.80	58.24	12.09	1.10	0.00	1.10	0.00
12.10	94.51	0.84	0.00	0.00	0.21	0.00
12.70	74.43	0.97	1.29	0.32	0.00	0.00
13.70	79.06	9.16	0.00	0.26	0.00	0.26
14.70	53.42	4.35	1.55	0.31	2.48	0.62
15.65	47.08	2.15	4.62	0.31	1.85	0.31
15.90	36.98	2.96	2.07	0.00	5.92	4.14
16.35	44.25	0.77	0.51	0.51	4.60	4.09
17.50	46.77	4.31	0.62	1.23	4.31	2.46
18.05	63.84	3.26	5.21	0.65	0.65	3.58
19.05	35.31	5.64	2.37	3.56	2.08	2.08
19.25	18.69	3.12	0.93	2.18	3.43	4.69
19.75	14.92	3.31	0.55	1.66	2.49	7.18
20.10	36.86	2.56	0.32	0.64	2.56	6.09
20.50	30.71	2.72	2.17	0.00	2.99	6.79
20.85	3.57	1.37	0.00	0.27	3.85	5.77
21.35	5.04	1.06	0.00	0.00	2.39	5.04

CORE S1 DATA

Sample Depth (m)	other <i>Criboelphidium</i>	<i>Elphidium</i> spp.	<i>Haynesina depressula</i> , <i>H. germanica</i>	<i>Quinqueloculina seminulum</i>	other <i>Quinqueloculina</i>	<i>Adelosina</i> spp.	<i>Siphonaperta</i> spp.
11.30	1.69	1.69	2.81	3.37	10.67	3.93	0.00
11.80	0.00	2.20	0.00	5.49	5.49	5.49	1.10
12.10	0.42	0.21	1.05	0.42	0.42	0.21	0.21
12.70	0.32	0.32	2.27	8.74	3.88	2.59	0.65
13.70	0.00	0.00	0.00	4.71	2.36	1.05	0.26
14.70	0.62	1.55	0.31	8.07	5.59	6.21	2.48
15.65	3.08	4.31	0.92	7.08	5.85	5.54	3.08
15.90	1.78	7.40	0.89	5.03	6.21	5.92	1.78
16.35	1.28	8.70	2.56	4.09	4.86	3.58	1.02
17.50	0.00	6.77	0.31	4.92	5.85	6.77	0.92
18.05	2.28	1.63	3.58	2.61	3.26	2.28	0.00
19.05	3.26	1.78	0.00	16.32	6.82	10.68	0.30
19.25	6.85	6.23	1.25	4.98	6.54	11.53	0.62
19.75	6.35	5.52	2.21	3.04	7.18	10.77	1.10
20.10	2.88	5.13	1.60	6.09	5.13	7.69	0.00
20.50	1.63	2.72	2.45	4.08	5.71	6.52	1.63
20.85	2.75	6.59	0.55	3.57	14.29	16.76	0.82
21.35	3.18	7.43	0.00	1.33	15.38	19.89	3.71

CORE S1 DATA

Sample Depth (m)	<i>Triloculina</i> spp.	<i>Miliolinella</i> spp.	<i>Textularia</i> spp.	<i>Buccella granulata</i>	<i>Rosalina</i> spp.	other Miliolidae	other taxa
11.30	3.93	0.00	0.00	0.56	0.00	0.00	6.74
11.80	1.10	0.00	0.00	1.10	0.00	0.00	5.50
12.10	0.42	0.00	0.00	0.00	0.00	0.00	1.08
12.70	1.29	0.00	0.00	0.00	0.00	0.32	2.61
13.70	2.09	0.00	0.00	0.00	0.00	0.00	0.79
14.70	6.52	0.00	1.86	0.00	0.00	0.31	3.75
15.65	4.31	0.00	0.92	0.92	0.00	2.46	5.21
15.90	9.47	0.30	5.03	0.59	0.00	0.00	3.53
16.35	8.44	0.77	5.37	0.26	0.00	2.56	1.78
17.50	7.69	0.62	2.77	0.62	0.00	1.85	1.21
18.05	1.95	0.33	0.98	0.33	0.00	1.95	1.63
19.05	3.56	0.00	1.78	0.59	0.00	0.60	3.27
19.25	9.03	2.18	11.21	2.18	0.31	0.31	3.74
19.75	9.12	3.04	11.88	3.59	0.28	0.56	5.25
20.10	9.62	0.96	7.05	1.28	0.00	0.32	3.22
20.50	14.40	2.99	1.36	1.09	4.35	0.81	4.88
20.85	14.84	4.95	4.95	1.37	2.75	3.84	7.14
21.35	17.51	1.06	3.18	1.59	4.24	3.71	4.26

Paper 6

**The application of a subtidal foraminiferal-based transfer function to
reconstruct Holocene palaeo-bathymetry of the Po delta,
Northern Adriatic Sea**

Rossi, V. and Horton, B.P.

**THE APPLICATION OF A SUBTIDAL FORAMINIFERAL-BASED
TRANSFER FUNCTION TO RECONSTRUCT HOLOCENE
PALAEO-BATHYMETRY OF THE PO DELTA, NORTHERN
ADRIATIC SEA**

Veronica Rossi ^{1,*} and Benjamin Peter Horton ²

¹Dipartimento di Scienze della Terra e Geologico-Ambientali, Università di Bologna,
Via Zamboni 67, 40126 Bologna, Italy

²Sea Level Research Laboratory, Department of Earth and Environmental Science,
University of Pennsylvania, Philadelphia, PA 19104-6316, USA

Abstract

We evaluated the potential of WA-PLS foraminiferal-based transfer functions to reconstruct the Holocene palaeo-bathymetric evolution of Po Delta area (Northern Adriatic Sea).

The Northern Adriatic transfer function (NATF) is based upon the largest modern adriatic database existing in literature (Jorissen, 1988). The relationship existing between observed and foraminiferal-predicted water depths indicated that accurate ($r^2_{\text{jack}} = 0.95$) and precise ($\text{RMSEP} = 5.14 \text{ m}$) reconstructions are possible. We applied the NATF to a fossil marine succession (40-meters long Core 1), which was recovered in the southern portion of Modern Po Delta and dated to the last ca. 5,500 cal yr BP. The transfer function produced 31 palaeo-water depth data with a specific error ranging from 5.2 to 5.6 m. All maximum water depth values (from $17.8 \pm 5.3 \text{ m}$ to $28.9 \pm 5.6 \text{ m}$) were recorded within inner shelf deposits (29-26.80 m core depth), containing an open-marine microfauna dominated by Miliolids and hyaline epiphytic taxa. The reliability of the paleo-bathymetric reconstruction was statistically confirmed by modern analogue techniques.

An abrupt decrease in water depth, from 28.9 m to 11.6 m, took place ca. 4,000-3,500 cal yr BP (around 26.80 m core depth), marking the passage to prodelta sedimentation characterized by elevated amounts of *Ammonia tepida*, *Ammonia parkinsoniana*, *Valvulineria perlucida* and *Criboelphidium granosum*. The whole prodelta succession, recorded between ca. 26,60-15 m core depth, was characterized by water depth values lower than $18.7 \pm 5.3 \text{ m}$. Following a typical progradational trend, the shallowest

bathymetric conditions (from 10.4 ± 5.3 m to 7.6 ± 5.3 m) were reached in correspondence of the uppermost prodelta deposits. Within the prodelta succession a minimal increase of palaeobathymetry is recorded between 25.10-20.50 m core-depth, in correspondence of clayey deposits containing high percentages of *Nonionella turgida*. These deposits are interpreted as the fossil record of a marginal mud-belt developed along the present Po Delta coastline during historical times (ca. 600 cal yr ago).

Keywords: transfer function; benthic foraminifers; palaeobathymetry; Po Delta; Holocene

INTRODUCTION

Integrated sedimentological and micropalaeontological analyses of Late Quaternary deposits buried beneath several Mediterranean coastal areas have been used to better understand the response of coastal environments to relative sea-level changes occurred in the recent past and develop depositional models (Bellotti and others, 2004; Leorri and Cearreta, 2004; Amorosi and others, 2004). The sensitivity of many microorganisms, especially benthic foraminifers, to several physical parameters, (e.g., salinity, organic content, oxygen percentage, nature of substrate and depth), has enabled the reconstruction of high-frequency palaeoenvironmental oscillations in the Late Quaternary period from sedimentary successions (Serandrei Barbero and others, 2004; Amorosi and others, 2005; Leorri and others, 2006). Recently, qualitative estimates have been replaced by quantitative reconstructions of specific physical parameters, such as elevation relative to sea level, organic carbon flux, salinity and sea surface temperature (e.g., Wollenburg and Kuhnt, 2000; Horton and Edwards, 2006).

The reliability of these quantitative reconstructions mostly depends on the quality of the modern training set, used for regression purposes, and the robustness of the relationship between the microfossil assemblages and a selected parameter (Birks, 1995). Although high-resolution palaeoenvironmental reconstructions have been recently performed on the Holocene subsurface deposits of the Po Basin (e.g., Amorosi and others, 2005), the palaeo-bathymetric signature of benthic foraminiferal associations have not been quantified yet. Jorissen (1987) argued that the present depth distribution of benthic foraminifers in the shallowest portion of Adriatic basin (10-100 meters) depends on

nutrients and oxygen content more than bathymetry itself. Food availability, in particular, appeared to be the main abiotic factor influencing the composition and the interspecific diversity of benthic microfauna (Jorissen and others, 1992; Donnici and Serandrei Barbero, 2002). Thus, the water depth distribution of foraminiferal species varies from basin to basin (e.g., Culver and Buzas, 1980, 1981) but, even so, depth relatable patterns are well developed and relatively easily recognized. Hayward and others (1999) noted that depth zonations at inner to mid shelf depths are finer than those of outer shelf and upper bathyal and mid bathyal or deeper depths. Furthermore, quantitative approaches (e.g., Culver, 1988; Horton and others, 2007) can be used to delineate finer zonation schemes.

Modern nutrients and oxygen content, as well as salinity and turbidity values, of the Po Delta are related to the distance from the main fluvial outputs, and consequently to a well-defined bathymetrical zone of the gently sloping platform. This relationship should have existed from the middle Holocene, when the Po River influence became significant and the Adriatic anti-clockwise current system was plausibly established (Jorissen, 1988; Cattaneo and others, 2004). Thus, within this limited chronological interval (from about 8,000 cal yr BP to present) reliable palaeo-depth reconstructions can be obtained for an appropriate shallow-marine succession of the Po Delta area.

The specific aims of this paper are, therefore, to: develop a subtidal Northern Adriatic foraminiferal based-transfer function (NATF) using the most comprehensive modern dataset available for the study area (Jorissen, 1988); and calibrate the NATF using core sequences from the Po Delta area to reconstruct the Holocene palaeo-bathymetry in the Po Delta area.

STUDY AREA

The Adriatic Sea is a narrow epicontinental basin (ca. 200 x 800 km), orientated roughly NW/SE in the central Mediterranean Sea. In the northern section of the Adriatic basin (Northern Adriatic Sea), a gently sloping platform with a low topographic gradient (ca. 0.02 degrees; Cattaneo and others, 2004) and an average depth of 35 m (Jorissen, 1988; Morigi and others, 2005) is present (Fig. 1). Off San Benedetto del Tronto, water depth increases up to 270 m, which is the maximum value recorded within the Central Adriatic basin (Jorissen, 1988). The deepest conditions (1,225 m) are reached south of Gargano Promontory in the Southern Adriatic Sea. The Adriatic Sea is connected with the Ionian Sea by the Strait of Otranto (about 750 m water depth).

The microtidal regime of the Adriatic area is strongly wave-influenced (Cavaleri, 2000). The whole basin is affected by a cyclonic thermohaline circulation, with a pronounced seasonal variability. In this respect, three water masses are distinguished (Paschini and others, 1993): a surficial (0-30 m), a Levantine Intermediate Water-LIW (30-130 m) and a deep layer. The surficial anti-clockwise circulation pattern governs the distribution of fluvial products (sediments and nutrients) on the shelf. As a consequence, a long-shore southward drift affects the Italian margin of the Adriatic Sea and distributes the suspended load, supplied by the adriatic rivers, to remarkable distances respect the entry points. The interplay of river-discharge and surface-water currents induces the deposition of a fine-grained, organic-rich zone parallel to the coast (mud-belt) and located at ca. 20-40 m depth in the Northern Adriatic Sea (Van der Zwaan and Jorissen, 1991). The total amount of fluvial discharge varies through time in relation to the seasonal cycles and

climatic changes. About one third of the total river runoff is supplied by the Po River and its tributaries (Kourafalou, 1999; Correggiari and others, 2005) through the Po Delta system (ca. 730 km²), located in the northern section of the Adriatic basin (Cencini, 1998) (Fig. 1).

The development of Po Delta system took place after the peak of Holocene marine transgression dated ca. 6,000 yr BP (middle Holocene), when the palaeoshoreline was located ca. 30 km landward respect is present position (Amorosi and Milli, 2001; Amorosi and Colalongo, 2005). At the beginning of Holocene age (ca. 10,000 yr BP) an abrupt eustatic rise led to the inundation of the wide alluvial plain developed in the study area during the last glacial period (Correggiari and others, 1996; Amorosi and others, 2003). Beneath the present Po Plain a vertical succession of paludal, lagoonal and marine deposits recorded the rapid sea-level rise that affected the study area up to ca. 6,000 yr BP (Amorosi and others, 2003, 2004). On the other hand, the recent documentation of a millennial-scale parasequence architecture in the subsurface deposits of SE Po Plain (Amorosi and others, 2005) indicates that a step-like sea-level rising trend occurred during the transgressive and the subsequent regressive period.

As a whole, the rate of sea level rise slowed down around 6,000 cal yr BP (Preti 1999; Lambeck and others, 2004), allowing the development of Po Delta system. During the relatively stable sea-level conditions, that characterized the highstand period, subsidence mainly supported the accumulation of coastal-deltaic sediments in the study area (Amorosi and others, 2004, submitted; Stefani and Vincenzi, 2005).

Owing to the interplay of climate and anthropic alteration, Po Delta system experienced a complex palaeogeographic and depositional evolution, reaching the present-day

configuration (Modern Po Delta) just ca. 350 years ago after the Porto Viro cut, operated by Venice Republic to preserve Venice Lagoon (Correggiari and others, 2005).

At present, the Modern Po Delta is a wave-dominated system evolving to a more cusped morphology during the last few decades (Del Cin, 1983), due to the decrease in sediment supply induced by several human regulations on the fluvial course.

RESEARCH APPROACH

The transfer function is a statistical technique developed by Imbrie and Kipp (1971), and extensively adopted in many areas of palaeoecology to produce quantitative palaeoenvironmental data (e.g., Jones and Juggins, 1995; Gasse and others, 1995; Gehrels and others, 2000; Charman, 2001; Edwards and others, 2004; Sawai and others, 2004). In order to assess the performance of this technique for subtidal foraminifera, a standard approach was followed (Birks, 1995). Firstly, the relationship between modern "training sets" of water depth and foraminiferal taxa from the Northern Adriatic shelf were empirically modeled to derive "ecological response functions". This is achieved by regression, expressing the foraminiferal data as a function of water depth. Secondly, the fossil foraminiferal assemblages from sediment samples are "calibrated" to produce estimates of paleo-water depth by applying the ecological response functions.

Modern database

The modern database created for the Adriatic Sea by Jorissen (1987, 1988) satisfies all the major assumptions required for quantitative palaeoenvironmental reconstructions (Imbrie and Kipp, 1971; Imbrie and Webb, 1981; Birks and others, 1990; Birks, 1995).

The foraminiferal dataset is composed of 285 grab samples and piston-core tops collected from the Gulf of Venice to the Strait of Otranto. Four environmental parameters were measured (water depth, percentage of organic matter, calcium carbonate and sand fraction) at each sampling site. Water depth was calculated by integrating the bathymetric map edited by Debrazzi and Segre (1960) for the Central Mediterranean Sea and the acoustic data recorded during the oceanographic cruise (Pigorini, 1967). Unfortunately no further information, such as the estimation of the error range, are available in literature.

We selected a subset of samples from the Northern Adriatic area (north of Conero Promontory, Ancona) for statistical analyses. This consisted of 112 samples (Fig. 1) and 45 most common taxa including species and upper taxonomic group at genera level. All samples prepared for foraminiferal analyses were washed through sieves of 63, 150 and 595 μm , but only the 150 μm fraction was counted (Jorissen, 1987, 1988). For each sample more than 250 specimens were counted. The agglutinated taxa, *Eggerella scabra* and *Reophax* spp., which are usually not preserved in fossil deposits due to the fragility of test were not included in the dataset. Furthermore, there was no distinction between live and dead foraminifera (Jorissen, 1987, 1988).

Fossil database: Core 1

A 40-metres long core (Core 1) was extruded using a wire-line perforation, which guaranteed an optimal percentage of recovery (more than 90%) and an undisturbed stratigraphic succession. Core 1 was located close to the modern Po Delta coastline (Fig. 1) and contained a thick and continuous record of shallow-marine clays containing a very rich microfauna (Fig. 2). A detailed description and interpretation of Core 1 facies associations have been recently carried out by Amorosi and others (submitted). Core elevation (1.8 m below mean sea level) was interpolated using three benchmarks reported in the topographic map (1:25,000) of Po Delta area.

We collected a total of 124 samples along the core length and prepared following standard methodology. Each sample was dried at 60 °C, washed with H₂O and H₂O₂ (35% vol.) through sieves of 63 µm (240-mesh) and dried again. The fraction greater than 125 µm was analyzed for the micropalaeontological content and a minimum count of 300 specimens of benthic foraminifers was performed. Unfortunately, 33 samples collected within the marine clays produced low counts, relating to the prodelta succession that can cause highly stressed conditions because of strong fluvial influences. Moreover, 10 samples collected within the upper 4 meters of prodelta deposits (proximal prodelta) were barren, as consequence of the excessive fluvial discharge due to the proximity of river mouths (see Fig. 2). Thus, 31 samples containing a marine countable microfauna, with 34 different taxa, form the fossil database that was processed for statistical analyses. Minor taxa (less than 2%) were excluded from the fossil dataset. Furthermore, several species were grouped together on the basis of their taxonomy and main ecological characteristics,

in order to make the two data sets more comparable. The taxonomic identification and ecological information regarding benthic foraminifers were mainly based on Jorissen publications (Jorissen, 1987, 1988). Further information were obtained from other specific papers, as Albani and Serandrei Barbero (1990), Cimerman and Langer (1991), Sgarrella and Moncharmont Zei (1993), Fiorini and Vaiani (2001) and Donnici and Serandrei Barbero (2002).

The chronological framework of Core 1 was provided by six radiocarbon ages (Table 1), performed by CEDAD laboratory (University of Lecce, Italy). Carbon-rich samples (peat, organic-rich clay, well-preserved shells of mollusk) were collected at specific stratigraphic levels, to temporally constrain the main sedimentological and microfossil facies associations. AMS measured ^{14}C activity of each sample was corrected for isotopic fractionation ($\delta^{13}\text{C}$ correction), before the conversion to ^{14}C age. Conventional ages, in sensu Stuiver and Polach (1977), were converted in calibrated ages, using software OxCal Ver. 3.10 based on the new dataset provided by Reimer et al. (2004). For the calculation of ages of mollusk shells, the Northern Adriatic marine reservoir correction, reported in literature ($\Delta R = -61 \pm 50$), was regarded. In text all ages are reported as calibrated year BP (cal yr BP).

Transfer function development

We developed foraminifera-based transfer functions using two specific programs, CANOCO for Windows 4.5 (ter Braak and Šmilauer, 2002) and C2 version 1.4.3 (Juggins, 2006). The ecological response of modern foraminifera to water depth was

modeled using detrended canonical correspondence analysis (DCCA), which estimates the length of variation of biological data. The gradient length of Northern Adriatic taxa was more than 2 standard deviation-SD (2.972), indicating a Gaussian unimodal distribution characterized by an optimum value and a tolerance range (Birks, 1995). We used weighted averaging partial least squares-WA-PLS regression to develop the subtidal transfer function, because it usually ensures the strongest relationship between biological data and the environmental parameter. WA-PLS takes into account any residual correlation not explained by the variable of interest (ter Braak and Juggins, 1993; ter Braak and others, 1993).

The performance of the screened transfer function (NATF) was provided by the Root Mean Square Error of Prediction (RMSEP) and the coefficient of determination (r^2), which are representative of the predictive abilities of the function and the strength of the relationship between observed and inferred values, respectively. Both parameters were calculated as "apparent", using the whole training set to generate the transfer function, and as "jack-knifing" (RMSEP_{jack} and r^2 _{jack}). Jack-knifing or leave-one-out cross validation method operates leaving out one sample in turn that is used to evaluate the prediction error and provide the overall predictive ability of the model. During the calibration process a statistical evaluation of the sample-specific error of prediction was quantified using the bootstrapping cross validation (1,000 cycles).

We used the modern analogue technique (MAT) to test the robustness of the paleo-water depth reconstructions. MAT identifies core samples that have a "good analogue" in the modern training set by means of the measure of dissimilarity between fossil and modern assemblages. We used the largest dissimilarity coefficient of the modern dataset as the

critical threshold to identify fossil samples with a "good modern analogue" (Woodroffe, 2006).

THE MODERN DATABASE AND THE ECOLOGICAL RESPONSE FUNCTIONS OF NORTHERN ADRIATIC

In the Adriatic Sea the general distribution pattern of benthic foraminifers was extensively studied by Jorissen (1987, 1988), revealing the presence of a bathymetric zonation roughly parallel to the Italian coast, especially in the Northern part of the basin. Jorissen (1987, 1988) performed statistical analyses (principal components analysis-PCA and R-mode cluster analysis) on the relative abundances of the 50 most abundant taxa, found within the modern samples of the Adriatic Sea.

Four biofacial units (Biofacial units I-IV), recognized on the basis of PCA analysis, reflect four different bathymetric zones. Indeed, the first two principal components show a strong correlation with the parameter water depth, whereas the third component seems to be correlated with sedimentological characteristics, as calcium carbonate content, which co-varies with the grain size, and organic matter percentage.

The Northern Adriatic area contains Biofacial units II, III and IV, whereas Biofacial I reflects deeper conditions (50-1,225 m) reached within the central and southern basin. Biofacial unit II (characterized by high amounts of *Ammonia*, *Elphidium*, *Nonion depressulum* and few species of Miliolids) occupies the nearshore zone (7.5-25 m) parallel to the Italian coast and characterized by remarkable organic content. Very high

percentages of calcium carbonate and nutrients deficiency characterize all the samples collected from the sandy platform (20-100 m) and composing Biofacial unit III (containing several ephyphitic taxa, as *Neocorbina terquemi*, *Rosalina brady*, *Asterigerinata mamilla*, *Elphidium crispum* and *Textularia* species). Finally, Biofacial unit IV (*Nonionella turgida*, *Bulimina marginata* and *Valvulineria bradyana*) represents the foraminiferal assemblage of the modern adriatic mud-belt (20-100 m), where fluvial runoff products (fine-grained particles and nutrients) are accumulated by surficial currents. In this high-stressed area, ample food availability and low oxygen concentration are the main limiting factors for benthic microfauna.

R-mode cluster analysis shows minor variations within the Biofacial units, reflecting subtle environmental gradients.

Based upon this qualitative relationship between bathymetry and general foraminiferal distribution in the Northern Adriatic Sea, we developed a WA-PLS foraminiferal transfer function. The WA-PLS transfer function produced results for five components. The choice of component depended upon the prediction statistics: RMSEP and r^2 . We chose component two for the transfer function because it performed significantly better than component one when jack-knifed errors were considered; prediction errors (RMSEP) were lower, and squared correlations (r^2) were higher (Table 2). To increase the predictive ability of transfer function we screened the modern samples. Jones and Juggins (1995) attested the necessity to exclude all samples characterized by an "observed minus predicted" value (residual) greater than the standard deviation of physical training set. Thus two samples (labeled 334 and 324 in Jorissen, 1988) were eliminated. This selection is justified by the anomalous relative percentages of nearshore taxa, which may be

considered as evidence of reworking within samples collected at depth > 60 m. Moreover, we excluded a rare taxon (*Sphaeroidina bulloides*) with an unreliable species coefficient (negative optimum water depth). Using component two, the relationship between observed and subtidal foraminiferal-predicted water depth was very strong (Fig. 3), a result that illustrated the robust performance of the WA-PLS transfer function ($r^2_{\text{jack}} = \text{ca. } 0.95$). These results indicated that reconstructions of former sea levels are possible ($\text{RMSEP}_{\text{jack}} = \text{ca. } 5.14 \text{ m}$).

CALIBRATION OF NORTHERN ADRIATIC TRANSFER FUNCTION TO CORE 1

Abundant benthic foraminifers were preserved within the shallow-marine deposits between ca. 15 and 29 m core depth, where three different foraminiferal assemblages (M, P and C; see Figs. 2 and 4) were distinguished. The lower stratigraphic interval (29-26.8 m) was mainly characterized by relatively high percentages of Miliolidae (18-41%), as *Adelosina*; *Miliolinella* and *Quinqueloculina*, hyaline epiphytic taxa (ca. 6.7-27%), mainly including *Asterigerinata mamilla*, *Neocorbina terquemi* and *Rosalina brady*, and *Elphidium* spp. (2.8-7.0%) (Fig. 2). Two samples collected between 28-27 m showed a different foraminiferal association (Association P in Fig. 2), containing high amounts of *Valvulineria perlucida* (listed as *Ammonia perlucida* in Jorissen, 1988).

At ca. 26.80 m the open-marine Association M was replaced by a fluvio-influenced microfauna (Association P), mainly composed of *Ammonia tepida*, *A. parkinsoniana*,

Valvulineria perlucida and *Criboelphidium* spp. (mainly *C. granosum*). Throughout the whole core succession, the relative percentages of these species, typical of a prodelta environment (Donnici and Serandrei Barbero, 2002), had a maximum abundance of 99%, 48.6% and 44.3%, respectively (Fig. 2).

Between 25.10 and 20.50 m core depth a *Nonionella turgida* assemblage was found (Association C). High amounts of *Nonionella turgida* (27.5-74.6%), were encountered in association with relatively low abundances of *Ammonia tepida* and *A. parkinsoniana* (3.6-29.4%).

At 20.50 m Association C was abruptly replaced by an oligotypic microfauna (Association P) almost entirely composed of *Ammonia tepida* and *A. parkinsoniana*, that show relative abundances > 80%.

From 15.60 m core-depth scarce or no foraminifers were found within the clayey deposits. Upward delta front sands (11.2-7.3 m) containing a transported, and delta plain deposits, totally barren in microfossils, capped the core succession (Fig. 2).

We applied the Northern Adriatic Transfer Function (NATF) to the fossil samples containing a countable microfauna to provide palaeo-water depth data (Fig. 4 and Table 3). All maximum water depth values (ranging from 17.8 ± 5.3 m to 28.9 ± 5.6 m) were recorded within the inner shelf deposits, which contain the foraminiferal association M. However, two samples (at 27.80 and 27.60 m core depth) collected from the shelf succession indicated an abrupt decrease of palaeobathymetry (9.5 ± 5.3 m and 13.4 ± 5.3 m, respectively).

The first significant peak of *Ammonia tepida* and *A. parkinsoniana* (64.6%), encountered within Association P at 26.60 m, corresponded to a pronounced decrease in water depth

from 28.9 m to 11.6 m. Predicted water depth lower than 18.7 ± 5.3 m characterized the whole prodelta succession, reaching the lowest values (ranging from 10.4 ± 5.3 m to 7.6 ± 5.3 m) between 20.50-15.60 m core depth, where an oligotipic *Ammonia tepida* and *A. parkinsoniana* assemblage was recorded (Figs. 2 and 4).

Samples containing high percentages of *Nonionella turgida* (Association C) show minimal variations of palaeobathymetry respect to the underlying prodelta deposits (association P), and a slightly increase in water depth mean value is recorded (ca. 14.2 m versus 13.7 m).

DISCUSSION

The relationship existing between bathymetry and benthic foraminiferal distribution patterns is still a controversial issue. Some authors argued that benthic microfauna is usually not related to a specific water depth range but rather to other environmental factors, firstly nutrients and oxygen content (Van der Zwaan and others, 1999; De Rijk et al., 2000). Anyway, these abiotic factors usually result strictly correlated to the bathymetric gradient of each basin.

The main role exerted by parameter "water depth" on modern adriatic foraminiferal assemblages has been already evidenced by Jorissen (1987, 1988), who distinguished four principal biofacial units related to different ecological niches of the Adriatic platform (from 7.5 to about 200 m).

The development of NATF confirms the strong correlation between general distribution of benthic foraminifers and bathymetry in the Northern Adriatic Sea. This inference is supported by other researchers, such as Natland (1933) and Bandy and Chierici (1966). They showed that the distribution of subtidal foraminifera could be related to bathymetry. However, biotic and abiotic environmental factors that control the distribution of foraminifera vary with depth, thus depth is simply a factor, along with latitude and longitude, in locating a sample in three-dimensional space (e.g. Buzas, 1974; Boltovskoy and Wright, 1976; Sen Gupta, 1977; Murray, 1991, 2001; Hayward and others, 1999, 2006; Morigi and others, 2005; Horton and others, 2007).

Calibration of NATF to Core 1 has produced reliable and accurate water depth data for a significant part of marine succession, contributing to the reconstruction of Po Delta bathymetric evolution during the last ca. 5,500 cal yr BP (Fig. 4).

To temporally constrain the palaeo-bathymetric oscillations, recorded by foraminiferal assemblages of Core 1, three age-depth models were used. Taking into account the variability of sedimentation rates suggested by radiocarbon datings (Table 1), inner shelf (29-26.80 m), lower prodelta (26.80-25.70 m) and upper prodelta (25.70-15.60 m) successions were separately treated. Within each stratigraphic interval sample ages were linearly extrapolated. However, such linear extrapolation doesn't consider minor variations in sediment supply, that probably occurred during the whole prodelta sedimentation.

Late Quaternary deposits of Core 1 were dominated by a transgressive-regressive depositional cycle (Figs. 2 and 4). The beginning of the Holocene transgression (dated to 10,200-9,550 cal yr BP) was marked by an abrupt superposition around 34 m core depth

of back-swamp clays, on alluvial deposits formed during the last glacial period (Amorosi and others, submitted). Upcore, transgressive barrier sands, rich in mollusk shells and transported foraminifera (mainly *Ammonia beccarii* and *Elphidium* spp.), documented a rapid landward migration of facies, with the onset of a marine transgression around 6,000 cal yr BP in the study area.

The continuing sea-level rise led to the deposition of marine clays containing a typical infralittoral microfauna (Association M). Such foraminiferal assemblage suggested the establishment of an inner-shelf environment with minor fluvial influence and a flourished vegetation cover at the sea bottom (Donnici and Serandrei Barbero, 2002). These deposits furnished water depth values ranging from about 29 to 18 m, suggesting that the peak of Holocene transgression took place between ca. 5,500-4,000 cal yr BP (Fig. 4) in the Po Delta area.

The abrupt decrease of palaeobathymetry recorded by two samples collected at 27.80 and 27.60 m within the inner shelf succession indicated a minor palaeoenvironmental change that induced the momentary establishment of shallower water depth conditions. The remarkable abundance of *Valvulineria perlucida* (Association P), a species commonly found in river-influenced environments characterized by large inputs of nutrients (Jorissen, 1988; Donnici and Serandrei Barbero, 2002), suggested an increase in fluvial influence, that preceded the onset of Po prodelta around 4,000 cal yr BP. This may be related to a local, autocyclic event, such as delta lobe switching, caused by unstable deltaic sedimentation during the earliest stages of progradation (Stefani and Vincenzi, 2005).

A prompt shift toward stable shallower conditions (less than 18 m) characterized prodelta deposits (26.80-15.60 m core depth). Samples containing Association P suggested low salinity and organic-rich conditions, characteristic of prodelta settings strongly influenced by fluvial discharge. At present a comparable microfauna (*Ammonia* and *Criboelphidium* assemblage) is commonly found in several deltaic systems at 10-22 meters of water depth (Jorissen, 1988; Murray, 1991; Hayward and others, 1999; Donnici and Serandrei Barbero, 2002).

On the other hand, Association C dominated by the opportunistic species *Nonionella turgida* is similar to that observed by Van der Zwaan and Jorissen (1991) in correspondence of the western flank of Po modern mud-belt, where finer fluvial products are concentrated by Adriatic long-shore currents. High nutrients content combined with seasonal low oxygen conditions favoured *Nonionella turgida*, that profited from such stressed conditions, and induced the substantial decrease of typical nearshore taxa (*Ammonia* and *Criboelphidium* species).

Although food availability and oxygen concentration seem to be the major factors controlling faunal changes within prodelta environment (Jorissen, 1987, 1988; Barmawidjaja and others, 1992), a slight increase in water depth distinguished Association C respect to Association P.

This subtle palaeobathymetric gradient is coherent with the onset of mud-belt sedimentation dated to ca. 600 cal yr ago (Fig. 4) at the core site. Po mud-belt formation was enhanced by a major natural avulsion, known as Rotta di Ficarolo (800 cal yr BP from Correggiari and others, 2005), that shifted northward, far from the core site, the active Po River branches, favoring the accumulation of Po River runoff products (finer

particles and nutrients) and the abandonment of all the delta lobes located in the southern portion of Delta, where Core 1 was performed.

Around 500 cal yr BP mud-belt sedimentation stopped, due to the progressive approaching of Po River mouths, and a typical fluvio-influenced microfauna (Association P) replaced *Nonionella turgida*-assemblage at ca. 20.50 m core depth.

The very high percentages of *Ammonia tepida* and *A. parkinsoniana* recorded within the upper prodelta succession (20.50-15.60 m core depth) are suggestive of a nearshore hypohaline setting subject to frequent freshwater outflows (Jorissen, 1988; Bellotti and others, 1994). Reasonably, the progressive approaching of fluvial mouths have induced shallower conditions typical of a proximal prodelta environment, as confirmed by our paleobathymetric reconstruction (palaeo-water depth data minor than 10 m), according to a typical progradational trend.

Moreover, the reliability of Core 1 palaeo-bathymetric curve, that is coherent with the relative sea level trend reported for the Northern Adriatic area by Lambeck and others (2004), is statistically confirmed by the examination of MAT results. Using Squared Euclidean distance as dissimilarity coefficient, 29 fossil samples from a total of 31 possess a modern analogue (Table 3). The exceptions are samples collected at 27.80 m and 20.65 m within the inner shelf and mud belt succession, respectively. The former contains a foraminiferal association dominated by *Valvulineria perlucida* (ca. 48.6%), with remarkable percentages of Miliolids (mainly *Quinqueloculina seminulum*) and *Criboelphidium granosum* (Association P). The latter is almost entirely composed of *Nonionella turgida* (ca. 74.7%), with low abundances of *Ammonia tepida* and *A. parkinsoniana* (Association C). In contrast the modern database does not include these

species with such elevated abundances (maximum 16.60% for *Valvulineria perlucida* and 42.3% for *Nonionella turgida*). Thus, the palaeo-water depth data estimated for samples 27.80 and 20.65 should be treated with caution. (Fig. 4).

CONCLUSIONS

The development of WA-PLS foraminiferal-based transfer functions, based upon a selected subset of the modern adriatic database created by Jorissen (1988), evidenced that benthic foraminifer distribution and bathymetry are highly correlated in the Northern Adriatic basin. The robust performance of NATF (Northern Adriatic Transfer Function) is guaranteed by the strong relationship existing between observed and subtidal foraminiferal-predicted water depths ($r^2_{\text{jack}} = 0.95$) and the possibility of accurate palaeo-bathymetric reconstructions (RMSEP = 5.14 m).

The application of NATF to a suitable fossil marine succession (Core 1), recovered from the southern portion of Modern Po Delta, furnished 31 reliable paleo-water depth data chronologically constrained between ca. 5,500-500 cal yr BP. The reliability of these data is statistically confirmed by the examination of MAT results. They evidenced that 29 samples from a total of 31 possess a good modern analogue.

These results contributed to the reconstruction of the recent paleo-bathymetric and palaeoenvironmental evolution of Po Delta area. The highest water depth values (ranging from 17.8 ± 5.3 m to 28.9 ± 5.6 m) were obtained from the transgressive-early regressive

inner shelf deposits, recorded at the bottom of the marine succession. These data suggested that the peak of transgression took place between ca. 5,500-4,000 cal yr BP. Shallower water conditions (less than 18 m) characterized the thick prodelta succession, formed during the recent development of Po Delta system (ca. 4,000-500 cal yr BP). An abrupt decrease in palaeobathymetry, from 28.9 m to 11.6 m, was recorded at the passage to prodelta clays, while the lowest water depth values (ranging from 10 to 7.5 m) characterized the uppermost deposits, according to a typical shallowing-upward, progradational trend.

Furthermore, NATF application evidenced the occurrence of high-frequency and subtle palaeobathymetric oscillations during the early and late regressive period. Two samples collected within the inner shelf succession indicated that an abrupt decrease in water depth (ca. 10 m) took place around 4,500 cal yr BP, maybe induced by autocyclic factors, as delta lobe switching. On the contrary, a slight increase of palaeobathymetry generally characterized mud-belt deposits, dated ca. 600-500 cal yr BP.

However, caution should be used with our predicted data, considering the different source of modern and fossil dataset and the possible influence on foraminiferal assemblages of post-depositional processes, as transport of tests.

Despite that, the results presented in this paper suggested that subtidal foraminiferal-based transfer functions can represent an useful tool to provide reliable and high-resolution palaeobathymetric data from subsurface deposits of modern deltaic systems.

Figure and table captions

Figure 1. Bathymetric map of the Northern Adriatic Sea with the location of modern samples (black dots) (from Jorissen, 1988). Core 1 site is also indicated.

Figure 2. Foraminiferal associations and relative frequencies of the most common taxa from Core 1. TS: Transgressive surface, RS: Ravinement surface, MFS: Maximum Flooding Surface (stratigraphy after Amorosi and others, submitted). Calibrated radiocarbon ages are also reported.

Figure 3. (a) Scatter plot showing the relationship between Observed water depth and Predicted water depth and (b) residuals versus Observed water depth, using WA-PLS transfer function (component 2).

Figure 4. Estimated palaeo-water depth values for Core 1. Samples without a good modern analogue are shown as empty squares. Gray area represents the error range of estimation (sample-specific error).

Table 1. Radiocarbon dating for Core 1 (conventional and calibrated ages).

Table 2. Statistics components of WA-PLS transfer functions. The shaded row corresponds to component 2, selected for calibration purposes (Northern Adriatic Transfer Function-NATF).

Table 3. Summary of palaeo-water depth predictions and sample-specific errors, generated by NATF for 31 samples of Core 1. For each sample foraminiferal association (F.A.) and fossil dissimilarity coefficient (Min. DC) are reported. The critical threshold used to distinguish samples without a good modern analogue is the largest dissimilarity coefficient obtained from the modern dataset (1088.28). Core samples without a modern analogue are highlighted in gray.

REFERENCES

Albani, A., and Serandrei Barbero, R., 1990, I Foraminiferi della Laguna e del Golfo di Venezia: *Memorie di Scienze Geologiche Padova*, v. 42, p. 271–341.

Amorosi, A., Colalongo, M. L., 2005, The linkage between alluvial and coeval nearshore marine successions: evidence from the Late Quaternary record of the Po River Plain, Italy, *in*: Blum, M. D., Marriott, S. B. and Leclair, S. F. (eds.), *Fluvial Sedimentology VII*, International Association of Sedimentologists Special Publication, vol. 35, p. 257–275.

———, and Milli, S., 2001, Late Quaternary depositional architecture of Po and Tevere river deltas (Italy) and worldwide comparison with coeval deltaic successions: *Sedimentary Geology*, v. 144, p. 357–375.

Amorosi, A., Centineo, M. C., Colalongo, M. L., Pasini, G., Sarti, G., and Vaiani, S. C., 2003, Facies architecture and Latest Pleistocene-Holocene depositional history of the Po Delta (Comacchio area). Italy: *The Journal of Geology*, v. 111, p. 39–56.

———, Centineo, M. C., Colalongo, M. L., and Fiorini, F., 2005, Millennial-scale depositional cycles from the Holocene of the Po Plain, Italy: *Marine Geology*, v. 222–223, p. 7–18.

——, Colalongo, M. L., Fiorini, F., Fusco, F., Pasini, G., Vaiani, S. C., and Sarti, G., 2004, Palaeogeographic and palaeoclimatic evolution of the Po Plain from 150-ky core records: *Global and Planetary Change*, v. 40, p. 55–78.

——, Dinelli, E., Rossi, V., Vaiani, S. C., and Sacchetto, M., submitted, Late Quaternary palaeoenvironmental evolution of the Adriatic coastal plain and the onset of Po River Delta: *Palaeogeography, Palaeoclimatology, Palaeoecology*.

Bandy, O. L., and Chierici, M. A., 1966, Depth–temperature evaluation of selected California and Mediterranean bathyal foraminifera: *Marine Geology*, v. 4, p. 259–271.

Barmawidjaja, D. M., Jorissen, F. J., Puskaric, S., and Van der Zwaan, G. J., 1992, Microhabitat selection by benthic foraminifera in the northern Adriatic Sea: *Journal Foraminiferal of Research*, v. 22, p. 297–317.

Bellotti, P., Caputo, C., Davoli, L., Evangelista, S., Garzanti, E., Pugliese, F., and Valeri, P., 2004, Morpho-sedimentary characteristics and Holocene evolution of the emergent part of the Ombrone River delta (southern Tuscany): *Geomorphology*, v. 61, p. 71–90.

Bellotti, P., Carboni, M. G., Di Bella, L., Palagi, I., and Valeri, P., 1994, Benthic foraminiferal assemblages in the depositional sequence of the Tiber Delta: *Bollettino della Società Paleontologica Italiana, Special Volume 2*, p. 29–40.

Birks, H. J. B., 1995, Quantitative palaeoenvironmental reconstructions, *in* Maddy, D., and Brew, J. S. (eds.), *Statistical Modelling of Quaternary Science Data: Technical Guide No. 5*: Quaternary Research Association, Cambridge, p. 161–236.

———, Line, J. M., Juggins, S., Stevenson, A. C. and ter Braak, C. J. F., 1990: Diatoms and pH reconstruction: *Philosophical Transactions of the Royal Society of London*, v. 327, p. 263–278.

Boltovskoy, E., and Wright, R., 1976, *Recent Foraminifera*: Dr. W. Junk, Publishers, The Hague, 515 p.

Buzas, M. A., 1974, Vertical distribution of *Ammobaculites* in the Rhode River, Maryland: *Journal of Foraminiferal Research*, v. 4, p. 144–147.

Cattaneo, A., Trincardi, F., Langone, L., Asioli, A., and Puig, P., 2004, Cliniform generation on Mediterranean margins: *Oceanography*, v. 17, no. 4, p. 105-117.

Cavaliere, L., 2000, The oceanography tower *Acqua Alta*, activity and prediction of sea states at Venice: *Coastal Engineering*, v. 39, p. 29–70.

Cencini, C., 1998, Physical processes and human activities in the evolution of the Po delta, Italy: *Journal of Coastal Research*, v. 14, p. 774–793.

Charman, D. J., 2001, Biostratigraphic and palaeoenvironmental applications of testate amoebae: *Quaternary Science Reviews*, v. 20, p. 1753– 1764.

Cimerman, F., and Langer, M. R., 1991, *Mediterranean Foraminifera: Slovenian* Academy of Science and Arts and Swiss Academy of natural Sciences, Ljubljana, 118 p.

Correggiari, A., Cattaneo, A., and Trincardi, F., 2005, Depositional patterns in the Holocene Po Delta system, in Bhattacharya, J. P., Giosan, L. (eds.), *River Deltas: Concepts, Models and Examples*. SEPM Special Publication, v. 83, p. 365–392.

Correggiari, A., Roveri, M., and Trincardi, F., 1996, Late Pleistocene and Holocene evolution of the Northern Adriatic Sea: *Il Quaternario*, v. 9, p. 697–704.

Culver, S. J., 1988, New foraminiferal depth zonation of the Northwestern Gulf of Mexico: *Palaios*, v. 3, p. 69-86.

——, and Buzas, M. A., 1980, Distribution of recent benthic foraminifera off the North America Atlantic coast: *Smithsonian Contribution to the Marine Science*, no. 6, 512 p.

——, and Buzas M. A. 1981, Distribution of recent benthic foraminifera in the Gulf of Mexico: *Smithsonian Contribution to the Marine Science*, no. 8, 898 p.

Dal Cin, R., 1983, I litorali del delta del Po e alle foci dell'Adige e del Brenta: caratteri tesiturali e dipersione dei sedimenti, cause dell'arretramento e previsioni sull'evoluzione future: Società Geologica Italiana, Bollettino, v. 102, p. 9–56.

De Rijk, S., Jorissen, F.J., Rohling, E.J., and Troelstra, S.R., 2000, Organic flux on bathymetric zonation of Mediterranean benthic Foraminifera: *Marine Micropaleontology*, v. 40, p. 151–166.

Debrazzi, E., and Segre, A. G., 1960, Carta Batimetrica del Mediterraneo Centrale: Mare Adriatico: Foglio n. 1253, Istituto Idrografico della Marina, Genova.

Donnici, S., and Serandrei Barbero, R., 2002, The benthic foraminiferal communities of the northern Adriatic continental shelf: *Marine Micropaleontology*, v. 44, p. 93–123.

Edwards, R. J., Wright, A. J., and Van De Plassche, O., 2004, Surface distributions of salt-marsh foraminifera from Connecticut, USA: modern analogues for high resolution sea-level studies: *Marine Micropaleontology*, v. 51, p. 1–21.

Fiorini, F., and Vaiani, S. C., 2001, Benthic foraminifers and transgressive-regressive cycles in the Late Quaternary subsurface sediments of the Po Plain near Ravenna (Northern Italy): *Bollettino della Società Paleontologica Italiana*, v. 40, p. 357–403.

Gasse, F., Juggins, S., and Khelifa, L. B., 1995, Diatom-based transfer functions for inferring past hydrochemical characteristics of African lakes: *Palaeogeography, Palaeoclimatology, Palaeoecology*, v. 117, p. 31–54.

Gehrels, W. R., 2000, Using foraminiferal transfer functions to produce high-resolution sea-level records from salt-marsh deposits. *Maine, USA: The Holocene*, v. 10, p. 367–376.

Hayward, B. W., Grenfell, H. R., Reid, C. M., and Hayward, K. A., 1999, Recent New Zealand shallow-water benthic foraminifera: taxonomy, ecologic distribution, biogeography, and use in paleoenvironmental assessment: *Institute of Geological and Nuclear Sciences Monograph*, v. 21, 258 p.

———, ——, Sabaa, A. T., Hayward C. M., and Neil, H. L., 2006, Ecological distribution of benthic foraminifera, offshore northeast New Zealand: *The Journal of Foraminiferal Research*, v. 36, p. 332–354

Horton, B. P., and Edwards, R. J., 2006, *Quantifying Holocene Sea Level Change Using Intertidal Foraminifera: Lessons from the British Isles*: Cushman Foundation for Foraminiferal Research, Special Publication no. 40, 97 p.

———, Culver, S. J., Hardbottle, M. I. J., Larcombe, P., Milne, G. A., Morigi, C., Whittaker, J. E., and Woodroffe, S. A., 2007, *Reconstructing Holocene sea-level change*

for the central great barrier reef (Australia) using subtidal foraminifera: *Journal of Foraminiferal Research*, v. 37, p. 327–343.

Imbrie, J., and Kipp, N., 1971, A new micropaleontological method for quantitative paleoclimatology: application to a late pleistocene caribbean core, in Turekian, K. K. (ed.), *The late Cenozoic glacial ages*. Yale University Press, New Haven, p. 71–181.

———, and Webb, T. III, 1981, Transfer functions: calibrating micropaleontological data in climatic terms, *in* Berger, A. (ed.), *Climatic variations and variability: facts and theories*. Dordrecht, D. Reidel, p. 125–134.

Jones, V. J., and Juggins, S., 1995, The construction of diatom-based chlorophyll transfer function and its application at three lakes on Signy Island (maritime Antarctic) subject to differing degrees of nutrient enrichment: *Freshwater Biology*, v. 34, p. 433–445.

Jorissen, F. J., 1987, The distribution of benthic foraminifera in the Adriatic Sea: *Marine Micropaleontology*, v. 12, p. 21–48.

Jorissen, F. J., 1988, Benthic foraminifera from the Adriatic Sea; principles of phenotypic variation: *Utrecht Micropaleontology Bulletins*, v. 37, 176 p.

Jorissen, F. J., Barmawidjaja, D. M., Puskaric, S., and Van der Zwaan, G. J., 1992, Vertical distribution of benthic foraminifera in the northern Adriatic Sea: the relation with the organic flux: *Marine Micropaleontology*, v. 19, p. 131–146.

Juggins, S., 2006, C2, Version 1.4.3: Newcastle University, UK, <http://www.campus.ncl.ac.uk/staff/Stephen.Juggins/index.html>.

Kourafalou, V. H., 1999, Processes studies on the Po River plume, North Adriatic Sea: *Journal of Geophysical Research*, v. 104, p. 29963–29985.

Lambeck, K., Antonioli, F., Purcell, A., and Silenzi S., 2004, Sea-level change along the Italian coast for the past 10,000 yr: *Quaternary Science Reviews*, v. 23, p. 1567–1598.

Leorri, E., and Cearreta, A., 2004, Holocene environmental development of the Bilbao estuary, northern Spain: sequence stratigraphy and foraminiferal interpretation: *Marine Micropaleontology*, v. 51, p. 75– 94.

———, Martin, R., and McLaughlin, P., 2006, Holocene environmental and parasequence development of the St. Jones Estuary, Delaware (USA): Foraminiferal proxies of natural climatic and anthropogenic change: *Palaeogeography, Palaeoclimatology, Palaeoecology*, v. 241, no. 3-4, p. 590-607.

Morigi, C., Jorissen, F. J., Fraticelli, S., Horton, B. P., Principi, M., Sabbatici, A., Capotondi, L., Curzi, P. V., and Negri, A., 2005, Benthic foraminiferal evidence for the formation of the Holocene mud-belt and bathymetrical evolution in the central Adriatic Sea: *Marine Micropaleontology*, v. 57, p. 25–49.

Murray, J. W., 1991, *Ecology and Palaeoecology of Benthic Foraminifera*: Longman Scientific and Technical, Harlow, England, 397 p.

——, 2001, The niche of benthic foraminifera, critical thresholds and proxies: *Marine Micropaleontology*, v. 41, p. 1–7.

Natland, M. L., 1933, The temperature and depth distribution of some Recent and fossil foraminifera in the southern California region: *Bulletin of the Scripps Institute of Oceanography, Technical Series*, v. 3, p. 225–230.

Paschini, E., Artegiani, A., and Pinardi, N., 1993, The mesoscale eddy field of the middle Adriatic during fall 1988: *Deep-Sea Research I*, v. 40, p. 1365–1377.

Pigorini, B., 1967, Aspetti sedimentologici del Mare Adriatico: *Memorie della Società Italiana di Scienze Naturali e del Museo Civico di Storia Naturale di Milano*, v. 16, no. 3, p. 131–199.

Preti, M., 1999, The Holocene transgression and the land-sea interaction south of the Po delta: *Giornale di Geologia*, v. 61, p. 143–159.

Reimer, P. J., Baillie, M. G. L., Bard, E., Bayliss, A., Beck, J. W., Bertrand, C. J. H., Blackwell, P. G., Buck, C. E., Burr, G. S., Cutler, K. B., Damon, P. E., Edwards, R. L., Fairbanks, R. G., Friedrich, M., Guilderson, T. P., Hogg, A. G., Hughen, K. A., Kromer, B., McCormac, F. G., Manning, S. W., Ramsey, C. B., Reimer, R. W., Remmele, S., Southon, J. R., Stuiver, M., Talamo, S., Taylor, F. W., van der Plicht, J., and Weyhenmeyer, C. E., 2004, IntCal04 Terrestrial radiocarbon age calibration: *Radiocarbon*, v. 46, p. 1029–1058.

Sawai, Y., Nagumo, T., and Horton, B. P., 2004, Diatom-based elevation transfer function along the Pacific coast of eastern Hokkaido, northern Japan — an aid in paleo-seismic study along the coasts near Kurile subduction zone: *Journal of Quaternary Science*, v. 23, p. 2467–2484.

Sen Gupta, B. K., 1977, Depth-distribution of modern benthic foraminifera on continental shelves of the world ocean: *Indian Journal of Earth Science*, v. 4, p. 60–83.

Serandrei Barbero, R., Albani, A. D., and Bonari, M., 2004, Ancient and modern salt marshes in the Lagoon of Venice: *Palaeogeography, Palaeoclimatology, Palaeoecology*, v. 202, no. 3-4, p. 229–244.

Sgarrella, F., and Moncharmont Zei, M., 1993, Benthic Foraminifera of the Gulf of Naples (Italy): systematics and autoecology: *Bollettino Società Paleontologica Italiana*, v. 32, p. 145–264.

Stefani, M., and Vincenzi, S., 2005, The interplay of eustasy, climate and human activity in the late Quaternary depositional evolution and sedimentary architecture of the Po Delta system: *Marine Geology*, v. 222–223, p. 19–48.

Stuiver, M., and Polach, H. A., 1977, Discussion: Reporting of ^{14}C data: *Radiocarbon*, v. 19, p. 355–363.

ter Braak, C. J. F., and Juggins, S., 1993, Weighted averaging partial least squares regression (WA-PLS): an improved method for reconstructing environmental variables from species assemblages: *Hydrobiologia*, v. 269/270, p. 485–502.

———, and Šmilauer, P., 2002, *CANOCO Reference Manual and User's Guide to CANOCO for Windows: Software for Canonical Community Ordination*, Microcomputer Power, Ithaca, NY, Version 4.5.

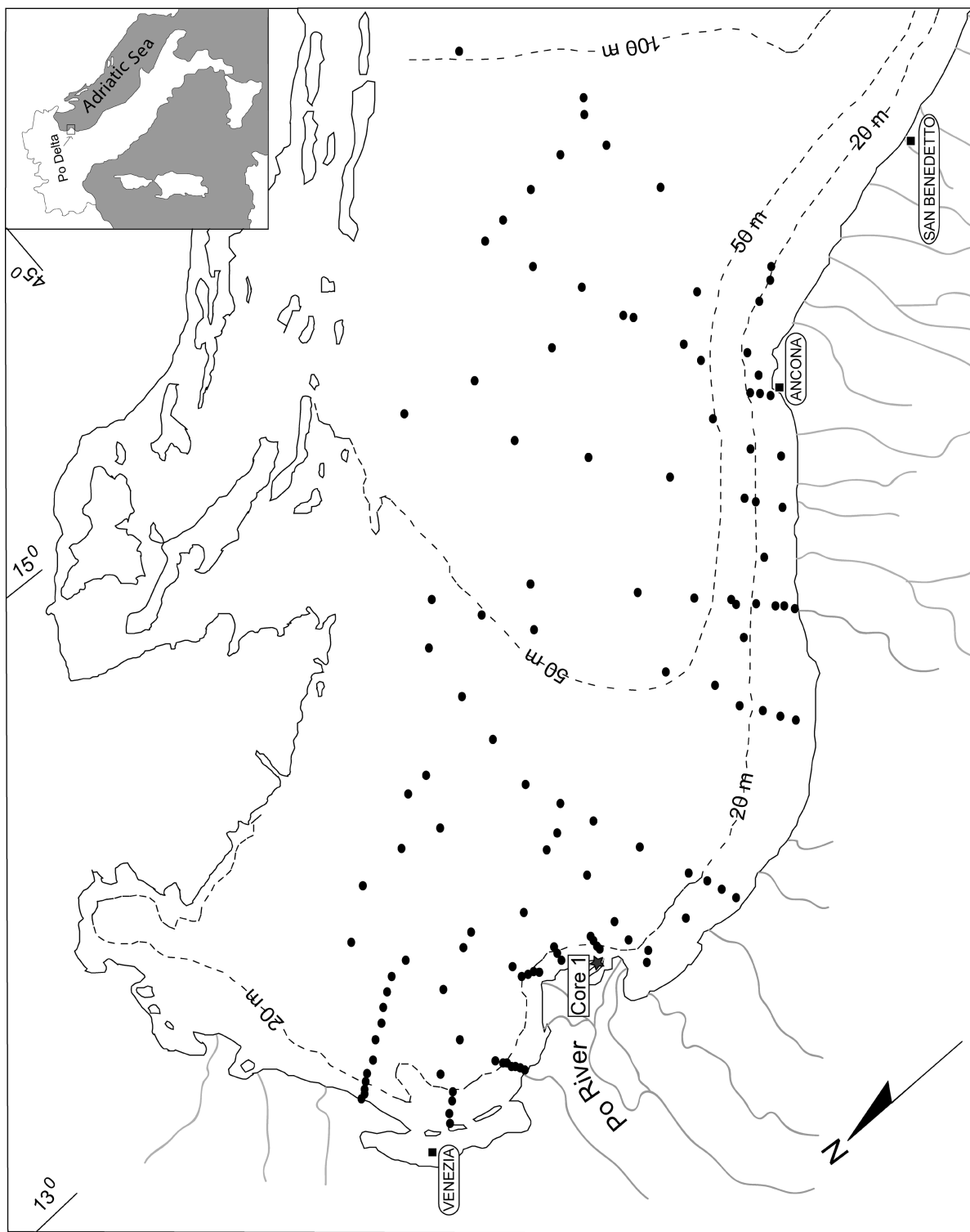
———, Juggins, S., Birks, H. J. B. and van der Voet, H., 1993. Weighted averaging partial least squares regression (WA-PLS): definition and comparison with other methods for species-environment calibration, *in* Patil, G. P., Rao, C. R. (eds.), *Multivariate Environmental Statistics*. North Holland, Amsterdam, p. 529–560.

Van der Zwaan, G. J., and Jorissen, F. J., 1991, Biofacial patterns in river-induced shelf anoxia. *in* Tyson, R. V., Pearson, T. H. (eds.), *Modern and Ancient Continental Shelf Anoxia*. Geological Society, Special Publication 58, p. 65–82.

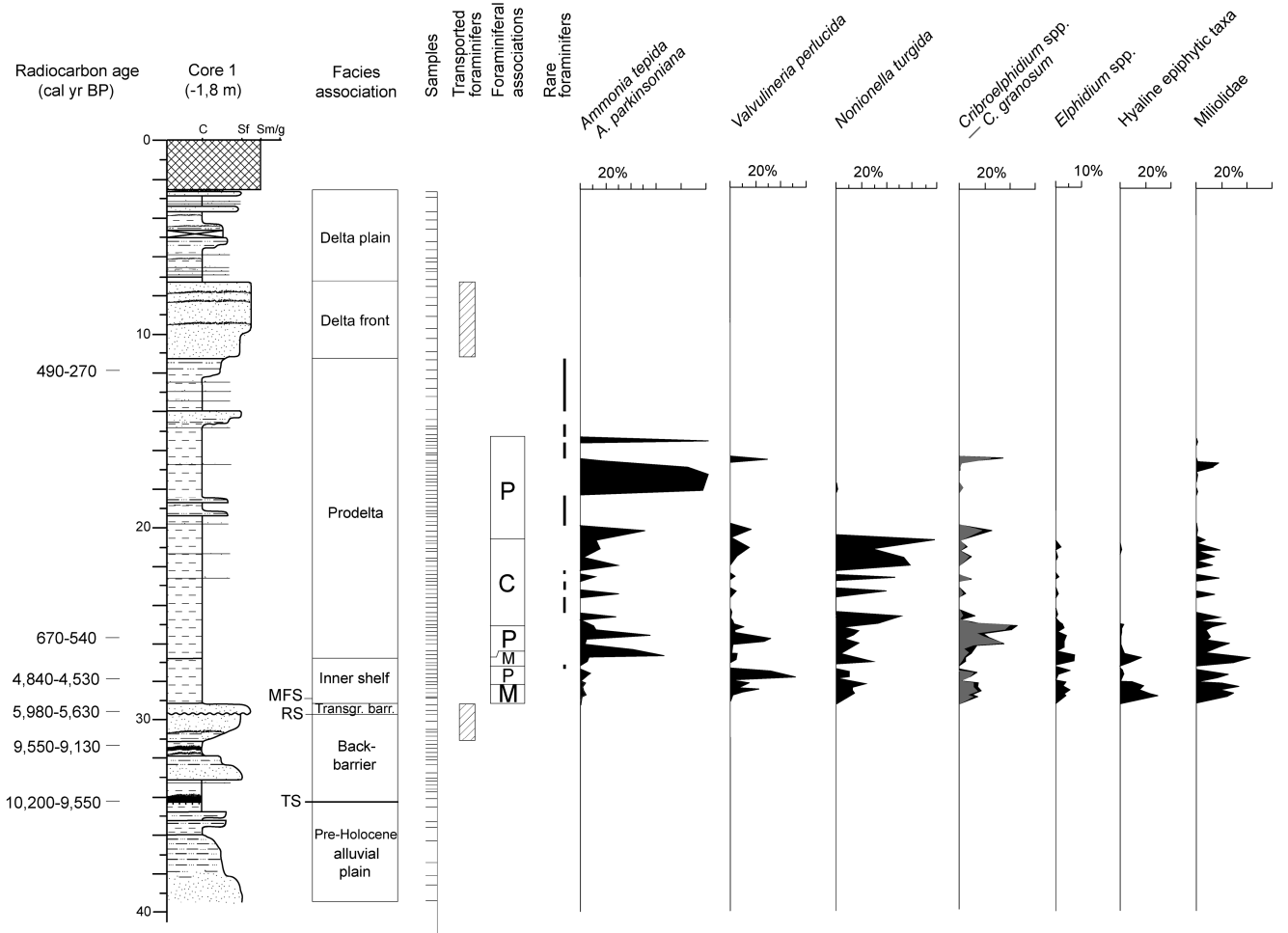
——, Duijnste, I. A. P., den Dulk, M., Ernst, S. R., Jannink, N. T., and Kouwenhoven, T. J., 1999, Benthic foraminifers: proxies or problems? A review of paleocological concepts: *Earth-Science Reviews*, v. 46, p. 213–36.

Wollenburg, J. E., and Kuhnt, W., 2000, The response of benthic foraminifers to carbon flux and primary production in the Arctic Ocean: *Marine Micropaleontology*, v. 40, no. 3, p. 189–231.

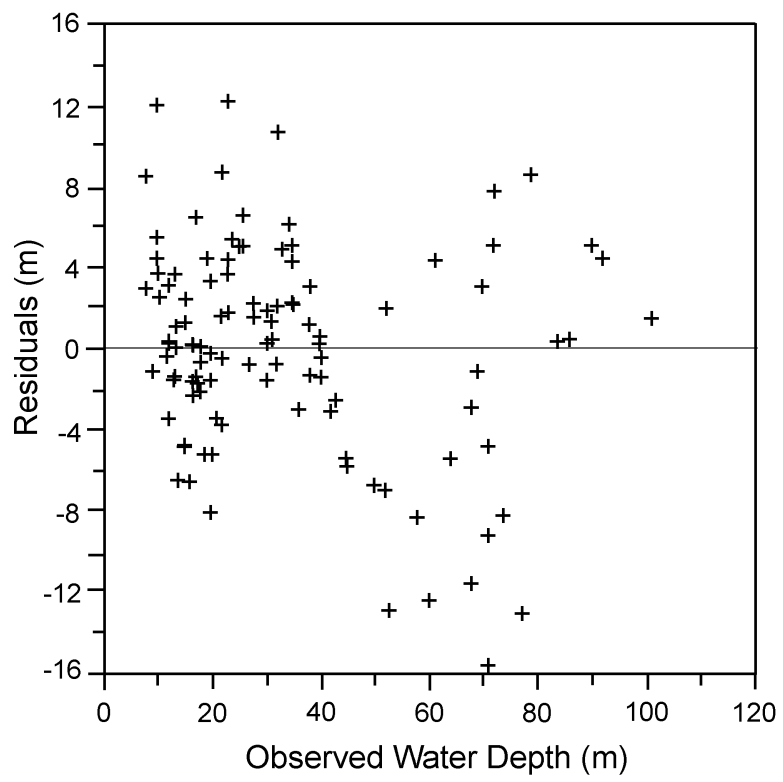
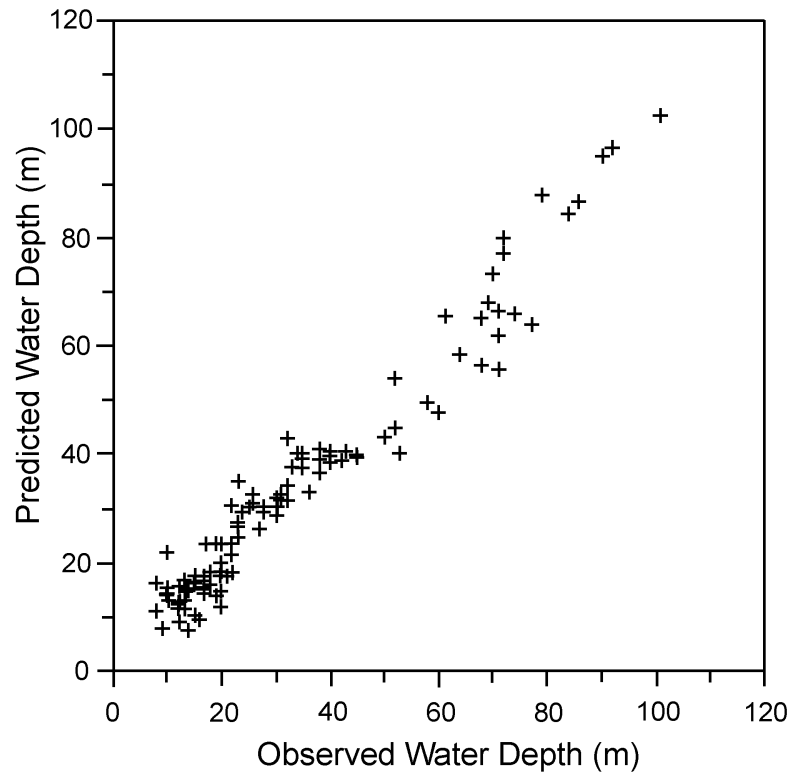
Woodroffe, S.A., 2006, Holocene relative sea-level changes in Cleveland Bay, North Queensland, Australia: Unpublished Ph.D. Thesis, University of Durham, Durham, UK, 155 p.



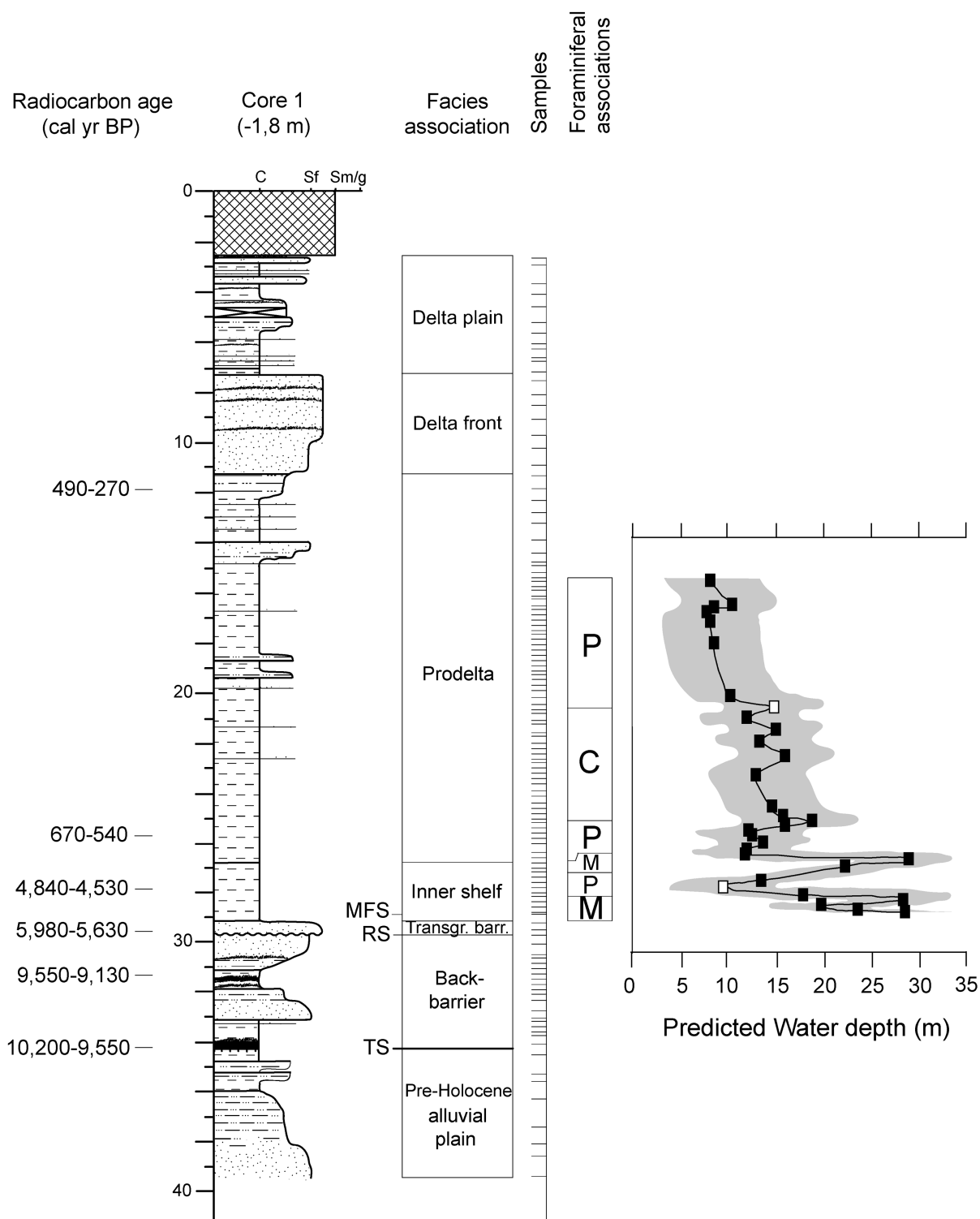
Rossi and Horton, Fig. 1



Rossi and Horton, Fig. 2



Rossi and Horton, Fig. 3



Rossi and Horton, Fig. 4

Sample core depth (m)	Conventional age (yr BP)	Calibrated age range (cal yr BP)		
		Max.	Mid.	Min.
11.80	273±50	490	380	270
25.70	622±50	670	605	540
27.80	4,165±55	4,840	4,685	4,530
29.50	5,383±55	5,980	5,805	5,630
31.35	8,404±100	9,550	9,340	9,130
34.16	8,797±100	10,200	9,875	9,550

Rossi and Horton, Table 1

Component	Apparent RMSE (m)	Apparent r^2	RMSEP_(jack) (m)	r^2_(jack)
1	7.03809	0.903143	7.38847	0.89337
2	4.74957	0.955875	5.1464	0.948206
3	4.10486	0.967047	4.64399	0.957827
4	3.63176	0.9742	4.30726	0.963712
5	3.21165	0.979824	4.08031	0.967447

Rossi and Horton, Table 2

Sample core depth (m)	F.A.	Estimated water depth (m)	Sample-specific error	Min. DC	Analogue
15.60	P	8.00086	5.4024	29.3764	good
16.55	P	10.384	5.31237	872.312	good
16.70	P	8.47961	5.33448	106.616	good
16.90	P	7.55633	5.34684	125.383	good
17.30	P	8.03171	5.40162	28.2873	good
18.10	P	8.42716	5.37362	11.3922	good
20.20	P	10.1447	5.21276	343.182	good
20.65	C	14.6947	5.57164	1772.18	no close
21.10	C	11.9411	5.28373	326.423	good
21.60	C	14.8658	5.4498	811.908	good
22.05	C	13.2807	5.40556	472.155	good
22.68	C	15.8539	5.38542	389.256	good
23.45	C	12.8346	5.29114	334.853	good
24.65	C	14.5795	5.34417	347.137	good
25.08	C	15.5921	5.27976	321.552	good
25.20	P	18.7218	5.28674	1067.53	good
25.40	P	15.8918	5.23333	1051.05	good
25.60	P	12.0891	5.20956	294.126	good
25.80	P	12.3474	5.29624	973.568	good
26.05	P	13.5844	5.27334	1044.9	good
26.40	P	11.9439	5.25244	381.699	good
26.60	P	11.619	5.27367	88.3179	good
26.80	M	28.8593	5.62941	521.212	good
27.05	M	22.2244	5.47153	458.02	good
27.60	P	13.362	5.27899	866.859	good
27.80	P	9.45914	5.39664	1828.19	no close
28.20	M	17.8358	5.26742	507.895	good
28.40	M	28.3841	5.66809	583.05	good
28.60	M	19.6338	5.30969	770.89	good
28.80	M	23.4808	5.39563	784.428	good
28.90	M	28.5875	5.3153	507.78	good

Rossi and Horton, Table 3

CICLI DEPOSIZIONALI SUB-MILANKOVIANI NELLE AREE COSTIERE: RECORD STRATIGRAFICO DI EVENTI CLIMATICO-EUSTATICI AD ALTA FREQUENZA

Cicli deposizionali sub-milankoviani ed eventi climatico-eustatici ad alta frequenza nel Tardiglaciale-Olocene inferiore

Nel corso dell'ultimo decennio è andata progressivamente rafforzandosi l'idea di una generale correlazione fra cicli deposizionali a scala sub-milankoviana, registrati nelle successioni tardoquaternarie di numerosi sistemi costieri attuali (Somoza et al., 1998; Amorosi et al., 2005; Boyer et al., 2005; Leorri et al., 2006), ed eventi climatico-eustatici relativi agli ultimi 14.000 anni calibrati circa (Bond et al., 1997; Liu et al., 2004; Mayewski et al., 2004).

Entro un contesto prettamente trasgressivo come quello del Tardiglaciale-Olocene inferiore, le superfici trasgressive o di *flooding*, che delimitano superiormente ed inferiormente questi cicli a scala circa millenaria o parasequenze (*sensu* Van Wagoner et al., 1990), possono essere verosimilmente correlate a momenti noti di rapida risalita del livello marino, avvenuti durante il processo di deglaciazione (post-20.000 anni calibrati fa). Dopo l'ultimo massimo glaciale, il riscaldamento globale del clima ha infatti provocato periodiche fasi di intenso scioglimento delle calotte glaciali (*MWP-melt water pulse*, Fairbanks et al., 1989; Bard et al., 1996; Liu et al., 2004), inducendo rapidi impulsi trasgressivi.

Ad ogni MWP fa seguito una fase di rallentamento nella risalita del livello marino che, unitamente a brevi periodi di deterioramento climatico, eventi freddi a impatto globale noti in letteratura come *Bond's event* (Bond et al., 1997) e/o *RCC-rapid climatic change* (Mayewski et al., 2004), può avere indotto la deposizione della porzione "regressiva" presente al tetto di ogni parasequenza.

Tuttavia, questo modello interpretativo semplifica di molto i complessi meccanismi di interazione fra clima, variazione del livello marino e

produzione/apporto di sedimenti a mare, spesso interessati anche da processi di retroazione (*feedback*) difficilmente prevedibili.

Le fasi di rilascio di enormi volumi di acqua dolce in mare (MWP), anticipando sistematicamente i principali eventi freddi compresi fra i 14.000 e i 7.000 anni calibrati, sembrano avere profondamente alterato non solamente il livello marino, ma anche il sistema di redistribuzione mondiale del calore, e di conseguenza il clima. Le simulazioni ottenute recentemente tramite modelli climatici basati sul doppio sistema "atmosfera-oceano" (Renssen et al., 2007) hanno contribuito a fare luce sulla relazione esistente fra eventi climatici freddi e oscillazioni eustatiche. In particolare, queste simulazioni hanno dimostrato che improvvise immissioni di grandi volumi di acqua dolce in mare possono indebolire la circolazione oceanica profonda, alterando il delicato equilibrio del sistema atmosfera-oceano.

Questa variabilità climatica ha certamente agito sulle terre emerse, andando ad alterare sia il *pattern* vegetazionale sia, in modo diretto e indiretto, la produzione e il trasporto verso mare di materiale clastico, favorendo importanti cambiamenti nella rete idrografica e nel rapporto portata liquida/portata solida.

Esiste dunque un unico complesso sistema atmosfera-oceano-terra che interagisce con il fattore climatico tramite azioni e retroazioni su una particolare scala temporale, quella millenaria-submillenaria, che maggiormente coinvolge l'uomo. La comprensione di questi meccanismi e delle loro conseguenze sui sistemi costieri nel recente passato può dunque aiutarci a prevedere l'evoluzione futura di queste aree densamente popolate.

Inquadramento cronologico: le datazioni al radiocarbonio

Al fine di verificare la stretta relazione fra parasequenze e noti eventi climatico-eustatici circa millenari del periodo Tardiglaciale-Olocene inferiore, è necessario disporre di un valido modello cronologico assoluto adatto per un'analisi ad alta risoluzione.

Ancora oggi il metodo del radiocarbonio (^{14}C), introdotto da Libby nel 1949 (Arnold & Libby, 1949), risulta essere lo strumento migliore per datare con precisione depositi appartenenti all'attuale interglaciale (post-20.000 anni circa). Questo metodo, che si basa sul decadimento naturale dell'isotopo radioattivo ^{14}C , necessita ovviamente di campioni ricchi in carbonio, sebbene la quantità minima richiesta sia stata negli ultimi decenni notevolmente ridotta grazie all'utilizzo di spettrometri di massa (analisi radiometriche AMS).

Il dato strumentale, corretto per il frazionamento isotopico ($\delta^{13}\text{C}$), fornisce un'età detta "convenzionale" riferita al 1950, l'anno zero di riferimento (BP-*before present*) per convenzione internazionale (Stuiver & Polach, 1977).

Questa età non può però essere considerata assoluta, in quanto affetta da un errore intrinseco nella formula di calcolo, dove la concentrazione del ^{14}C in atmosfera è considerata stabile nel tempo. In realtà esistono vari *trend* di variabilità (a lungo, medio e breve periodo), riconosciuti e documentati per il Tardoquaternario-Olocene (Stuiver & Kra, 1986). L'età convenzionale deve essere quindi soggetta ad un processo di calibrazione, per correggere questo errore sistematico noto come effetto DeVries.

In natura esistono materiali che conservano traccia della concentrazione del ^{14}C nell'atmosfera del passato e dei quali è nota l'età assoluta. Fra questi, in particolare i tronchi degli alberi, le successioni lacustri e i coralli, databili rispettivamente tramite il conteggio degli anelli di accrescimento (dendrocronologia) o delle varve, e il metodo di datazione assoluta U/Th.

In letteratura, per differenti intervalli temporali esistono numerose curve e tabelle/*dataset* di calibrazione, che possono fornire età assolute fra loro sensibilmente differenti, rispetto allo *standard* di precisione richiesto, pur partendo dalla medesima

età convenzionale. Per questo motivo non dovrebbero essere messe a confronto fra loro età ottenute utilizzando metodi e curve di calibrazione differenti, come può accadere quando vengono presi in considerazione dati pubblicati in letteratura da diversi autori e appartenenti ad aree studio differenti.

In questo capitolo vengono riportate esclusivamente età calibrate, ottenute applicando all'intero *dataset* il programma CALIB versione 5.1. (Stuiver & Reimer, 1993; Stuiver et al., 2005) e le curve di riferimento attualmente più accreditate: IntCal04 (Reimer et al., 2004) e Marine04 (Hughen et al., 2004), rispettivamente per i campioni terrestri e marini.

Le corrispondenti età convenzionali, dalle quali sono state ottenute le età calibrate, provengono sia dalle aree costiere direttamente studiate nell'ambito di questo progetto di ricerca (Piana costiera dell'Arno e Delta del Po) che da altre zone deltizio-costiere attuali di varie parti del mondo, i cui dati sono riportati in letteratura.

Esistono tuttavia intervalli cronologici del Tardiglaciale-Olocene inferiore (quali 12.600-12.300 anni calibrati BP; 11.700-11.300 anni calibrati BP; 9.900-9.600 anni calibrati BP e 9.000-8.750 anni calibrati BP), noti come *plateau*, durante i quali la curva di calibrazione varia debolmente attorno ad un valore all'incirca costante (Mellars, 1990; Stuiver et al., 1998; Blackwell et al., 2006). La presenza di tali *plateau* aumenta il margine di incertezza relativo alla datazione.

Durante il processo di calibrazione di campioni marini (prevalentemente gusci di molluschi) è stato inoltre considerato l'effetto di *reservoir*, che provoca un'età apparente più vecchia di quella reale. Questo effetto è causato dalla notevole differenza fra il tempo di residenza del carbonio nel sistema oceanico rispetto all'atmosfera (Olsson, 1983).

Il fattore di correzione (ΔR) da applicare per eliminare l'effetto di *reservoir* varia da luogo a luogo, a causa della complessità del sistema di circolazione oceanico. Il valore di ΔR locale, che per ogni area geografica può in buona approssimazione essere considerato costante, è disponibile *online* unitamente al programma di calibrazione CALIB (<http://calib.qub.ac.uk/calib/>).

Il fattore climatico nell'evoluzione stratigrafica e ambientale della Piana costiera dell'Arno e del Delta del Po

L'analisi stratigrafico-paleoambientale effettuata nel corso di questo studio ha evidenziato la presenza di cicli deposizionali sub-milankoviani con periodicità millenaria e submillenaria entro i depositi trasgressivi di età tardiglaciale-olocenica (circa 15.000-7.000 anni calibrati fa) della Piana costiera dell'Arno (Paper 2-3) e Delta del Po (Paper 4).

In particolare, studi pollinici effettuati su due sondaggi chiave della Piana dell'Arno hanno permesso di documentare una buona correlabilità cronologica e una stretta relazione di causa-effetto fra noti eventi climatico-eustatici circa millenari e lo sviluppo e l'architettura delle parasequenze (Paper 3). Per la prima volta tre eventi climatici freddi, i due principali dell'attuale interglaciale (Younger Dryas-YD e l'evento degli 8.200 anni calibrati), e un ulteriore evento datato attorno ai 10.400 anni calibrati, sono stati riconosciuti e documentati da un punto di vista stratigrafico-deposizionale, con una chiara connotazione in termini di facies.

I dati ottenuti dalle due aree prese in esame sono ora messi a confronto (Figura 1), al fine di evidenziare similitudini e differenze di carattere generale nella risposta deposizionale e ambientale a recenti variazioni climatico-eustatiche ad alta frequenza.

La finestra temporale analizzata (15.000-7.000 anni calibrati fa) corrisponde di fatto all'intervallo prettamente trasgressivo dell'attuale interglaciale, durante il quale i fattori allociclici, di natura climatico-eustatica, risultano in genere predominanti su quelli autociclici (Amorosi e Milli, 2001). In contesti di valle incisa, come nel caso dell'Arno, possono inoltre essersi preservati elevati spessori di depositi trasgressivi fini, prevalentemente in facies estuarina, favorendo così l'individuazione di cicli deposizionali ad alta frequenza.

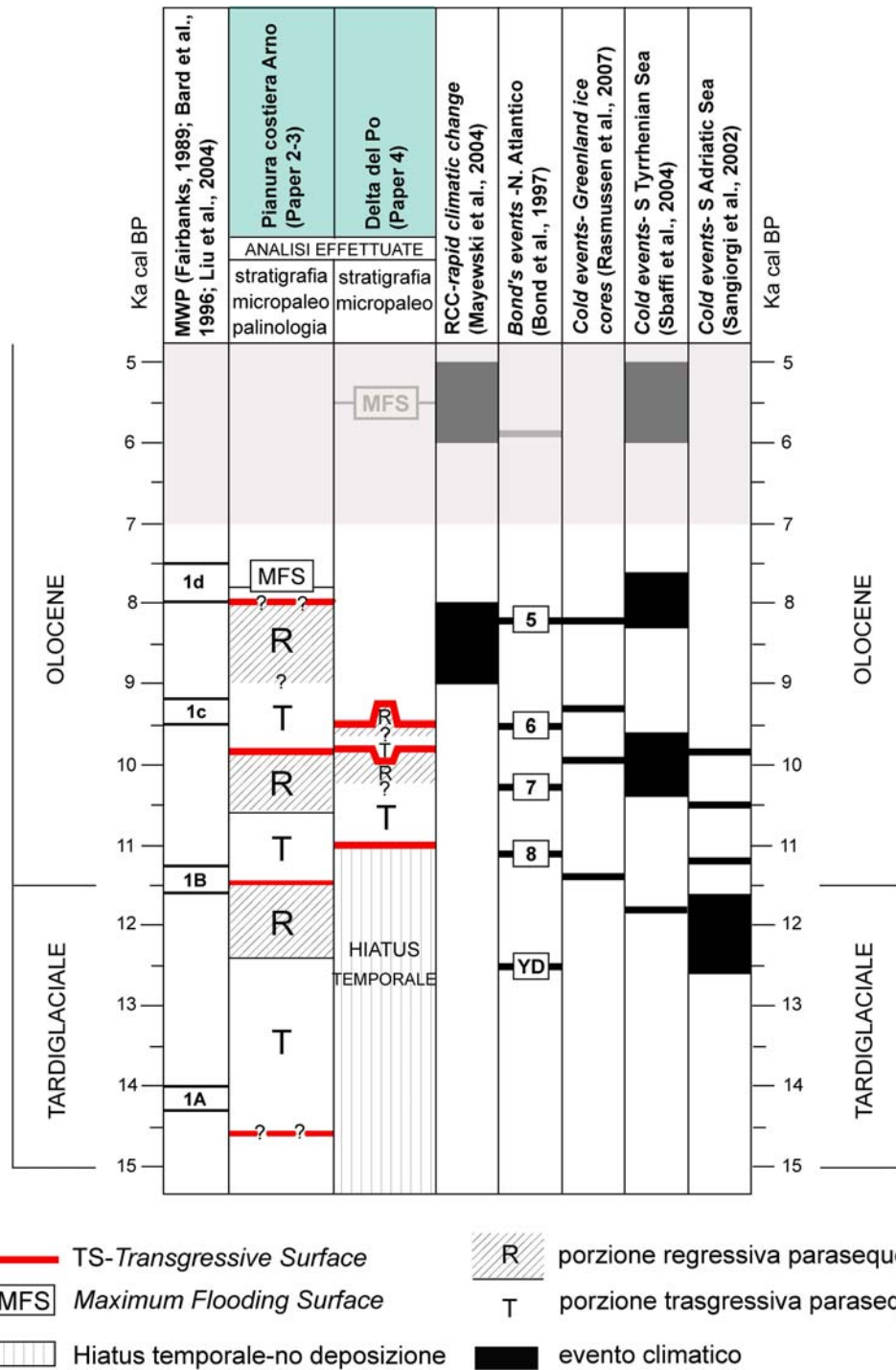


Figura 1. Schema di confronto e correlazione fra eventi climatico-eustatici ad alta frequenza di impatto mondiale e cicli deposizionali sub-milankoviani presenti nelle successioni trasgressive di età tardiglaciale-olocenica della Piana costiera dell'Arno e del Delta del Po.

Nella colonna di sinistra in Figura 1 sono indicate per confronto le quattro principali fasi di risalita eustatica del livello marino, note in letteratura come MWP 1A (14.300-14.000 anni calibrati), MWP 1B (11.600-11.300 anni calibrati), mwp 1c (9.500-9.200 anni calibrati) e mwp 1d (8.000-7.500 anni calibrati) (Fairbanks et al., 1989; Bard et al., 1996; Liu et al., 2004).

Nella parte destra della figura sono invece riportati i dati di letteratura relativi agli eventi climatici freddi riconosciuti a scala globale (RCC di Mayewski et al., 2004) o extraregionale-Nord Atlantico (*Bond's event* di Bond et al., 1997), tramite l'integrazione di differenti indicatori paleoclimatici. Sono inoltre raffigurati i principali eventi freddi registrati nelle carote di ghiaccio della Groenlandia (Rasmussen et al., 2007), indicativi delle condizioni termiche dell'atmosfera alle alte latitudini dell'emisfero settentrionale, e quelli di carattere locale riconosciuti entro le successioni marine profonde del Mar Tirreno (Sbaffi et al., 2004) e del Mar Adriatico (Sangiorgi et al., 2002).

A seconda del grado di dettaglio fornito dall'indicatore paleoclimatico-ambientale e dal metodo di datazione utilizzato, gli eventi freddi riconosciuti possono avere un'estensione temporale più o meno ampia (Fig. 1).

Entro la spessa successione trasgressiva, di età tardiglaciale-olocenica, della piana costiera dell'Arno sono state riconosciute tre parasequenze, ognuna con una chiara connotazione climatica (Paper 2 e Paper 3). Al contrario, nel Delta del Po l'assenza di riempimenti di valle incisa, quindi di un elevato spessore di depositi trasgressivi, impedisce la registrazione di tutti e quattro i principali eventi trasgressivi-MWP e di molti eventi di deterioramento climatico globale.

La trasgressione registrata alla base del riempimento di valle incisa nella Piana dell'Arno avviene durante una fase calda del Tardiglaciale, probabilmente riferibile all'interstadiale Bølling-Allerød, come indicato dalle analisi polliniche presentate in Paper 3. Questa superficie trasgressiva è correlabile con la prima fase di rapida risalita post-glaciale del livello marino (MWP-1A) avvenuta fra i 14.300-14.000 anni calibrati fa, considerando il margine di errore introdotto dall'interpolazione della datazione.

A questa prima fase trasgressiva segue una fase di regressione deposizionale, i cui depositi chiudono al tetto la parasequenza di età tardiglaciale. Le analisi polliniche consentono di interpretare questi depositi regressivi come l'espressione fisica dell'evento freddo YD.

La superficie trasgressiva successiva, che segna la base della parasequenza sovrastante, è databile all'inizio dell'Olocene, grazie a chiare evidenze polliniche, e di conseguenza correlabile al MWP-1B. Il corpo regressivo che chiude questa parasequenza è temporalmente correlabile all'evento climatico freddo compreso fra 10.500 e 10.000 anni calibrati (probabile *Bond's event 7*), riconosciuto sia nelle carote di ghiaccio (Rasmussen et al., 2007) che nei depositi marini del Mediterraneo (Sangiorgi et al., 2002; Sbaffi et al., 2004).

Un'ulteriore trasgressione, che sembra anticipare di poco l'inizio del mwp-1c (Fig. 1), è registrata in corrispondenza di una successiva fase di miglioramento climatico, evidenziata dalle analisi polliniche nella paleovalle dell'Arno (Paper 3). Lo sfasamento temporale fra superficie trasgressiva e mwp-1c può essere spiegato considerando il margine di approssimazione del modello cronologico adottato, che dipende sia dalla posizione del campione datato rispetto alla superficie trasgressiva sia dall'errore introdotto dalla misura radiometrica e dal processo di calibrazione.

Questa superficie trasgressiva delimita inferiormente la terza e ultima parasequenza identificata all'interno del riempimento della paleovalle dell'Arno. La porzione superiore, a carattere regressivo, di questa parasequenza mostra affinità pollinica e cronologica con il noto evento freddo degli 8.200 anni calibrati (Alley et al., 1997; Klitgaard-Kristensen et al., 1998; Nesje and Dahl, 2001; Baldini et al., 2002; Diefendorf et al., 2006; Thomas et al., 2007).

La trasgressione immediatamente successiva ha anch'essa una chiara espressione di facies sedimentaria e pollinica (Paper 3) ed è correlabile all'ultima fase di rapido innalzamento del livello marino (mwp-1d), immediatamente antecedente il momento di massima ingressione marina (espresso dalla MFS-*maximum flooding surface*).

L'assenza di uno spesso riempimento di valle incisa ha impedito una registrazione altrettanto dettagliata e completa degli eventi climatico-eustatici ad alta frequenza nella successione trasgressiva del Delta del Po. In questo caso la prima trasgressione

documentata è infatti datata a circa 11.000 anni calibrati ed è correlabile all'impulso trasgressivo di base Olocene (MWP-1B), uno dei maggiori dell'attuale interglaciale con un innalzamento del livello marino quantificabile in circa 20 metri in 300 anni (Fairbanks et al., 1989; Liu et al., 2004). Il ritardo nella registrazione di MWP-1B, così come l'assenza di depositi relazionabili al periodo pre-olocenico/tardiglaciale (vedi Fig. 1), sono verosimilmente legati alla caratteristica geometria ad *onlap* dei depositi trasgressivi su di una paleomorfologia articolata, ereditata dal precedente periodo glaciale.

Come in Arno, al di sotto del Delta del Po sono documentati sia l'impulso eustatico mwp-1c che l'evento freddo dei 10.500-10.000 anni calibrati (*Bond's event 7*), evidenziati rispettivamente da una chiara superficie trasgressiva e dal corpo regressivo nella parte sommitale della parasequenza compresa fra 11.000 e i 10.000 anni calibrati.

Nell'area del Delta del Po è però presente un'ulteriore parasequenza, databile fra i 9.800 e i 9.500 anni calibrati fa, indicativa di una ciclicità submillenaria forse dovuta a un evento freddo datato a circa 9.500 anni calibrati (*Bond's event 6*). Questo evento non ha lasciato alcuna evidenza stratigrafica entro la successione trasgressiva della Piana dell'Arno, dove fattori locali possono averne inibito gli effetti sulla sedimentazione o più semplicemente a causa del fatto che la scarsa risoluzione entro depositi estuarini può essere insufficiente alla sua identificazione.

Considerati i problemi connessi alla preservazione di cicli sedimentari di questo tipo entro successioni costiere e le già citate difficoltà di correlazione cronologica, è altamente improbabile che tutti gli eventi climatici ad alta frequenza riconosciuti in letteratura possano trovare una chiara espressione di facies nel record sedimentario di ogni area costiera presa in esame. L'interazione di numerosi fattori locali e il diverso grado di sensibilità degli indicatori paleoclimatico-ambientali disponibili costituiscono inoltre un ulteriore problema.

A tal proposito, un chiaro esempio è fornito dal noto evento freddo pre-boreale o *PBO-Preboreal oscillation*, datato a circa 11.400-11.200 anni calibrati fa e documentato tramite vari indicatori paleoclimatici a scala mondiale (Lotter et al., 1992; Björk et al., 1996; Bond et al., 1997; Rasmussen et al., 2007). Questo evento

sembra non avere lasciato traccia evidente nel record sedimentario sia della Piana costiera dell'Arno che del Delta del Po. La rapida risalita eustatica/MWP-1B alla base dell'Olocene ha in questo caso probabilmente annullato qualsiasi possibile effetto della PBO sulla sedimentazione costiera, a favore di un chiaro e continuo *trend* trasgressivo fino a circa 10.500 anni calibrati fa.

In conclusione, è possibile riconoscere un segnale climatico-eustatico sulla architettura deposizionale delle successioni trasgressive di età tardiglaciale-olocenica della Piana dell'Arno e del Delta del Po. Differenze nella preservazione e nella registrazione di eventi climatico-eustatici, circa millenari, noti a livello globale, sono legate a fattori paleomorfologici e paleoambientali a carattere locale.

Registrazione stratigrafica di eventi climatico-eustatici circa millenari nelle successioni costiere di età tardiglaciale-olocenica: confronto e correlazione a scala mondiale

La letteratura più recente, in particolare quella riferibile all'ultimo decennio, mette in evidenza la presenza, a scala mondiale, di cicli deposizionali ad alta frequenza entro successioni tardiglaciale-oloceniche presenti nel sottosuolo di sistemi costieri attuali (Somoza et al., 1998; Amorosi et al., 2005; Boyer et al., 2005; Leorri et al., 2006).

Alla luce dei risultati ottenuti in questo studio per l'area dell'Arno e del Delta del Po, si è tentato di verificare in che misura eventi climatico-eustatici di età tardiglaciale-olocenica possano essere fisicamente riconosciuti (cicli deposizionali sub-milankoviani) e correlati a scala mondiale. A questo scopo, i dati di letteratura sono stati parzialmente rivisti e reinterpretati (Fig. 2) per garantire l'uniformità del dato cronologico, tramite l'utilizzo di datazioni assolute ottenute con il programma CALIB 5.1. e le curve IntCal04 e Marine04 (vedere paragrafo "Il modello cronologico: le datazioni al radiocarbonio").

I dati sedimentologico-stratigrafici presentati in Figura 2, che comprendono l'ubicazione delle superfici trasgressive e la suddivisione in parasequenze, derivano da sistemi deltizi e costieri, distinti per l'area mediterranea e per quella extra-mediterranea (dall'Oceano Atlantico settentrionale al Pacifico occidentale). I dati sono ulteriormente ordinati distinguendo nell'ambito dell'area mediterranea dati provenienti dalla zona costiera del mare Adriatico, del bacino tirrenico e di quello algero-provenzale. Per l'area extra-mediterranea sono invece presentati dati provenienti dal Golfo di Biscaglia, dall'Atlantico nord-occidentale e dal Pacifico occidentale.

Le aree prese in esame in questo lavoro sono evidenziate in celeste e comprendono, oltre alla Piana dell'Arno e al delta attuale del Po, dati inediti della pianura bolognese (Fig. 2), dove è stato recentemente analizzato un sondaggio a carotaggio continuo profondo 30 metri.

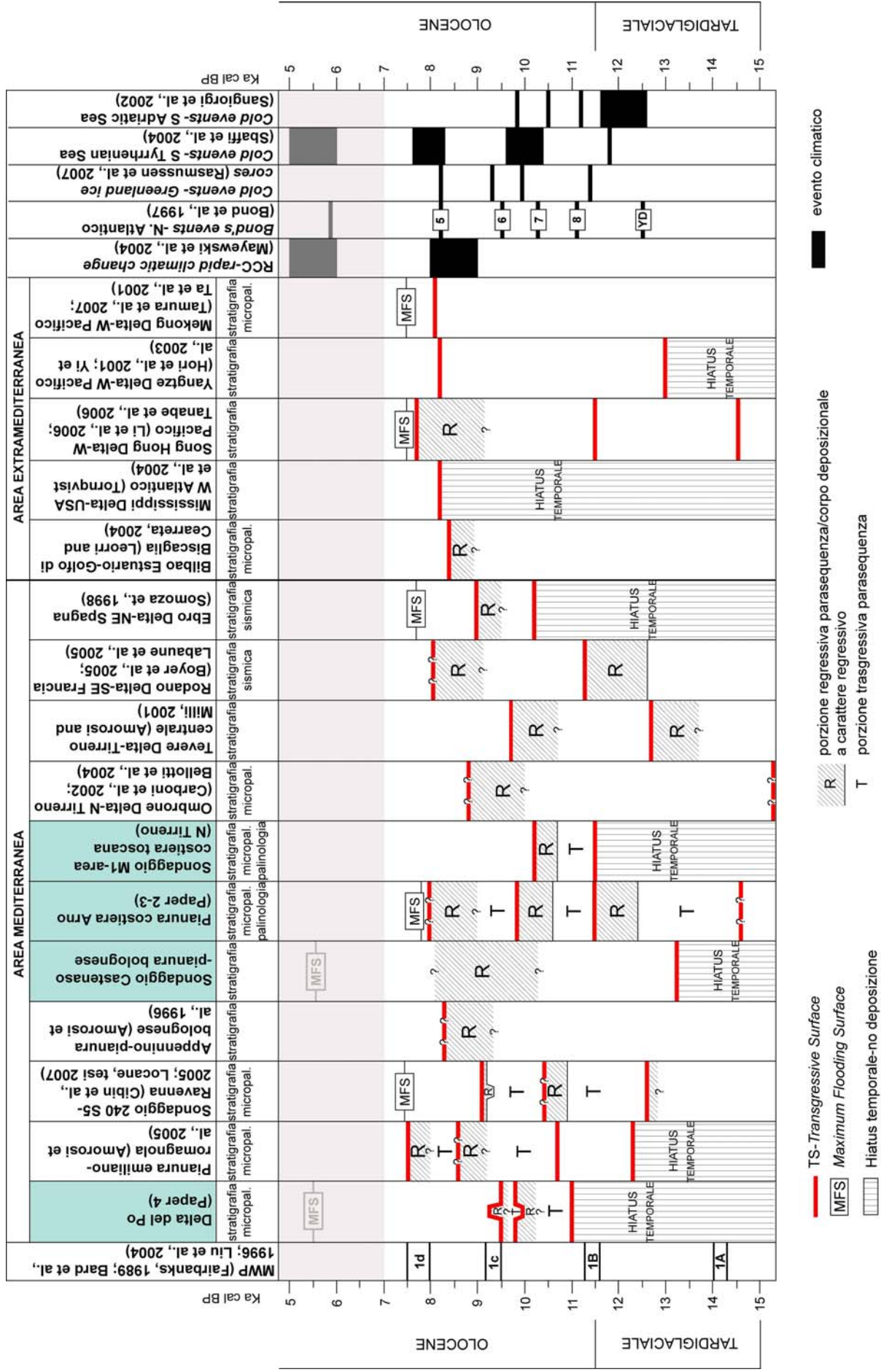


Figura 2. Schema di confronto e correlazione globale fra eventi climatico-eustatici circa millenari di impatto mondiale e cicli deposizionali sub-milankoviani presenti nelle successioni trasgressive tardi-glaciale-oloceniche di sistemi costieri attuali.

La mancanza, soprattutto in letteratura, di datazioni direttamente o strettamente riferibili alle superfici stratigrafiche di interesse, quali le superfici trasgressive e il limite basale dei corpi sedimentari regressivi, in molti casi comporta un notevole grado di incertezza nell'interpretazione (Fig. 2). Nella Pianura Padana, nell'estuario dell'area di Bilbao, nel delta del Tevere, del Rodano, dello Yangtze e del Mekong alcune superfici evidenziate dalle analisi stratigrafiche non sono databili tramite i dati di letteratura disponibili e, per questo motivo, non sono riportate in Figura 2.

Sono inoltre indicate, come in Figura 1, le quattro principali fasi di risalita eustatica del livello marino-MWP e gli eventi climatici freddi compresi fra i 15.000-7.000 anni calibrati.

Al di là di una inevitabile dispersione del dato stratigrafico (Fig. 2), facilmente prevedibile considerando che sono state messe a confronto aree differenti, geograficamente lontane e studiate tramite diverse metodologie (analisi stratigrafiche, micropaleontologiche e sismiche), è possibile distinguere alcuni elementi comuni a gran parte delle aree costiere prese in considerazione.

Le superfici trasgressive sono in generale elementi stratigrafici ben correlabili attraverso le differenti successioni in esame; tuttavia, a causa della paleomorfologia locale che, come discusso nella sezione precedente, può indurre ritardi nella trasgressione in corrispondenza di paleoalti strutturali, e del margine di incertezza che il processo di uniformazione delle datazioni comporta, è possibile che lo stesso evento trasgressivo non dia origine in aree diverse ad una superficie sincrona di trasgressione. E' stato osservato come la paleomorfologia di alcune aree costiere possa addirittura impedire la preservazione dell'intera successione tardiglaciale e, di conseguenza, la registrazione della trasgressione pre-olocenica attribuibile al MWP-1A (vedi Delta del Po e Delta dell'Ebro in Figura 2).

In generale, evidenze stratigrafiche del MWP-1A sono ben preservate nei contesti di valle incisa riconosciuti per l'area del Mediterraneo nella piana costiera dell'Arno e per il Pacifico occidentale nel delta del Song Hong e dello Yangtze. La mancanza di datazioni impedisce di evidenziare, in Figura 2, la presenza di depositi trasgressivi di età pre-olocenica anche per la successione di valle incisa del Mekong.

In altre aree costiere, dove non esistono condizioni paleomorfologiche favorevoli di valle incisa, la trasgressione legata al MWP-1A è comunque registrata, ma subisce un notevole ritardo, come nel caso della pianura emiliano-romagnola (Fig. 2).

La trasgressione successiva di inizio Olocene è invece generalmente ben documentata nella quasi totalità delle successioni prese in esame e facilmente correlabile con l'impulso trasgressivo di notevole intensità 1B (MWP-1B: 11.600-11.300 anni calibrati).

Una maggiore dispersione temporale caratterizza invece la trasgressione successiva, databile fra i 10.000-9.000 anni calibrati. Questa superficie trasgressiva, pur essendo correlabile con il mwp-1c (9.500-9.200 anni calibrati), può avere risentito dell'influenza di fattori locali sulla sedimentazione, considerata la minore intensità dell'impulso trasgressivo 1c rispetto ai due precedenti.

La TS più evidente e globalmente meglio registrata su scala mondiale è quella presente al tetto della successione trasgressiva (TST). Il graduale riempimento delle valli incise e in generale delle paleomorfologie ereditate dal periodo glaciale ha reso presumibilmente le aree in esame maggiormente comparabili dal punto di vista fisiografico in questa fase, favorendo una minore dispersione del dato stratigrafico attorno all'impulso trasgressivo noto come mwp-1d (8.000-7.500 anni calibrati BP). In certe aree costiere la TS è prossima o coincide con il momento di massima ingressione marina, materializzato dalla MFS (*maximum flooding surface*). Questo può essere dovuto, almeno in parte, alla sensibilità dell'indicatore paleoambientale utilizzato e, di conseguenza, al grado di risoluzione dell'analisi stratigrafica effettuata.

Analogamente a quanto osservato per le fasi climatiche calde, ossia per gli episodi trasgressivi, anche gli eventi climatici freddi a carattere globale sembrano avere una chiara espressione di facies nel *record* sedimentario delle successioni costiere su scala globale, sebbene le conseguenze della variabilità climatica sulla sedimentazione siano complesse e probabilmente interessate da parametri locali.

Nonostante le particolari condizioni fisiografiche di molte delle aree in esame durante la fase tardiglaciale abbiano impedito la registrazione dell'evento freddo noto come Younger Dryas, quest'ultimo (ove preservato) e l'evento degli 8.200 anni

calibrati sembrano essere in generale gli episodi freddi meglio rappresentati (Fig. 2). A questi eventi corrispondono i principali momenti di deterioramento climatico avvenuti durante l'attuale interglaciale, con una diminuzione della temperatura in media dell'ordine di qualche grado (circa 2-5 °C) e variazioni nel tasso di umidità, che hanno fortemente influenzato l'evoluzione deposizionale-ambientale delle aree alluvionali e costiere.

Una chiara registrazione dello Younger Dryas è presente unicamente in contesti di valle incisa, quali ad esempio quelli ricostruiti nel sottosuolo della Piana dell'Arno e del delta del Rodano. Per quanto riguarda le successioni di riempimento di valle incisa della zona costiera del Pacifico occidentale, chiare evidenze sedimentologico-stratigrafiche di depositi regressivi tardiglaciali non sembrano essere deducibili dall'osservazione dei dati di letteratura. Tuttavia, analisi polliniche effettuate in un sondaggio ubicato nel delta dello Yangtze hanno evidenziato la presenza, fra i 13.000-11.000 anni calibrati, di una fase di deterioramento climatico (periodo freddo e arido) correlabile allo YD (Yi et al., 2003).

I dati pollinici sono i principali indicatori in grado di fornire una caratterizzazione climatica delle successioni sedimentarie, spesso avvalorando l'interpretazione di superfici stratigrafiche e importanti cambiamenti di facies. Nel caso della Piana dell'Arno (Paper 3), lo spettro pollinico consente di interpretare due dei tre corpi regressivi riconosciuti nella parte superiore delle parasequenze come espressione fisica rispettivamente dello YD e dell'evento 8.200 anni calibrati. Analogamente, nel delta del Song Hong le analisi polliniche hanno permesso di riconoscere nel corpo regressivo di età più recente la fase fredda degli 8.200 anni calibrati (Li et al., 2006; Tanabe et al., 2006).

Là dove non siano disponibili i dati pollinici, è l'affinità cronologica dell'evento regressivo a fare presupporre questo tipo di interpretazione-correlazione di carattere climatico (Fig. 2). L'evento degli 8.200 anni calibrati, in particolare, sembra essere ben rappresentato in numerose aree costiere ed è inoltre l'unico ad avere una propria espressione fisica anche entro successioni sedimentarie di aree alluvionali, quali ad esempio il margine della pianura bolognese (Fig. 2).

Più difficoltosa è invece l'interpretazione climatica dei corpi regressivi registrati in molte delle successioni costiere in esame fra gli 11.000 e i 9.000 anni calibrati circa (vedi Figura 2). La tipologia dei dati a disposizione e il grado di approssimazione fornito dalle datazioni al radiocarbonio (compresa la presenza di *plateau*) impediscono di correlare questi corpi regressivi a uno specifico evento climatico freddo compreso fra lo YD e quello degli 8.200 anni calibrati. Nella letteratura mondiale esistono evidenze geologiche di almeno tre eventi climatici (noti come *Bond's event* 8, 7 e 6) con periodicità millenaria-submillenaria durante i primi 2.000 anni dell'Olocene (Bond et al., 1997; Rasmussen et al., 2007). E' per questo motivo ancor più difficile un'attribuzione specifica di un generico evento regressivo ad uno di questi eventi.

Concludendo, l'architettura deposizionale delle successioni trasgressive (vedi Figura 2) documenta chiaramente la forte influenza che la variabilità eustatica e climatica circa millenaria hanno avuto sulla sedimentazione costiera mondiale durante il Tardiglaciale-Olocene inferiore (circa 14.000-7.000 anni calibrati fa).

In alcuni casi fattori paleomorfologici e paleoambientali locali possono avere indebolito o addirittura obliterato, come nel caso della mancata preservazione dei depositi tardiglaciali, evidenze stratigrafiche (quali superfici trasgressive e corpi regressivi al tetto di parasequenze) di specifici impulsi trasgressivi (MWP) ed eventi climatici freddi a carattere globale. Per questo motivo, in generale, le successioni trasgressive di riempimento di valli incise risultano essere quelle meglio predisposte per una registrazione dettagliata, ma soprattutto completa, degli eventi climatico-eustatici avvenuti fra i 14.000 e i 7.000 anni calibrati.

Bibliografia

Alley, R.B., Mayewski, P., Sowers, T., Stuiver, M., Taylor, K., Clark, P. 1997. Holocene climatic instability: a prominent widespread event 8200 yr ago. *Geology* 25, 483–486.

Amorosi, A., Milli, S. 2001. Late Quaternary depositional architecture of Po and Tevere river deltas (Italy) and worldwide comparison with coeval deltaic successions. *Sedimentary Geology* 144, 357–375.

Amorosi, A., Farina, M., Severi, P., Preti, D., Caporale, L., Di Dio, G. 1996. Genetically related alluvial deposits across active fault zones: an example of alluvial fan-terrace correlation from the upper Quaternary of the southern Po Basin, Italy. *Sedimentary Geology* 102, 275–295.

Amorosi, A., Centineo, M. C., Colalongo, M. L., Fiorini, F. 2005. Millennial-scale depositional cycles from the Holocene of the Po Plain, Italy. *Marine Geology* 222-223, 7–18.

Arnold, J. R., Libby, W. F. 1949. Age Determinations by Radiocarbon Content: Checks with Samples of Known Age. *Science* 110, 678–680.

Baldini, J. U. L., McDermott, F. and Fairchild, I. J. 2002: Structure of the 8200-year cold event revealed by a speleothem trace element record. *Science* 296, 2203–06.

Bard, E., Hamelin, B., Arnold, M., Montaggioni, L., Cabioch, G., Faure, G., Rougerie, F. 1996. Deglacial sea-level record from Tahiti corals and the timing of global meltwater discharge. *Nature* 382, 241–244.

Bellotti, P., Caputo, C., Davoli, L., Evangelista, S., Garzanti, E., Pugliese, F., Valeri, P. 2004. Morpho-sedimentary characteristics and Holocene evolution of the emergent part of the Ombrone River delta (southern Tuscany). *Geomorphology* 61, 71–90

Björck, S., Kromer, B., Johnsen, S. J., Bennike, O., Hammarlund, D., Lehmdahl, G., Possnert, G., Rasmussen, T. L., Wohlfarth, B., Hammer, C. U., Spurk, M. 1996. Synchronised terrestrial–atmospheric deglacial records around the North Atlantic. *Science* 274, 1155–1160.

Blackwell, P. G., Buck, C. E., Reimer, P. J. 2006. Important features of the new radiocarbon calibration curves. *Quaternary Science Reviews* 25, 408–413.

Bond, G., Showers, W., Cheseby, M., Lotti, R., Almasi, P., deMenocal, P., Priore, P., Cullen, H., Hajdas, I., Bonani, G. 1997. A pervasive millennial scale cycle in North Atlantic Holocene and glacial climate. *Science* 278, 1257–1266.

Boyer, J., Duvail, C., Le Strat, P., Gensous, B., Tesson, M. 2005. High resolution stratigraphy and evolution of the Rhône delta plain during Postglacial time, from subsurface drilling data bank. *Marine Geology* 222-223, 267–298.

Carboni, M.G., Bergamin, L., Di Bella, L., Iamundo, F., Pugliese, N. 2002. Palaeoecological evidences from foraminifers and ostracods on Late Quaternary sea-level changes in the Ombrone river plain (central Tyrrhenian coast, Italy). *Geobios Mémoire spécial* 24, 40–50.

Cibin, U., Severi, P., Roveri, M. 2005. Carta Geologica d'Italia alla scala 1:50.000. Foglio 240-241 Forlì-Cesena. APAT. Regione Emilia-Romagna.

Diefendorf, A. F., Patterson, W. P., Mullins, H. T., Tibert, N., Martini, A. 2006. Evidence for high-frequency late Glacial to mid-Holocene (16,800 to 5,500 cal yr

B.P.) climate variability from oxygen isotope values of Lough Inchiquin, Ireland. *Quaternary Research* 65, 78–86.

Fairbanks, R. G. 1989. A 17,000-year glacio-eustatic sea level record: influence of glacial melting rates on the Younger Dryas event and deep ocean circulation. *Nature* 342, 639–642.

Hori, K., Saito, Y., Zhao, Q., Cheng, X., Wang, P., Sato, Y., Li, C. 2001. Sedimentary facies of the tide-dominated paleo-Changjiang (Yangtze) estuary during the last transgression. *Marine Geology* 177, 331–351.

Hughen, K. A., Baillie, M. G. L., Bard, E., Beck, J. W., Bertrand, C. J. H., Blackwell, P. G., Buck, C. E., Burr, G. S., Cutler, K. B., Damon, P. E., Edwards, R. L., Fairbanks, R. G., Friedrich, M., Guilderson, T. P., Kromer, B., McCormac, G., Manning, S., Ramsey, C. B., Reimer, P. J., Reimer, R. W., Remmele, S., Southon, J. R., Stuiver, M., Talamo, S., Taylor, F. W., van der Plicht, J., Weyhenmeyer, C. E. 2004. Marine04 marine radiocarbon age calibration, 0-26 cal kyr BP. *Radiocarbon* 46, 1059–1086.

Klitgaard-Kristensen, D., Sejrup, H-P., Hafliðason, H., Johnsen, S., Spurk, M. 1998. A regional 8200 cal yr BP cooling event in northwest Europe, induced by final stages of the Laurentide ice-sheet deglaciation? *Journal of Quaternary Science* 13, 165–169.

Labaune, C., Jouet, G., Berné, S., Gensous, B., Tesson, M., Delpeint, A. 2005. Seismic stratigraphy of the Deglacial deposits of the Rhône prodelta and of the adjacent shelf. *Marine Geology* 222-223, 299–311.

Leorri, E., Cearreta, A. 2004. Holocene environmental development of the Bilbao estuary, northern Spain: sequence stratigraphy and foraminiferal interpretation. *Marine Micropaleontology* 51, 75–94.

Leorri, E., Martin, R., McLaughlin, P. 2006. Holocene environmental and parasequence development of the St. Jones Estuary, Delaware (USA): Foraminiferal proxies of natural climatic and anthropogenic change. *Palaeogeography, Palaeoclimatology, Palaeoecology* 241, 590–607.

Li, Z., Saito, S., Matsumoto, E., Wang, Y., Tanabe, S., Vu, Q.L. 2006. Climate change and human impact on the Song Hong (Red River) Delta, Vietnam, during the Holocene. *Quaternary International* 144, 4–28.

Liu, J. P., Milliman, J. D., Gao, S., Cheng, P. 2004. Holocene development of the Yellow River's subaqueous delta, North Yellow Sea. *Marine Geology* 209, 45–67.

Locane, R. 2007. Analisi micropaleontologica ed evoluzione paleoambientale di una successione lagunare olocenica del sottosuolo della Pianura Padana. Tesi di Laurea Triennale in Scienze Geologiche. Università degli Studi di Bologna.

Lotter, A. F., Eicher, U., Siegenthaler, U., Birks, H. J. B. 1992. Late-glacial climatic oscillations as recorded in Swiss Lake sediments. *Journal of Quaternary Science* 7, 187–204.

Mayewski, P. A., Rohling, E. E., Stager, J. C., Karlen, W., Maasch, K. A., Meeker, L. D., Meyerson, E. A., Gasse, F., van Kreveld, S., Holmgren, K., Lee-Thorp, J., Rosqvist, G., Rack, F., Staubwasser, M., Schneider, R. R., Steig, E. J. 2004. Holocene climate variability. *Quaternary Research* 62, 243–255.

Mellars, P. 1990. A major 'plateau' in the radiocarbon time-scale at c. 9650 b.p.: the evidence from Star Carr (North Yorkshire), *Antiquity* 64, 836–841.

Rasmussen, S. O., Vinther, B. M., Clausen, H. B., Andersen, K. K. 2007. Early Holocene climate oscillations recorded in three Greenland ice cores. *Quaternary Science Reviews* 26, 1907–1914.

Reimer, P. J., Baillie, M. G. L., Bard, E., Bayliss, A., Beck, J. W., Bertrand, C. J. H., Blackwell, P. G., Buck, C. E., Burr, G. S., Cutler, K. B., Damon, P. E., Edwards, R. L., Fairbanks, R. G., Friedrich, M., Guilderson, T. P., Hogg, A. G., Hughen, K. A., Kromer, B., McCormac, F. G., Manning, S. W., Ramsey, C. B., Reimer, R. W., Remmele, S., Southon, J. R., Stuiver, M., Talamo, S., Taylor, F. W., van der Plicht, J., Weyhenmeyer, C. E. 2004. IntCal04 Terrestrial radiocarbon age calibration. *Radiocarbon* 46, 1029–1058.

Renssen, H., Goosse, H., Fichefet, T. 2007. Simulation of Holocene cooling events in a coupled climate model. *Quaternary Science Reviews* 26, 2019–2029.

Sangiorgi, F., Capotondi, L., Brinkhuis, H. 2002. A centennial scale organic-walled dinoflagellate cyst record of the last deglaciation in the South Adriatic Sea (Central Mediterranean). *Palaeogeography, Palaeoclimatology, Palaeoecology* 186, 199–216.

Sbaffi, L., Wezela F.C., Curzia, G., Zoppi U. 2004. Millennial- to centennial-scale palaeoclimatic variations during Termination I and the Holocene in the central Mediterranean Sea. *Global and Planetary Change* 40, 201–217.

Somoza, L., Barnolas, A., Arasa, A., Maestro, A., Rees, J. G., Hernandez-Molina, F. J. 1998. Architectural stacking patterns of the Ebro delta controlled by Holocene high-frequency eustatic fluctuations, delta-lobe switching and subsidence processes. *Sedimentary Geology* 117, 11–32.

Stuiver, M., Polach, H. A. 1977. Discussion: Reporting of ¹⁴C data. *Radiocarbon* 9, 355– 363.

Stuiver, M., Kra, R. 1986. Calibration Issue. *Radiocarbon* 28, 805–1030.

Stuiver, M., Reimer, P. J. 1993. Extended ¹⁴C data base and revised CALIB 3.0 ¹⁴C Age calibration program. *Radiocarbon* 35, 215–230.

Stuiver, M., Reimer P. J., Bard, E., Beck, J. W., Burr, G. S., Hughen, K. A., Kromer, B., McCormac, G., van Der Plicht, J., Spurk, M. 1998. Intcal98 radiocarbon age calibration, 24000–0 cal BP. *Radiocarbon* 40, 1041–1083

Stuiver, M., Reimer, P. J., Reimer, R. W. 2005. CALIB 5.0.
<http://calib.qub.ac.uk/calib/>

Ta, T.K.O., Nguyen, V.L., Tateishi, M., Kobayashi, I., Saito, Y. 2001. Sedimentary facies, diatom and foraminifer assemblages in a late Pleistocene-Holocene incised-valley sequence from the Mekong River Delta, Bentre Province, Southern Vietnam: the BT2 core. *Journal of Asian Earth Sciences* 20, 83–94.

Tamura, T., Saito, Y., Sieng, S., Ben, B., Kong, M., Choup, S., Tsukawaki, S. 2007. Depositional facies and radiocarbon ages of a drill core from the Mekong River lowland near Phnom Penh, Cambodia: Evidence for tidal sedimentation at the time of Holocene maximum flooding. *Journal of Asian Earth Sciences* 29, 585–592.

Tanabe, S., Saito, Y., Vu, Q.L., Hanebuth, T.J.J., Ngo, Q.L., Kitamura, A. 2006. Holocene evolution of the Song Hong (Red River) delta system, northern Vietnam. *Sedimentary Geology* 187 (1-2), 29–61.

Thomas, E. R., Wolff, E. W., Mulvaney, R., Steffensen, J. P., Johnsen, S. J., Arrowsmith, C., White, J. W. C., Vaughn, B., Popp, T. 2007. The 8.2 kyr event from Greenland ice cores. *Quaternary Science Reviews* 26, 70–81.

Törnqvist, T., Bick, S.J., González, J.L., van der Borg, K., de Jong, A.F.M. 2004. Tracking the sea-level signature of the 8.2 ka cooling event: New constraints from the Mississippi Delta. *Geophysical Research Letters* 31, L23309, doi:10.1029/2004GL021429.

Van Wagoner, J. C., Mitchum, R. M., Campion, K. M., Rahmanian, V. D. 1990. Siliclastic sequence stratigraphy in well logs, cores and outcrops: concepts for high resolution correlations of time and facies. *American Association of American Petroleum Geologists. Methods in Exploration* 7 Barbara H. Lidtz, Tulsa.

Yi, S., Saito, Y., Zhao, Q., Wang, P. 2003. Vegetation and climate changes in the Changjiang (Yangtze River) delta, China, during the past 13,000 years inferred from pollen records. *Quaternary Science Reviews* 22, 1501–1519.

Appendice

The Sedimentary Record of the 2005 Hurricane Season from the Mississippi and Alabama Coastlines

Horton, B.P., Rossi, V. and Hawkes, A.D.

The Sedimentary Record of the 2005 Hurricane Season from the Mississippi and Alabama Coastlines

Benjamin P. Horton^{a*} Veronica Rossi^b and Andrea D. Hawkes^a

^a Sea Level Research Laboratory, Department of Earth and Environmental Science, University of Pennsylvania, Philadelphia, PA 19104-6316, USA

^b Dipartimento di Scienze della Terra e Geologico-Ambientali, Università di Bologna, Via Zamboni 67, 40126 Bologna, Italy

*Corresponding author: Tel: +1 215 573 5388; Fax: +1 215 898 0964; E-mail: bphorton@sas.upenn.edu.

Abstract

The instrumental record of hurricane activity is too short to fully capture the occurrence of the rare but most destructive hurricanes. Therefore, obtaining a record of present and past landfalling hurricanes, and their extent of geological and ecological impacts, is one means to assess future risk, reveal the spatial and temporal variability of hurricane activity and decipher its relationship with global climatic changes. We rapidly dispatched survey teams to collect the readily available, but perishable data of Hurricanes Katrina and Rita storm surge from two salt marshes in Mississippi and one salt marsh in Alabama. In Mississippi we recorded Hurricane Katrina storm surge heights greater than 7.5 m North American Vertical Datum 88 (NAVD88) with inland extents in excess of 700 m, whereas in Alabama the maximum recorded storm surge was 3.43 m NAVD88. At one salt marsh in Mississippi we recorded the maximum inland extent and elevation of maximum penetration of Hurricane Rita as 370 m and 3.43 m NAVD88, respectively.

We observed a three-dimensional distribution of hurricane-induced storm surge deposits that tapered landward, overlying salt marsh sediment. There was a sharp or erosional boundary between the pre-storm surge and storm surge sedimentary units, which was accompanied by a change in color and lithology. The overlying storm surge sediment unit was coarser than the pre-storm surge unit with a lower organic content. The thickness of the Hurricane Katrina and Rita storm surge sediments ranged from 9 cm to 13 cm and approximately 7 cm, respectively. Foraminiferal analyses revealed a virtual absence of tests within the storm surge sediments, whereas abundant agglutinated foraminifera were found in the underlying salt marsh deposits.

Keywords: Hurricane; Sedimentology; Micropaleontology; Paleotempestology; Gulf Coast

1. Introduction

A major obstacle in producing reliable predictions of catastrophic environmental changes is a lack of data on time scales longer than the short instrumental record. Nevertheless, the pending disaster along the Gulf Coast, in particular the New Orleans region, has been forecasted since the 19th century (e.g. Twain, 1882; McPhee, 1989; Louisiana Department of Natural Resources, 1998; Turnipseed et al., 1998; Fischetti, 2001; Bourne, 2004; Laska, 2004; Tidewell, 2004; Enserink and Bohannon, 2005; Travis, 2005). The increase in the frequency and intensity of tropical cyclones that has been identified by instrumental records and linked to human-induced climate change is the subject of much recent scientific debate (Levitus et al., 2000, 2001; Emanuel, 2005; Webster et al., 2005; Greening et al., 2006). Increasingly, hurricane activity is viewed as a process by which the climate system cools the oceans and atmosphere in the tropical zone. Since hurricanes draw their energy from warm ocean waters and given the predicted warming of the atmosphere and surface-ocean waters, it is reasonable to expect that the climate system will generate more frequent and/or more intense hurricanes to achieve this cooling (e.g., Kerry, 2001, 2003; Mann and Kerry, 2006; Elsner, 2007; Sriviver and Huber, 2007). Webster et al. (2005) suggested the number of category 4 and 5 hurricanes (Saffir-Simpson Scale) has doubled globally over the past 35 years and the total number of hurricanes in the western North Atlantic basin has increased in conjunction with warming sea-surface temperatures. Nyberg et al. (2007) also stated that hurricane activity in the North Atlantic Ocean has increased significantly since 1995. However, they suggested that changes in the magnitude of vertical wind shear will have a significant influence on future hurricane activity. The importance of stratigraphic and paleoenvironmental records was recently highlighted by Donnelly and Woodruff (2007), who studied a Caribbean lagoon and concluded that intense hurricane activity in the western North Atlantic Ocean over the past 5,000 years was controlled by El Niño and the West African Monsoon.

Every hurricane, however, that makes landfall has the potential to leave a signal within the sediment deposited by its storm surge (Cahoon, 2006; Sallenger et al., 2006). Identification of storm surge deposits is often based on anomalous sand deposits in an environment where such a deposit is unusual, such as lakes and marshes (e.g. Reed, 1989; Liu and Fearn, 1993, 2000; Donnelly et al., 2001a, b; Sedgwick and Davis, 2003; van de Plassche et al., 2004; Turner et al., 2006). In addition, storm surge deposits have been identified through microfossil analysis (e.g. foraminifera) where species show abrupt changes in assemblage and provide an additional technique to either support existing lithostratigraphic characteristics or importantly, distinguish storm surge sediment where lithostratigraphic characteristics are inadequate (Parsons, 1998; Collins et al., 1999; Hippensteel and Martin, 1999, 2000; Scott et al., 2003; Cochran et al., 2005). These lithological and micropaleontological techniques have revealed significant and generally synchronous centennial to millennial scale variability of intense hurricane activity throughout western North Atlantic. For example, Liu and Fearn (1993, 2000) and Liu (2004) established that the hurricane landfall along the Gulf Coast was more frequent between 3800 and 1100 years ago. They concluded that at least twelve category 4 or 5 hurricanes made landfall. In contrast, a quiescent period occurred between 1000 years ago and present when only one storm of category 4 or 5 struck the Gulf Coast, occurring about 500 year ago. A similar pattern has been observed from back-barrier marshes from southeastern Massachusetts (Buynevich and Donnelly, 2006) and back-barrier lagoons in Puerto Rico (Woodruff et al., 2004, 2005).

The landfalling Hurricanes Katrina and Rita provide access to unique and perishable geological and ecological data along the Gulf Coast (e.g. Travis 2005). We made measurements of the local topography, storm surge heights and extent of inundation within salt marsh environments from the Mississippi and Alabama coastlines (e.g. Turnipseed et al., 1998; Stumpf et al., 1999; Sallenger, 2000; Fischetti, 2001; USGS, 2005). We compared the sedimentology (grain size and organic content) and micropaleontology (foraminifera) of pre-storm surge and storm surge

sediment from Hurricanes Katrina and Rita to provide proxies to reconstruct past hurricane strikes.

2. Hurricanes Katrina and Rita

Tropical Depression Katrina formed in the Bahamas on August 23, 2005 and two days later achieved Category 1 hurricane status while turning west toward South Florida. Moving over the eastern Gulf of Mexico it rapidly increased its strength and reached Category 5 hurricane status on August 28 with maximum wind speeds of approximately 280 km/h and a minimum central pressure of 902 mb; the fourth lowest on record at that time for an Atlantic storm (NOAA-National Climatic Data Center, 2005). Before making landfall on the northern Gulf Coast, Katrina weakened to a strong Category 3 hurricane that created wave heights of over 16 m about 80 km east of the mouth of the Mississippi River (NOAA Buoy 42040). Early on Monday August 29, Katrina made landfall on the coast of Louisiana with a maximum wind speed of about 200 km/h and a central pressure of 920 mb (Fig 1). A few hours later and more than 110 km east of Hurricane Katrina's landfall, Dauphin Island, experienced sustained wind speeds of 122 km/h with gusts up to 164 km/h (NOAA-National Climatic Data Center, 2005).

Tropical Depression Rita formed in the Turks and Caicos Islands on September 18, 2005, and acquired hurricane status (Category 2) near the Florida coastline on 20 September. The storm quickly intensified and by the afternoon of September 21 achieved Category 5 hurricane status 434 km south-southeast of the mouth of Mississippi River. Hurricane Rita had peak wind speeds of 288 km/h and a minimum central pressure of 897 mb; the third lowest on record for an Atlantic storm (NOAA-National Climatic Data Center, 2005). Rita was a Category 3 status when it made landfall on September 24 with an estimated wind speed of 190 km/h (NOAA-National Climatic Data Center, 2005).

3. Study areas

Several geological or biological proxies are potentially useful in reconstructing past hurricane strikes, but so far the proxy that has proven the most useful is overwash sand layers deposited in the sediments of coastal lakes and marshes (e.g. Liu and Fearn, 1993, Liu, 2004, 2006; Donnelly and Woodruff, 2007). We selected three salt marsh sites (Ocean Springs, and St. Andrews, Mississippi, and Dauphine Island, Alabama) based on satellite images, aerial maps and preliminary site reconnaissance that met the following criteria: Hurricanes Katrina and/or Rita sediment was present; minimal site cleanup and reconstruction had been initiated; and a population was present for eyewitness accounts (Fig. 1).

Ocean Spring, Mississippi is located on the Gulf Coast, 40 km east of the region where the eye of Katrina came ashore in Plaquemines Parish, Louisiana. The study site consisted of an armoured shoreline, which protected a *Spartina alterniflora* and *Juncus roemerianus* marsh and woodland. A channel toward the back of the marsh feeds into the Gulf of Mexico. Scattered one and two storey housing is found within the woodland. St. Andrews, Mississippi lies further eastwards along the Gulf Coast, 50 km from the landfall of Katrina. The study site consisted of a narrow beach, which bordered the coastal road. A *Juncus roemerianus* marsh is enclosed by woodlands and is connected to the Gulf of Mexico by a small channel. St. Andrews Golf Course and its residential community have reclaimed much of the woodland and marsh. Dauphin Island is located directly south of Mobile, Alabama and 110 km east of the landfall of Katrina. The impacts of past and present hurricanes on this barrier island have previously been published (e.g. Sallenger et al., 2006); the island suffered overwash and breaches from Hurricanes Lili, Ivan and Dennis. The study site is towards the east of the island, where a *Juncus roemerianus* marsh is found landward of a beach lined by one and two-story stilted housing.

4. Methods

We made measurements of local topography, storm surge flow depth and inland extent along cross-shore transects at Ocean Springs and St. Andrews, Mississippi, and Dauphine Island, Alabama. Site evaluations were augmented by formal interviews with the residents. Due to the removal of benchmarks and local tide gauges, we set up a temporary benchmark (TBM) at each site using a fixed object, such as the concrete base of a water tower. The height above local sea level of the TBM was determined by staff and autolevel. This raw elevation was reduced to the accepted North American Vertical Datum 88 (NAVD88) by reference to the tide charts for the time the measurements were taken. Repeated measurements suggest the elevation of the TBM relative to NAVD88 is accurate to ± 10 cm. The location of each TBM was determined using a Leica SR530 GPS system to a horizontal accuracy of better than ± 5 m. From the TBM a series of leveled transects perpendicular to the coastline were conducted in order to establish the elevation of (i) the major geomorphic features and (ii) the elevation of high water marks above NAVD88. Other features (roads, coastline, housing, vegetation, etc) were mapped using GPS or digitized from aerial photographs and satellite imagery.

Following the methodology of the National Institute of Standards and Technology (NIST) (Link et al. 2006), U.S. Corps of Engineers (Gutierrez et al., 2006) and FEMA (FEMA, 2006a, b, c) we measured high water marks from the storm surges of Hurricanes Katrina and Rita using watermarks defined by water marks on buildings, scars on trees and rafted debris (Fig. 2a, b). The interpretation of watermarks on buildings is less straightforward, as discussed by Horton et al. (in press), and we have assumed that watermarks on the outside walls parallel to the direction of surge flow provide the most reliable estimates. The National Hurricane Center (2005) defines storm surge as “An abnormal rise in sea level accompanying a hurricane or other intense storm,

and whose height is the difference between the observed level of the sea surface and the level that would have occurred in the absence of the cyclone. Storm surge is usually estimated by subtracting the normal or astronomic high tide from the observed storm tide.”

Through detailed stratigraphic analyses, we selected a trench that was representative of the local salt marsh at each site. The trenches ran perpendicular to the shore to a depth of approximately 0.5 m. We photographed and stratigraphically described the sediment profiles using Tröels-Smith (1955) nomenclature. A 5 cm³ sample was taken for grain size and organic content, and 5 cm³ volume sample for foraminiferal analyses at 1 cm vertical sampling intervals.

4.1. Grain size analysis

We determined the grain size distribution using a Beckman Coulter laser particle-size analyzer (Beckman Coulter, 1999) following the sediment preparation procedures of Goff et al. (2004) and Hawkes et al. (2007). Grain sizes were based on Wentworth scale (1922). Organic content of the sediments was determined by loss on ignition following the procedures of Ball (1964), Bondevik et al. (1997) and Heiri et al. (2001). We used Principal Component Analysis (PCA) to detect, describe and classify patterns within the grain size and organic content distributions (following Brown, 1985; Ferrini and Flood, 2006). PCA is an ordination technique, which represents samples as points in multi-dimensional space where similar samples plot close together and dissimilar samples apart.

4.2. Foraminiferal analysis

Foraminiferal analysis followed the standard methods (e.g. Scott et al., 2001; Horton and Edwards, 2006; Murray, 2006). The identifications were confirmed to primary and secondary

type specimens from the Smithsonian Institution, Washington D.C. We stored samples in buffered ethanol. For surface samples we added the protein-specific stain rose Bengal to enable identification of foraminifera living at the time of collection and thus, allow the analyses of live, dead and total assemblages (e.g. Walton, 1952; Scott and Medioli, 1980a, b). Rose Bengal is used extensively to differentiate living from dead foraminifera (e.g. Scott and Medioli, 1980a; Murray and Bowser, 2000; Murray, 2006).

5. Results

5.1. Ocean Springs, Mississippi

Eyewitnesses stated that the storm surge of Hurricane Rita did not penetrate inland at Ocean Springs perhaps due to the seawall. Thus, we assume the general form and extent of the storm surge deciphered from watermarks and physical damage was solely from Hurricane Katrina (Fig. 3). As the storm surge came ashore perpendicular to the W-E shoreline, the maximum high water mark was 6.0 m above land elevation. The surge ran inland for 725 m to an elevation 7.35 m NAVD88. Extensively damaged housing was found throughout the study area, indicating that the storm surge penetrated inland with significant force.

Stratigraphic investigation of a sand sheet that was deposited on a salt marsh behind the armored shoreline revealed that it tapered landwards. We took samples from a 50 cm trench (Fig. 4), which was located 60 m inland at an elevation of 0.87 m NAVD88. We used field descriptions and grain size distributions to distinguish five stratigraphic units. These are confirmed by the PCA Axis 1 results, which show a significant change in score at each boundary. From the base of the trench, Unit OS1 was composed of c. 60% very fine grained silt and 20% clay with an lack of sand. The contact between units OS1 and OS2 was diffuse, with the overlying unit (23 cm to 19 cm) having a notable increase in fine and medium grained sand. Within unit OS3, the coarse grain

material was replaced by very fine-medium silt with the presence of plant macrofossils. The upper contact between the organic silt-clay (OS3) and the overlying sand (OS4), which was presumably laid down by the storm surge of Hurricane Katrina, was abrupt and erosive. The underlying herbaceous plants from the organic clay-silt were still in their growth position but have been pushed over in a landward direction. Unit OS4 was composed of c. 65% medium sand and c. 30% coarse sand from 9.5 cm to 1 cm. The fifth stratigraphical unit (unit OS5) was from 1 cm to 0 cm and showed a significant reduction of coarse grained sand.

The foraminifera showed a clear presence versus absence between the Hurricane Katrina storm surge sand deposit and the remaining stratigraphical units (Fig. 5). Units OS1 to OS3 and OS5 were dominated by agglutinated species such as *Arenoparrella mexicana*, *Haplophragmoides* spp. and *Trochammina inflata*, which are indicative of salt marsh environments. The number of foraminifera differed between stratigraphical units: Units OS1 and OS3 had total counts greater than 200 individuals per 5 cm³ with a mean of 323 ± 133 individuals per 5 cm³; whereas OS2 had a significant reduction to <155 individuals per 5 cm³. Foraminifera were absent within Unit OS4 and were in very low numbers within OS5 (38 individuals per 5 cm³). The assemblage of OS5 was similar to the other units, however some of the individuals were juveniles and living at the time of collection.

5.2. St. Andrews, Mississippi

Local residents described the maximum penetration of Hurricanes Katrina and Rita (Fig. 6). Both storm surges came ashore perpendicular to the shoreline crossing a small beach, a coastal road and penetrating St. Andrews golf course. Hurricane Katrina broke the foundations of a 20 m high water tower and carried it 50 m landwards onto the salt marsh (Fig. 2c). Based upon eyewitness accounts we believe that the detailed surveys at St. Andrews record the storm surge heights of

Hurricane Katrina. Watermarks along the coastline were identified as high as 8.26 m NAVD88 (storm surge depth 6.12 m). However, these were on walls facing the direction of flow and hence are considered an over estimate of the storm surge height. Watermarks on walls parallel to the direction of flow, and on electricity poles, suggest a storm surge depth of 5.23 m at the coast, decreasing to 0.88 m 745 m inland (Fig. 6). The maximum penetration of Katrina's storm surge was 780 m inland at an elevation of 6.52 m NAVD88. The maximum inland extent of Rita was 370 m with an elevation of maximum penetration of 3.43 m NAVD88.

We investigated the local stratigraphy of the salt marsh that was overlain by a sand sheet. The salt marsh enclosed by woodland and connected to the Gulf of Mexico by a small tidal creek. We selected a trench that was located 130 m inland at an elevation of 0.91 m NAVD88. Field and grain size analysis of sediment samples collected from the trench revealed eight stratigraphical units that alternate between fine grained organic units and coarser grained sand (Fig. 2d), which was supported by the PCA Axis 1 scores (Fig. 7). Unit SA1 was found at the base of the 50 cm trench consisting of silt and clay (>50% very fine to medium silt in all samples) with organics. This fine grained unit was overlain by Unit SA2, which consisted of a pronounced increase in fine to medium grain sand. Unit SA2 was found between 46 cm and 43 cm. Unit SA3 returned to fine grained silt-clay but with a lower organic content. The upper boundary at 34 cm was sharp and erosional. The overlying stratigraphical unit SA4 was dominated by fine and to medium grained sand between 34 cm and 25 cm (>44% in all samples). There was again a return to a fine grained unit with organics (25 cm to 19 cm). Unit SA5 had a sharp upper contact with the overlying fine and medium grained sand (SA6), which was found between 19 cm and 10 cm. There was a notable increase in very fine grained sand and organic content between 10 cm and 7 cm (SA7) before a return to a coarser grained sediment from 7 cm to 0 cm (SA8). The grain size distribution of SA8 showed a coarsening upward sequence; fine and very fine grained sand was

gradually replaced by medium and coarse grained sand. Based upon eyewitness reports we propose that SA6 and SA8 were laid down by the storm surges of Katrina and Rita, respectively.

The number of foraminifera at St. Andrews, Mississippi was low throughout the trench (Fig. 8) and the presence versus absence again supported the lithostratigraphical units. The coarse grained units SA2, SA4, SA6 and SA8 showed either an absence of foraminifera or very low counts (<12 individuals per 5 cm³), whereas the fine grain units were dominated by a mixed agglutinated and calcareous assemblage (e.g. *Haplophragmoides* spp., *Miliammina fusca*, *Trochammina inflata* and *Criboelphidium* spp.) indicative of a low marsh environments. It is interesting to note a relatively high number of foraminifera (>21 individuals per 5 cm³) was found in Unit SA7.

5.3. Dauphine Island, Alabama

Eyewitnesses attest that the storm surges of Hurricanes Katrina and Rita both made landfall along the island with the storm surge of the former event being much higher. There was extensive damage to buildings on this island as the result of Hurricane Katrina (Fig. 9). Because many houses had been destroyed or substantially repaired, it was difficult to obtain measurements of storm surge height close to the coast. Nevertheless, watermarks at locations 200 m to 300 m inland, some of which were protected by a 200 m wide beach, indicate storm surge depths of approximately 1.50 m. Local informants indicated that the storm surges of Katrina and Rita overwashed Dauphine Island from the Gulf into the Sound, thus the concept of inland extent does not apply.

Stratigraphical analysis of a sand sheet within a marsh on the lee of Dauphine Island indicated that it tapered landward. We selected a trench that was located 500 m inland from the Gulf at an elevation of 0.46 m NAVD8. From field and laboratory analyses we identified seven units; PCA

Axis 1 scores showed significant differences across stratigraphic contacts (Fig. 10). DI1 was found at the base of the trench to 49 cm. It consisted of an organic clay-silt with an absence of coarse sand. Overlying DI1 was a thin unit (DI2; 49 cm to 48 cm) with a pronounced increase in coarse grained sand (> 15%). An organic silt sand was found between 48 cm and 29 cm (DI3), which was overlain by another coarser grained unit between 29 cm and 21 cm (DI4; medium-coarse sand >30%). There was subsequently a return to an organic silt sand between 21 cm and 20 cm (DI5). This unit was abruptly overlain by a medium grained sand between 20 cm and 7 cm (DI6). The final unit (DI7) was also a coarse grained sand, although the grain size distributions suggested a fining upward sequence; coarse grained sand was gradually replaced by medium and fine grained sand. The boundary between DI6 and DI7 was very diffuse but with an increase in organics.

Foraminifera were found throughout the 50 cm trench except for samples within the upper most units (DI6 and DI7). Units DI1 to DI5 were dominated by agglutinated species such as *Ammobaculites* spp., *Arenoparella mexicana*, *Haplophragmoides* spp. and *Miliammina fusca*, indicative of a salt marsh environment (Fig. 11). There is a notable reduction in the number of foraminifera (4 individuals per 5 cm³) in DI2. Within DI6 and DI7 foraminifera only exist in very low numbers at their boundary (7 cm to 8 cm) and in the upper most sample. The surface sample assemblage is dominated by calcareous foraminifera such as *Ammonia* spp. and *Haynesina germanica*, which are indicative of estuarine environments.

6. Discussion

6.1. Storm surge inland penetration and water depth

Katrina's extensive size and the strength of the system just prior to landfall caused high storm surges in many coastal areas of Louisiana, Mississippi and Alabama. The storm surge heights

varied along the Gulf Coast and an accurate measurement of them is complicated by many factors (e.g. failures of tide gauges and the complete destruction of the buildings in many localities). A maximum high water mark of about 8 m NAVD88 was observed along the western coast of Mississippi (Mississippi Emergency Operation Center) with an inland penetration, suggested by the damage survey, of at least 9.6 km in many locations and up to about 19 km along bays and rivers (Link et al., 2006).

Further east along the Mississippi coast, large portions of Gulfport and Biloxi were flooded by a storm surge of about 6 m to more than 7 m NAVD88 (Link et al., 2006). Estimations of high water marks for the local county (Jackson) by the U.S. Corps of Engineers (2006) were between 3.5 m and 9 m NAVD88 (Gutierrez et al., 2006). Fritz et al. (2007) suggest the surge penetrated at least 10 km inland in many portions of coastal Mississippi and up to 20 km inland along bays and rivers. In Ocean Springs and St. Andrews we recorded similar high water marks (7.70 m NAVD88 and 7.83 m NAVD88, respectively) although the inland penetration was less than 1 km due to relief of the coastal lowlands and the presence of woodlands and wetlands in both study sites. An important ecosystem service of coastal wetlands is protection of inland human infrastructure (e.g. Dixon and Weight, 1995; Moeller et al., 1996; Fritz and Blount, 2007). There is some evidence that coastal mangrove forests reduced inland flooding and damage to infrastructure from the 2004 Indian Ocean tsunami (Dahdouh-Guebas et al., 2005; Kandasamy and Narayanasamy, 2005; Bird et al., 2007; Horton et al., in press). It is not clear how these findings translate to the Gulf Coast where forest and wetland morphology is much different and storm surges are driven by winds (Costanza et al., 2006; Greening et al., 2006).

Katrina produced a lesser but still massive surge along the Alabama coast, with surge heights from 1.5 m NAVD88 to more than 3 m NAVD88 recorded at Mobile and about 1.8 m NAVD88 along Dauphin Island (NOAA-National Climatic Data Center, 2005). Fritz et al. (2007) suggest

that storm surge heights of the Alabama Barrier Islands were between 3.5 and 5.5 m above mean sea level. Our measurements are consistent with a maximum recorded high water mark of 3.43 m NAVD88.

With respect to Hurricane Rita, only a few direct observations of high water marks were available (NIST, 2006). Rita produced a very significant storm surge of 4.6 m at Cameron in the southwest Louisiana (near the landfall site) and high water marks of about 3 m to 1.8 m were recorded in many other sites of southwest Louisiana (NIST, 2006). McGee et al. (2006) reported that the storm surge of Hurricane Rita brought saline waters 20 km inland onto coastal wetlands. Along the southeastern Louisiana coastline, the same areas that had already been impacted by the surge from Hurricane Katrina were flooded by a surge of about 2.3 m to 1.2 m. We can only estimate the maximum inland extent of Rita (370 m) and elevation of maximum penetration (3.43 m NAVD88) at St. Andrews, Mississippi.

6.2. Stratigraphy and Sedimentology

Hurricane storm surges can cause large scale redistribution of sediments resulting in sediment deposition, erosion, compaction, disruption of vegetated substrates or some combination of these (Morgan et al., 1958; Liu and Fearn, 1993, 2000; Nyman et al., 1995; Donnelly et al., 2001a, b; Cahoon, 2003, 2006; Sedgwick and Davis, 2003; Sallenger et al., 2006; Turner et al., 2006, 2007; Burkett et al., 2007). Although these effects are readily observable rarely have storm impacts on coastal wetlands been measured directly (Cahoon, 2006). At each of our study sites we observed a three-dimensional distribution of a sand sheet that tapered landward overlying salt marsh sediment. At Ocean Springs a 9.5 cm thick layer of medium to coarse grain sand was deposited by the storm surge of Hurricane Katrina. However, at both St. Andrews and Dauphine Island we believe that Hurricanes Katrina and Rita deposited separate sedimentary packages. At these study

sites two coarse grained units that were identifiable in the field were separated by a decrease in grain size and/or an increase in organic content, which was supported by multivariate analysis.. Furthermore, eyewitnesses described significant deposition of sediment from both events. Moreover, foraminiferal analysis showed a small, but notable presence of foraminifera between the sedimentary packages. The sedimentary thicknesses of Hurricanes Katrina and Rita at St. Andrews and Dauphine Island were 9 cm and 7 cm, and 13 cm and 7 cm, respectively. It has been recognized that hurricanes are capable of introducing sediments onto salt marshes (Turner et al., 2006). For example, Bauman et al. (1984) found between 1.4 cm and 2.2 cm of sediment accretion in salt marshes of Barataria Bay, Louisiana following Hurricane Bob (>1 m storm-surge) and tropical storm Claudette. A similar thickness of sediment deposition (2.2 cm) was observed by Rejmánek et al. (1988) in the marshes of the Atchafalaya Delta, Louisiana after Hurricane Danny in 1985 (>2 m storm surge). Cahoon et al. (1995) and Nyman et al. (1995) documented between 2 cm and 6 cm, and 0 cm and 9 cm, respectively, in marshes of Louisiana following the landfall of Hurricane Andrew (2 m storm surge). Notably, Turner et al. (2006) measured between 0 cm and 68 cm (mean of 5.8 cm) of hurricane-induced sedimentation at 198 locations along the Gulf Coast following Hurricanes Katrina and Rita.

A comparison of the grain size distributions among our study sites reveals the complex nature of sediment deposition. At Ocean Springs field description and grain size distribution recorded one massive coarse and medium sand unit indicating high energy surge flow and rapid mass deposition (Nanayama et al., 2000; Donnelly et al., 2001a, b; Goff et al, 2004). However, at St. Andrews and Dauphine Island we recorded coarsening upwards and fining upwards sequences, respectively, in Hurricane Rita's storm surge sedimentary unit. Generally storm inundation is gradual and prolonged consisting of many waves with relatively little return flow until after the main flooding event. Coarsening upward sequences signify a renewed flow energy by the arrival of a subsequent wave or increased energy during backflow. In contrast, fining upward sequences

reflect the gradual decrease in flow energy to a point where increasingly smaller particles fall out of suspension. This generally occurs as flow naturally decreases with time or as it inundates landward and energy is lost with distance or flow is prematurely slowed by geomorphology or topography (Goff et al., 2004).

The difference between the pre-storm surge and storm surge sediment at our study sites was defined by the following characteristics: a sharp or erosional boundary between sedimentary units, which was accompanied by a change in color and lithology; and the overlying storm surge sediment was coarser than the pre-storm surge unit with a lower organic content. With respect to paleotempestology, the stratigraphical analyses of all study sites revealed coarse grained units that may relate to previous hurricane-induced sedimentation. Although the abrupt boundaries were commonly absent and there was some sediment mixing, these coarse grained units were readily identified in the field and through grain size analysis. Similarly, Liu and Fearn (2000) inferred from sediment cores from Western Lake, Florida, that coarse grained sand unit overlying finer, organic-rich sediment represent catastrophic hurricanes of category 4 or 5 intensity.

6.3. Foraminiferal analysis

A small number of studies have noted that storm surges may not apparent be from the sedimentology alone, but are better recognized based on a combination of lithological and micropaleontological analysis (Hippensteel and Martin, 1999). For example, Collins et al. (1999), Scott et al. (2003) and Cochran et al. (2005) all found unusually high populations and an increase in species diversity of calcareous foraminifera within storm layers. Furthermore, Hippensteel and Martin (1999, 2000) and Hippensteel et al. (2005) inferred that sedimentary layers of Oligo-Miocene deepwater benthic foraminifera (e.g. *Uvigerina* spp., *Siphogenerina* spp.) separated by

mud-rich layers containing shallow-water foraminifera such as *Ammonia beccarii* and *Elphidium* spp. are indicative of hurricane deposits.

In contrast, our foraminiferal analysis revealed a virtual absence of tests within the coarse grained storm surge sediments, although they were present within the fine grained organic sediments. These *in-situ* assemblages were dominated by agglutinated taxa such as *Arenoparella mexicana*, *Haplophragmoides* spp., *Miliammina fusca* and *Trochammina inflata*, which are indicative of salt marsh environments (e.g. Scott and Medioli, 1980b, de Rijk, 1995; Horton and Edwards, 2006; Murray, 2006). The absence of foraminifera may be due to initial size of the standing crop of the source material, the number of individuals that reproduce, frequency of reproduction and number of progeny (Murray, 2006). Reproduction results in the foraminifera cell vacating the test. Therefore, all empty tests, either from reproduction or death are added to the death assemblage (Horton and Murray, 2007). All life assemblages are subject to variations in production and the death assemblages are affected by its cumulative effects (Horton and Murray, 2006). Although, seasonal hypoxia on the Louisiana shelf is widespread (Rabalais et al., 2000; Rabalais and Turner, 2001) and thus, may cause significant environmental stress to the foraminiferal population (Alve, 1995a), there is always a sizeable benthic foraminiferal assemblage in surface sediments (Platon et al., 2005). With greater certainty, foraminifera would indeed be rare in a sand substrate with no or insignificant fine grained material, especially if the source of the sand was a beach sand or dune sand. In non-carbonate areas, foraminifera are extremely rare in beach sands because of taphonomy, and absent in coastal dunes.

Alternatively, the absence of foraminifera within the storm surge sediment may be due to post-depositional changes. Post-depositional changes are the result of diagenetic processes such as preservation of foraminifera and transportation of tests (Murray, 1991). The tests of calcareous foraminifera will be subject to dissolution due to the low pH of the underlying salt marsh

sedimentary units at all the study sites (Scott and Medioli, 1980b; Williams, 1989; Jonasson and Patterson, 1992, de Rijk; 1995; Edwards and Horton, 2000). Transportation by suspended load is selective and depends on overall size and specific gravity of the foraminifera (Murray, 1965; Nichols and Norton, 1969; Berger, 1970). Thus, foraminifera may be winnowed out during a storm surge and deposited when flow energy had reduced substantially to allow the tests to fall out of suspension. However, most foraminifera, especially those with thick shells (e.g. rotalids) have a specific density very similar to quartz grains.

Finally, it is worth noting that low numbers of foraminifera were present in the surface sample of all study sites. Some of these individuals were juveniles and living at the time of collection. Benthic foraminifera are known to disperse and effectively colonize new or remediated settings such as a storm surge deposit (e.g. Buzas and Culver, 1994; Alve, 1995b), yet their dispersal mechanisms are poorly understood (Alve, 1999; Alve and Goldstein, 2003).

7. Conclusions

A major obstacle in producing reliable predictions of catastrophic environmental changes is a lack of data on time scales longer than the short instrumental record. Obtaining a record of present and past events, and the extent of coastal impacts, is one means to assess future risk and test the possibility that the recent cluster of hurricane events along the Gulf Coast may be linked to global environmental change.

We rapidly dispatched survey teams to collect the data from Hurricanes Katrina and Rita storm surge along the Alabama and Mississippi coastline. We made high resolution ground surveys of local topography, storm surge flow depth and flow direction. In Mississippi we recorded Hurricane Katrina storm surge heights greater than 7.5 m NAVD88 with inland extents greater

than 750 m. Katrina produced a lesser but still massive surge along the Alabama coast, with a maximum recorded storm surge depth of 3.43 m NAVD88. We could only estimate the maximum inland extent of Rita (370 m) and elevation of maximum penetration (3.43 m NAVD88) at St. Andrews, Mississippi.

We examined sediment deposit thickness and character along cross-shore transects at our study sites. We measured and described the deposits in the field and performed sedimentological, foraminiferal and statistical analyses. We observed a three-dimensional distribution of storm surge deposits that tapered landward overlying salt marsh sediment. The difference between the pre-storm surge and storm surge sediment was defined by the following characteristics: a sharp or erosional boundary between sedimentary units accompanied by a change in color and a change in lithology; and the overlying storm surge sediment was coarser than the pre-storm surge unit with a lower organic content. The thickness of the Hurricanes Katrina and Rita storm surge sediments ranged from 9 cm to 13 cm and 7 cm, respectively.

Foraminiferal analyses supported the sedimentological analyses; all three sites revealed a virtual absence of tests within the storm surges sediments. Furthermore, there were notable reductions in the number of individuals in all coarse grained units within the sedimentary sequences, possibly indicative of paleostorm deposits. Foraminifera were present in the underlying salt marsh sediments and in low numbers in the surface sample of all study sites.

Acknowledgments

We acknowledge and greatly appreciate research funding provided by a special topic award from the National Science Foundation (SES-0522133) and Dipartimento di Scienze della Terra e Geologico-Ambientali, Università di Bologna. In addition we gratefully thank the Design and

Imaging Unit of the Department of Geography, University of Durham for the illustrations. Finally, we thank the graduate students from Department of Earth and Environmental Science University of Pennsylvania (Andrew 'Derby' Kemp, Chris Bernhardt, Jamie Bedison, Kyo Tanoë and Simon Engelhart) and Matt Wright for their field assistance.

References

Alve, E., 1995a. Benthic foraminiferal responses to estuarine pollution. A review. *Journal of Foraminiferal Research* 25, 190-203.

Alve, E., 1995b. Benthic foraminiferal distribution and recolonization of formerly anoxic environments in Drammensfjord, southern Norway. *Marine Micropaleontology* 25, 169-186.

Alve, E., 1999. Colonization of new habitats by benthic foraminifera: A review. *Earth-Science Review* 46, 167–185.

Alve, E., Goldstein, S. T., 2003. Propagule transport as a key method of dispersal in benthic foraminifera (Protista). *Limnology Oceanography* 48, 2163–2170.

Ball, D.F., 1964. Loss-on-ignition as an estimate of organic matter and organic carbon in non-calcareous soils. *Journal of Soil Science* 15, 84-92.

Bauman, R., Day, J. J.W., Miller, C., 1984. Mississippi deltaic wetland survival: sedimentation versus coastal subsidence. *Science* 224 (6), 1093-1095.

Beckman Coulter, 1999. Beckman Coulter LS 13320 Series Particle size analyzer. Beckman Coulter, Inc. California, pp. 12.

Berger, W.H., 1970. Planktonic foraminifera: selective solution and the lysocline. *Marine Geology* 8, 111-138.

Bird, M., Cowie, S., Hawkes, A., Horton, B.P., Macgregor, C., Ong, J.E., Shau Hwai, A.T., Tiong Sa, T., Zulfigar, Y., 2007. Indian Ocean Tsunami – environmental and socio-economic impacts in Langkawi, Malaysia. *The Geographical Journal*, 173, doi: 10.1111/j.1475-4959.2007.00224..

Bondevik, S., Svendsen, J.I., Mangerud, J., 1997b. Tsunami sedimentary facies deposited by the Storegga tsunami in shallow marine basins and coastal lakes, western Norway. *Sedimentology* 44, 1115-1131.

Brown, A. G., 1985. Traditional and multivariate techniques in the interpretation of floodplain sediment grain size variations. *Earth Surface Processes and Landforms* 10, 281-291.

Bourne, J.K., 2004. Gone with the Water. *National Geographic*, October, 88-105.

Burkett, V., Groat, C.G., Reed, D., 2007. Hurricanes Not the Key to a Sustainable Coast. *Science* 315, 1366-1367.

Buynevich, I.V., Donnelly, J.P., 2006. Geological signatures of barrier breaching and overwash, southern Massachusetts, U.S.A. *Journal of Coastal Research* SI 39, 112-116

Buzas, M.A., Culver, S.J., 1994. Species pool and dynamics of marine paleocommunities. *Science* 264, 1439–1441.

Cahoon, D.R., 2006. A review of major storm impacts on coastal wetland elevations. *Estuaries and Coasts* 29 (6A), 889-898.

Cahoon, D.R., Hensel, P., Rybczyk, J., McKee, K., Proffitt, C.E., Perez, B., 2003. Mass tree mortality leads to mangrove peat collapse at Bay Islands, Honduras after Hurricane Mitch. *Journal of Ecology* 91 (6), 1093-1105.

Cahoon, D.R., Reed, D., Day, J.J.W., 1995. Estimating shallow subsidence in microtidal salt marshes of the southeastern United States: Kaye and Barghoorn revisited. *Marine Geology* 128 (1), 1-9.

Cochran, U.A., Berryman, K.R., Middledhall, D.C., Hayward, B.W., Southall, K., and Hollis, C.J., 2005. Towards a record of Holocene tsunami and storms for northern Hawke's Bay, New Zealand. *New Zealand Journal of Geology and Geophysics*, 48, 507-515.

Collins, E.S., Scott, D.B., Gayes, P.T., 1999. Hurricane records on the South Carolina coast: Can they be detected in the sediment record? *Quaternary International* 56, 15-26.

Costanza, R., Mitsch, W.J., Day, J.W., 2006. A new vision for New Orleans and the Mississippi Delta: Applying ecological economics and ecological engineering. *Frontiers in Ecology and the Environment* 4, 465-472.

Dahdouh-Guebas, F., Jayatissa, L.P, Di Nitto, D., Bosire, J.O., Lo Seen, D., Koedam, N., 2005. How effective were mangroves as a defence against the recent tsunami? *Current Biology* 15 (12), 443-447.

Dixon M., Weight R., 1995. Managing coastal realignment – case study at Orplands sea wall, Blackwater Estuary, Essex. In: Halcrow, W. (Ed.), *Saltmarsh management for flood defense*, London, NRA.

Donnelly, J.P., Woodruff, J.D. 2007. Intense hurricane activity over the past 5,000 years controlled by El Niño and the West African Monsoon. *Nature* 447, 465-468.

Donnelly, J.P., Bryant, S.S., Butler, J., Dowling, J., Fan, L., Hausmann, N., Newby, P.N., Shuman, B., Stern, J., Westover, K., Webb, T. III, 2001b. A 700-year sedimentary record of intense hurricane landfalls in southern New England. *Geological Society of America Bulletin* 113, 714-727.

Donnelly, J.P., Roll, S., Wengren, M., Butler, J., Lederer, R., Webb, T. III, 2001a. Sedimentary evidence of intense hurricane strikes from New Jersey. *Geology* 29, 615-618.

Edwards, R.J., Horton, B.P., 2000. High Resolution Records of Relative Sea-Level Change from U.K. Salt-marsh Foraminifera. *Marine Geology* 169, 41-56.

Elsner, J.B., 2007. Tempests in time. *Nature* 447, 647-649.

Emanuel, K., 2005. Increasing destructiveness of tropical cyclones over the past 30 years. *Nature* 436, 686-688.

Enserink, M., Bohannon, J., 2005. News Focus: Questioning the 'Dutch Solution'. *Science* 309, 1809.

FEMA, 2006a. High Water Mark Collection for Hurricane Katrina in Louisiana. FEMA-1603-DR-LA, Task Orders 412 and 419, Federal Emergency Management Agency, Denton, Texas.

FEMA, 2006b. Final Coastal and Riverine High Water Mark Collection for Hurricane Katrina in Mississippi. FEMA-1604-DR-MS, Task Orders 413 and 420, Federal Emergency Management Agency, Atlanta, Georgia.

FEMA, 2006c. High Water Mark Collection for Hurricane Katrina in Alabama. FEMA-1605-DR-AL, Task Orders 414 and 421, Federal Emergency Management Agency, Atlanta, Georgia.

Ferrini, V. L. and Flood, R.D., 2006. The effects of fine-scale surface roughness and grain size on 300 kHz multibeam backscatter intensity in sandy marine sedimentary environments. *Marine Geology* 228, 153-172.

Fischetti, M., 2001. Drowning New Orleans. *Scientific American* 285, 76-84.

Fritz, H.M., Blount, C., 2007. Role of forests and trees in protecting coastal areas against cyclones. In: *Coastal Protection in the Aftermath of the Indian Ocean Tsunami: What Role for Forests and Trees?* Proceedings of an FAO Regional Technical Workshop, Khao Lak, Thailand, 28–31 August 2006. FAO, Bangkok.

Fritz, H. M., Blount, C., Sokoloski, R., Singleton, J., Fuggle, A., McAdoo, B. G., Moore, A., Grass, C., Tate, B., (2007. "Hurricane Katrina storm surge distribution and field observations on the Mississippi Barrier Islands." *Estuarine, Coastal and Shelf Science* 74 (1-2): 12-20.

Goff, J., McFadgen, B.G., Chagué-Goff, C., 2004. Sedimentary differences between the 2002 Easter storm and the 15th-century Okoropungo tsunami, southeastern North Island, New Zealand. *Marine Geology* 204 (1-2), 235-250.

Greening, H., Doering, P., Corbett, C., 2006. Hurricane impacts on coastal ecosystems. *Estuaries and Coasts* 29 (6A), 877-879.

Gutierrez, C. M., Cresanti, R., Jeffrey, W.A., 2006. Performance of Physical Structures in Hurricane Katrina and Hurricane Rita: A Reconnaissance Report NIST Technical Note 1476, US Department of Commerce, Washington, DC.

Hawkes, A.D., Bird, M., Cowie, S., Grundy-Warr, C., Horton, B.P., Aileen Tan, S.H., Law, L., Macgregor, C., Nott, J., Ong, J.E., Rigg, J., Robinson, R., Tan-Mullins, M., Tiong Sa, T., Yasin, Z., Aik, L.W., 2007. Sediments deposited by the 2004 Indian ocean tsunami along the Malaysia-Thailand peninsula. *Marine Geology*, 242, 169-190.

Heiri, O., Lotter, A.F., Lemcke, G., 2001. Loss on ignition as a method for estimating organic and carbonate content in sediments: reproducibility and comparability. *Journal of Paleolimnology* 25, 101-110.

Hippensteel, S.P., Martin, R.E., 1999. Foraminifera as an indicator of overwash deposits, barrier island sediment supply, and barrier island evolution, Folly Island, South Carolina. *Palaeogeography, Palaeoclimatology, Palaeoecology* 149, 115–125.

Hippensteel, S.P., Martin, R.E., 2000. Foraminifera of storm-generated washover fans: Implications for determining storm frequency in relation to sediment supply and barrier island evolution, Folly Island, South Carolina, 351-369. In: Martin, R.E. (Ed), *Environmental Micropaleontology*. Kluwer Academic/Plenum Publishers, New York, pp. 481.

Hippensteel, S.P., Martin, R.E., 1999. Foraminifera as an indicator of overwash deposits, barrier island sediment supply, and barrier island evolution, Folly Island, South Carolina: *Palaeogeography, Palaeoclimatology, Palaeoecology* 149, 115–125.

Hippensteel, S.P., Martin, R.E., Harris, M. S., 2005. Records of prehistoric hurricanes on the South Carolina coast based on micropaleontological and sedimentological evidence, with comparison to other Atlantic Coast records: Discussion. *GSA Bulletin* 117, 250-253.

Horton, B.P., Edwards, R.J., 2006. Quantifying Holocene Sea Level Change Using Intertidal Foraminifera: Lessons from the British Isles. *Cushman Foundation for Foraminiferal Research, Special Publication* 40, pp. 97.

Horton, B.P., Murray, J.W., 2006. Patterns in cumulative increase in live and dead species from foraminiferal time-series of Cowpen Marsh, Tees Estuary, UK: implications for sea-level studies. *Marine Micropaleontology* 58, 287-315.

Horton, B.P., Murray, J.W., 2007. The roles of elevation and salinity as primary controls on living foraminiferal distributions: Cowpen Marsh, Tees Estuary, UK. *Marine Micropaleontology*, 63, 169-186.

Horton, B.P., Bird, M.I., Cowie, S.A., Ong, J.E., Hawkes, A., Tan S.H., Gong, W.K., Colin Macgregor, C., The, T.S., Yasin, Z., in press. Indian Ocean tsunami – environmental and socio-economic impacts in Penang, Malaysia. *Singapore Journal of Tropical Geography*.

Jonasson, K.E., Patterson, R.T., 1992. Preservation potential of salt marsh foraminifera from the Fraser River delta, British Columbia. *Micropaleontology* 38, 289-301.

Kandasamy, K., Narayanasamy, R., 2005. Coastal mangrove forests mitigated tsunami. *Estuarine, Coastal and Shelf Science* 65, 601-606.

Kerry, E., 2001. The contribution of tropical cyclones to the oceans' meridional heat transport. *Journal of Geophysical Research* 106, 771-778.

Kerry, E., 2003. Tropical cyclones. *Annual Review of Earth and Planetary Sciences* 31, 75-104.

Laska, S., 2004. What if Hurricane Ivan Had Not Missed New Orleans? *Natural Hazards Observer* 29, 5-6.

Levitus, S., Antonov, J., Boyer, T.P., Stephens, C., 2000. Warming of the World Ocean. *Science* 287, 2225-2229.

Levitus, S., Antonov, J., Wang, T.L., Delworth, K., Dixon, W., Broccoli, A.J., 2001. Anthropogenic warming of earth's climate system. *Science* 292, 267-270.

Link, L.E., Jaeger, J.J., Stevenson, J., Stroupe, W., Mosher, R.L., Martin, D., Garster, J.K., Zilkoski, D.B., Ebersole, B.A., Westerwink, J.J., Resio, D.T., Dean, R.G., Sharp, M.K., Steedman, R.S., Duncan, J.M., Moentenich, B.L., Howard, R., Harris, J., Fitzgerald, S., Moser, D.A., Canning, P., Foster, J., Muller Jr. B.C., 2006. Performance Evaluation of the New Orleans and Southeast Louisiana Hurricane Protection System: Draft Final Report of the Interagency Performance Evaluation Task Force (IPET), United States Army Corps of Engineers (USACE), vols. 1-9.

Liu, K.B., 2004. Paleotempestology: Geographic solutions to hurricane hazard assessment and risk prediction. In: Janelle, D., Warf, B., Hansen, K. (Eds), *WorldMinds: Geographical Perspectives on 100 Problems*. Kluwer Academic Publishers, Dordrecht, pp. 443-448.

Liu, K., Fearn, M.L., 1993. Lake-sediment record of late Holocene hurricane activities from coastal Alabama. *Geology* 21, 793-796.

Liu, K., Fearn, M.L., 2000. Reconstruction of prehistoric landfall frequencies of catastrophic hurricanes in northwestern Florida from lake sediment records. *Quaternary Research* 54, 238-245.

Louisiana Coastal Wetlands Conservation and Restoration Task Force and Wetlands Conservation and Restoration Authority, 1998. *Coast 2050: Toward a sustainable coastal Louisiana*. Louisiana Department of Natural Resources, Baton Rouge, LA.

Mann, M., Kerry E., 2006. Atlantic hurricane trends linked to climate change. *EOS* 87, 233-241.

McGee, B.D., Goree, B.B., Tollett, R.W., Woodward, B.K., Kress, W.H., 2006. Hurricane Rita Surge Data, Southwestern Louisiana and Southeastern Texas, September to November 2005. U.S. Geological Survey Data Series 220.

McPhee, J., 1989. *The control of nature*. Collins Publishers, Toronto, pp. 272.

Moeller, I., Spencer, T., French, J., 1996. Wind wave attenuation over saltmarsh surfaces: preliminary results from Norfolk, England. *Journal of Coastal Research* 12, 1009-1016.

Morgan, J.P., Nichols, L.G., Wright, M., 1958. Morphological effects of hurricane Audrey on the Louisiana coast. Coastal Studies Institute Report 58-3. LSU, Baton Rouge, La 70803, pp. 53.

Murray, J.W., 1965. On the foraminifera of the Plymouth Region. *Journal of the Marine Biological Association of the United Kingdom* 45, 481-505.

Murray, J.W., 1991. *Ecology and palaeoecology of benthic foraminifera*. Longman Scientific and Technical, Harlow, England, 397 pp.

Murray, J.W., 2006. *Ecology and Applications of Benthic Foraminifera*. Cambridge University Press, pp. 426.

Murray, J.W., Bowser, S.S., 2000. Mortality, protoplasm decay rate, and reliability of staining techniques to recognize 'living' foraminifera: a review. *Journal of Foraminiferal Research* 30, 66-77.

Nanayama, F., Shinego, K., Satake, K., Shimokawa, K., Koitabashi, S., Miyasaka, S., Ishii, M., 2000. Sedimentary differences between the 1993 Hokkaido-nensei-oki tsunami and the 1959 Miyakojima typhoon at Taisei, southwestern Hokkaido, northern Japan. *Sedimentary Geology*, 135, 255-264.

National Hurricane Center, 2005, <http://www.nhc.noaa.gov/ms-word/> http://www.nhc.noaa.gov/ms-word/TCR-AL182005_Rita.doc

Nichols, M.M., Norton, W., 1969. Foraminiferal populations in a coastal plain estuary. *Palaeogeography, Palaeoclimatology, Palaeoecology* 6, 197-213.

NOAA's National Climatic Data Center, 2005. Hurricane Katrina a climatological perspective – preliminary report.

Nyberg, J., Malmgren, B.A., Winter, A., Jury, M.R., Kilbourne K.H., Quinn, T.M., 2007. Low Atlantic hurricane activity in the 1970s and 1980s compared to the past 270 years. *Nature* 447, 698-701.

Nyman, J.A., Crozier, C.R., DeLaune, R.D., 1995. Roles and patterns of hurricane sedimentation in an estuarine marsh landscape. *Estuarine Coastal and Shelf Science* 40, 665-679.

Parsons, M.L., 1998. Salt marsh sedimentary record of the landfall of hurricane Andrew on the Louisiana Coast: diatoms and other paleoindicators. *Journal of Coastal Research* 14, 939-950.

van de Plassche, O., Wright, A.J., van der Borg, K., de Jong, A.F.M., 2004. On the erosive trail

of a 14th and 15th century hurricane in Connecticut (USA) salt marshes. *Radiocarbon* 46, 775-784.

Platon, E., Sen Gupta, B.K., Rabalais, N.N., Turner, R.E., 2005. Effect of seasonal hypoxia on the benthic foraminiferal community of the Louisiana inner continental shelf: The 20th century record *Marine Micropaleontology* 54, 263-283.

Rabalais, N.N., Turner, R.E., 2001. Hypoxia in the northern Gulf of Mexico: description, causes and changes. In: Rabalais, N.N., Turner, R.E. (Eds.), *Coastal Hypoxia: Consequences for Living Resources and Ecosystems*, American Geophysical Union Coastal and Estuarine Studies, vol. 58. American Geophysical Union, Washington, pp. 1– 36.

Rabalais, N.N., Smith, L.E., Harper Jr., D.E., Justic, D., 2001. Effects of seasonal hypoxia on continental shelf benthos. In: Rabalais, N.N., Turner, R.E. (Eds.), *Coastal Hypoxia: Consequences for Living Resources and Ecosystems*. American Geophysical Union, Washington, pp. 211 –240.

Rabalais, N.N., Turner, R.E., 2001. Hypoxia in the northern Gulf of Mexico: description, causes and changes. In: Rabalais, N.N., Turner, R.E. (Eds.), *Coastal Hypoxia: Consequences for Living Resources and Ecosystems*. American Geophysical Union Coastal and Estuarine Studies 58, American Geophysical Union, Washington, pp. 1– 36.

Reed, D.J., 1989. Patterns of sediment deposition to subsiding coastal salt marshes, Terrebonne Bay, Louisiana: The role of winter storms. *Estuaries* 12, 222-227.

Rejmánek, M., Sasser, C.E., Peterson, G.W., 1988. Hurricane-induced sediment deposition in a gulf coast marsh. *Estuarine, Coastal and Shelf Science* 27 (2), 217-222.

de Rijk, S., 1995. Salinity control on the distribution of salt marsh Foraminifera (Great Marshes, Massachusetts). *Journal of Foraminiferal Research* 25, 156-166.

Sallenger, A.H. Jr., 2000. Storm impact scale for barrier islands. *Journal of Coastal Research* 16, 890-895.

Sallenger, A.H., Stockdon, H.F., Fauver, L., Hansen, M., Thompson, D., Wright, C.W., Lillycrop, J., 2006. Hurricanes 2004: An Overview of Their Characteristics and Coastal Change. *Estuaries and Coasts* 29, 880-888.

Scott, D.B., Medioli, F.S., 1980a. Living vs. total foraminifera populations: Their relative usefulness in paleoecology. *Journal of Paleontology* 54, 814-831.

Scott, D.B., Medioli, F.S., 1980b. Quantitative studies of marsh foraminifera distribution in Nova Scotia: implications for sea-level studies. *Journal of Foraminiferal Research, Special Publication* 17, 1-58.

Scott, D.B., Collins, E.S., Gayes, P.T., Wright, E., 2003. Records of prehistoric hurricanes on the South Carolina coast based on micropaleontological and sedimentological evidence, with comparison to other Atlantic Coast records. *GSA Bulletin* 115, 1027-1039.

Scott, D.B., Medioli, F.S., Schafer, C.T., 2001. *Monitoring in coastal environments using foraminifera and thecamoebian indicators*. Cambridge University Press, London, pp. 175.

Sedgwick, P.E., Davis, R.A., 2003. Stratigraphy of washover deposits in Florida: Implications for recognition in the stratigraphic record. *Marine Geology* 200, 31-48.

Sriver, R.L., Huber, M., 2007. Observational evidence for an ocean heat pump induced by tropical cyclones, *Nature* 447, 577-580.

Stumpf, R., Morgan, K., Peterson, R., Krohn, M.D., Sallenger, A.H., 1999. Mapping impacts of Hurricanes Fran and Bertha on the North Carolina coast. *Coastal Sediments* 99, 1826-1835.

Tidewell, M., 2004. *Bayou Farewell: the Rich Life and Tragic Death of Louisiana's Cajun Coast*. Vintage Publishers, pp. 368.

Travis, J., 2005. News: Scientists' Fears Come True as Hurricane Floods New Orleans. *Science* 309, 1656-1659.

Trøels-Smith, J., 1955. Characterization of unconsolidated sediments. *Danmarks Geologiske Undersogelse, Series IV* 3, 38-73.

Turner, E.R., Baustian, J.J., Swenson, E.M., Spicer, J.S., 2006. Wetland Sedimentation from Hurricanes Katrina and Rita. *Science* 314, 449-452.

Turner, E.E., Baustian, J.J., Swenson, E.M., Spicer, J.S., 2007. Response: Hurricanes Not the Key to a Sustainable Coast. *Science* 315, 1367-1368.

Turnipseed, D.P., Giese, G., Pearman, J.L., Farris, G., Krohn, M.D., Sallenger, A., 1998. Hurricane Georges: headwater flooding, storm surge, beach erosion, & habitat destruction on the central Gulf coast. United States Geological Survey Water Resources Investigations Report, 98-4231.

Twain, M., 1882. The flood still Rising, 497 – 500. In: Teacher, L. (Ed.), *The Unabridged Mark Twain*, Port City Press, Baltimore, pp. 1289.

United States Geological Survey, 2005. Hurricane and Extreme Storm Impact Studies.

Walton, W.R., 1952. Techniques for recognition of living foraminifera. *Contributions from Cushman foundation for Foraminiferal Research* 3, 56-60.

Webster, P.J., Holland, G.J., Curry, J.A., Chang, H.-R., 2005. Changes in Tropical Cyclone Number, Duration, and Intensity in a Warming Environment. *Science* 309, 1844-1846.

Wentworth, C.K., 1922. A scale of grade and class terms for clastic sediments. *Journal of Geology* 30, 377-392.

Williams, H.F.L., 1989. Foraminiferal zonation on the Fraser River Delta and their application to paleoenvironmental interpretations. *Palaeogeography, Palaeoclimatology, Palaeoecology* 73, 39-50.

Woodruff, J.D., Donnelly, J.P., Scileppi, E., 2004. Sedimentary archives of extreme flooding events in the Northeastern Caribbean. *Eos, Transactions, American Geophysical Union* 85 (47), Fall Meet. Suppl. Abstract H41C-0304.

Woodruff, J.D., Donnelly, J.P., Tierney, J., Scileppi, E., Giosan, L., 2005. Geochemical and sedimentological evidence of varying intense hurricane activity and precipitation patterns from the Caribbean during the late Holocene. *Eos, Transactions, American Geophysical Union* 86 (52) Fall Meet. Suppl. Abstract PP14B-03.

Figures

- Fig. 1 Location of Ocean Springs, Mississippi, St. Andrews, Mississippi, and Dauphine Island, Alabama study sites along the Gulf Coast. The paths of Hurricane Katrina and Rita are shown.
- Fig. 2 High water marks from Hurricane Katrina's storm surge: (a) thin film of mud on buildings; and (b) water and sediment in an exterior light. (c) The final resting position of water tower at St. Andrews, Mississippi and (d) the sedimentary sequence from a core extruded from St. Andrews, Mississippi showing sedimentary units SA3 to SA8.
- Fig. 3 Location Map of Ocean Springs, Mississippi, showing geomorphology and buildings that were impacted by the storm surges. The two numbers show the elevation (m NAVD88) and water depth (m), respectively. The maximum penetration of Hurricane Katrina is shown.
- Fig. 4 Grain size distribution and organic content (OM) of Ocean Springs, Mississippi. Principal Component Analysis (PCA) Axis 1 score is shown. Schematic stratigraphic column follows Tröels-Smith nomenclature (1955).
- Fig. 5 Foraminiferal analysis of Ocean Springs, Mississippi. Schematic stratigraphic column following Tröels-Smith nomenclature (1955), location of sample and total number of individuals per 5 cm³ are shown.
- Fig. 6 Location Map of St. Andrews, Mississippi, showing geomorphology and buildings that

were impacted by the storm surges. The two numbers show the elevation (m NAVD88) and water depth (m), respectively. The maximum penetration of Hurricane Katrina and Rita are revealed.

Fig. 7 Grain size distribution and organic content (OM) of St. Andrews, Mississippi. Principal Component Analysis (PCA) Axis 1 score is shown. Schematic stratigraphic column follows Tröels-Smith nomenclature (1955).

Fig. 8 Foraminiferal analysis of St. Andrews, Mississippi. Schematic stratigraphic column following Tröels-Smith nomenclature (1955), location of sample and total number of individuals per 5 cm³ are shown.

Fig. 9 Location Map of Dauphine Island, Alabama, showing geomorphology and buildings that were impacted by the storm surges. The two numbers show the elevation (m NAVD88) and water depth (m), respectively.

Fig. Grain size distribution and organic content (OM) of Dauphine Island, Alabama.
10 Principal Component Analysis (PCA) Axis 1 score is shown. Schematic stratigraphic column follows Tröels-Smith nomenclature (1955).

Fig. Foraminiferal analysis of Dauphine Island, Alabama. Schematic stratigraphic column
11 following Tröels-Smith nomenclature (1955), location of sample and total number of individuals per 5 cm³ are shown.

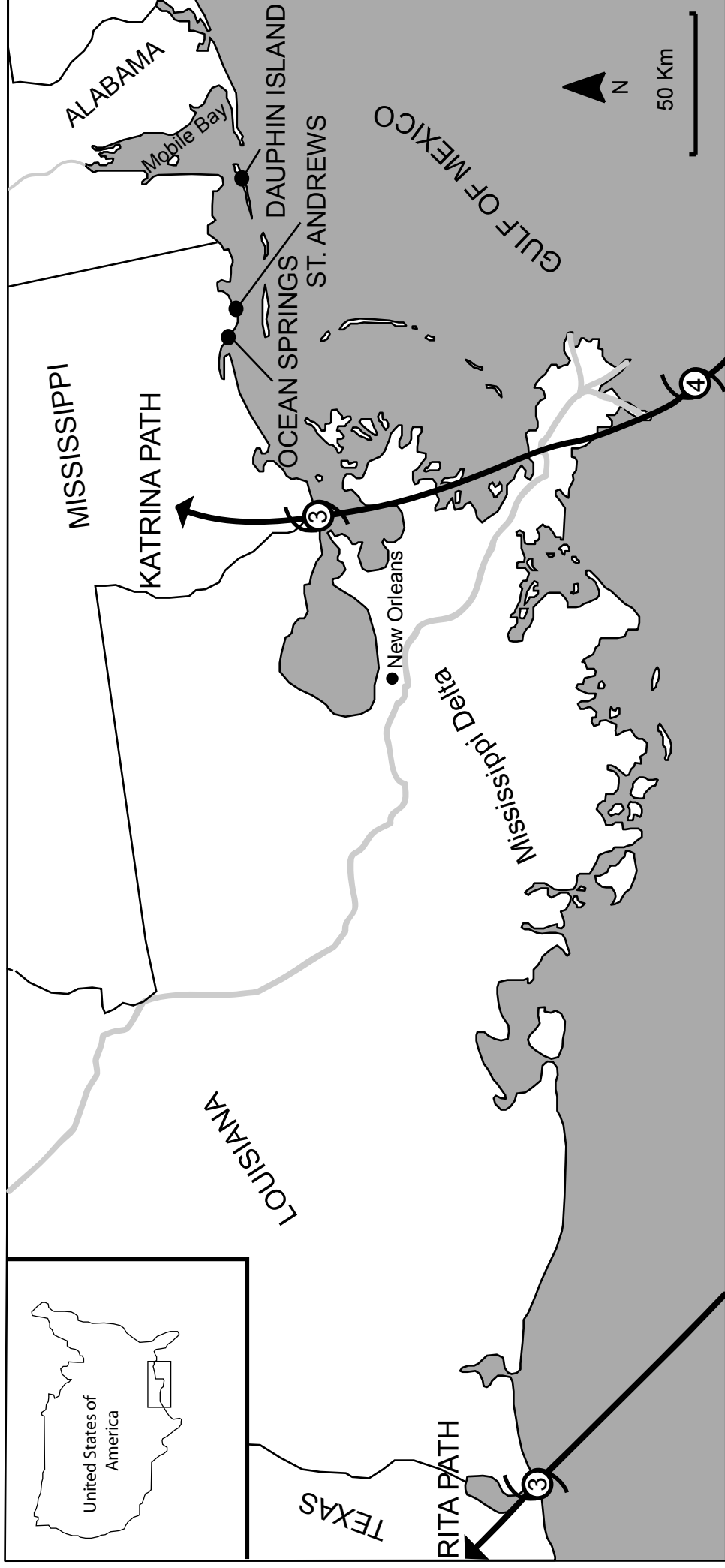


Figure 1

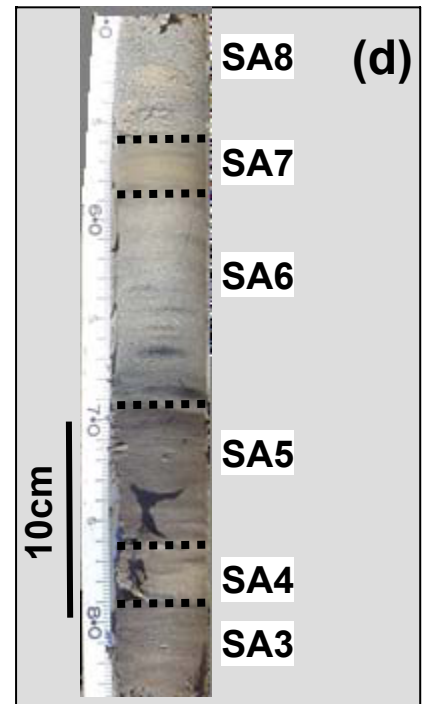
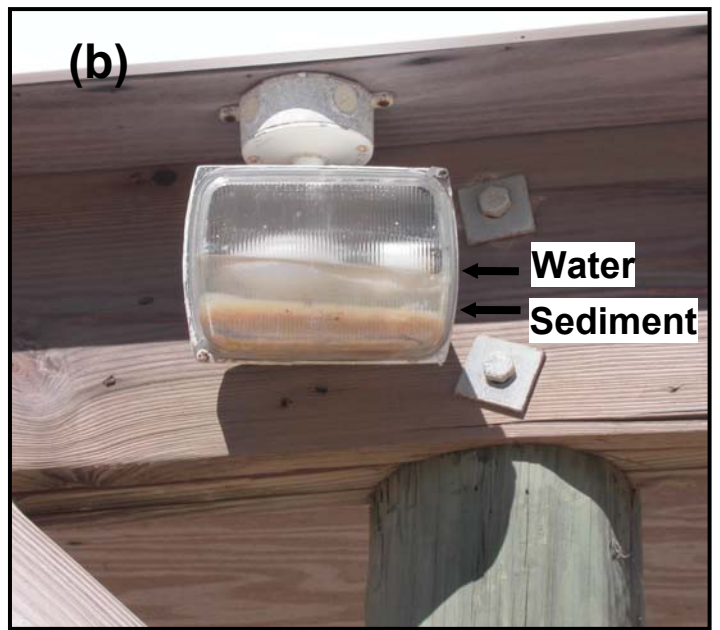


Figure 2

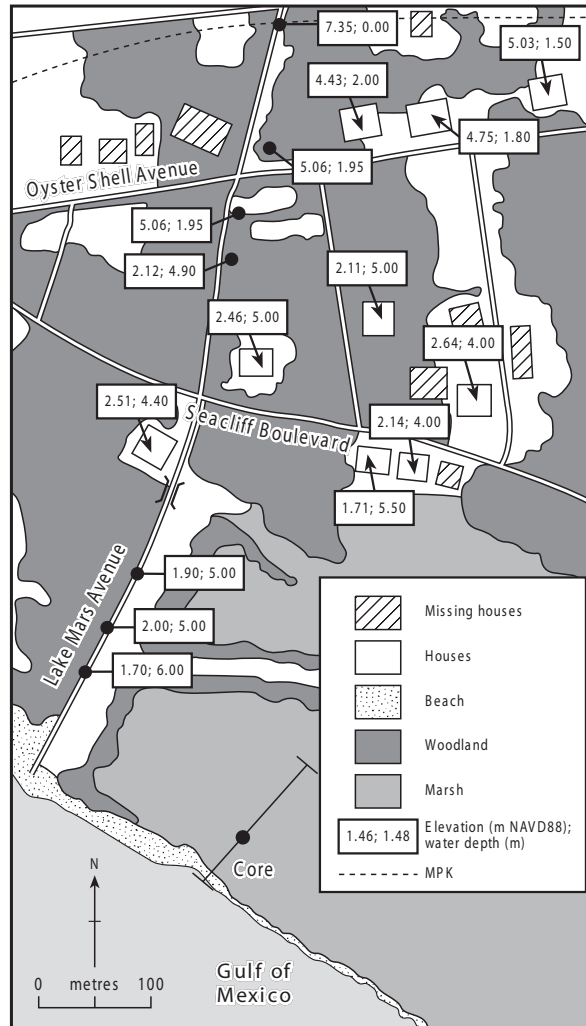


Figure 3

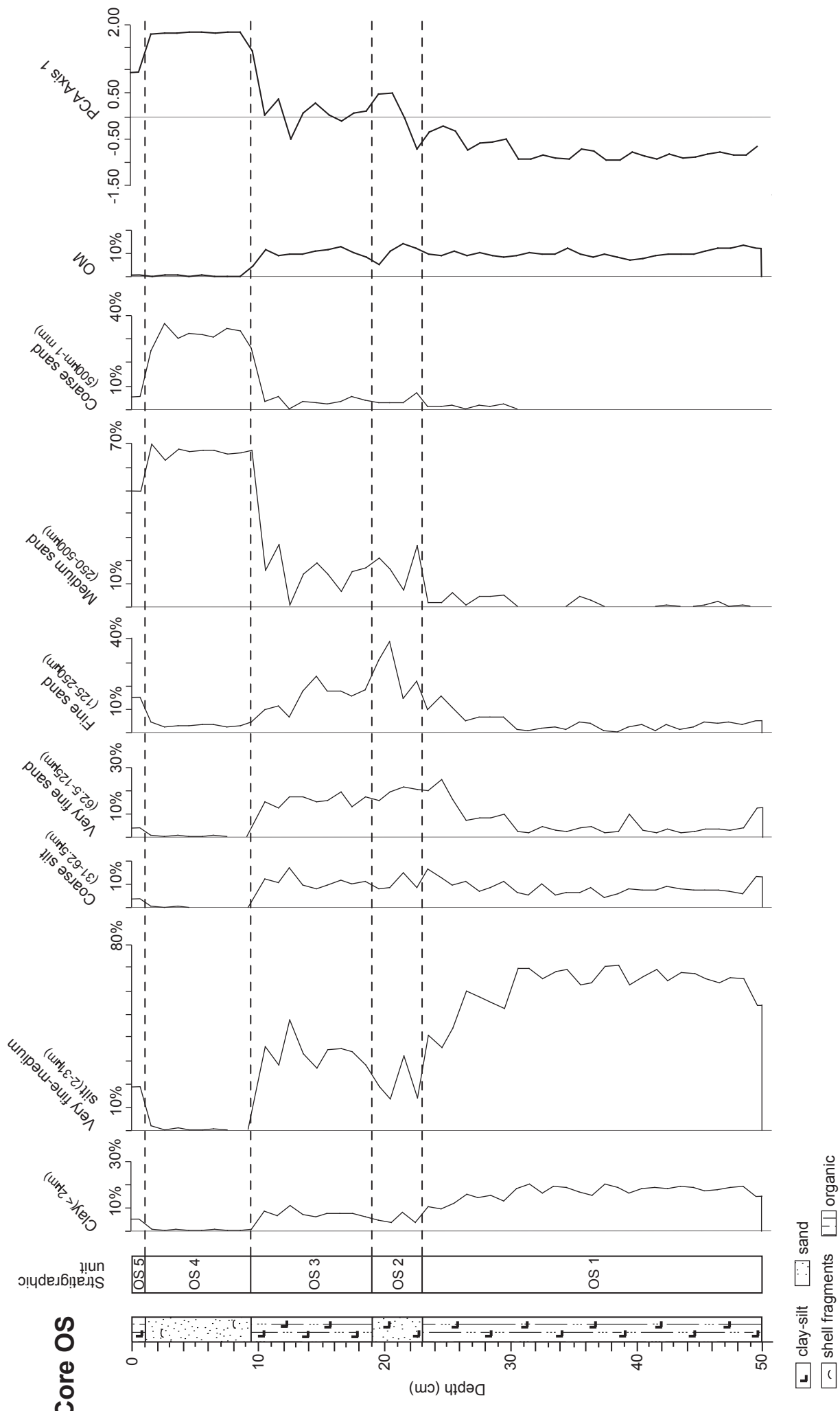


Figure 4

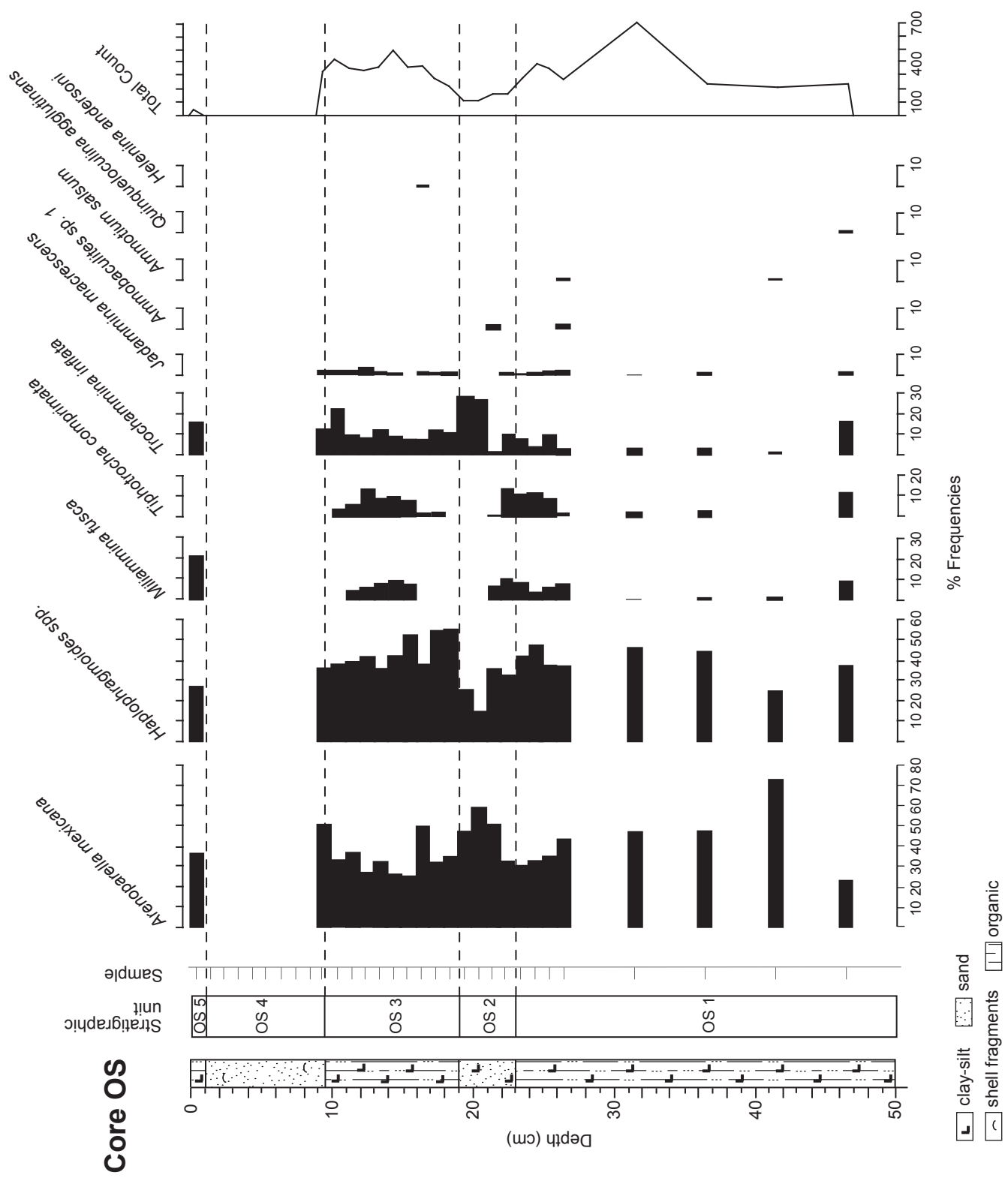


Figure 5

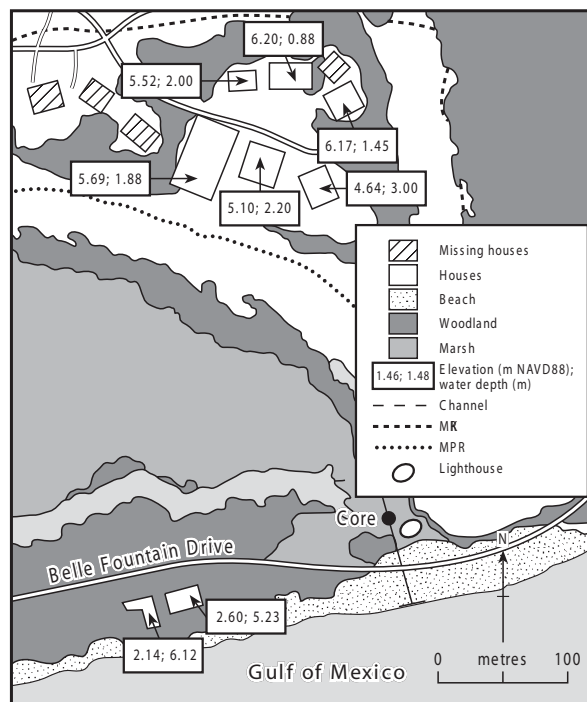


Figure 6

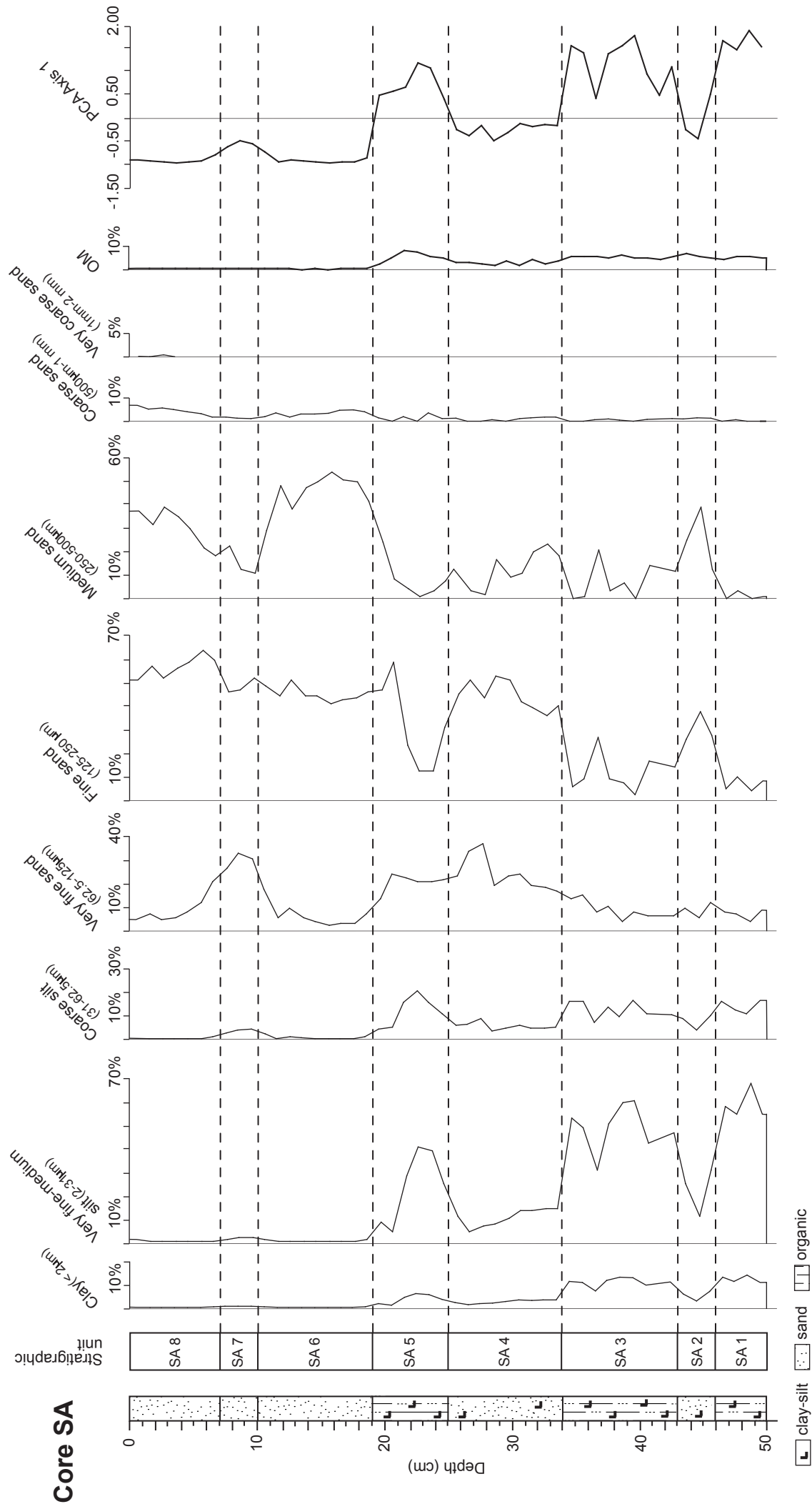


Figure 7

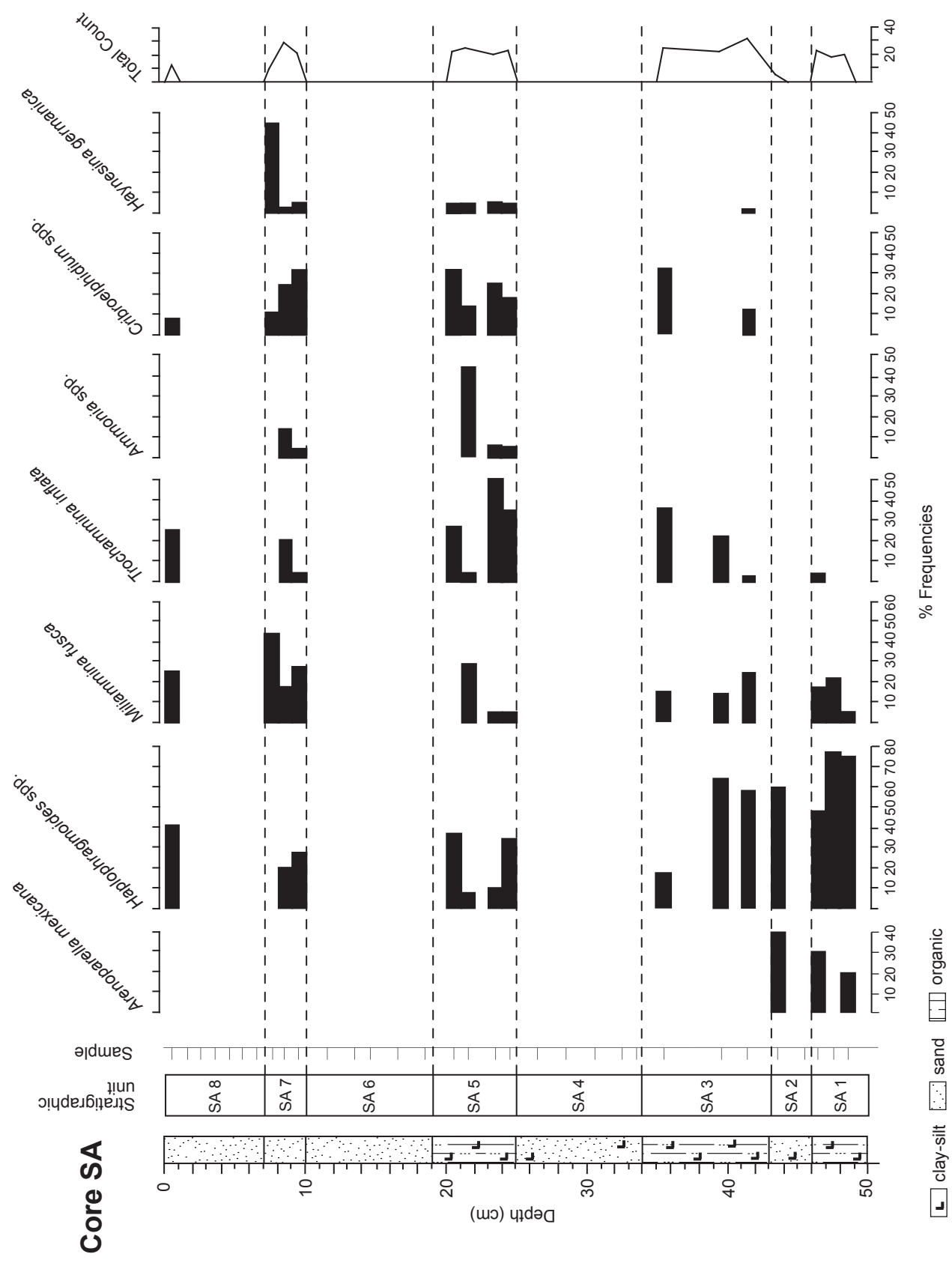


Figure 8

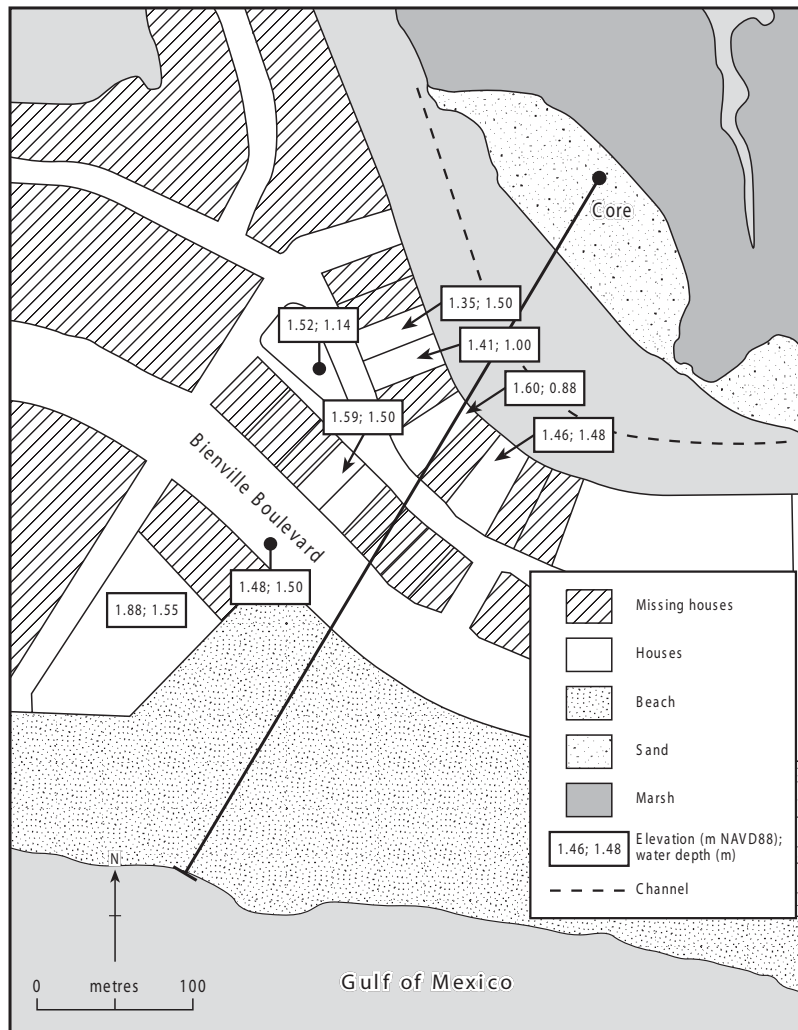


Figure 9

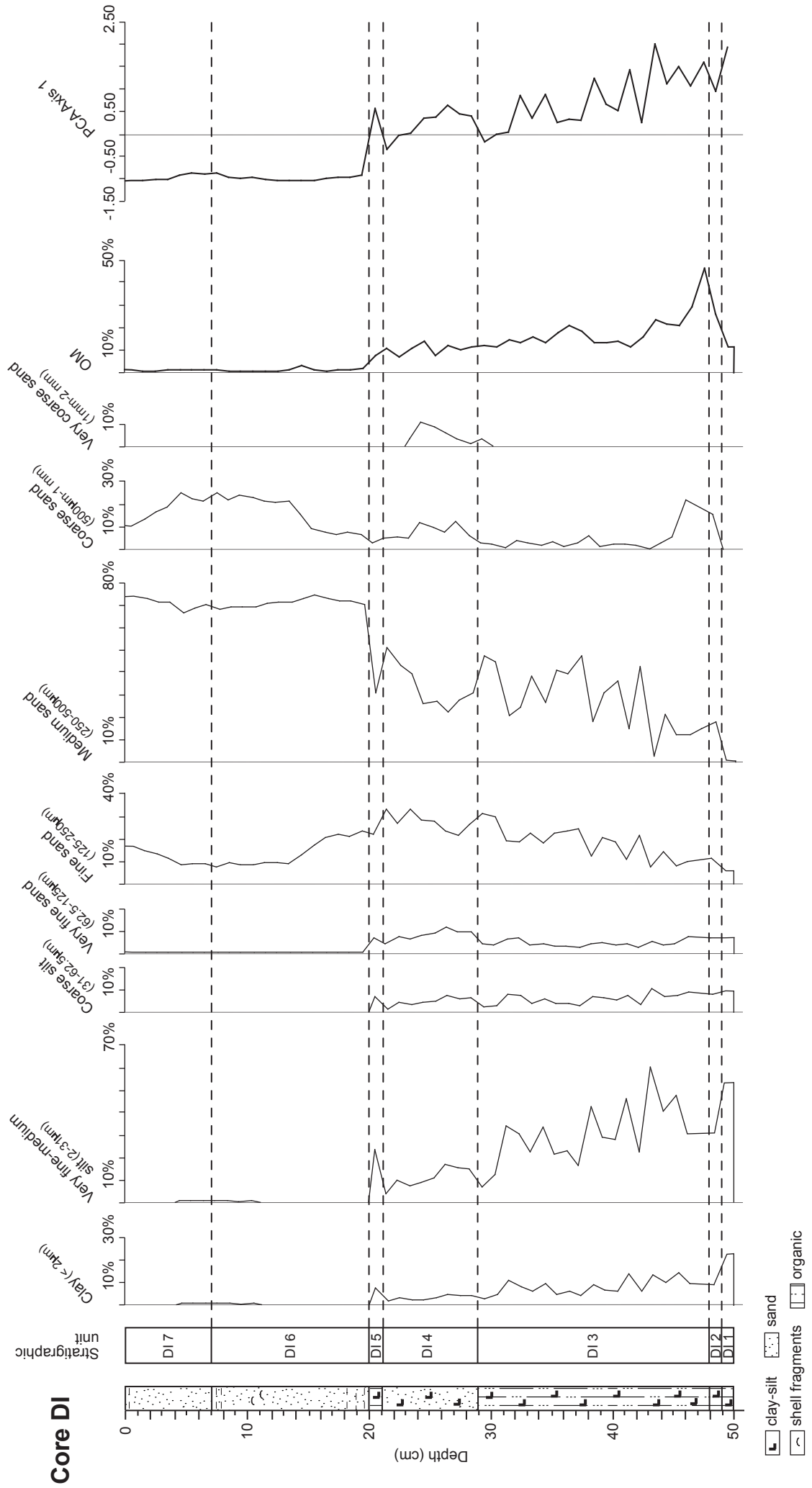


Figure 10

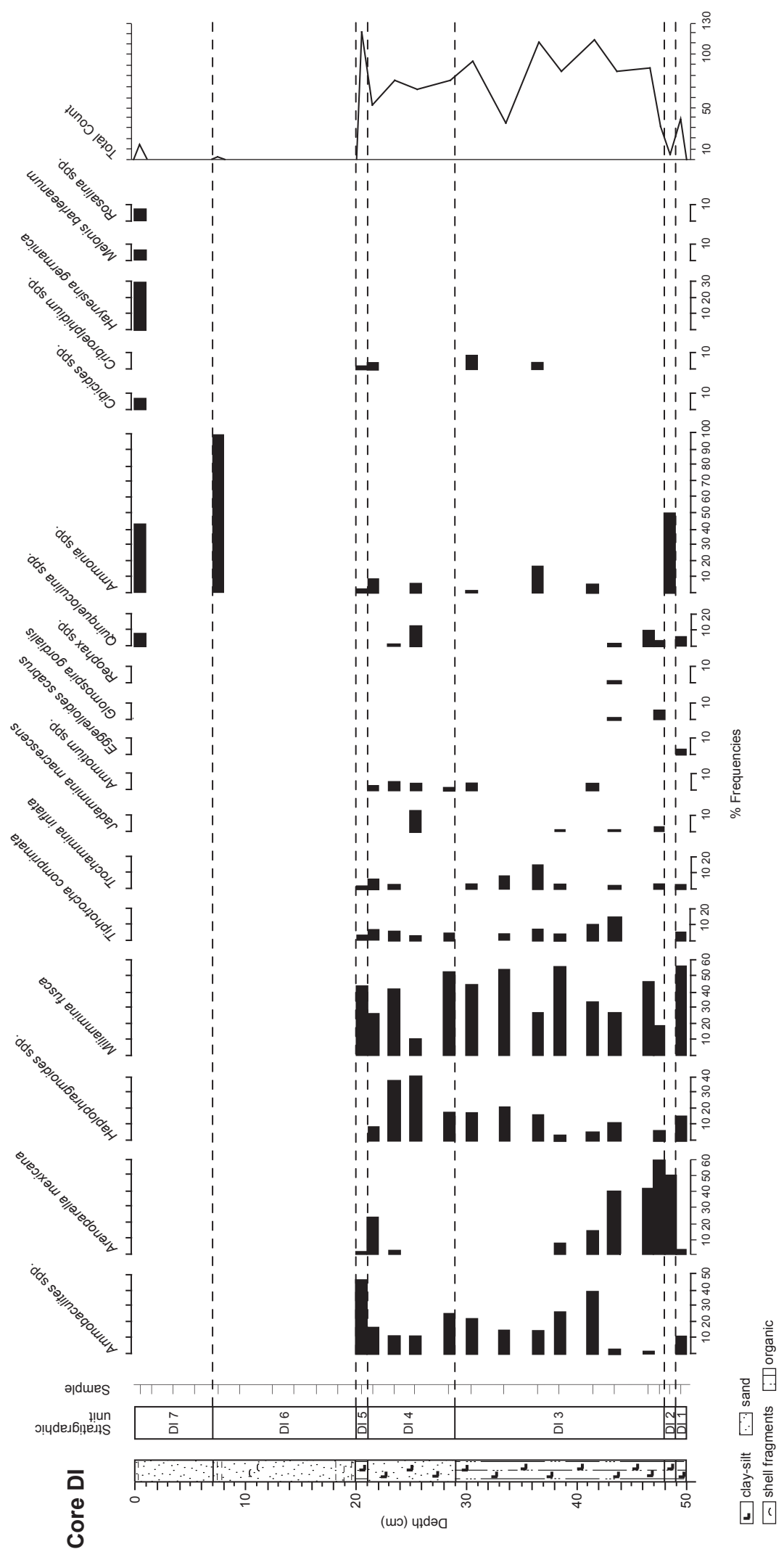


Figure 11

Ringraziamenti

Voglio ringraziare tutti coloro che hanno contribuito a realizzare questo lavoro e che mi sono stati vicini durante i tre anni di dottorato.

In particolar modo desidero ringraziare:

il Prof. Alessandro Amorosi per la supervisione dell'intero lavoro.

il Dott. Stefano Claudio Vaiani e il Dott. Giovanni Sarti dell'Università di Pisa per la loro disponibilità e per le discussioni riguardanti i dati micropaleontologici e stratigrafici.

Le mie amiche e colleghe Dott. Margherita Aguzzi e Dott. Marianna Ricci Lucchi che mi hanno sempre sostenuto e aiutato, ma anche regalato il nome di Ronni. Un grazie va infine a tutti gli amici e colleghi, Fabio, Federico, Franz, Giovanna, Nunzia e gli altri, senza i quali questi tre anni non sarebbero stati un così bel ricordo.

Desidero inoltre ricordare con riconoscenza la Prof. Maria Luisa Colalongo che mi ha insegnato molto nonostante la malattia.

